Systematik, Taxonomie und Phylogeographie der „Tasmanischen Berggarnelen“ der Gattung *Anaspides* (Anaspidesidae, Anaspidacea, Malacostraca)

Kumulative Dissertation

zur

Erlangung des akademischen Grades

doctor rerum naturalium (Dr. rer. nat.)

am Lehrstuhl für Allgemeine und Spezielle Zoologie

des Instituts für Biowissenschaften

an der Mathematisch-Naturwissenschaftlichen Fakultät

der Universität Rostock

vorgelegt von

Christoph Gert Höpel, geb. am 25.12.1993 in Grevesmühlen

aus Dassow

Rostock, den 14.08.2025

https://doi.org/10.18453/rosdok_id00005639

Gutachter:

Prof. Dr. Stefan Richter, Universität Rostock, Institut für Biowissenschaften, Allgemeine und Spezielle Zoologie

Prof. Dr. Uwe Fritz, Senckenberg Naturhistorische Sammlungen Dresden, Museum für Tierkunde

Dekan: Prof. Dr. Oliver Kühn

Jahr der Einreichung: 2025

Jahr der Verteidigung: 2025

Inhaltsverzeichnis

Zusammenfassung III

1 Einleitenden Zusammenfassung 1

1.1 Umfang der Dissertationsschrift 1

1.2 Einleitung 3

1.2.1 Entdeckungsgeschichte und Taxonomie der Anaspidesidae 3

1.2.2 Verbreitung und Habitat 7

1.2.3 Ökologie 10

1.2.4 Klima, Geomorphologie und Höhlen Tasmaniens 11

1.2.5 Höhlenbesiedlung 13

1.3 Ziele der Dissertation 14

1.4 Ergebnisse und Diskussion 16

1.4.1 Systematik der Anaspidesidae 16

1.4.2 Taxonomie und Verbreitung von *Anaspides* 18

1.4.2.1 *Anaspides tasmaniae* 18

1.4.2.2 *Anaspides driesseni* Höpel et al., 2023 21

1.4.3 Artbildung, Phylogeographie und *Anaspides richardsoni* als paraphyletische Art . 22

1.4.4 Höhleneinwanderung und Populationsgenetik 29

1.5 Ausblick und weiterführende Analysen 33

1.6 Literaturverzeichnis 35

2 Höpel, C. G., Ahyong, S. T., & Richter, S. (2021). Genetic structure and new occurrence records of the iconic Tasmanian mountain shrimp *Anaspides tasmaniae* (Thomson, 1893)(Anaspidesidae: Anaspidacea) reveal relictual distribution in southern Tasmania. Australian Journal of Zoology, 68(1), 45-53. 41

3 Höpel, C. G., Richter, S., & Ahyong, S. T. (2023). A new species of Tasmanian mountain shrimp, *Anaspides driesseni* sp. nov. (Malacostraca, Anaspidacea, Anaspidesidae). Records of the Australian Museum, 75(1), 25-43. 51

4 Höpel, C. G., Yeo, D., Ahyong, S. T., Meier, R., & Richter, S. (2023). First mitochondrial genomes of Anaspidacea (Malacostraca, Crustacea) and the phylogenetic relationships of

mountain shrimps (*Anaspides* Thomson, 1894) and their relatives within Anaspidesidae. Journal of Crustacean Biology, 43(2), ruad028. 71

5 Höpel, C. G., Ahyong, S. T., Kapun, M., Schwentner, M., & Richter, S. (2025). Phylogeography of the *Anaspides richardsoni* species clade (Anaspidacea, Anaspidesidae): glaciation and recolonization of the Tasmanian Central Plateau and the question of paraphyletic species. Cladistics. (https://doi.org/10.1111/cla.70005) 82

6 Höpel, C. G., Ahyong, S. T., Eberhard, S., Fordyce, S., Kapun, M., Schwentner, M., & Richter, S. Comparative phylogeography and speciation in correlation with cave colonization in Tasmanian mountain shrimps (*Anaspides*, Anaspidacea, Crustacea). Zoological Journal of the Linnean Society. (Under review).....106

Eigenständigkeitserklärung der Kapitel 2-6.....137

Selbstständigkeitserklärung 141

Lebenslauf 142

Danksagung 148

Zusammenfassung

Die Anaspidacea stellen eine einzigartige, jedoch wissenschaftlich bislang wenig untersuchte Ordnung innerhalb der Malacostraca (Höhere Krebse) dar und kommen ausschließlich im Süßwasser vor. Aufgrund ihrer großen morphologischen Übereinstimmung mit einem triassischen Fossil und vieler für die Malacostraca plesiomorph angenommener Merkmale, werden sie häufig als lebende Fossilien bezeichnet. Dies gilt insbesondere für die „Tasmanischen Berggarnelen“ der Gattung *Anaspides* Thomson, 1894. Bis zum Jahr 2023 waren lediglich sieben Arten beschrieben, von denen die meisten ein sehr begrenztes Verbreitungsgebiet aufweisen. Während einige Arten ausschließlich epigäische Gewässer besiedeln, zeigen andere sowohl Oberflächen- als auch Höhlenformen, und wiederum andere gelten als obligate Höhlenbewohner. Die vorliegende Dissertation liefert neue Erkenntnisse zu der Systematik, Taxonomie, Phylogeographie, Populationsgenetik und Artbildung der „Tasmanischen Berggarnelen“ (*Anaspides*). Neben morphologischen Analysen kamen insbesondere genetische Methoden wie die Sanger-Sequenzierung, Genome Skimming und ddRAD-Analysen zum Einsatz. Unsere Untersuchungen ermöglichten die präzise Bestimmung der Verbreitungsgrenzen der meisten Arten und stellten disjunkte Verbreitungsgebiete in Zusammenhang mit pleistozänen Vergletscherungen, wie etwa bei den Arten *Anaspides tasmaniae* Thomson, 1893 und *Anaspides driesseni* Höpel et al., 2023. Letzte wurde im Rahmen dieser Arbeit neu beschrieben. Mithilfe genetischer Daten konnte gezeigt werden, dass diese Art mehrfach Wasserscheiden über Bergplateaus überquert haben muss. Darüber hinaus klärten Analysen des vollständigen mitochondrialen Genoms die meisten phylogenetischen Verwandtschaftsverhältnisse innerhalb der Familie Anaspidesidae. Es konnte eindeutig gezeigt werden, dass *Paranaspides* Smith, 1908 die Schwestergruppe von *Anaspides* darstellt. Auch innerhalb der Gattung *Anaspides* wurden die meisten Beziehungen aufgelöst, wobei aber auch zwei Artkomplexe identifiziert wurden. Darüber hinaus wurde das Grundmusters der Genanordnung bei Anaspidacea rekonstruiert und Hypothesen über die Verwandtschaftsbeziehungen der Anaspidacea innerhalb der Malacostraca diskutiert. Die populationsgenetischen Analysen mittels ddRAD erlaubten schließlich eine detaillierte Auflösung der Verwandtschaftsverhältnisse innerhalb des „Central Clade“-Artkomplexes. Dabei wurden fünf monophyletische Arten identifiziert, davon drei bislang unbeschriebene, von denen vier innerhalb verschiedener genetischer Linien der Art *A. richardsoni* Ahyong, 2016 stehen. Im Zuge dessen werden Artbildungsprozesse diskutiert und das Konzept von *A.*

richardsoni als „paraphyletische“ Art eingeführt. Die detaillierten populationsgenetischen Daten zeigen eine starke Korrelation zwischen Lokalität und genetischem Signal, bei dem so gut wie jeder Fundort als eigenständige genetische Population ausgewiesen werden konnte. Auf Grundlage dieser Daten wurden glaziale Refugien sowie die Wiederbesiedlung ehemals vergletscherter Gebiete auf dem Zentralplateau Tasmaniens rekonstruiert. Abschließend widmet sich die Arbeit der Besiedlung von Höhlensystemen und den damit verbundenen Speziationsprozessen. Im Fokus steht die obligat höhlenbewohnende Art *A. eberhardi* Ahyong, 2016. Hier konnte eine einmalige Besiedlung des subterranen Lebensraums mit anschließender unterirdischer Ausbreitung und Diversifikation festgestellt werden. Diese Prozesse stehen in engem Zusammenhang mit geomorphologischen Veränderungen infolge pleistozäner Vergletscherungen. Aufgrund der heute allopatrischen Populationen von *A. eberhardi* und *A. richardsoni*, der genetischen Daten sowie der glazialen Historie der Region wird die „climatic relict hypothesis“ als das plausibelste Modell für die Höhlenbesiedlung angenommen. Darüber hinaus wurden die Populationsstruktur und unterirdischen Wanderbewegungen von *A. eberhardi* rekonstruiert und diskutiert.

Summary

The Anaspidacea represent an enigmatic but scientifically understudied order within the Malacostraca (higher crustaceans) and are exclusively found in freshwater habitats. Due to their strong morphological resemblance to a Triassic fossil and the presence of numerous traits considered plesiomorphic for Malacostraca, they are often referred to as living fossils. This is especially true for the Tasmanian Mountain Shrimps of the genus *Anaspides* Thomson, 1894. As of 2023, only seven species had been described, most of which exhibit highly restricted distribution ranges. While some species inhabit exclusively epigean waters, others display both surface and cave-dwelling forms, and yet others are considered obligate cave dwellers. This dissertation provides new insights into the systematics, taxonomy, phylogeography, population genetics, and speciation of Tasmanian Mountain Shrimps (*Anaspides*). In addition to morphological analyses, genetic methods such as Sanger sequencing, genome skimming, and ddRAD analyses were employed. Our investigations enabled precise delineation of the distribution of most species and linked disjunct distribution patterns to Pleistocene glaciations, as observed in *Anaspides tasmaniae* Thomson, 1893 and *Anaspides driesseni* Höpel et al., 2023. The latter was newly described in the course of this

study. Genetic data revealed that this species must have crossed watersheds multiple times via mountain plateaus. Furthermore, analyses of complete mitochondrial genomes resolved most phylogenetic relationships within the family Anaspidesidae. It was shown that *Paranaspides* Smith, 1908 is the sister group to *Anaspides*. Within the genus *Anaspides*, most relationships were resolved as well, however, two distinct species complexes were identified. Additionally, the ground pattern of the gene order in Anaspidacea was reconstructed, and hypotheses regarding the phylogenetic placement of Anaspidacea within Malacostraca were discussed. Population genetic analyses using ddRAD ultimately allowed for a detailed resolution of relationships within the "Central Clade" species complex. Five monophyletic species were identified (with three previously undescribed ones), of which four are grouping within several distinct genetic lineages of *A. richardsoni* Ahyong, 2016. In this context, speciation processes are discussed, and the concept of *A. richardsoni* as a "paraphyletic" species is introduced. The detailed population genetic datasets further reveal a strong correlation between locality and genetic signal, with nearly every sampling site representing a distinct genetic population. Based on these findings, glacial refugia and the postglacial recolonization of formerly glaciated areas on Tasmania's Central Plateau were reconstructed. Finally, the study addresses the colonization of cave systems and associated speciation processes. The obligate cave-dwelling species *A. eberhardi* Ahyong, 2016 is of particular interest. Our data suggests a single colonization event of the subterranean habitat, followed by underground dispersal and diversification. This processes were heavily influenced by geomorphological changes due to Pleistocene glaciations. Given the current allopatric populations of *A. eberhardi* and *A. richardsoni*, the genetic signal, and the glacial history of the region, the "climatic relict hypothesis" is proposed as the most plausible model for this cave colonization. Additionally, the population structure and subterranean migration patterns of *A. eberhardi* were reconstructed and discussed.

1 Einleitenden Zusammenfassung

Die vorliegende kumulative Dissertationsschrift besteht aus 6 Kapiteln. Sie umfasst die einleitende Zusammenfassung (Kapitel 1) und die zugrundeliegenden vier angenommenen Publikationen (Kapitel 2-5), sowie ein weiteres eingereichtes und sich im Review (2. Runde) befindendes Publikationsmanuskript (Kapitel 6).

1.1 Umfang der Dissertationsschrift

Kapitel 1 stellt die einleitende Zusammenfassung der Dissertationsschrift dar. Es bietet eine inhaltliche Einführung in die Thematik, leitet zu den zentralen Fragestellungen der Arbeit über und fasst die Ergebnisse der zugrundeliegenden Publikationen (Kapitel 2-6) zusammen, wobei diese in einen übergeordneten wissenschaftlichen Kontext eingeordnet werden. Im ersten Teil wird auf die Entdeckungsgeschichte der Familie der Anaspidesidae, ihre Taxonomie, sowie ihre Verbreitung, ihr Habitat und ihre Ökologie eingegangen. Der besondere Fokus liegt dabei auf den „Tasmanischen Berggarnelen" der Gattung *Anaspides* Thomson, 1894. Darüber hinaus werden das Klima, die Geomorphologie und die Höhlensysteme Tasmaniens vorgestellt. In diesem Zusammenhang werden auch grundlegende Prinzipien und Modelle zur Einwanderung in Höhlen erläutert. Im Anschluss werden die Ziele und Fragestellungen der Dissertation dargestellt. Danach folgt eine Zusammenfassung und Diskussion der zentralen Inhalte der zugrundeliegenden Publikationen (Kapitel 2-6), beginnend mit der Systematik der Familie Anaspidesidae und der Gattung *Anaspides*. Es folgen Ausführungen zu Aspekten der Verbreitung und Taxonomie, die in der Beschreibung einer neuen Art mündeten. Im weiteren Verlauf werden phylogeographische Muster und Prozesse der Artbildung innerhalb der Gattung *Anaspides* diskutiert, insbesondere im Zusammenhang mit den pleistozänen Vergletscherungen Tasmaniens. Ein besonderer Schwerpunkt liegt hierbei auf den genetischen Daten und konzeptionellen Überlegungen zur Paraphylie der Art *A. richardsoni* Ahyong, 2016. Abschließend erfolgt eine vertiefte inhaltliche Auseinandersetzung mit der Höhlenbesiedlung durch *Anaspides*, einschließlich der Charakteristika subterraner Populationen und möglicher unterirdischer Wanderbewegungen.

Kapitel 2 behandelt die Verbreitung und genetische Struktur der ehemals als weit verbreitet geltenden Art *Anaspides tasmaniae* Thomson, 1892, welche aber nach der Revision von Ahyong (2016) auf ein sehr kleines Gebiet im Osten und Südosten des Mt. Wellington beschränkt ist. Es werden die Ergebnisse zweier Forschungs- und Sammelreisen (2017, 2019)

sowie der Sanger-Sequenzierungen verschiedener Genabschnitte bei 48 Individuen von *A. tasmaniae* von sieben Fundorten dargestellt und diskutiert. Es werden die genauen Verbreitungsgrenzen aufgezeigt und die Funde neuer, vom Ursprungsgebiet weit entfernter (>50 km), Populationen vorgestellt. Darüber hinaus werden syntope Vorkommen mit anderen Arten beschrieben. Diese disjunkten Populationen werden hinsichtlich historischer Verbreitungsprozesse im Kontext pleistozäner Vergletscherungen diskutiert.

Kapitel 3 stellt die Neubeschreibung der Art *Anaspides driesseni* Höpel et al., 2023 dar. Es werden die artspezifischen Merkmale beschrieben, als Zeichnungen dargestellt und weitere, für die Gattung *Anaspides* als besonders taxonomisch wichtige, Merkmale identifiziert. Darüber hinaus werden hochauflösende Fotos der ersten Antenne (Antennula) der neuen Art sowie ihrer Schwesterart *A. swaini* Ahyong, 2015 gezeigt und das genaue Verbreitungsgebiet dieser Art dargestellt. Darüber hinaus wird die genetische Distanz zu anderen *Anaspides*-Arten und die genetische Vielfalt innerhalb von *A. driesseni*, welche mittels Sanger Sequenzierung ermittelt wurde, gezeigt und hinsichtlich phylogeographischer Prozesse diskutiert.

Kapitel 4 beschreibt die Analyse der mitochondrialen Genome und Systematik der Anaspidesidae und einer unbeschriebenen Art der Gattung *Micraspides* Nicholls, 1931 (Koonungidae, Anaspidacea). Es wird dargestellt, wie mittels Genome Skimming und anschließender Annotation die ersten vollständigen Mitogenome der Anaspidacea rekonstruiert wurden. Es werden die verschiedenen Genanordnungsmuster innerhalb der Anaspidesidae diskutiert und das Grundmuster der Anaspidacea rekonstruiert. Diese wird in den Kontext der Phylogenie der Höheren Krebse (Malacostraca) eingeordnet und potentielle Schwestergruppenverhältnisse diskutiert. Darüber hinaus werden die phylogenetischen Verwandtschaftsbeziehungen innerhalb der Anaspidesidae und insbesondere innerhalb der Gattung *Anaspides* dargestellt und diskutiert.

Kapitel 5 beschäftigt sich mit der sogenannten „Central Clade“, einem Artkomplex der über große Teile Zentral- und Nordtasmanien verbreitet ist, insbesondere auf dem zentralen Bergplateau. Es werden die sechs Arten dieses Komplexes vorgestellt und morphologisch eingeordnet. Darüber hinaus werden die Ergebnisse einer detaillierten ddRAD-Analyse, erweitert durch einige Sanger-Sequenzierungsdaten, dargelegt und diskutiert. Hierbei werden Aspekte der Artbildung, Populationsgenetik und Phylogeographie behandelt. Die Artbildung betreffend werden die Arten auf ihren Artstatus getestet und dieser anhand der genetischen

und morphologische Daten diskutiert. Insbesondere im Fokus steh dabei die Arten *A. richardsoni* Ahyong, 2016 und *A. spinulae* Williams, 1965. Hierbei wurde *A. richardsoni* als paraphyletisch rekonstruiert und es findet eine wissenschaftstheoretische Auseinandersetzung mit Thema der Artabgrenzung sowie der Mono- beziehungsweise Paraphylie von Arten statt. Die Art *A. spinulae*, welche als evolutiv sehr jung angesehen wird, wird hinsichtlich ihres Alters, dem Einfluss der letzten Vergletscherungen Tasmaniens und potentiellen Genflusses mit anderen Arten besprochen. Im Folgenden werden die phylogeographischen Prozesse, insbesondre im Hinblick auf glaziale Refugien und der Wiederbesiedlung des Zentralplateau diskutiert.

Kapitel 6 widmet sich vertieft den Höhlenpopulationen und der Besiedlung subterraner Habitate, wobei auch Aspekte der Artbildung beleuchtet werden. Im Zentrum steht die ausschließlich in den Höhlen des Junee-Florentine Karsts vorkommende Art *Anaspides eberhardi* Ahyong, 2016. Ihre Verwandtschaftsbeziehungen zu *A. richardsoni* sowie zu *Anaspides* sp. nov. 2, die ebenfalls in dieser Region vorkommen und ihr genetisch am nächsten stehen, werden eingehend untersucht. Die Ergebnisse einer detaillierten ddRAD-Analyse werden zusammengefasst und diskutiert. Dabei werden Hinweise auf Genfluss zwischen *A. eberhardi* und *A. richardsoni* sowie das syntope Vorkommen von *A. eberhardi* und *Anaspides* sp. nov. 2 dargestellt und eingeordnet. Darüber hinaus werden am Beispiel von *A. eberhardi* und auf Basis genetischer Daten, paläoklimatischer Rekonstruktionen und geomorphologischer Prozesse die gängigen Modelle für rezente Besiedlungen von Höhlen („climatic relict hypothesis“, CRH vs. „adaptive shift hypothesis“ ASH) diskutiert. Der geografische Ursprung der Höhlenbesiedlung wird aufgezeigt und unterirdische Wanderbewegungen sowie Populationsstrukturen werden rekonstruiert. Diese werden phylogeographisch eingeordnet und im Kontext der pleistozänen Vergletscherungen interpretiert.

1.2 Einleitung

1.2.1 Entdeckungsgeschichte und Taxonomie der Anaspidesidae

Die Anaspidacea bilden eine der Ordnungen der Malacostraca (Höheren Krebse) und weisen eine Gondwana-Verbreitung auf, die sich von Australien (einschließlich Tasmanien) über Neuseeland bis nach Südamerika (Argentinien, Chile) erstreckt. Die größte Artenvielfalt findet sich in Südostaustralien, insbesondere auf der Insel Tasmanien, wo vier der fünf rezenten

Familien vorkommen: Anaspidesidae, Koonungidae, Psammaspididae und Stygocarididae. Historisch wurden die Anaspidacea häufig gemeinsam mit den Bathynellacea (Brunnenkrebse) unter dem Taxon Syncarida zusammengefasst. Diese Einordnung basiert jedoch auf nur wenigen Apomorphien, wie dem ausschließlichen Vorkommen im Süßwasser und dem Fehlen eines Carapax (Calman, 1909). Aufgrund der begrenzten morphologischen Übereinstimmungen wurden im Laufe der Zeit verschiedene alternative Schwestergruppenverhältnisse vorgeschlagen. So vermutete Siewing (1956) die Anaspidacea als Schwestergruppe der Decapoda, während Richter und Scholz (2001) sie als Schwestergruppe der Euphausiacea + Peracarida identifizierten. Neuste molekulare Untersuchungen (Schwentner et al., 2018; Bernot et al., 2023) deuten auf ein Schwestergruppenverhältnis mit den Euphausiacea hin. Darüber hinaus werden die Anaspidacea häufig auch als „lebende Fossilien" bezeichnet, aufgrund der starken Ähnlichkeit zum triassischen Fossil *Anaspidites antiquus* Chilton, 1929 aus dem Hawkesbury Sandstone (Brookvale, New South Wales, Australien) und den vielen, für den Grundbauplan der Malacostraca, als plesiomorph angenommenen Merkmalen. Diese umfassen unter anderem eine minimale Tagmatisierung, ein nur mit dem ersten Thoraxsegment verschmolzenes Cephalon, eine fast vollständige Ausprägung aller Thorakopoden mit zwei blattartigen Kiemen und sehr gut ausgeprägten thorakopodalen Exopoditen (Smith, 1908, 1909; Manton, 1930; Schram & Hessler, 1984; Schramm, 1986; Schminke, 1996; Ahyong, 2016). Die Bezeichnung als „lebende Fossilien" trifft insbesondere auf die in Tasmanien endemische Familie der Anaspidesidae zu, und hier vor allem auf die Gattung *Anaspides*.

Die erste Art der Anaspidacea, *Anaspides tasmaniae*, wurde 1892 von Thomson auf dem Mt. Wellington in Tasmanien entdeckt und 1893 von ihm beschrieben. Zuerst den Schizopoda zugeordnet (Mysidacea + Euphausiacea, Thomson, 1894), errichtete Calman (1904) eine eigenständige Ordnung innerhalb der Malacostraca, die Anaspidacea. 1908 entdeckte Smith weitere Populationen von *Anaspides tasmaniae* in den Hartz Mountains, auf dem Mount Field und dem Mount Rufus. Darüber hinaus entdeckte und beschrieb er aus dem Great Lake, (Tasmanien) mit *Paranaspides lacustris* Smith, 1908, eine weitere Art und Gattung innerhalb der Familie der Anaspidesidae. Diese Gattung zeichnet sich durch einen mysidenartigen Habitus aus. 1965 beschrieb Williams mit *Anaspides spinulae* die zweite *Anaspides*-Art, welche ausschließlich im Lake St. Clair (Tasmanien) vorkommt. Im selben Jahr dokumentierte Williams (1965b) auch erstmals das Vorkommen von *Anaspides* in Höhlen. Die dritte Gattung der

Anaspidesidae, *Allanaspides*, wurde 1970 von Swain et al. beschrieben und umfasst die zwei Arten *Allanaspides helonomus* (Swain et al., 1970) und *Allanaspides hickmani* (Swain et al., 1971). In den folgenden Jahrzehnten führten weitere Untersuchungen in Tasmanischen Gewässern zu einer erheblichen Vergrößerung des Verbreitungsgebiets von *Anaspides tasmaniae.* Es wurden Höhlenpopulationen mit unterschiedlichen Anpassungsgraden dokumentiert, sowie eine größere morphologische Vielfalt innerhalb der Populationen von *A. tasmaniae* festgestellt. Dies führte zu Vermutungen, dass es sich um mehrere Arten, statt einer weit verbreiteten, handeln könnte (Goede, 1967; Lake & Coleman, 1977; O'Brien, 1990). Diese wurde auch durch die ersten genetischen Untersuchungen von Jarman und Elliot (2000) sowie Andrew (2005) gestützt. Erst Ahyong (2015, 2016) war jedoch in der Lage, fünf neue Arten von *Anaspides* zu unterscheiden und zu beschreiben (*A. clarkei* Ahyong, 2015*, A. eberhardi, A. jarmani* Ahyong, 2015*, A. richardsoni, A. swaini* Ahyong, 2015). Darunter waren mit *A. clarkei* und *A. eberhardi* zwei obligat höhlenbewohnende Arten sowie mehrere Arten (*A. richardsoni, A. swaini, A. jarmani*) mit Oberflächen- als auch Höhlenpopulationen. Darüber hinaus beschrieben Ahyong et al. (2017) eine weitere Art von *Paranaspides*, *Paranaspides williamsi* Ahyong et al., 2017*,* aus Arthurs und Woods Lake.

Als wichtigste Merkmale bei der Artunterscheidung werden häufig sexual Merkmale wie die männlichen Geschlechtsorgane oder andere mit der Kopulation assoziierte Strukturen herangezogen (Eberhard, 1985). Solche Merkmale sind bei den Arten der Gattung *Anaspides* die Form des männlichen Kopulationsorgans (Petasma) und die Anzahl und Form der „clasping spines" (dornenartige Setae am 7. Segment des inneren Flagellums der 1. Antenne) (Abb. 1). Nur die Männchen tragen diese „clasping spines" und es wird vermutet das sie sich mithilfe dieser dornenartigen Setae am Weibchen festklammern. Die Anzahl der „clasping spines" variiert hierbei je nach Art zwischen 1–5 und scheint einer starken sexuellen Selektion zu unterliegen. So haben *A. richardsoni* und *A. eberhardi* jeweils einen „clasping spine", während *A. spinulae*, *A. swaini* und *A. tasmaniae* zwei haben (Abb. 1). *Anaspides jarmani* und *A. clarkei* besitzen 3-4, respektive 3-5 „clasping spines". Weiteres wichtige artspezifische Merkmale sind die Form und Bedornung des Telsons, die Anzahl der pleopodalen Endopoden, die pleonale Bedornung sowie die Größe beim Erreichen der Geschlechtsreife. Letzteres ist insbesondere bei der Art *A. spinulae* auffällig, die bereits bei einer Körperlänge von 14–15 mm geschlechtsreif wird, während die meisten anderen Arten dies durchschnittlich erst bei 18–23 mm erreichen. Unterschiede in den genannten Merkmalen veranlassten Ahyong (2016) zur

Spekulation über noch weitere, unbeschriebene Arten. Er identifizierte mehrere morphologische Formen, beispielsweise innerhalb von *A. swaini* (Form 1-3, Ahyong 2016). Im Gegensatz zu *Anaspides* weißt *Paranaspides* einen markanten (garnelenartigen) Knick im ersten Pleonsegment auf und besitzt keine sexuell dimorphen Antennen. Zudem zeigt *Paranaspides* eine insgesamt stärkere Bedornung. Die beiden Arten innerhalb von *Paranaspides* werden hauptsächlich anhand der Merus Länge des Maxillipeden, der Länge der Dornenreihe am uropodalen Exopoden, sowie an kleinen Unterschieden der Petasmata unterschieden (Ahyong et al., 2017). Ebenso wie *Paranaspides* zeigt auch *Allanaspides* keine geschlechtsspezifischen Unterschiede an den Antennen, unterscheidet sich jedoch in anderen Merkmalen deutlich von den übrigen Vertretern der Familie Anaspidesidae. Das auffälligste Merkmal ist das Vorhandensein eines Fenestra dorsalis, welches vermutlich dem Ionentransport und der Exkretion dient. Diese Struktur stellt vermutlich eine Anpassung an die sauren Gewässer dar, in denen diese Tiere leben (pH <5, Driessen & Mallick, 2007). Darüber hinaus hat *Allanaspides* keinen Exopoditen mehr am 7. Thorakopoden, keine Epipodite an den ersten Thorakopoden und auch keine pleopodalen Endopoden. Die beiden bekannten *Allanaspides*-Arten unterscheiden sich vor allem durch die Form und Farbe des Fenestra dorsalis, welches bei *Allanaspides hickmani* rechteckig und rot ist während es bei *Allanaspides helonomus* oval und durchsichtig ist (Swain et al., 1971).

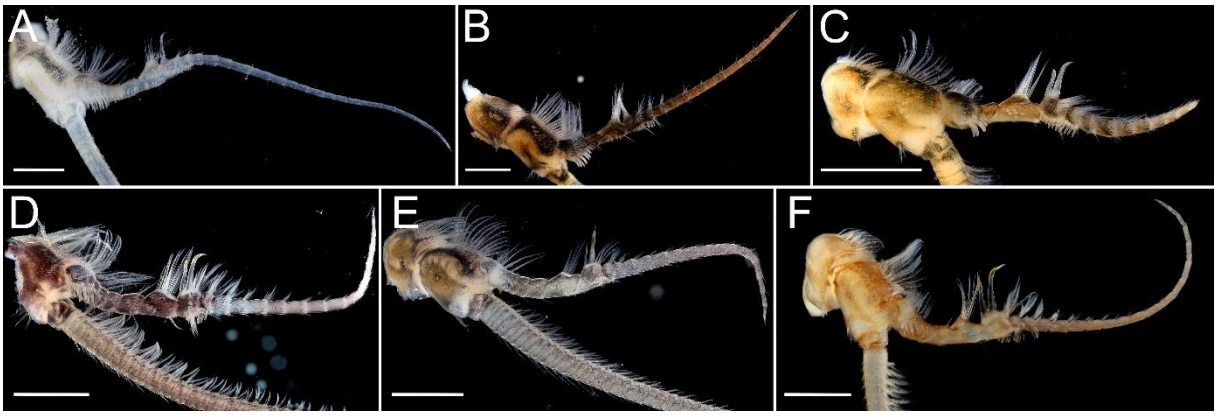


Abbildung 1: Inneres Flagellum der 1. Antenne mit den „clasping spines“ (nur bei Männchen) bei *Anaspides* spp. (A) *A. eberhardi*; (B) *A. richardsoni*; (C) *A. spinulae*; (D) *A. tasmaniae*; (E) *A. swaini* (Form 1 nach Ahyong 2016); (F) *A. swaini* (Frankland Range, Form 2 nach Ahyong 2016). Weißer Maßstab: 1 mm.

Richter et al. (2018) konnten durch molekulargenetische Analysen die Mehrzahl der morphologisch beschriebenen Arten und Artgruppen bestätigen, darunter beide Arten der Gattungen *Paranaspides* und *Allanaspides* sowie A*. tasmaniae, A. swaini, A. richardsoni* und die Artgruppe *A. clarkei/A. jarmani*. Allerdings traten auch einige taxonomisch problematische

Fälle zutage. So wurden die Arten *A. eberhardi* und *A. spinulae* als genetische Linien innerhalb von *A. richardsoni* identifiziert, was Zweifel an ihrem Artstatus aufkommen ließ. Darüber hinaus deuteten erhöhte genetische Distanzen innerhalb von *A. swaini* auf die mögliche Existenz bislang unbeschriebener Arten hin. Es variierten auch die phylogenetischen Beziehungen zwischen den Arten je nach analysiertem Gen.

1.2.2 Verbreitung und Habitat

Anaspides, sowie alle übrigen Vertreter der Anaspidesidae (*Paranaspides, Allanaspides*), kommen ausschließlich im Süßwasser vor. Sie sind endemisch auf Tasmanien und zeigen eine bemerkenswerte horizontale wie auch vertikale Verbreitung. *Anaspides* bevorzugt dabei Habitate in höheren Lagen, meist über 700 m Höhe, kann aber gelegentlich auch in geringeren Höhen angetroffen werden (>350 m) (Smith, 1908; Siewing, 1959; Williams, 1965a, 1965b; O´Brien, 1990; Ahyong, 2016). Sie besiedeln Bergseen, -tümpel, -pools als auch kleinere Gebirgsbäche und –flüsse (Abb. 2). Darüber hinaus finden sich Populationen von *Anaspides* in zahlreichen Höhlensystemen auf der gesamten Insel (Abb. 3). Der Haupteinflussfaktor auf die Verbreitung scheint die Wassertemperatur und -qualität zu sein (Williams, 1965a; Swain & Reid, 1983; O´Brien, 1990). Obwohl sie zeitweise auch höhere Temperaturen tolerieren können, bevorzugen sie kalte und klare Gewässer.

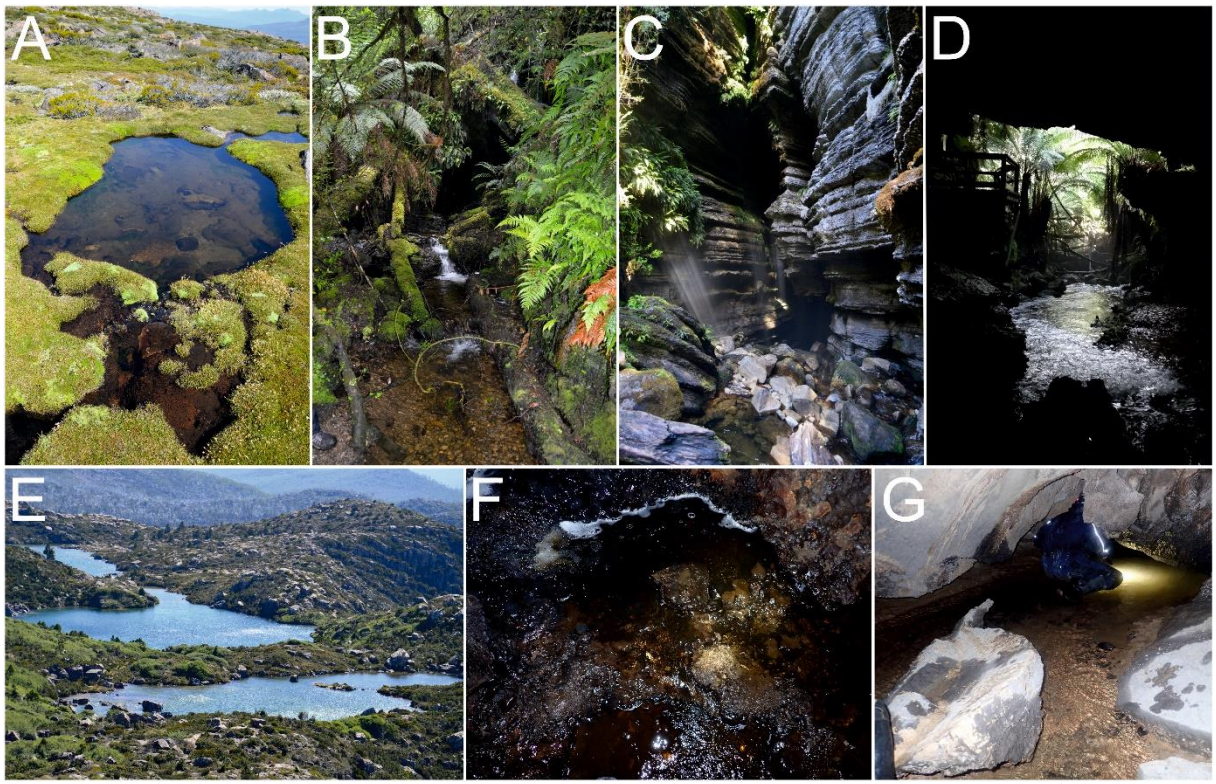


Abbildung 2: Typische *Anaspides* spp. Habitate. (A) Bergpool am Mt. Field West; (B) Gebirgsbach im temperaten Regenwald; (C) Garths Creek am Höhleneingang zur Growling Swallet Cave; (D) Junee River am Höhlenausgang der Junee Cave; (E) Robert Tarn, McKenzie Tarn und Johnston Tarn auf dem Tarn Shelf (Bergplateau) im Mt. Field Nationalpark; (F) kleiner Höhlenpool in einem Höhlenbach in der Höhle JF-104; (G) Höhlenfluss in der Welcome Stranger Cave.

Von den bislang sieben beschriebenen Arten der Gattung *Anaspides* kommen zwei ausschließlich in epigäischen Gewässern vor (*A. tasmaniae*, *A. spinulae*), zwei weitere ausschließlich in Höhlen (*A. clarkei*, *A. eberhardi*), während die übrigen drei Arten sowohl oberirdische als auch subterrane Lebensräume besiedeln (*A. jarmani*, *A. richardsoni*, *A. swaini*) (Ahyong, 2015, 2016). Die Mehrzahl dieser Arten weist ein äußerst begrenztes Verbreitungsgebiet auf (Abb. 3). So wurde *A. spinulae* bislang ausschließlich im Lake St. Clair nachgewiesen und stellt die einzige Art der Gattung dar, die in einem der großen tasmanischen Seen vorkommt (Abb. 3). *Anaspides eberhardi* ist ausschließlich in Höhlengewässern des Junee-Florentine Karsts anzutreffen (Abb. 2D, F, G und 3), während *A. clarkei* auf Höhlen im Südosten Tasmaniens in den Karstregionen von Ida Bay und Hastings beschränkt ist.

Die vormals als weit verbreitet geltende Art *A. tasmaniae* wurde infolge der taxonomischen Revision durch Ahyong (2016) auf ein kleines Gebiet im Osten und Südosten des Mt. Wellington nahe Hobart eingegrenzt (Abb. 3). Lediglich zwei Arten lassen sich als weit verbreitet klassifizieren: *A. richardsoni* und *A. swaini*. Das Verbreitungsgebiet von *A. richardsoni* erstreckt sich von Zentraltasmanien mit dem Mt. Field Nationalpark über große Teile des Zentralplateaus bis in den Norden (z. B. Mole Creek Karst) und Nordwesten Tasmaniens (z. B. Black Bluff Range, West Coast Range). *Anaspides swaini* besiedelt ein ausgedehntes Areal von Südwesttasmanien mit der Arthurs Range, Frankland Range und dem Mt. Anne über Zentraltasmanien (Mt. Field) bis in den Nordwesten (Abb. 3). Trotz zum Teil überlappender Verbreitungsgebiete treten syntope Vorkommen bei *Anaspides* äußerst selten auf (Ahyong, 2016) (Abb. 3).

Die beiden Arten der Gattung *Paranaspides* besiedeln ausschließlich die größeren Seen des östlichen Teils des tasmanischen Zentralplateaus. *Paranaspides lacustris* wurde im Great Lake sowie in der angrenzenden Shannon Lagoon nachgewiesen, während *P. williamsi* im Arthurs Lake und Woods Lake vorkommt (Abb. 3). Obwohl eine Pumpstation existiert, die den Great Lake und den Arthurs Lake miteinander verbindet, konnten bislang keine syntopen Vorkommen oder artifiziell verbrachte Tiere festgestellt werden (Ahyong et al., 2017).

Die natürlichen Lebensräume der Gattung *Allanaspides* sind die stark sauren Knopfgrasmoore („buttongrass moorlands“) im Südwesten Tasmaniens, insbesondere in der Umgebung des Lake Pedder und Lake Gordon (Abb. 3). Dort sind sie in den oberflächlichen Überschwemmungsgebieten und Tümpeln mit Flusskrebsgängen anzutreffen, welche sie in Trockenperioden und den regelmäßig auftretenden Buschbränden als Rückzugsorte nutzen. Die beide Arten können syntop auftreten (Abb. 3) (Swain et al., 1970; Swain et al., 1971; Swain, 2000; Driessen & Mallick, 2007; Driessen et al., 2014).

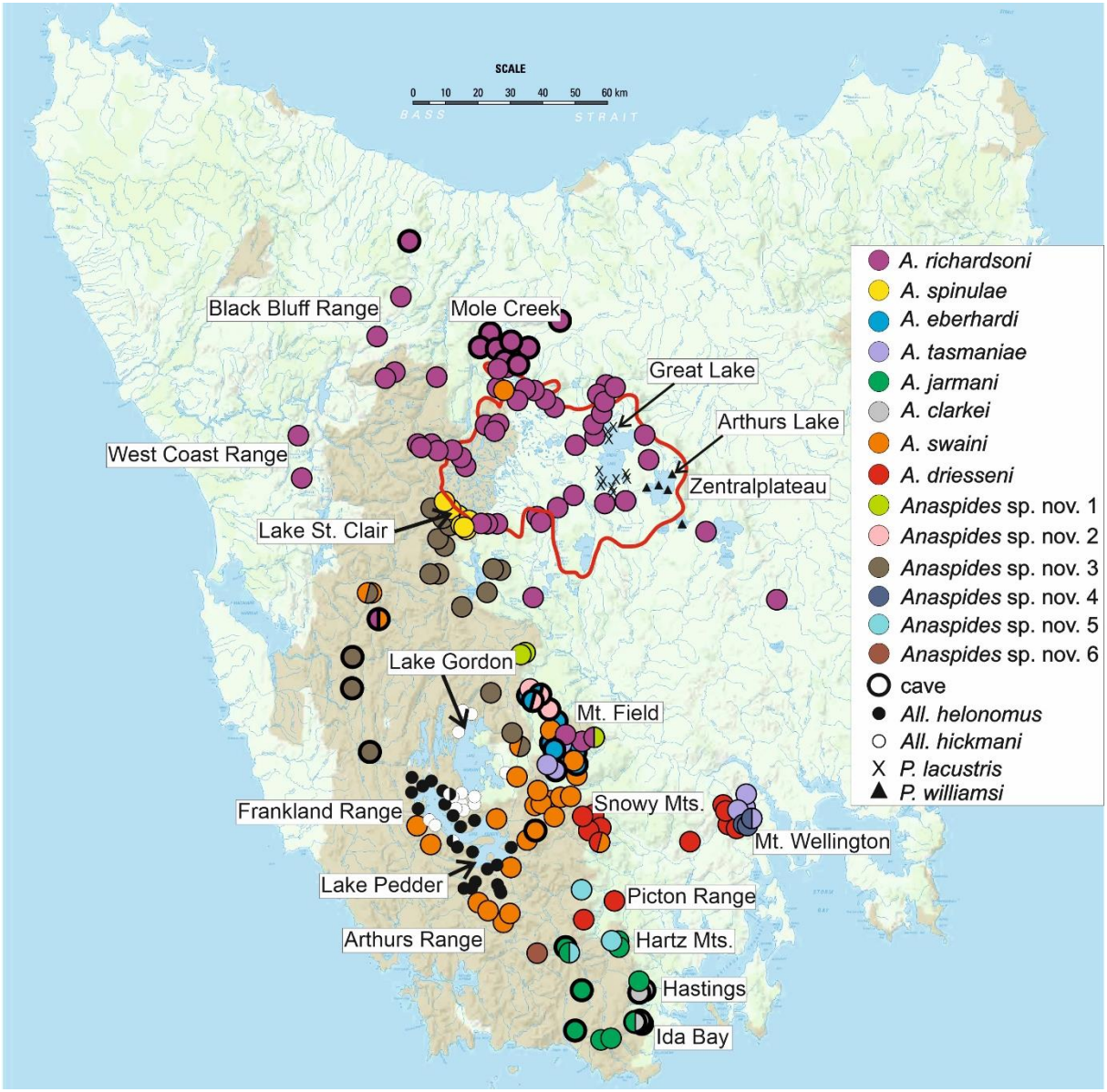


Abbildung 3: Topologisch-hydrologische Karte Tasmaniens mit den Verbreitungsgebieten der acht beschriebenen und sechs unbeschriebenen *Anaspides*-Arten (Stand 14.08.2025, alle Fundorte von Ahyong 2016 und der eigenen Sammelreisen inkludiert). Die rote Linie zeigt die Ausdehnung des Zentralplateaus an. Zweifarbige Kreise weisen syntope Vorkommen aus. Kreise mit dicker schwarzer Umrandung weisen Höhlenpopulationen aus. Die Basiskarte wurde bearbeitet und verändert basierend auf der Tasmanian catchment map, Tasmanian Government, Department of Primary Industries, Parks, Water & Environment, 13.09.2016.

1.2.3 Ökologie

Adulte Tiere der Gattung *Anaspides* können eine Gesamtlänge (Spitze des Rostrums bis Telson-Spitze) von bis zu 5 cm und ein Alter von vier bis fünf Jahren erreichen. Sie gelten als omnivor und ernähren sich von Algen, Detritus, Kaulquappen, Anneliden und Insektenlarven. Hierbei sind sie in der Lage, Beutetiere zu ergreifen, die ähnliche oder sogar größer als sie selbst sind (Swain & Reid, 1983). Zudem wurde beobachtet, dass sie zur Wasseroberfläche schwimmen, sich dort umdrehen und die Oberfläche nach Nahrungspartikeln absuchen. Das Schwimmen ähnelt jedoch sehr dem normalen Laufverhalten auf dem Grund und unterliegt den selben kinematischen Prinzipien (Grams & Richter, 2021). Dieses Verhalten der Nahrungssuche ist insbesondere in ruhigen Gewässern wie Bergseen und Gebirgstümpeln zu beobachten (Smith, 1908; Hickman, 1936). Es wurde auch mehrfach Kannibalismus dokumentiert (Smith, 1908; Swain & Reid, 1983). Zu den Prädatoren zählen andere wirbellose Tiere, die in Tasmanien endemischen Galaxiiden sowie eingeführte Fischarten wie die Bachforelle (*Salmo trutta*), die Regenbogenforelle (*Oncorhynchus mykiss*) und der Bachsaibling (*Salvelinus fontinalis*). Nichtsdestotrotz gibt es sympatrische Vorkommen von *Anaspides*, Galaxiiden und Forellen (Williams, 1965a; Swain & Reid, 1983; O'Brien, 1990) sowie den Nachweis von *Anaspides*-Resten aus Bachsaiblings und Forellenmägen. Generell lässt sich jedoch ein überwiegendes Fehlen von *Anaspides* in Fisch besiedelten Gewässern feststellen (O'Brien, 1990). Bis zum Jahre 2022 konnte die Paarung (Spermatophorenübertragung) bei *Anaspides* nicht direkt beobachtet werden. Bekannt war lediglich, dass die Männchen Spermatophoren produzieren und diese mittels des Petasma in die Spermatheka (Spermien-Speicherorgan an den achten Thorakopoden) der Weibchen übertragen. Uns gelang es jedoch erste Aufnahmen der Paarung zu machen, bei denen zu sehen ist, dass sich das Männchen tatsächlich mit den „clasping spines" am Kopf des Weibchens festhält (Abb. 4).



Abbildung 4: Paarung bei *Anaspides richardsoni* im Robert Tarn. Das Männchen (oben) klammert sich mit Hilfe der „clasping spines" am Weibchen (unten) fest. Foto: Markus Grams

Die Weibchen legen wenige, relativ große Eier ab und befestigen diese einzeln unter Rinde, an Algenmatten, Wasserpflanzen oder Steinen (Smith, 1908; Hickman, 1936). *Anaspides* besitzt keine Larvenform und die juvenilen Tiere ähneln nach dem Schlupf weitgehend den adulten Tieren (Hickman, 1936). Die Eiablage erfolgt ganzjährig, mit einem Maximum zwischen Oktober und November. Eier, welche im Frühling und Sommer gelegt werden, schlüpfen nach 32–35 Tagen, während Eier die im Herbst oder Winter abgelegt werden, zunächst in einem frühen Zellstadium verharren und ihre weitere Entwicklung erst im darauffolgenden Frühling beginnen (Hickman, 1936). Bemerkenswert ist, dass *Anaspides* im Gegensatz zu anderen Malacostraca einen nach vorne oder oben gerichteten caridoiden Fluchtreflex zeigt (Smith, 1908; Grams & Richter, 2021). Darüber hinaus sind sie in der Lage, mehrere Tage außerhalb des Wassers zu überleben und sich über kurze Distanzen an Land fortzubewegen (Swain & Reid, 1983). *Paranaspides* ist im Vergleich zu *Anaspides* deutlich kleiner (max. 16 mm bei *P. williamsi*, max. 25 mm bei *P. lacustris*). Im Gegensatz zur hauptsächlich benthischen Lebensweise von *Anaspides,* weißt *Paranaspides* einen eher benthisch-pelagischen Lebensstil auf. Die Ernährung erfolgt vorwiegend durch Filtration, ergänzt durch die Aufnahme von Detritus, Algen, Pilzhyphen, Wasserpflanzen und Diatomeen (Manton, 1930; Williams, 1965a). *Paranaspides* weist einen univoltinen Lebenszyklus auf und erreicht ein Alter von bis zu 18 Monaten.

Über die Ökologie von *Allanaspides* ist bisher wenig bekannt. Sie weisen, genau wie *Paranaspides,* einen univoltinen Lebenszyklus auf. Die Paarungszeit erstreckt sich über einen längeren Zeitraum von Spätherbst bis Frühsommer, während der Schlupf der Jungtiere von Hochsommer bis Frühling erfolgt.

1.2.4 Klima, Geomorphologie und Höhlen Tasmaniens

Tasmanien zeichnet sich durch ein kühles, maritimes und gemäßigtes Klima aus, mit abnehmenden Niederschlägen und steigenden Temperaturen von West nach Ost (O'Brien, 1990; Tyler, 1992). Die heutigen klimatischen Bedingungen, sowie die Geomorphologie wurde maßgeblich durch pleistozäne Klimaveränderungen und insbesondere die damit einhergehenden Vergletscherungen der Tasmanischen Hochebenen und Bergketten geprägt. Tasmanien gehört zu den wenigen Regionen der Südhalbkugel, die während des Pleistozäns eine starke Vergletscherung aufwiesen. Die maximale Eisausdehnung dieser Periode wird in das frühe Pleistozän datiert (1.5–2.5 mya), wobei es keine exakte Datierung für dieses Ereignis

gibt. Barbetti und Colhoun (1988) konnten zeigen, dass aufgrund der umgekehrten magnetischen Polarität in geschichteten Tonablagerungen von Seen, diese Vergletscherungen älter als 0,785 Millionen Jahre sind. Die Gletscher dieser ersten großen Vergletscherung hatten eine Dicke von 500–800 m und bedeckten eine Fläche von 7000 km², insbesondere auf dem Zentralplateau und den westlichen Gebirgszügen (Kiernan, 1990; Augustinus, 1999; Coulhoun et al., 2010). Bis heute konnten mindestens zehn individuelle Eisvorstöße im Verlauf des Pleistozäns nachgewiesen werden. Allgemein gilt, dass die späteren Vergletscherungen weniger ausgedehnt waren. Das letzte glaziale Maximum (LGM) ereignete sich vor etwa 22.000 bis 17.000 Jahren im marinen Isotopenstadium 2 (MIS 2). Während dieses Zeitraums bedeckte Eis noch eine Fläche von rund 1100 km² und erreichte eine Dicke von bis zu 250 m. Die am stärksten betroffenen Regionen dieser Vergletscherung waren wieder das Zentralplateau und die westlichen Gebirgszüge, aber auch mehrere Gebirgsregionen im Süden und Südwesten Tasmaniens waren von Vergletscherungen betroffen. Die Temperaturen lagen während dieser letzten Periode der Vergletscherungen um etwa 6–10 °C unter den heutigen Werten, und die Schneegrenze war um rund 1000–1500 m abgesenkt.

Des Weiteren zeichnet sich Tasmanien auch dadurch aus, dass es über 300 Karstgebiete mit über 4000 dokumentierten Höhlen gibt, welche sich über eine Gesamtfläche von etwa 400.000 ha erstrecken (Clark, 1999; Sharples, 2002). Einige diese unterirdischen Höhlensysteme erstrecken sich dabei über mehr als 35 km und Tasmanien hat mit Delta Variant die tiefste Höhle Australiens. Obwohl die meisten tiefen unterirdischen Höhlen und Gänge bereits im späten Mesozoikum und Känozoikum anfingen sich heraus zu bilden (der älteste verlässliche Nachweis für eine Höhlenbildung in Tasmanien stammt aus dem mittleren Devon, Coulhoun et al., 2010), hatten die pleistozänen Vereisungen erhebliche Auswirkungen auf die Karstgebiete der Insel und spielten eine zentrale Rolle bei der Entstehung und Entwicklung von Höhlensystemen (Jennings & Sweeting, 1959; Kiernan, 2005). Insbesondere Schmelzwasserströme und glaziale Sedimente sorgten immer wieder für verschiedenste Modifikation von Höhlengängen und Wasserwegen (z.B. Verschlüsse und Öffnungen von Höhlenein- und ausgängen sowie niedrigerer Ebenen).

1.2.5 Höhlenbesiedlung

Die Besiedlung von extrem Habitaten wie Höhlen zählen zu den spannendsten Fragestellungen der Evolutionsbiologie, mit welchen sich bereits Charles Darwin beschäftigte (Darwin, 1859). Permanente Dunkelheit und limitierte Nahrungsverfügbarkeit zählen zu den vielen Herausforderungen für höhlenbewohnende Organismen. Phylogenetische Systematik und Phylogeographie können die Grundlage bilden, um Höhlenbesiedlungsprozesse zu verstehen und herauszufinden, ob Besiedlungen vielfach unabhängig stattgefunden haben oder einmalige Ereignisse waren, gefolgt von unterirdischer Ausbreitung. Diese Informationen sind essenziell, um zu klären, ob spezifische Merkmale der Höhlenanpassung einmalig entstanden oder mehrfach konvergent entwickelt wurden (Juan et al., 2010). Verschiedene Modellsysteme wurden hierbei bereits bei den Crustacea untersucht, wie zum Beispiel die Atyidae (von Rintelen et al. 2012) oder Flusskrebse aus dem Süden der USA mit vielen sehr alten Höhleneinwanderungen (Buhay & Crandall, 2005; Stern et al., 2017). Die wohl am besten untersuchten Modellsysteme für Höhlenbesiedlung und subterrane Ausbreitungsprozesse sind jedoch *Asselus aquaticus* und seine Verwandten, sowie die Amphipoden Gattung *Niphargus* und die Art *Gammarus minus*. Während es sich bei *Asselus aquaticus* und seiner Verwandten um mehrfach unabhängige, jedoch sehr junge, Höhlenbesiedlung handelt (Verovnik & Konec, 2019), finden wir bei *Niphargus* eine einmalige Höhlenbesiedlung mit subterraner Radiation (Borko et al., 2022). Auch für mehrere Arten der Gattung *Anaspides* konnten Richter et al. (2018) bereits unabhängige Kolonisierungsvorgänge nachweisen.

Typische troglomorphe Merkmale bei Crustaceen umfassen den Verlust der Pigmentierung, die Reduktion der Augen und optischen Neuropile sowie die Verlängerung der sensorischen Anhänge, insbesondere der ersten und zweiten Antenne. Hierbei werden zwei Klassen solcher Merkmale unterschieden, „regressive“ und „konstruktive“ Merkmale. Während die Verlängerung der Antennen oder der Zugewinn von olfaktorischen und Mechanorezeptoren als echte Anpassungen (konstruktive Merkmale) gelten, entstehen regressive Merkmale häufig durch neutrale Evolution und nicht durch Selektion, wobei energetische oder pleiotrope Effekte ebenfalls eine Rolle spielen können (Borowski, 2010).

Für rezente Höhlenbesiedlungsereignisse wurden zwei unterschiedliche Modelle der Artbildung vorgeschlagen. Für gemäßigte Zonen hypothetisiert die „climatic relict hypothesis“ (CRH), dass Höhlen infolge klimatischer Veränderungen (z. B. Vergletscherung, Desertifikation) passiv als Refugien besiedelt wurden (Peck & Finston, 1993; Holsinger, 2000;

Rivera et al., 2002). Während der Existenz in der Höhle treten neutrale oder „regressive“ Mutationen auf (z. B. Verlust von Pigmentierung, Reduktion der Augen), die möglicherweise, jedoch nicht zwingend, mit adaptiven Veränderungen im Zusammenhang mit reproduktiver Isolation einhergehen. Die ursprüngliche epigäische Population stirbt entweder aus oder bleibt nur noch in geographisch weit entfernten Gebieten erhalten, was dem klassischen Modell der allopatrischen Artbildung entspricht. Dem gegenüber steht die „adaptive shift hypothesis“ (ASH), die von einer aktiven Besiedlung der Höhlen durch Oberflächenorganismen ausgeht. Die reproduktive Isolation erfolgt hierbei in Parapatrie als Folge unterschiedlicher ökologischer Anpassung (Peck & Finston, 1993; Desutter-Grandcolas & Grandcolas, 1996). Da auch im Rahmen der CRH Anpassungen eine Rolle spielen können, liegt der entscheidende Unterschied nicht in der Anpassung selbst, sondern im Fehlen (CRH) beziehungsweise dem Vorhandensein (ASH) von Genfluss während der Divergenzphase (Niemiller et al., 2008).

1.3 Ziele der Dissertation

Die Anaspidacea zählen zu den am wenigsten erforschten Taxa innerhalb der Höheren Krebse (Malacostraca). Erst durch die Arbeiten von Ahyong (2015, 2016), in denen er fünf neue Arten der Gattung *Anaspides* beschrieb, sowie durch die anschließenden umfassenderen molekulargenetischen Untersuchungen von Richter et al. (2018) an der Familie Anaspidesidae rückte dieses Taxon wieder stärker in den wissenschaftlichen Fokus. Ahyong (2016) zeigte, dass die meisten Arten ein sehr begrenztes Verbreitungsgebiet aufweisen. Bei den beiden verbliebenden, weiter verbreiteten Arten konnte er eine größere morphologische Variabilität zwischen den Regionen feststellen, was bereits zu ersten Spekulationen über weitere, bislang unbeschriebene *Anaspides*-Arten führte. Darüber hinaus beschrieb er zwei obligat höhlenbewohnende Arten und belegte, dass einige Arten sowohl epigäische als auch subterrane Populationen besitzen. Bei den Höhlenpopulationen konnten unterschiedliche Grade der Höhlenanpassung aufgezeigt werden.

Die Studie von Richter et al. (2018) bestätigte molekulargenetisch viele der zuvor beschriebenen Arten der Anaspidesidae. Zudem identifizierten die Autoren zwei Artkomplexe mit bislang ungeklärten phylogenetischen Verwandtschaftsverhältnissen sowie eine erhöhte genetische Variabilität innerhalb einiger weiterer Arten. Ihre Ergebnisse deuten außerdem darauf hin, dass es innerhalb der Gattung *Anaspides* mehrfach zu unabhängigen Einwanderungen in Höhlen gekommen sein muss (mehr als vier Ereignisse), die vermutlich im

Zusammenhang mit den pleistozänen Vergletscherungen stehen. Die vorliegende Arbeit verfolgt das Ziel, die durch die Arbeiten von Ahyong (2016) und Richter et al. (2018) aufgeworfenen Fragen zu klären und weitere Einblicke in die Systematik, Taxonomie, Phylogeographie, Artbildung und Populationsgenetik der Tasmanischen Berggarnelen der Gattung *Anaspides* zu geben. Es sollen folgende Fragestellungen beantwortet werden:

I Wie sind die phylogenetischen Beziehungen innerhalb der Familie der Anaspidesidae? Bildet *Paranaspides* die Schwestergruppe zu *Anaspides* oder steht sie innerhalb von *Anaspides*?

II Inwieweit lassen sich die morphologisch beschriebenen Arten durch molekulargenetische Daten stützen, insbesondere im Fall von *A. eberhardi* und *A. spinulae*? Gibt es genetische und/oder morphologische Hinweise auf weitere bisher unbeschriebene Arten? Wo verlaufen die genauen Verbreitungsgrenzen der von Ahyong (2015, 2016) neu beschriebenen Taxa, und existieren darüber hinaus syntope Vorkommen oder zusätzliche Höhlenpopulationen?

III Welche Auswirkungen hatten die pleistozänen Vergletscherungen auf die heutige Verbreitung der Arten beziehungsweise Populationen? Wo befanden sich die glazialen Refugien, und wie erfolgte die postglaziale Wiederbesiedlung des tasmanischen Zentralplateaus?

IV Wie hoch ist die Ausbreitungsfähigkeit von *Anaspides*? In welchem räumlichen Maßstab lassen sich Populationen differenzieren und wie stark sind diese genetisch voneinander isoliert?

V Wie viele unabhängige Besiedlungsereignisse von Höhlen lassen sich bei *Anaspides* rekonstruieren und zu welchem Zeitpunkt fanden sie statt? Welches Besiedlungsmodell („climatic relict hypothesis“ vs. „adaptive shift hypothesis“) erklärt diese Höhleneinwanderungen am plausibelsten? Wie stark sind die Höhlenpopulationen und Höhlen miteinander verbunden?

1.4 Ergebnisse und Diskussion

1.4.1 Systematik der Anaspidesidae

Dieser Abschnitt ist eine Synopsis des Kapitels 4: Höpel, C. G., Yeo, D., Ahyong, S. T., Meier, R., & Richter, S. (2023). First mitochondrial genomes of Anaspidacea (Malacostraca, Crustacea) and the phylogenetic relationships of mountain shrimps (*Anaspides* Thomson, 1894) and their relatives within Anaspidesidae. Journal of Crustacean Biology, 43(2), ruad028.

Obwohl die molekulargenetischen Untersuchungen von Richter et al. (2018) einen Großteil der morphologisch beschriebenen Arten bestätigen konnten, warfen sie zugleich auch weitere Fragen auf, insbesondere bezüglich der phylogenetischen Verwandtschaftsverhältnisse der Arten und Artengruppen zueinander. So wurde *Paranaspides* je nach analysiertem Gen (COI, 16S, 28S), mal als Schwestergruppe zu *Anaspides* oder aber innerhalb von *Anaspides* gefunden. *Anaspides tasmaniae* wurde entweder als Schwestergruppe zur „Central Clade“ (Artkomplex benannt nach Richter et al., 2018, umfasst *A. richardsoni* + *A. eberhardi* + *A. spinulae*) oder zu der Central Clade + *A. swaini* gefunden. Die Central Clade wurde in COI als Schwestergruppe aller übrigen *Anaspides*-Arten identifiziert während in 16S die *A. jarmani*/*A. clarkei*-Artengruppe die Schwestergruppe zu allen anderen war. Außerdem war *A. eberhardi* nur in 16S vertreten und *A. driesseni* (Höpel et al., 2023a) fehlte gänzlich. *Anaspides clarkei* und *A. jarmani* waren je nach Gen paraphyletisch zueinander.

Zur Klärung der Verwandtschaftsverhältnisse innerhalb der Anaspidesidae und insbesondere innerhalb von *Anaspides* wurden die vollständigen oder fast vollständigen mitochondrialen Genome mittels Genome Skimming von 24 Individuen allen bekannten Arten rekonstruiert und annotiert. Zusätzlich wurden die vollständigen 18S und 28S Sequenzen aller 24 Individuen mittels Sanger-Sequenzierung generiert. Es wurde ein kombinierter Datensatz der proteinkodierenden Gene des Mitogenoms, 16S, 12S, 28S und 18S genutzt, um mittels Bayesian Inference (BI), Maximum Likelihood (ML) und Maximum Parsimony (MP) phylogenetische Verwandtschaftsdiagramme zu berechnen.

Die hier rekonstruierten Mitogenome stellen die ersten vollständigen mitochondrialen Genome der Anaspidacea dar. Es wurden 20 vollständige und 4 fast vollständige Mitogenome rekonstruiert und annotiert. Bei allen vollständig assemblierten Mitogenomen konnten die, für die Metazoa typischen, 13 proteincodierenden Gene, die 2 RNA-Gene, sowie die 22 Transfer-RNAs gefunden werden. Die Länge der mitochondriellen Genome schwankt hierbei

zwischen 15213–17962 Basenpaaren. Auffällig ist der sehr hohe A+T Gehalt in allen vollständig rekonstruierten Mitogenomen, der in einigen Fällen bis zu 75.5 % betrug. Es konnten darüber hinaus fünf verschieden Genanordnungen auf dem Mitogenom festgestellt werden und das Grundmuster der Anaspidacea rekonstruiert werden, welches sich in einer Stelle vom Grundmuster der Tetraconata unterscheidet. Dieser Unterschied besteht in der Translokation und dem Reversal (Umkehr der Leserichtung) des tRNA-L1 Gens. Des Weiteren haben die beiden Arten von *Paranaspides* eine weitere Translokation, genau wie die beiden Arten von *Allanaspides*. *Allanaspides hickmani* weist darüber hinaus noch eine Verdopplung des tRNA-L1 Genes auf. In *Micraspides* sp., welche als Außengruppe genutzt wurde, konnten sogar vier Versionen (Verdopplungen) des tRNA-L2 Genes festgestellt werden. *Micraspides* gehört zur Familie den Koonungidae innerhalb der Anaspidacea, die allgemein hin als Schwestergruppe der Anaspidesidae angesehen werden (Schminke, 1975; Schramm & Hessler, 1984; Grosso & Peralta, 2002).

Die aus den Analysen resultierenden phylogenetischen Verwandtschaftsdiagramme (BI, ML, MP) unterscheiden sich nur marginal voneinander (unterschiedliche Position eines Individuums in ML). So ist *Allanaspides*, wie auch bei Richter et al. (2018) Schwestergruppe zu allen übrigen Vertretern der Anaspidesidae. Auch die Position von *Paranaspides* kann abschließend geklärt werden. So ist *Paranaspides* Schwestergruppe zu *Anaspides*. Innerhalb von *Anaspides* ist die Artengruppe um *A. clarkei* und *A. jarmani* Schwestergruppe der übrigen Arten. Hierbei brachte die Analyse eine paraphyletische Art *A. jarmani* in Bezug auf *A. clarkei* hervor. Zukünftige Studien, insbesondere mittels populationsgenetischer Methoden, sind erforderlich um die genauen Verwandtschaftsverhältnisse innerhalb der Gruppe aufzulösen. Der nächste Abzweig umfasst die beiden Arten *A. swaini* und *A. driesseni*, welche ein Schwestergruppenverhältnis aufweisen. *Anaspides swaini* wird hierbei repräsentiert von zwei Individuen die zur morphologischen Form 1 nach Ahyong (2016) gehören. Danach folgt *A. tasmaniae* welche Schwestergruppe zur Central Clade (*A. richardsoni*, *A. eberhardi* und *A. spinulae*) + *A. swaini* (Form 2) ist. Höpel et al. (2023b) schlagen ein Hinzufügen von *A. swaini* Form 2 zur Central Clade vor. Innerhalb der Central Clade ist *A. swaini* Form 2 Schwestergruppe zu den übrigen Arten, während *A. spinulae* und *A. eberhardi* innerhalb verschiedener Linien von *A. richardsoni* stehen. Dabei ist *A. eberhardi* am nächsten verwandt zur *A. richardsoni* Linie vom Mt. Field, welches auch die geographisch nächste Population ist, während *A. spinulae* Schwestergruppe zur Linien von *A. richardsoni* welche vom Tributary to

Travellors Rest River ist. Dies ist ebenfalls die geographische dichteste Population. Weitere populationsgenetische Untersuchungen (Kapitel 5, Höpel et al., 2025) waren abschließend in der Lage, die genauen Verwandtschaftsverhältnisse innerhalb der Central Clade sowie den Artstatus der Einzelarten aufzulösen und konzeptualisierten *A. richardsoni* als paraphyletische Art.

Die für das Grundmuster der Anaspidacea apomorphe Translokation des tRNA-L1 genes kann ebenfalls im Grundmuster der Euphausiacea („Krill“) festgestellt werden (basierend auf vier untersuchten Mitogenomen), welches darüber hinaus noch eine weitere Translokation aufweist. Dies liefert einen weiteren Hinweis auf ein mögliches Schwestergruppenverhältnis zwischen Euphausiacea und Anaspidacea, welches durch Schwenter et al. (2018) molekulargenetisch identifiziert wurde. Auch Grams et al. (2023) fanden weitere Hinweise auf ein mögliches Schwestergruppenverhältnis aufgrund verschiedener Merkmale der Laufbeine (Thorakopoden). Diese Merkmale umfassten unter anderem: Übereinstimmungen im Carpus-Propodus Gelenks, der Unterteilungsstruktur der Basis und dem Vorhandensein eines posterioren Sklerits zwischen Basis und Exopoditen.

1.4.2 Taxonomie und Verbreitung von *Anaspides*

Dieser Abschnitt ist in zwei Teile untergliedert, welche zu großen Teilen eine Synopsis der Kapitel 2: Höpel, C. G., Ahyong, S. T., & Richter, S. (2021). Genetic structure and new occurrence records of the iconic Tasmanian mountain shrimp *Anaspides tasmaniae* (Thomson, 1893)(Anaspidesidae: Anaspidacea) reveal relictual distribution in southern Tasmania. Australian Journal of Zoology, 68(1), 45-53 und Kapitel 3: Höpel, C. G., Richter, S., & Ahyong, S. T. (2023). A new species of Tasmanian mountain shrimp, *Anaspides driesseni* sp. nov. (Malacostraca, Anaspidacea, Anaspidesidae). Records of the Australian Museum, 75(1), 25-43 darstellen, erweitert durch bisher unveröffentlichte Daten.

1.4.2.1 *Anaspides tasmaniae*

Anaspides tasmaniae war die erste beschriebene Art der Anaspidacea (Thomson, 1893) und galt lange Zeit als weitverbreitet in ganz Tasmanien. Die Typuslokalität ist der Mt. Wellington, an dessen Fuß die Tasmanischen Hauptstadt Hobart liegt. Nach der Revision von Ahyong (2016) und der Neubeschreibung von fünf Arten (Ahyong 2015, 2016) schrumpfte das Verbreitungsgebiet von *A. tasmaniae* auf wenige Orte östlich und südöstlich des Mt. Wellington (Abb. 3) zusammen. Damit hatte *A. tasmaniae* eines der kleinsten

Verbreitungsgebiete aller *Anaspides*-Arten. Darüber hinaus gilt *A. tasmaniae* an einigen der alten Fundorte bereits als verschwunden, vermutlich bedingt durch das größer werdende Stadtgebiet Hobarts. Die übrigen Orte verteilen sich auf drei Wassereinzugsgebiete, während die übrigen Wassereinzugsgebiete um den Mt. Wellington von *A. driesseni* (ehemals *A. swaini* Form 3) besiedelt werden (Höpel et al., 2023a). Obwohl der Wellington Park zwar als Schutzgebiet gilt, hat er dennoch keinen Nationalpark-Status und der diskutierte Bau einer Seilbahn als Touristenattraktion auf die Spitze des Mt. Wellington könnte das Verbreitungsgebiet noch weiter verkleinern.

Um das genaue Verbreitungsgebiet sowie die Populationsstruktur von *A. tasmaniae* zu bestimmen, wurden extensive Suchen in und auf dem Mt. Wellington im Rahmen von zwei Forschungsreisen in 2017 und 2019 (sowie später nochmals in 2024 und 2025) durchgeführt und mittels Sanger-Sequenzierung die Gene COI, 16S und 28S untersucht (Höpel et al. 2021). Später wurden dann auch ddRAD-Methoden angewendet (unveröffentlichte Daten). Alle Tiere wurden morphologisch untersucht. Dabei unterscheidet sich *A. tasmaniae* von anderen Vertretern der Gattung *Anaspides* durch die Kombination von zwei „clasping spines“, dem verlängerten und gleichmäßig abgerundeten Telson mit einer gleichmäßigen Reihe von kleinen Dornen, dem Vorhandensein von vier Paaren pleopodaler Endopoden und der Form des Telsons. Insbesondere die Form des Telsons ist hierbei einzigartig im Vergleich zu allen übrigen *Anaspides*-Arten und erwies sich als verlässliches Merkmal zur Artabgrenzung.

Trotz des Fundes einiger neuer Standorte an der Ost und Südost Seite des Mt. Wellington während unserer Forschungsreisen bleibt das Verbreitungsgebiet von *Anaspides tasmaniae* weiterhin beschränkt auf die drei bekannten Wassersysteme. Darüber hinaus bestätigte eine intensive Suche auf dem Plateau des Mt. Wellington das Fehlen von *A. tasmaniae*, sowie auch das von *A. driesseni*. Während der Forschungsreisen 2024 und 2025 konnte sogar eine potentiell neue Art in zwei der drei von *A. tasmaniae* besiedelten Wassersystemen gefunden werden. Diese kommt syntop mit *A. tasmaniae* an einem Fundort vor (Abb. 3). Erste genetische Untersuchungen zeigen, dass diese Art Schwestergruppe von *A. swaini* ist (unveröffentlicht).

Am bemerkenswertesten war jedoch, dass während der Sammlungsreise nach Tasmanien 2017 es uns erstmals, und sehr überraschend, gelang *A. tasmaniae* außerhalb des bekannten Verbreitungsgebietes nachzuweisen. Es wurden Populationen 50 km entfernt vom Mt. Wellington im und um den Mt. Field Nationalpark in Zentraltasmanien entdeckt. Weitere

Reisen in 2019, 2022 und 2023 erweiterten die Anzahl der von *Anaspides* besiedelten Standorte im Mt. Field Nationalpark. So konnten *A. tasmaniae* bis heute an 13 Standorten in diesem Gebiet nachgewiesen werden (Kapitel 2, Abb. 1, 3 + unveröffentlichte Daten). Die meisten dieser Standorte sind dabei kalte Bergbäche in Höhen zwischen 500 - 650 m, welche vom Plateau des Mt. Field herabfließen. Gesammelt wurde *A. tasmaniae* hierbei vor allem kurz (100-200 m) vor oder direkt in Höhleneingängen. Diese Höhlen gehören zum Junee-Florentine Karst an den Hängen des Mt. Field. Hierbei wurde *A. tasmaniae* auch an zwei Stellen syntop mit *A. swaini* gefunden. Drei weitere Fundorte waren kalte Bäche im Tiefland (300–350 m). Des Weiteren gelang uns auch der Erstnachweis von zwei Höhlenpopulationen von *A. tasmaniae* (Risby Basin Cave, Abb. 5 und Tom Smith Cave). Tiere dieser beiden Populationen können als „leicht“ höhlenangepasst (stärkere Depigmentierung, leichte Reduktion der Augen, leichte Verlängerung der Antennen) angesehen werden.



Abbildung 5: Adultes *Anaspides tasmaniae* Weibchen aus der Risby Basin Cave.

Die genetischen Daten der Sanger Sequenzierung ergeben in COI ebenfalls eine klare Trennung von den Populationen des Mt. Wellington und des Mt. Field mit mindestens sechs Mutationen Unterschied, was auf eine natürliche Verbreitung von *A. tasmaniae* hindeutet und eine Translokation durch den Menschen unwahrscheinlich macht. Die wahrscheinlichste Erklärung ist das *A. tasmaniae* während glazialer Zeiten einen größeren Bereich besiedelte und dies nacheiszeitliche Refugien sind. Obwohl 50 km zwischen dem Mt. Wellington und dem Mt. Field liegen gehören alle Fundorte von *A. tasmaniae* zur selben großen Wassereinzugsgebiet, dem Derwent River Einzugsgebiet.

1.4.2.2 *Anaspides driesseni* Höpel et al., 2023

Bereits 2016 beschrieb Ahyong in seiner Revision der Gattung *Anaspides* drei morphologische Formen innerhalb von *A. swaini*, die jeweils eine geographische Korrelation zu verschiedenen Regionen Tasmaniens aufwiesen. Form 1 besitzt ein vorwiegend südwestliches Verbreitungsgebiet, das sich von der Arthurs Range über die Frankland Range, den Mt. Anne und die Snowy Mountains bis zum Mt. Field erstreckt. Diese Form war auch Gegenstand der Untersuchungen von Richter et al. (2018), die hohe intraspezifische genetische Distanzen zwischen Individuen feststellten die in Flüssen entlang der Müller Road gesammelt wurden. Auch hier zeigte sich eine weitgehende Übereinstimmung zwischen Fundort und genetischer Linie (COI), wenngleich es einzelne Ausnahmen gab. Form 2 weist ein nördliches Verbreitungsgebiet jenseits des Lake Gordon auf. Es erstreckt sich von der Westseite des Lake St. Clair südwärts bis zu den Wentworth Hills und dem Frenchman Cap. Diese Form ist auch in Höhlen des Nicholls-Range-Karstsystems sowie des Franklin-River-Karstsystems südlich des Frenchman Cap zu finden, wo sie offenbar von oberirdischen Populationen isoliert ist (Eberhard et al., 1992). Form 3 besitzt eine östliche bis südöstliche Verbreitung, die sich von der Wellington Range im Osten über die Snowy Mountains bis zur Picton Range im Südosten erstreckt.

Um zu klären, ob es sich bei den von Ahyong (2016) beschriebenen morphologischen Formen um eigenständige Arten oder lediglich um populationsspezifische Unterschiede handelt, wurden die im Australian Museum vorhandenen Exemplare durch während zweier Forschungsreisen in den Jahren 2017 und 2019 gesammelte Tiere von *A. swaini* ergänzt und sowohl morphologisch als auch molekulargenetisch untersucht. Dabei wurden die Gene COI, 16S und 28S mittels Sanger-Sequenzierung analysiert.

Diese Untersuchungen führten zur Neubeschreibung einer neuen Art *Anaspides driesseni* Höpel et al., 2023, welche der morphologischen Form 3 entspricht. Die wichtigsten Unterscheidungsmerkmale sind die Kombination von zwei kurzen „clasping spines“, der Form des Telson (z.B. breiter als lang), das Vorhandensein von vier Paaren pleopodaler Endopoditen, der Form und Beborstung des inneren Flagellums der 1. Antenne sowie das Erreichen der Geschlechtsreife bei durchschnittlich 26–28 mm Körpergröße. Insbesondere letzteres ist als bemerkenswert zu betrachten da *A. driesseni* die einzige Art mit diesem Merkmal ist, während die meistens anderen *Anaspides*-Arten die Geschlechtsreife bei durchschnittlich 18–23 mm erreichen. Auch molekulargenetisch konnte *A. driesseni* eindeutig

als eigenständige Art klassifiziert werden, mit signifikanten genetischen Unterschieden in allen untersuchten Genen (8.4–14.2 % pairwise distance in COI zu allen übrigen *Anaspides*-Arten). Genau wie bei *A. tasmaniae* zeig auch *A. driesseni* ein disjunktes Verbreitungsgebiet mit einer etwa 25 km breiten Lücke zwischen der Wellington Range und den Snowy Mountains auf. Genau wie bei *A. tasmaniae* schließen wir auch hier eine anthropogene Translokation aus und postulieren ein ehemals deutlich größeres Verbreitungsgebiet mit Tieflandpopulationen während glazialer Perioden. Darüber hinaus kommt *A. driesseni* in zwei großen Wassereinzugsgebieten vor (Derwent River und Huon River) und unsere Daten deuten auf ein mehrfaches Überschreiten der Wasserscheiden zwischen den beiden Systemen hin. Die plausibelste Erklärung scheint hierbei ein Überqueren der Wasserscheiden über Bergplateaus, welche temporär durch Überschwemmungen, sumpfige Gebiete, Schnee und Schneeschmelze verbunden sein können, zu sein. Weitere Sammlungsreisen in 2022, 2023, 2024 und 2025 bestätigten das eingeschränkte Verbreitungsgebiet von *A. driesseni* in Südosttasmanien und lieferten Hinweise auf eine weitere unbeschriebene Art welche sich von den Hartz Mountains über den Mount Bobs bis hin zur Picton Range erstreckt (bisher noch als *A. swaini* beschrieben von diesen Fundorten) (Abb. 3). Dies führte zu einer erneuten morphologischen Analyse der südlichsten Populationen von *A. driesseni*, die erste Hinweise darauf liefern, dass es sich bei einigen dieser Populationen um die besagte neue Art handeln könnte, möglicherweise mit syntopen Vorkommen zusammen mit *A. driesseni* (unveröffentlicht).

In *Anaspides swaini* Form 1 hingegen konnten keine artspezifischen Unterschiede zwischen den Fundorten und COI-Linien (teilweise mit über 10 % Unterschied in der pairwise distance) gefunden werden, weshalb sie weiterhin als *A. swaini sensu stricto* geführt werden. Dies wurde auch durch ddRAD-Analysen an Tieren, welche diese hohen genetischen Distanzen aufweisen, aus sechs Flüssen entlang der Müller Road bestätigt. Dabei zeigte sich eine klare Auftrennung der Populationen nach Gewässersystem, jedoch nicht nach COI-Linien.

1.4.3 Artbildung, Phylogeographie und *Anaspides richardsoni* als paraphyletische Art

Dieser Abschnitt ist eine Synopsis des Kapitels 5, Höpel, C. G., Ahyong, S. T., Kapun, M., Schwentner, M., & Richter, S. (2025). Phylogeography of the *Anaspides richardsoni* species clade (Anaspidacea, Anaspidesidae): glaciation and recolonization of the Tasmanian Central

Plateau and the question of paraphyletic species. Cladistics. (https://doi.org/10.1111/cla.70005)

Als Williams (1965a) die zweite Art der Gattung *Anaspides*, *A. spinulae*, beschrieb, diskutierte er bereits, ob es sich hierbei nicht auch um eine Ökomorphe von *A. tasmaniae* handeln könnte, entschied sich jedoch letztlich dafür, sie als eigenständige Art zu beschreiben. Auch O'Brien (1990) griff diese Fragestellung auf und zeigte, dass es auf dem Zentralplateau morphologische Formen gab, zu diesem Zeitpunkt noch als *A. tasmaniae* geltend, welche ebenfalls eine starke Bedornung aufwiesen, ähnlich der von *A. spinulae*. Ahyong (2016) sprach sich in seiner Revision der Gattung *Anaspides* ebenfalls für die Eigenständigkeit von *A. spinulae* als Art aus und lieferte weitere wichtige Merkmale zur Artabgrenzung. So besitzt *A. spinulae* zwei „clasping spines", während *A. richardsoni* genau wie alle stärker bedornte Formen von *A. richardsoni* nur einen „clasping spine" aufweisen. Darüber hinaus erreicht *A. spinulae* die Geschlechtsreife bei deutlich geringerer Körpergröße. Die molekulargenetischen Untersuchungen von Richter et al. (2018) zeigten erstmals, dass *A. richardsoni*, *A. spinulae* und die obligat subterran lebende Art *A. eberhardi* einen Artkomplex bilden. Dieser wurde aufgrund des Hauptvorkommens der drei Arten auf dem Zentralplateau als „Central Clade" bezeichnet. Diese Region ist zugleich diejenige Tasmaniens, die am stärksten von pleistozänen Vergletscherungen betroffen war. Ahyong (2016) hypothetisierte, dass diese Vergletscherungen eine Rolle in der Artbildung gespielt haben könnten, etwa bei *A. spinulae*, die den vollständig vergletscherten Lake St. Clair nach der Eiszeit entweder neu besiedelt oder in tieferen Wasserschichten überdauert haben musste. Auch die Ausbildung verschiedener morphologischer Formen, etwa bei *A. swaini* oder *A. richardsoni*, könnte durch diese klimatischen Veränderungen beeinflusst worden sein. Richter et al. (2018) brachten zudem die mehrfachen Höhleneinwanderungen von *Anaspides* mit den geomorphologischen Veränderungen durch die Vergletscherungen der Karstsysteme in Verbindung. Im Jahr 2023 erweiterten Höpel et al., basierend auf phylogenetischen Analysen vollständiger Mitogenome, die Central Clade um *A. swaini* Form 2 und spekulierten, dass es sich hierbei um eine eigenständige Art handeln könnte. Während der Forschungsreisen in den Jahren 2022, 2023, 2024 und 2025 wurden darüber hinaus zwei weitere potenziell neue Arten entdeckt, die im Mt. Field Nationalpark und dem angrenzenden Florentine Valley vorkommen. Erste morphologische Untersuchungen legen nahe, dass auch diese beiden Arten eng mit der Central Clade verwandt sind oder ihr sogar angehören.

Zur Klärung der genauen Verhältnisse innerhalb der Central Clade sowie zur Bestimmung des Artstatus der einzelnen Linien wurden neben der Untersuchung einzelner Genabschnitte mittels Sanger-Sequenzierung (COI, 16S, 28S) auch ddRAD-Analysen durchgeführt, um ein detailliertes Bild auf Populationsebene zu erhalten. Der Vorteil von ddRAD gegenüber der Analyse einzelner Gene liegt darin, dass nicht nur einzelne Genabschnitte mit wenigen Mutationen, sondern tausende Loci mit zehntausenden SNPs (single nucleotide polymorphisms) verglichen werden können. Das angewandte ddRAD-Protokoll orientierte sich größtenteils an Schwentner und Lörz (2021), wobei kleinere Modifikationen des Workflows vorgenommen wurden (siehe Kapitel 5, Höpel et al., 2025). Die daraus resultierenden Datensätze wurden mittels verschiedener phylogenetischer Methoden analysiert. Zur Untersuchung der Verwandtschaftsverhältnisse zwischen Arten, Linien und Populationen wurden phylogenetische Bäume mittels Maximum Likelihood (Programm: IQTree 2), Maximum Parsimony (Programm: TNT v1.6) sowie ungewurzelte phylogenetische Netzwerke (Programm: SplitsTree) erstellt. Zur weiteren Analyse der Populationsstruktur, Abstammungsgemeinschaften und genetischen Austauschprozessen wurden fineRADstructure, PCA (principial component analysis) und STRUCTURE-Analysen durchgeführt. Historischer Genfluss und Introgression wurden zusätzlich mit D-Statistiken (ABBA-BABA-Test mittels Dsuite) sowie Treemix untersucht.

Die für diese Studie analysierten Individuen wurden vorab morphologisch untersuch und konnten eindeutig den folgenden Arten zugeordnet: *A. richardsoni*, *A. spinulae*, *A. eberhardi*, *Anaspides* sp. nov. 1, *Anaspides* sp. nov. 2 und *Anaspides* sp. nov. 3. Letztere entspricht *A. swaini* Form 2 aus Ahyong (2016). Ausschlaggebend für die Zuordnung waren insbesondere Anzahl, Form und Position der „clasping spines“, die Form und Bedornung des Telsons, die Bedornung der Pleurite sowie die Körpergröße beim Erreichen der Geschlechtsreife. So besitzen *A. richardsoni* und *A. eberhardi* jeweils nur einen „clasping spine“ während alle anderen Arten zwei „clasping spines“ haben. Bei *Anaspides* sp. nov. 1 sind diese in einer vertikalen Achse angeordnet, während sie bei den anderen Arten in einer horizontalen stehen. *Anaspides spinulae* und *Anaspides* sp. nov. 2 werden geschlechtsreif bei deutlich geringerer Körpergröße als die übrigen Arten (13–15 mm gegenüber 18–23 mm bei den anderen Arten). *Anaspides spinulae* und *Anaspides* sp. nov. 2 zeichnen sich darüber hinaus auch durch eine starke Bedornung der Pleurite aus. *Anaspides eberhardi* besitzt ein verlängertes Telson mit wenigen großen Dornen (in der Regel genau acht), während bei *A. spinulae* die Dornen

unterschiedlich groß sind. Bei allen übrigen Arten ist eine gleichmäßige Dornenreihe mit >40 Dornen in adulten Tieren festzustellen, mit den durchschnittlich höchsten Werten bei *A. richardsoni* (normallerweise >50 in adulten Tieren). Basierend auf der Topologie der Verwandtschaftsdiagramme gehen wir davon aus, dass ein einzelner „clasping spine“ den plesiomorphen Zustand darstellt und es innerhalb der Central Clade drei Reversals hin zu zwei „clasping spines“ gegeben hat in *Anaspides* sp. nov. 2 und 3 sowie in *A. spinulae* (siehe Kapitel 5, Abb. 10).

In sämtlichen Analysen zeigt sich eine starke Korrelation zwischen Lokalität und genetischer Linie (Kapitel 5, Abb. 2-5). Besonders deutlich wird dies in der fineRADstructure-Analyse, die zweifelsfrei belegt, dass nahezu jeder Fundort (einige teils nur wenige hundert Meter voneinander entfernt) eine eigenständige, genetisch klar abgrenzbare Population darstellt. Die genetische Übereinstimmung zwischen Individuen desselben Fundorts ist dabei höher als zwischen denen verschiedener Fundorten. Dies unterstreicht das äußerst geringe Ausbreitungspotenzial von *Anaspides* und macht die Gattung zu einem idealen Modellsystem für phylogeographische Studien.

Die phylogenetischen Verwandtschaftsdiagramme zeigen weitgehend übereinstimmende Topologien, insbesondere in den tiefen Knotenpunkten (basal abzweigende Gruppen), mit sehr hohen Unterstützungswerten (Kapitel 5, Abb. 2). Unterschiede treten lediglich bei einigen abgeleiteten Linien von *A. richardsoni* und *A. spinulae* auf, was sich vor allem in einer Polytomie im MP-Baum widerspiegelt (Kapitel 5, Abb. 2). Mit Ausnahme von *A. richardsoni* sind alle genannten Arten „monophyletisch“ (eigenständige Linien). *Anaspides* sp. nov. 1 bildet die Schwestergruppe zu allen übrigen Arten. Diese Art kommt syntop im Lake Nicholls (Mt. Field Nationalpark) mit *A. richardsoni* vor, wobei keine Anzeichen von Hybridisierung und Genfluss zwischen den beiden Arten festgestellt werden konnte. Während der Sammlungsreise 2025 konnte *Anaspides* sp. nov. 1 zusätzlich in zwei benachbarten Bergbächen am Wylds Craig im Norden des Florentine Valley nachgewiesen werden (unpubliziert). Aufgrund ihrer phylogenetischen Position, des Sympatrietests mit *A. richardsoni* sowie klarer morphologischer Merkmale besteht kein Zweifel daran, dass es sich um eine eigenständige Art handelt.

Die übrigen vier Arten (*A. eberhardi*, *A. spinulae*, *Anaspides* sp. nov. 2 und 3) stehen innerhalb diverser Linien von *A. richardsoni* (Kapitel 5, Abb. 2, 10). *Anaspides eberhardi* bildet die Schwestergruppe zur *A. richardsoni*-Linie der Populationen des Mt. Field Plateaus. Beide

zusammen sind Schwestergruppe zu allen übrigen *A. richardsoni*-Linien + *Anaspides* sp. nov. 2 und 3 + *A. spinulae*. Der nächste Abzweig ist *Anaspides* sp. nov. 2, gefolgt von der *A. richardsoni*-Linie aus den Höhlen der Lightning Plains (nur geringe Anpassungen an das Höhlenleben), und anschließend von *Anaspides* sp. nov. 3 (sieben untersucht Populationen). Die nachfolgenden Linien sind diverse *A. richardsoni*-Linien vom Zentralplateau und Umgebung, den westlichen Bergketten sowie die „monophyletische" Linie von *A. spinulae*. Je nach Analyse sind 12 (ML) bzw. 6 Linien (MP) paraphyletisch zu *A. spinulae*. *Anaspides spinula*e ist in allen Fällen die Schwestergruppe zur Population aus der Clarence Lagoon (Population D in Höpel et al., 2025). Diese beiden sind wiederum Schwestergruppe zur *A. richardsoni*-Population aus dem Tributary to Travellers Rest River (Population C in Höpel et al., 2025), wie bereits bei Höpel et al. (2023b) gezeigt wurde. Diese Lokalitäten sind die geographisch nächsten *A. richardsoni*-Populationen zum Lake St. Clair. Die basal stehenden sieben Linien von *A. richardsoni* kommen an den früheren Eisrändern der maximalen Vergletscherung vor, was im Folgenden noch thematisiert wird. Auch die PCA und STRUCTURE-Analysen identifizieren eigenständige Cluster für die einzelnen Arten sowie für den Großteil der *A. richardsoni*-Linien, insbesondere jene der tiefen Verzweigungen. Nichts desto trotz können in den fineRADstructure, STRUCTURE und DSuite-Analysen leicht erhöhte geteilte genetische Information zwischen *A. richardsoni* und *A. spinulae* (Population C + D vs. *A. spinulae*) nachgewiesen werden. Gleiches wurde auch zwischen bestimmten Populationen von *Anaspides* sp. nov. 3 (Populationen e, f, g, Kapitel 5, Abb. 4-6, 11) und der Gruppe von *A. richardsoni* Populationen C + D + *A. spinulae* festgestellt. Die Populationen von *Anaspides* sp. nov. 3 e, f, g liegen auf der Westseite des Lake St. Clair und sind die geographisch dichtesten zum Lake St. Clair. Auch in der Treemix-Analyse kann ein genetisches Signal von *A. spinulae* in die Population e, f, g von *Anaspides* sp. nov. 3 festgestellt werden, was einen historischen Genfluss zwischen den beiden Arten nahelegt. Im Gegensatz dazu kann keine Hybridisierung oder Genfluss zwischen *A. eberhardi* und *Anaspides* sp. nov. 2 festgestellt werden, obwohl beide Arten syntop vorkommen. Allerdings wurden nur wenige Populationen untersucht. Weiterführende Untersuchungen hierzu finden sich in Kapitel 6. Obwohl viele der basalen Linien auch in den COI-Daten als eigenständige Linien erscheinen, bestehen einige Diskrepanzen zu den nuklearen Daten, teils bedingt durch Introgressionen.

Aufgrund der eigenständigen („monophyletischen") genetischen Linien der Arten *A. eberhardi*, *Anaspides* sp. nov. 2 und 3, klaren artspezifischen Merkmalen, und im Fall von *A.*

eberhardi und *Anaspides* sp. nov. 2 dem Sympatrietest, können alle klar als eigenständige Arten angesehen werden. Auch bei *A. spinulae*, trotz genetischer Nähe zu *A. richardsoni* und Hybridisierungsereignissen mit *Anaspides* sp. nov. 3, spricht die genetische eigenständige („monophyletische“) Linie sowie klare morphologische und ökologische Merkmale (einzige *Anaspides*-Art in einem großen See) für eine eigenständige Art. Es wird angenommen, dass *A. spinulae* eine sehr junge Art ist, die möglicherweise erst während oder kurz nach der letzten Eiszeit (17.000–22.000 Jahre vor heute) entstanden ist, da der Lake St. Clair zu dieser Zeit vollständig vergletschert war. Dies würde auch die genetische Nähe zu benachbarten *A. richardsoni*-Populationen und die Hybridisierung mit *Anaspides* sp. nov. 3 erklären. Möglicherweise erklärt dies auch das Vorhandensein von zwei „clasping spines“ bei *A. spinulae* im Gegensatz zu nur einem bei *A. richardsoni*. Solche jungen, nacheiszeitlichen Arten wurden bereits von Roman et al. (2018) und Secci-Petretto et al. (2023) beschrieben.

Der interessanteste und zugleich komplizierteste Fall ist wohl der von *A. richardsoni*. Wir argumentieren das *A. richardsoni* eine „paraphyletische“ Art. So könnte es sich hierbei zwar auch um mehrere „kryptische“ Arten handeln, wobei es unser Meinung nach keine objektive Entscheidungsgrundlage für die Wahl dieser geben kann. So könnten es drei „kryptische“ Arten sein: die Linie vom Mt. Field, die Linie von den Lightning Plaines und einer weiteren Art die alle übrigen Linien vom Zentralplateau und den Westliche Bergkletten einschließt, wobei die letzte dann *A. spinulae* inkludieren könnte oder auch nicht. Letzteres würde ebenfalls wieder zu einer Paraphylie von *A. richardsoni* führen, während die Inkludierung von *A. spinulae* zu einer Auflösung der taxonomisch diagnostischen Merkmale führen würde. Innerhalb der letzten Linie (Zentralplateau/westlichen Bergketten) könnte es sich aber ebenfalls um 6-12, je nach Analyse, „kryptische“ Arten handeln, da alle diese Linien ebenfalls klar allopatrisch vorkommen. Das größte Problem ist das zwischen allen *A. richardsoni*-Linien, insbesondere den basal abzweigenden, keine morphologischen Unterschiede gefunden werden konnten, weder durch die detaillierte Analyse von Ahyong (2016) noch durch eigene Untersuchungen. Diese arbiträre Einteilung neuer Arten würde darüber hinaus zu einer extrem großen taxonomischen und diagnostischen Instabilität der Arten führend, da keine Artunterscheidungsmerkmale, weder morphologisch noch ökologisch herangezogen werden könnten. Auch die Beschreibung von Unterarten ist in diesem Fall problematisch, da auch diese, morphologische Unterschiede aufweisen müssen (Mayr, 1969). Zudem wurde historischer und rezenter Genfluss zwischen mehreren, auch basal stehenden *A. richardsoni*-

Linien festgestellt. Schlussendlich handelt es sich unser Meinung nach bei der Central Clade und *Anaspides richardsoni* um ein klassisches Beispiel für allopatrische Artbildung, bei der sich bereits einige Populationen einer weitverbreiteten Art (*A. richardsoni*) aufgrund von sexueller oder ökologischer Selektion in neue Arten entwickelt haben, während viele andere Linien dies noch nicht getan haben (Mayr, 1942; Baker, 2005). Solche Speziationsprozesse und „paraphyletische" Arten sind bereits bei Süßwasserfischen (Barluenga et al., 2006; Secci-Petretto et al., 2023) und Laufkäfern (Fujisawa et al., 2019) beschrieben und werden wohl in Zukunft durch den Einsatz von modernen genetische Methoden wie ddRAD oder Genomanalysen häufiger erkannt werden.

Mithilfe unseres hochauflösenden ddRAD-Datensatzes konnten wir glaziale Refugien sowie, zumindest in Teilen, die Wiederbesiedlung des Zentralplateaus rekonstruieren. Dieses Gebiet war während der pleistozänen Vergletscherungen mehrfach von Eis bedeckt, wobei die größte Ausdehnung des Eisschildes im frühen Pleistozän stattfand. Die Vergletscherungen führten zwangsläufig zum lokalen Aussterben oder zur Verdrängung der dortigen Populationen. Wie bereits gezeigt, weist *Anaspides* nur eine sehr geringe Ausbreitungsfähigkeit auf, sodass lediglich Populationen in den Randbereichen der Vergletscherung überdauern konnten. Für die detaillierte Analyse der Refugien und Wiederbesiedlung betrachten wir ausschließlich das Cluster jener Linien, die heute auf dem Zentralplateau und den westlichen Bergketten vorkommen (Kapitel 5, Populationen C-W + *A. spinulae*). Auffällig ist, dass die vier basalen Linien dieses Clusters allesamt an den ehemaligen Eisrändern der größten Vergletscherung (Linda-Vergletscherung) lokalisiert sind. Unsere Daten deuten zudem darauf hin, dass von den meisten dieser frühen Refugien keine Wiederbesiedlung des Plateaus erfolgt ist. Da spätere Vergletscherungen weniger weitreichend waren, konnten sich in deren Randbereichen dieser Ereignisse weitere Refugien bilden. Die endgültige Wiederbesiedlung des Plateaus erfolgte dann hauptsächlich aus einem nördlich gelegenen Refugium sowie in geringerem Maße aus dem Südwesten, aus der Region nahe dem Lake St. Clair. Bemerkenswert ist, dass südöstlich des maximalen Eisrandes keine Refugien identifiziert werden konnten. Die Population nahe der Pine Tier Lagoon, die heute in dieser Region außerhalb der ehemaligen maximalen Vergletscherung vorkommt, ist genetisch ganz klar als Wiederbesiedlung dieser Region von Norden her, spezifisch den 30 km entfernt gelegenen Walls of Jerusalem, zu kennzeichnen. Dies ist einer der wenigen Fälle von längeren Wanderbewegungen bei *Anaspides,* aber durch die Zugehörigkeit zum selben Flusssystem zu erklären.

1.4.4 Höhleneinwanderung und Populationsgenetik

Dieser Abschnitt ist eine Synopsis des Kapitels 6, Höpel, C. G., Ahyong, S. T., Eberhard, S., Fordyce, S., Kapun, M., Schwentner, M., & Richter, S. Comparative phylogeography and speciation in correlation with cave colonization in Tasmanian mountain shrimps (*Anaspides*, Anaspidacea, Crustacea). Zoological Journal of the Linnean Society. (Under review)

Tasmanien, mit seiner Vielzahl an Karstgebieten, gilt als ideales Gebiet zur Erforschung der Evolution subterranen Lebens und der Kolonisation von Höhlen. *Anaspides* kann dabei als ein hervorragendes Modellsystem zur Untersuchung dieser Prozesse betrachtet werden. Erstmals 1965 durch Williams (1965b) in Höhlen nachgewiesen, konnten im Laufe der Jahre zahlreiche weitere von *Anaspides* besiedelte Höhlen identifiziert werden (O'Brien, 1990; Eberhard, 1992; Ahyong, 2016). Ahyong (2015, 2016) beschrieb sogar zwei obligat höhlenbewohnende Arten (*A. clarkei*, *A. eberhardi*). Richter et al. (2018) zeigten erstmals phylogenetisch, dass es mehrere unabhängige Einwanderungen in diese unterirdischen Habitate gegeben haben muss. Sie identifizierten mindestens vier unabhängige Besiedlungsereignisse, vermuteten jedoch deutlich mehr, da nur ein Teil der zahlreichen Höhlenpopulationen untersucht werden konnte. Die Ergebnisse von Richter et al. (2018) deuten darauf hin, dass diese Einwanderungen im Pleistozän stattgefunden haben und mit glazialen Phänomenen wie der Öffnung von Höhleneingängen durch Schmelzwasser in Verbindung stehen. Für solche rezenten Höhlenbesiedlungen werden zwei Haupttheorien diskutiert: die „climatic relict hypothesis" (CRH) und die „adaptive shift hypothesis" (ASH). Die CRH besagt, dass Höhlen infolge klimatischer Veränderungen passiv als Refugien besiedelt werden, wobei die ursprüngliche epigäische Population ausstirbt (oder geographisch weit entfernt lebt). Während der Phase der Separation findet dabei kein Genfluss statt. Die ASH hingegen geht von einer aktiven Besiedlung der Höhlen aus, bei der während der Divergenzphase Genfluss zwischen epigäischen und subterranen Populationen besteht (Niemiller et al., 2008).

Zur Untersuchung solcher evolutionären Prozesse im Zusammenhang mit Höhlenleben und -besiedlung haben wir ddRAD-Sequenzierung als Methode angewandt (siehe Abschnitt 1.4.3 sowie Kapitel 5 und 6 für detaillierte Informationen zur Methodik), da sie in der Lage ist rezente Separationsereignisse und populationsgenetische Unterschiede aufzulösen. Zusätzlich wurden mittels Sanger-Sequenzierung Teile des COI-Gens analysiert. Unser Fokus lag insbesondere auf der Höhlenart *A. eberhardi* und ihren geographisch sowie genetisch

nächsten Verwandten. *Anaspides eberhardi* bildet die Schwestergruppe zu *A. richardsoni* vom Plateau des Mt. Field und kommt syntop mit *Anaspides* sp. nov. 2 (Kapitel 5, Höpel et al., 2025) in zwei Höhlen im Florentine Valley vor.

Das Untersuchungsgebiet umfasst den Mt. Field Nationalpark sowie die angrenzenden Täler und den darunterliegenden Junee-Florentine Karst in Zentraltasmanien. Dieses Karstgebiet erstreckt sich über eine Fläche von mehr als 18.500 Hektar und beherbergt über 600 dokumentierte Höhlen (Eberhard, 1998). Der Karst erhebt sich bis zu 400 Meter an den Hängen des Mt. Field und enthält die tiefsten Höhlen Australiens. Wie viele andere Karstsysteme in Tasmanien wurde auch der Junee-Florentine Karst stark durch pleistozäne Vergletscherungen und glaziale Überformungen beeinflusst. Große Mengen glazialer Sedimente können Höhlengänge verschließen, Wasserläufe umlenken und Einzugsgebiete verändern. Das nacheiszeitliche Abschmelzen kann solche Passagen durch starke Schmelzwasserströme wieder öffnen und die Bildung neuer Höhlenabschnitte fördern. Auch das Plateau des Mt. Field war während der letzten Eiszeiten nahezu vollständig von Eis bedeckt.

Wir konnten insgesamt 347 Individuen der Arten *Anaspides eberhardi*, *A. richardsoni*, *Anaspides* sp. nov. 1 und *Anaspides* sp. nov. 2 mittels ddRAD- und Sanger-Sequenzierung untersuchen (261 Individuen in ddRAD, 293 im COI-Datensatz). Die Proben stammen aus 32 Lokalitäten, darunter 14 verschiedene Höhlen. Die ddRAD-Daten wurden mithilfe verschiedener phylogenetischer Methoden analysiert. Es wurden Verwandtschaftsdiagramme und Netzwerke berechnet (Maximum Likelihood, Maximum Parsimony, Splitstree) sowie Populationsstruktur, Genfluss und Introgressionsereignisse ermittelt (PCA, STRUCTURE, fineRADstructure, Dsuite, Treemix; siehe Kapitel 6: Material & Methoden). Darüber hinaus wurde die Verbreitung der entfernt verwandten Arten *A. swaini* und *A. tasmaniae* im Gebiet des Mt. Field Nationalparks detailliert dokumentiert. Wie bereits in Höpel et al. (2025) festgestellt, zeigt sich eine Diskrepanz zwischen den nuklearen ddRAD-Daten und den mitochondrialen COI-Daten. Mehrfache Introgressionen im COI-Datensatz werden angenommen, weshalb dieser Datensatz im Folgenden nur punktuell diskutiert wird (für eine ausführlichere Analyse siehe Kapitel 6).

Anaspides eberhardi wurde in elf Höhlen des Junee-Florentine Karsts nachgewiesen. In drei dieser Höhlen tritt die Art syntop mit *Anaspides* sp. nov. 2 auf (Kapitel 6, Abb. 1, sowie unveröffentlichter Neufund in 2025). Darüber hinaus wurde *Anaspides* sp. nov. 2 in zwei

weiteren Höhlen und zwei Oberflächengewässern in der Nähe von Höhleneingängen und -ausgängen im Florentine Valley gefunden. *Anaspides richardsoni* besiedelt die Bergseen, -tümpel und Gebirgspools des Mt. Field Plateaus und wurde syntop mit *Anaspides* sp. nov. 1 im Lake Nicholls nachgewiesen, welche im Mt. Field Nationalpark ausschließlich dort vorkommt. *Anaspides swaini* und *A. tasmaniae* besiedeln die Bergbäche, die vom Plateau abfließen, und wurden dabei insbesondere in der Nähe von Höhleneingängen gefangen.

Wie bereits in Höpel et al. (2025) können die ddRAD-Daten, erweitert durch eine größere Anzahl an Individuen und Lokalitäten, die Monophylie von *A. eberhardi* und *Anaspides* sp. nov. 2 bestätigen. Trotz syntoper Vorkommen an mehreren Fundorten können keine Hinweise auf Genfluss zwischen *A. eberhardi* und *Anaspides* sp. nov. 2 gefunden werden, was erneut auf zwei klar getrennte Arten hinweist. *Anaspides eberhardi* bildet die Schwestergruppe zur *A. richardsoni*-Linie der Populationen des Mt. Field Plateaus. Im Gegensatz zu Höpel et al. (2025) können wir jedoch einen Fall von leichtem Genfluss zwischen *A. richardsoni* und *A. eberhardi* feststellen. Unsere Analysen zeigen ein schwaches, unidirektionales Signal von Genfluss ausgehend von *A. richardsoni* in *A. eberhardi*, genauer gesagt von einer Population im Quellgebiet des Garths Creek (Kapitel 6, Abb. 1, Population Nr. 12) in einige Individuen einer Höhlenpopulation (Porcupine Pot-Gormenghast Cave-Growling Swallet-Niggly Cave) von *A. eberhardi*. Das stärkste Signal wurde in elf Individuen aus Growling Swallet, Niggly Cave und Porcupine Pot nachgewiesen, wobei die meisten Individuen mit diesem Signal hierbei aus der Growling Swallet stammen. Dies ist auch jene Höhle in welche der Garths Creek einfließt (Abb. 2C). Der Garths Creek fällt jedoch nach dem Eintritt in die Höhle über 300 Meter in die Tiefe und die ersten Individuen von *A. eberhardi* können erst in den tieferen Ebenen der Höhle angetroffen werden, während der Bach am Eingang von *A. swaini* besiedelt wird. Dieses Introgressionssignal konnte auch in zwei Individuen im COI-Datensatzes gefunden werden. Interessanterweise weisen einige *A. eberhardi* aus der Growling Swallet und Niggly Cave, insbesondere, aber nicht ausschließlich jene mit Genflusssignal, eine erhöhte Anzahl von Telson-Dornen auf (15–23), im Gegensatz zu den sonst artspezifischen acht Dornen (in seltenen Fällen 7–9). Dies könnte mit dem genetischen Einfluss von *A. richardsoni* zusammenhängen. Dennoch widerlegt dieser sehr lokale und vermutlich einmalige Genfluss nicht den Artstatus von *A. eberhardi*.

Wie bereits in Höpel et al. (2025) zeigt auch dieser ddRAD-Datensatz eine starke Korrelation zwischen Fundort und genetischer Population. Die obligate Höhlenart *A. eberhardi* bildet in

nahezu jeder Höhle eine eigenständige, genetisch isolierte Population. Eine Ausnahme stellt das unterirdische Junee-River-Flusssystem dar, das sechs untersuchte Höhlen miteinander verbindet. Hier zeigen sich nur drei genetisch unterscheidbare Populationen: Individuen aus Porcupine Pot, Gormenghast Cave, Niggly Cave und Growling Swallet bilden eine gemeinsame Population, während die Höhle Khazad Dum und die Junee Cave jeweils eigene Populationen darstellen. Die Junee Cave ist zugleich der einzige Ausstrom des Höhlensystems. Bemerkenswert ist, dass die Population der Junee Cave genetische Signale der beiden anderen Populationen aufweist, jedoch in einem spezifischen Verhältnis und mit erhöhten Fst-Werten zu den anderen beiden Populationen, sodass sie klar als eigenständig klassifiziert werden kann. Dies deutet darauf hin, dass Wanderbewegungen innerhalb des Höhlensystems zwischen den drei Populationen begrenzt sind.

Der Topologie des phylogenetischen Verwandtschaftsdiagramms folgend lässt sich der Ursprung von *A. eberhardi* eindeutig im Florentine Valley verorten (beide basal abzweigenden Linien innerhalb der „monophyletischen" Linie von *A. eberhardi* aus dem Florentine Valley). Die Höhlen des Florentine Valley sind hydrologisch vom Junee-River-Flusssystem getrennt. Unsere molekulare Uhr legt nahe, dass die Besiedlung der Höhlen im Pleistozän stattgefunden hat, mit einem Mindestalter von 0,93 Millionen Jahren, möglicherweise aber bereits vor 2,19 Millionen Jahren. Jede Höhle des Florentine Valley beherbergt jeweils eine eigenständige Population. Aufgrund der genetischen Linien und der geomorphologischen Struktur (das Florentine Valley ist ein Karstgebiet mit flachem Relief und kurzen Höhlensystemen) kann keine rezente Verbindung zwischen den Höhlenpopulationen nachgewiesen werden. Eine Ausnahme bilden die nahegelegenen Höhlen Nameless Spring und Settlement Cave, zwischen derer Populationen wir nur geringe Populationsunterschiede festgestellt haben und ein regelmäßiger genetischer Austausch angenommen wird. Dies wird auch durch die Anwesenheit der schwach höhlenangepassten Art *Anaspides* sp. nov. 2 in beiden Höhlen gestützt, die vermutlich keine unterirdischen Verbindungen nutzen kann und dadurch deutlich stärkere Populationsunterschiede zeigt.

Der nächste Schritt in der Besiedlung der Höhlen des Junee-Florentine Karsts durch *A. eberhardi* war der Übergang vom Florentine Valley in das unterirdische Flusssystem des Junee River. Lange Zeit wurde angenommen, dass diese beiden Gewässersysteme hydrologisch und geologisch voneinander getrennt sind. Es konnte jedoch eine Höhle identifiziert werden, die genau auf der vermuteten Grenze liegt, in der das einfließende Wasser in beide Systeme

abgeleitet wird. Unsere Ergebnisse stützen diese Annahme und legen nahe, dass dies der wahrscheinlichste Weg war, über den *A. eberhardi* in das Junee-River-Flusssystem gelangte. Dieser Übergang könnte im Zusammenhang mit hydrologischen und geomorphologischen Veränderungen während glazialer Perioden stehen. So beschreibt Kiernan (2018), dass Teile des heutigen Junee-River-Flusssystems ehemals zum Florentine-Wassereinzugsgebiet gehörten und sich die Höhlensysteme und Wasserläufe durch glaziale Prozesse veränderten.

Unsere Daten unterstützen die „climatic relict hypothesis“ als Modell für die Höhlenbesiedlung. Wir postulieren, dass die Höhlen des Florentine Valley während glazialer Perioden passiv als Refugien besiedelt wurden, während die epigäische Populationen von *A. richardsoni* auf dem Plateau verschwanden und nur noch in geographisch entfernten Regionen vorkam. Trotz der heutigen räumlichen Nähe werden alle Höhleneingänge von den genetisch nicht näher verwandten Arten *A. swaini* und *A. tasmaniae* besiedelt, und es existieren keine parapatrischen Übergangsbereiche zwischen *A. richardsoni* und *A. eberhardi*. Auch liegt der Ursprung von *A. eberhardi* im Florentine Valley und nicht dem direkt den Mt. Field und sein Plateau angrenzendes Junee-River-Flusssystem. Darüber hinaus konnten wir zwar relativ rezenten, lokal begrenzten Genfluss feststellen, der aber eindeutig nach der Divergenzphase der beiden Arten stattgefunden haben muss und unsere Daten zeigen kein Signal für weiteren historischen Genfluss während der Divergenzphase.

1.5 Ausblick und weiterführende Analysen

Durch die Möglichkeit, eine Vielzahl an Forschungsreisen durchzuführen, waren wir in der Lage, den Großteil der bekannten Verbreitung von *Anaspides* sowie alle bekannten Arten und morphologischen Formen (Ahyong, 2016) zu sammeln. Dabei konnten wir die Verbreitung vieler Arten präziser eingrenzen und zahlreiche neue Fundorte dokumentieren, darunter auch diverse neue Höhlenpopulationen. Erste morphologische Untersuchungen identifizierten sechs bislang unbeschriebene Arten (Abb. 3), die sich klar voneinander abgrenzen lassen. Auch in diesen Fällen erwiesen sich die von Ahyong (2015, 2016) sowie Höpel et al. (2023a) beschriebenen diagnostischen Merkmale als ausschlaggebend. Die neuen Arten unterscheiden sich unter anderem in der Form und Anzahl der „clasping spines“, der Form des Petasmas, der Form und Bedornung des Telsons und der pleonalen Bedornung. Unsere genetischen Analysen (ddRAD und Sanger-Sequenzierung) bestätigen diese sechs Arten, sodass deren formale Beschreibung zeitnah erfolgen soll. Die meisten dieser Arten weisen ein

begrenztes Verbreitungsgebiet auf, was insbesondere das bekannte Areal von *A. swaini* weiter einschränkt. Darüber hinaus liefern die ddRAD-Untersuchungen weitere spannende Erkenntnisse und Fragestellungen im Hinblick auf Höhlenimmigration, Artbildung und Populationsgenetik, die in zukünftigen Publikationen behandelt werden sollen.

Ein Beispiel hierfür sind die Höhlen- und Oberflächenpopulationen des Mole Creek Karst sowie benachbarter Zentralplateau-Habitate von *A. richardsoni*. Erste vorläufige Daten deuten darauf hin, dass es sich, im Gegensatz zum Mt. Field und *A. eberhardi*, um mindestens zwei, möglicherweise sogar fünf unabhängige Höhleneinwanderungen in einem relativ kleinen Gebiet handeln könnte. Oberflächen- und Höhlenformen beziehungsweise -populationen kommen parapatrisch und in einigen Fällen sogar sympatrisch vor. Unsere Ergebnisse legen nahe, dass einige dieser Kolonisationsereignisse den Kriterien der „adaptive shift hypothesis" entsprechen, das zweite Modell für rezente Höhlenbesiedlung. In zwei Fällen konnten wir klaren Genfluss zwischen Oberflächen- und Höhlenpopulationen nachweisen. Zudem weist jede Höhle eine eigene genetische Population auf, welche im Gegensatz zu *A. eberhardi*, auch morphologisch deutlich unterscheidbar ist. Dies spiegelt sich unter anderem im Grad der Höhlenanpassung wieder. So zeigen beispielsweise die Tiere aus der Honeycomb Cave eine stark ausgeprägte Höhlenanpassung mit nahezu vollständig reduzierten Augen und optischen Neuropilen sowie extrem verlängerten ersten und zweiten Antennen. Im Gegensatz dazu weisen Höhlenpopulationen des Marakoopa-Systems lediglich leichte Reduktionen (mehr oder weniger vollständig ausgebildete Augen und optische Neuropile) und moderate Verlängerungen auf (Rohr, 2024). In einigen Höhlensystemen (<5 km) konnten sogar bis zu zwei genetisch und morphologisch leicht unterschiedliche Populationen identifiziert werden. Dieses Karstsystem mit seinen Höhlen bietet neue und äußerst spannende Einblicke in die Thematik der Höhlenbesiedlung und zeigt das verschiedene Populationen von *A. richardsoni* auf unterschiedlichen Stufen der Höhlenanpassung und Speziation (vergleiche de Queiroz, 2007) stehen, die jedoch bislang keine neuen Arten darstellen.

Ein weiteres Beispiel ist der Artkomplex *A. jarmani*/ *A. clarkei*. *Anaspides clarkei* stellt eine obligate Höhlenart dar, während *A. jarmani* sowohl epigäische als auch subterrane Populationen umfasst. Der morphologischen Klassifizierung von Ahyong (2015, 2016) folgend, deuten unsere ddRAD-Daten darauf hin, dass sich die beiden Arten an syntopen Fundorten frei miteinander kreuzen können, sodass eine klare Artabgrenzung nicht möglich ist. Wir fanden zudem morphologische Zwischenformen beider Arten. Nach klassischer Morphologie

wäre *A. clarkei* als polyphyletisch zu betrachten, mit zwei unabhängigen Höhleneinwanderungen in die Karstsysteme von Ida Bay und Hastings. Eine neue taxonomische Klassifikation sowie eine erneute morphologische Analyse der Tiere sind daher erforderlich. Darüber hinaus konnte eine weitere unabhängige Einwanderung innerhalb von *A. jarmani* in das Karstsystem am Precipitous Bluff festgestellt werden. Die Individuen dieser Höhlen weisen eine verspätete Ausbildung des vollständigen Satzes an „clasping spines“ auf, was zu Folge hat das bereits geschlechtsreife Individuen erst zwei „clasping spines“ besitzen und erst mit weiterem Wachstum die für *A. jarmani* typischen 3-5 (in der Regel vier) „clasping spines“ ausbilden. Innerhalb von *A. clarkei* konnten eigenständige genetische Populationen für die meisten Höhlen nachgewiesen werden. Das Exit-Cave-System mit über 30 km unterirdischer Flusspassagen scheint mehrere Populationen zu beherbergen. Die genetischen Grundlagen dieser Höhlenanpassungen sind noch völlig unerforscht und stellen ein völlig eigenes Forschungsfeld dar, vergleichbar denen von Höhlenfischen (Trajano et al. 2010).

1.6 Literaturverzeichnis

Ahyong, S. T. (2015). Preliminary diagnoses of three new species of Tasmanian mountain shrimps, *Anaspides* Thomson, 1894 (Syncarida, Anaspidacea, Anaspididae). *Zootaxa, 3957*(5), 596.

Ahyong, S. T. (2016). The Tasmanian mountain shrimps, *Anaspides* Thomson, 1894 (Crustacea, Syncarida, Anaspididae). *Records of the Australian Museum, 68*(7), 313-364.

Ahyong, S. T., Schwentner, M., & Richter, S. (2017). The Tasmanian Lake Shrimps, *Paranaspides* Smith, 1908 (Crustacea, Syncarida, Anaspididae). *Records of the Australian Museum, 69*(4), 259-275.

Andrew, J. (2005). Biogeography and systematics of the Tasmanian mountain shrimps of the family Anaspididae (Crustacea: Syncarida). Doktorarbeit, University of Tasmania.

Augustinus, P. C. (1999). Reconstruction of the Bulgobac glacial system, Pieman River basin, western Tasmania. *Australian Geographical Studies, 37*(1), 24-36.

Baker, J. M. (2005). Adaptive speciation: the role of natural selection in mechanisms of geographic and non-geographic speciation. *Studies in History and Philosophy of Science Part C: Studies in History and Philosophy of Biological and Biomedical Sciences, 36*(2), 303-326.

Barbetti, M., & Colhoun, E. A. (1988). Reversed magnetization of glaciolacustrine sediments from western Tasmania. *Search, 19*(3), 151-153.

Barluenga, M., Stölting, K. N., Salzburger, W., Muschick, M., & Meyer, A. (2006). Sympatric speciation in Nicaraguan crater lake cichlid fish. *Nature, 439*(7077), 719-723.

Bernot, J. P., Owen, C. L., Wolfe, J. M., Meland, K., Olesen, J., & Crandall, K. A. (2023). Major revisions in pancrustacean phylogeny and evidence of sensitivity to taxon sampling. *Molecular Biology and Evolution, 40*(8), msad175.

Borko, Š., Altermatt, F., Zagmajster, M., & Fišer, C. (2022). A hotspot of groundwater amphipod diversity on a crossroad of evolutionary radiations. *Diversity and Distributions, 28*(12), 2765-2777.

Borowski, R. (2010): *The evolutionary genetics of cave fishes: convergence, adaptation and pleiotropy*. In: Trajano, E., Bichuette, M.E. & Kapoor, B.G. (Eds.): Biology of subterranean fishes, 115-139. CRC Press Boca Raton, FL, USA.

Buhay, J. E., & Crandall, K. A. (2005). Subterranean phylogeography of freshwater crayfishes shows extensive gene flow and surprisingly large population sizes. *Molecular Ecology, 14*(14), 4259-4273.

Calman, W. T. (1904). On the classification of the Crustacea Malacostraca. *Journal of Natural History, 13*(74), 144-158.

Calman, W. T. (1909). *Crustacea*. In E. R. Lankester (ed.): A treatise on zoology, Part 7, 1–346. A. & C. Black, London, England.

Chilton, C. (1929). Notes on a fossil shrimp from Hawkesbury sandstones. *Journal of the Royal Society of New South Wales, 62*, 366-368.

Clarke, A. (1999). Surface disturbance threats to karst faunas in Tasmania, Australia. *Proceedings of the 1999 National Cave and Karst Management Symposium, Southeastern Cave Conservancy, Chattanooga*, 23-47.

Colhoun, E. A., Kiernan, K., Barrows, T. T., & Goede, A. (2010). Advances in Quaternary studies in Tasmania. *Geological Society, London, Special Publications, 346*(1), 165-183.

Darwin, C. R. (1859). On the origin of species by means of natural selection, or the preservation of favoured races in the struggle for life. John Murray, London, England.

De Queiroz, K. (2007). Species concepts and species delimitation. *Systematic biology, 56*(6), 879-886.

Desutter-Grandcolas, L., & Grandcolas, P. (1996). The evolution toward troglobitic life: a phylogenetic reappraisal of climatic relict and local habitat shift hypotheses. *Mém Biospéol, 23*, 57-63.

Driessen, M. M., & Mallick, S. A. (2007). The life history of *Allanaspides hickmani* Swain, Wilson & Ong, 1971 (Syncarida, Anaspididae). *Crustaceana, 80*(10), 1171-1192.

Driessen, M. M., Mallick, S. A., Thurstans, S., Smith, B., & Brereton, R. N. (2014). Distribution and conservation status of two endemic Tasmanian crustaceans, *Allanaspides hickmani* and *Allanaspides helonomus* (Syncarida: Anaspididae). *Papers and Proceedings of the Royal Society of Tasmania, 148*, 17-25.

Eberhard R. (1998). Planning for karst management in multiple–use forest: The Junee–Florentine karst study. *Tasforest–Hobart, 10*, 33–48.

Eberhard, S. (1992). The invertebrate cave fauna of Tasmania: ecology and conservation biology. Doktorarbeit, University of Tasmania.

Eberhard, W. G. (1985). Sexual selection and animal genitalia. Harvard University Press, Cambridge, MA, USA.

Fujisawa, T., Sasabe, M., Nagata, N., Takami, Y., & Sota, T. (2019). Genetic basis of species-specific genitalia reveals role in species diversification. *Science Advances, 5*(6), eaav9939.

Goede, A. (1967). Tasmanian cave fauna: character and distribution. *Helictite, 5,* 71-86.

Grams, M., & Richter, S. (2021). Locomotion in *Anaspides* (Anaspidacea, Malacostraca)–insights from a morpho-functional study of thoracopods with some observations on swimming and walking. *Zoology, 144*, 125883.

Grams, M., Klinger, M., & Richter, S. (2023). Neither leg nor jaw—nor always the same: a critical revision of the eumalacostracan maxilliped. *Zoological Journal of the Linnean Society, 197*(4), 965-1004.

Grosso, L., & Peralta, M. (2002). *Patagonaspides* gen. n.; *P. sandroruffoi* sp. n. (Crustacea, Syncarida). First phreatobite species of a new anaspidacean family discovered in Patagonia with cladistic analysis of Stygocaridinea (Anaspidacea). *Bolletino del Museo Civico di Storia Naturale di Verona*, *26*, 105–118.

Hickman, V. V. (1936). The embryology of the syncarid crustacean, *Anaspides tasmaniae. Papers and Proceedings of the Royal Society of Tasmania*, 1-36.

Holsinger, J. R. (2000). *Ecological derivation, colonization, and speciation*. In H. Wilkens, D. C. Culver & W.F. Humphreys (Eds.): Ecosystems of the World 30: subterranean ecosystems, 399-416. Elsevier Academic, Amsterdam, Niederlande.

Höpel, C. G., Ahyong, S. T., & Richter, S. (2021). Genetic structure and new occurrence records of the iconic Tasmanian mountain shrimp *Anaspides tasmaniae* (Thomson, 1893)(Anaspidesidae: Anaspidacea) reveal relictual distribution in southern Tasmania. *Australian Journal of Zoology, 68*(1), 45-53.

Höpel, C. G., Ahyong, S. T., Kapun, M., Schwentner, M., & Richter, S. (2025). Phylogeography of the *Anaspides richardsoni* species clade (Anaspidacea, *Anaspides* spp.) - glaciation and recolonisation of the Central Plateau and the question of paraphyletic species. *Cladistics.*

Höpel, C. G., Richter, S., & Ahyong, S. T. (2023a). A new species of Tasmanian mountain shrimp, *Anaspides driesseni* sp. nov. (Malacostraca, Anaspidacea, Anaspidesidae). *Records of the Australian Museum, 75*(1), 25-43.

Höpel, C. G., Yeo, D., Ahyong, S. T., Meier, R., & Richter, S. (2023b). First mitochondrial genomes of Anaspidacea (Malacostraca, Crustacea) and the phylogenetic relationships of mountain shrimps (*Anaspides* Thomson, 1894) and their relatives within Anaspidesidae. *Journal of Crustacean Biology, 43*(2), ruad028.

Jarman, S. N., & Elliott, N. G. (2000). DNA evidence for morphological and cryptic Cenozoic speciations in the Anaspididae,'living fossils' from the Triassic. *Journal of Evolutionary Biology, 13*(4), 624-633.

Jennings, J. N., & Sweeting, M. M. (1959). Underground breach of a divide at Mole Creek, Tasmania. *Australian Journal of Science, 21*(8), 261-262.

Juan, C., Guzik, M. T., Jaume, D., & Cooper, S. J. (2010). Evolution in caves: Darwin's 'wrecks of ancient life in the molecular era. *Molecular Ecology, 19*(18), 3865-3880.

Kiernan K. (2018). Eroding the Edges of Nature. Fullers Publishing Pty Ltd, Hobart, Australien.

Kiernan, K. (1990). The extent of late Cenozoic glaciation in the Central Highlands of Tasmania, Australia. *Arctic and Alpine Research, 22*(4), 341-354.

Kiernan, K. (2005). Tasmania's cold caves: an island of alpine karst. *Cave Mania 2005 Downunder at Dover,* 40-48.

Lake, P. S., & Coleman, D. J. (1977). On the subterranean syncarids of Tasmania. *Helictite, 15*, 12-17.

Manton, S. M. (1930). Notes on the Habits and Feeding Mechanisms of *Anaspides* and *Paranaspides* (Crustacea, Syncarida). *Proceedings of the Zoological Society of London, 100*(3), 791-800.

Mayr, E. (1969). The biological meaning of species. *Biological Journal of the Linnean society, 1*(3), 311-320.

Mayr, E., 1942. Systematics and the Origin of Species. Columbia University Press, NY, USA.

Nicholls, G. E. (1931). *Micraspides calmani*, a new syncaridan from the west coast of Tasmania. *Zoological Journal of the Linnean Society, 37*(254), 473-488.

Niemiller, M. L., Fitzpatrick, B. M., & Miller, B. T. (2008). Recent divergence with gene flow in Tennessee cave salamanders (Plethodontidae: *Gyrinophilus*) inferred from gene genealogies. *Molecular ecology, 17*(9), 2258-2275.

O'Brien, D. P. (1990). The conservation status of the mountain shrimp (*Anaspides tasmaniae* and *Anaspides spinulae*): a report on its distribution, ecology and taxonomy, including recommendations for management. Department of Parks, Wildlife and Heritage, Hobart, Tasmania.

Peck, S. B., & Finston, T. L. (1993). Galapagos islands troglobites: the questions of tropical troglobites, parapatric distributions with eyed-sister-species, and their origin by parapatric speciation. *Mémoires de Biospéologie, 20*, 19-37.

Richter, S., & Scholtz, G. (2001). Phylogenetic analysis of the Malacostraca (Crustacea). *Journal of Zoological Systematics and Evolutionary Research, 39*(3), 113-136.

Richter, S., Schwentner, M., Wirkner, C. S., & Ahyong, S. T. (2018). Phylogeny and species diversity of Tasmanian mountain shrimps and their relatives (Crustacea, Anaspidesidae). *Zoologica Scripta, 47*(1), 84-105.

Rivera, M. A. J., Howarth, F. G., Taiti, S., & Roderick, G. K. (2002). Evolution in Hawaiian cave-adapted isopods (Oniscidea: Philosciidae): vicariant speciation or adaptive shifts? *Molecular Phylogenetics and Evolution, 25*(1), 1-9.

Rohr, T. S. (2024). Morphologische Untersuchung der Anpassungen an Höhlen der Tasmanischen Berggarnelen (*Anaspides*, Anaspidacea, Malacostraca). (Bachelorarbeit, Universität Rostock)

Roman, I., Bourgeois, Y., Reyes-Velasco, J., Jensen, O. P., Waldman, J., & Boissinot, S. (2018). Contrasted patterns of divergence and gene flow among five fish species in a Mongolian rift lake following glaciation. *Biological Journal of the Linnean Society, 125*(1), 115-125.

Schminke, H. K. (1975). Phylogenie und Verbreitungsgeschichte der Syncarida (Crustacea, Malacostraca). *Verhandlungen Zoologische Gesellschaft Bochum*, 384-388.

Schminke, H. K. (1996). *Crustacea, Krebse.* In W. Westheide & R. Rieger (Eds.): Spezielle Zoologie, 1. Teil: Einzeller und Wirbellose Tiere, 501-581. Fischer, Stuttgart, Deutschland.

Schram, F. R., & Hessler, R. R. (1984). *Anaspidid Syncarida*. In N. Eldredge & S. M. Stanley (Eds.): Living fossils, 192-195. Springer, NY, USA.

Schram, F.R. (1986). *Crustacea*. Oxford University Press, NY, USA.

Schwentner, M., & Lörz, A. N. (2021). Population genetics of cold-water coral associated Pleustidae (Crustacea, Amphipoda) reveals cryptic diversity and recent expansion off Iceland. *Marine Ecology, 42*(1), e12625.

Schwentner, M., Richter, S., Rogers, D. C., & Giribet, G. (2018). Tetraconatan phylogeny with special focus on Malacostraca and Branchiopoda: highlighting the strength of taxon-specific matrices in phylogenomics. *Proceedings of the Royal Society: Biological Sciences, 285*(1885), 20181524.

Secci-Petretto, G., Englmaier, G. K., Weiss, S. J., Antonov, A., Persat, H., Denys, G. P., ... & Froufe, E. (2023). Evaluating a species phylogeny using ddRAD SNPs: Cyto-nuclear discordance and introgression in the salmonid genus *Thymallus* (Salmonidae). *Molecular Phylogenetics and Evolution, 178*, 107654.

Sharples, C. (2002). Data Dictionary and Metadata for the Tasmanian Karst Atlas vol. 2: Digital Dataset.

Siewing, R. (1956). Untersuchungen zur Morphologie der Malacostraca (Crustacea). *Zoologische Jahrbücher, Abteilung für Anatomie und Ontogenie der Tiere, 75*, 39–176.

Siewing, R. (1959). *Syncarida*. In M. G. Bronn (ed.): Klassen und Ordnungen des Tíerreichs, 5, 1-121. Akademische Verlagsgesellschaft Geest & Portig, Leipzig, Deutschland.

Smith, G. W. (1908). Preliminary account of the habits and structure of the Anaspididae, with remarks on some other fresh-water Crustacea from Tasmania. *Proceedings of the Zoological Society of London, 80*(543), 465-473.

Smith, G. W. (1909). On the Anaspidacea, living and fossil. *Journal of Cell Science, 2*(211), 489-578.

Stern, D. B., Breinholt, J., Pedraza-Lara, C., López-Mejía, M., Owen, C. L., Bracken-Grissom, H., & Crandall, K. A. (2017). Phylogenetic evidence from freshwater crayfishes that cave adaptation is not an evolutionary dead-end. *Evolution, 71*(10), 2522-2532.

Swain, R. (2000). The life history and habitat of *Allanaspides helonomus* (Syncarida: Anaspididae). *Crustacean Issues, 12*, 283-290.

Swain, R., & Reid, C. I. (1983). Observations on the life history and ecology of *Anaspides tasmaniae* (Thomson)(Syncarida: Anaspididae*). Journal of Crustacean Biology, 3*(2), 163-172.

Swain, R., Wilson, I. S., & Ong, J. E. (1971). A new species of *Allanaspides* (Syncarida, Anaspididae) from southwestern Tasmania. *Crustaceana,* 196-202.

Swain, R., Wilson, I. S., Hickman, J. L., & Ong, J. E. (1970). *Allanaspides helonomus* gen. et sp. nov. (Crustacea: Syncarida) from Tasmania. *Records of the Queen Victoria Museum, 35*, 1-13.

Thomson, G. M. (1893). Notes on Tasmanian Crustacea, with descriptions of new species. *Papers & Proceedings of the Royal Society of Tasmania*, 45-76.

Thomson, G. M. (1894). On a freshwater schizopod from Tasmania. *Transactions of the Linnean Society of London 6,* 285–303.

Trajano, E., Bichuette, M.E. & Kapoor, B.G. (2010). Biology of subterranean fishes. CRC Press Boca Raton, FL, USA.

Tyler, P. A. (1992). A lakeland from the dreamtime - the second founders' lecture. *British Phycological Journal, 27*(4), 353-368.

Verovnik, R., & Konec, M. (2019*). Asellus aquaticus: A model system for historical biogeography*. In W. B. White, D. C. Culver, & T. Pipan (Eds.): Encyclopedia of caves, Chapter 11, 76–84. Elsevier Academic, Amsterdam, Niederlande.

von Rintelen, K., Page, T. J., Cai, Y., Roe, K., Stelbrink, B., Kuhajda, B. R., & von Rintelen, T. (2012). Drawn to the dark side: a molecular phylogeny of freshwater shrimps (Crustacea: Decapoda: Caridea: Atyidae) reveals frequent cave invasions and challenges current taxonomic hypotheses. *Molecular Phylogenetics and Evolution, 63*(1), 82-96.

Williams, W. D. (1965a). Ecological notes on Tasmanian Syncarida (Crustacea: Malacostraca). with a description of a new species of *Anaspides*. *Internationale Revue der gesamten Hydrobiologie und Hydrographie, 50*(1), 95- 126.

Williams, W. D. (1965b). Subterranean occurrence of *Anaspides tasmaniae* (Thomson, 1893) (Crustacea, Syncarida). *International Journal of Speleology, 1*(3), 7.

2 **Höpel, C. G., Ahyong, S. T., & Richter, S. (2021). Genetic structure and new occurrence records of the iconic Tasmanian mountain shrimp *Anaspides tasmaniae* (Thomson, 1893)(Anaspidesidae: Anaspidacea) reveal relictual distribution in southern Tasmania. Australian Journal of Zoology, 68(1), 45-53.**

CSIRO PUBLISHING

Australian Journal of Zoology
https://doi.org/10.1071/ZO20100

Genetic structure and new occurrence records of the iconic Tasmanian mountain shrimp *Anaspides tasmaniae* (Thomson, 1893) (Anaspidesidae : Anaspidacea) reveal relictual distribution in southern Tasmania

Christoph G. Höpel[A,C], *Shane T. Ahyong*[B] *and Stefan Richter*[A]

[A]Allgemeine and Spezielle Zoologie, Institut für Biowissenschaften, Universität Rostock, Universitätsplatz 2, 18055 Rostock, Germany.
[B]Australian Museum Research Institute, Australian Museum, 1 William Street, Sydney, NSW 2010, Australia, *and* School of Biological, Earth and Environmental Sciences, University of New South Wales, Kensington, NSW 2052, Australia.
[C]Corresponding author. Email: christoph.hoepel@uni-rostock.de

Abstract. The iconic 'mountain shrimps' of the genus *Anaspides* Thomson, 1894, are endemic to Tasmania, inhabiting various freshwater habitats such as mountain tarns and creeks, as well as streams inside caves. They are often labelled as 'living fossils' because of their close resemblance to their Triassic relatives. Prior to 2015, only two species were recognised but recent studies have uncovered a total of at least seven species. The type species of *Anaspides*, *A. tasmaniae* (Thomson, 1893), was previously believed to occur throughout Tasmania, but following a review in 2016, this species was confirmed only from a small range on the east and south-east side of Mt Wellington, with *Anaspides* from other parts of Tasmania referable to other species. We herein provide a detailed assessment of the distribution and genetic structure of *A. tasmaniae* based on extensive field surveys throughout the ranges of all species of *Anaspides*. The distribution of *A. tasmaniae* is extended to include four separate localities in and around the Mt Field National Park, 50 km north-west of Mt Wellington. The recovered genetic structure of *A. tasmaniae* based on 48 specimens indicates that the disjunct distribution is unlikely to be the result of artificial translocation but, instead, probably reflects postglacial relictualisation of a formerly continuous range present during Pleistocene glacial maxima. Of particular interest is the record of syntopy in *Anaspides*, observed at the entrance of Khazad Dum cave, where both *A. tasmaniae* and *A. swaini* inhabit the inflow stream.

Keywords: Anaspidacea, Anaspidesidae, *Anaspides tasmaniae*, conservation, endemic, genetic structure, glaciation, mountain shrimp, relictual distribution, Tasmania.

Received 23 December 2020, accepted 11 March 2021, published online 9 April 2021

Introduction

The mountain shrimps of the genus *Anaspides* Thomson, 1894 (Anaspidesidae: Ahyong and Alonso-Zarazaga 2017) are endemic to Tasmania and are probably the most iconic freshwater invertebrates of the island (Ahyong 2016; Ahyong and Alonso-Zarazaga 2017). *Anaspides* occurs in a variety of freshwater surface habitats such as mountain tarns, creeks, streams, and pools, as well as subterranean streams in caves all over Tasmania. Although *Anaspides* spp. are found in surface waters between 150 m and approximately 1500 m above sea level (asl), they mainly occur in high-altitude areas above 700–800 m asl. *Anaspides* is often referred to as a 'living fossil' because of its close resemblance to Triassic relatives. The first species of *Anaspides* was discovered in 1892 by G. M. Thomson, who collected specimens on Mt Wellington, which he initially named *Anaspis tasmaniae* Thomson, 1893 (but later corrected to *Anaspides tasmaniae*) (Thomson 1894). In 1908, Smith enlarged the known distribution of *Anaspides*, finding populations on the Hartz Mts, Mt Field and Mt Read. A second species of *Anaspides*, *A. spinulae* Williams, 1965, was described from Lake St Clair (Williams 1965*a*). In the same year, Williams reported the first records of *Anaspides* from caves (Williams 1965*b*). Further investigations in caves and surface waters revealed further occurrences and higher morphological variation in *Anaspides*, as well as molecular evidence for undiscovered diversity (Goede 1967; Lake and Coleman 1977; O'Brien 1990; Jarman and Elliott 2000).

Journal compilation © CSIRO 2021

Our current taxonomic knowledge is based significantly on the investigations of Ahyong (2015, 2016), which led to recognition of five new species: *A. clarkei* Ahyong, 2015, *A. jarmani* Ahyong, 2015, *A. swaini* Ahyong, 2015, *A. eberhardi* Ahyong, 2016 and *A. richardsoni* Ahyong, 2016. *Anaspides richardsoni* occurs in the northern half of Tasmania from the West Coast Range, east to Cradle Mountain, Gunns Plains and Mole Creek, across the Central Plateau, and south to Mt Field, whereas *A. swaini* has a more central-south-western distribution, being reported from the Wellington Range over the Snowy Range and Arthur Range to the flanks of lakes Pedder and Gordon, and north to the vicinity of Lake St Clair. Moreover, Ahyong (2016) reported morphological differences within these widespread species, especially within *A. swaini*, recognising three subtly different, geographically discrete forms, which might represent separate species (currently under study). The remaining species have narrow ranges and are morphologically rather consistent. *Anaspides spinulae* occurs only within Lake St Clair, *A. eberhardi* is present only in caves of the Junee–Florentine karst and *A. jarmani* and *A. clarkei* are found in just a few localities in south-east Tasmania. Finally, *A. tasmaniae*, formerly believed to be widespread over the whole island in surface waters and caves, now appeared to be limited to a small range on the east and south-east side of Mt Wellington above 450 m asl with no known cave occurrences. Richter *et al*. (2018), using molecular data, largely corroborated the major species clades of Ahyong (2016) and recovered a monophyletic *A. tasmaniae*, with different sister group relationships depending on the gene fragment used.

Anaspides tasmaniae is readily distinguished from other species of the genus by the combination of well developed eyes, the presence of two antennular clasping spines in adult males, the elongated telson with an evenly rounded posterior margin lined with closely set spinules and a male pleopod I, in which the retinacular lobe is visible in lateral view (Ahyong 2016). In particular, the elongated telson with an evenly rounded posterior margin and the form of the antennular inner flagellum makes it easy to distinguish from other *Anaspides* species.

We herein provide a detailed assessment of distribution and genetic structure of *A. tasmaniae* based on extensive recent field surveys throughout the ranges of all species of *Anaspides*, extend the known distribution of *A. tasmaniae* to an area in the Junee–Florentine Karst, 50 km north-west of Mt Wellington and provide evidence of sympatry of two species of *Anaspides* at the entrance of the Khazad Dum cave.

Material and methods

Specimens were collected during two extensive field surveys in February 2017 and March 2019, sampling widely throughout the range of all species of *Anaspides*. In total, 37 specimens of *A. tasmaniae* were collected and newly sequenced for this study (see Table S1, Supplementary Material). In addition, a total of 9 COI, 11 16S rRNA and one 28S rRNA sequence from the study by Richter *et al*. (2018) were included. The newly sequenced specimens were collected using hand nets and preserved directly in 80–95% ethanol. Specimens were identified based on morphology following Ahyong (2015, 2016).

Tissue was removed from the 8th thoracopod or from the pleopods of the specimens. The DNA extraction was performed with the innuPrep Forensic Kit (Analytik Jena) and the DNeasy Blood and Tissue Kit (Qiagen) following the manufacturer's instruction. Three markers were partially sequenced: mitochondrial cytochrome *c* oxidase subunit I (COI) and 16S rRNA as well as the nuclear 28S rDNA. The polymerase chain reaction (PCR) had a total volume of 30 µL containing 3 µL of each primer (each 10 µM), 3 µL 10 × buffer (Sigma Aldrich), 3 µL dNTP mix (2 mM, Biozym), 2.58 µL $MgCl_2$ (25 mM, Sigma Aldrich), 0.12 µL Taq-polymerase (Sigma Aldrich), 10.71 µL ultrapure water and 4.5 µL of the DNA extract. Primers were LCO2 (5′-TCN ACH AAY CAT AAA GAY ATT GGA AC-3′) (Richter *et al*. 2018), HCO2198 (5′-TAA ACT TCA GGG TGA CCA AAA AAT CA-3′) (Folmer *et al*. 1994) for COI, 16Sa (5′- CGC CTG TTT ATC AAA AAC AT-3′), 16Sb (5′-CTC CGG TTT GAA CTC AGA TCA-3′) (Xiong and Kocher 1991) for 16S and rd4.8a (5′-ACC TAT TCT CAA ACT TTA AAT GG-3′) and rd7b1 (5′-GAC TTC CCT TAC CTA CAT-3′) (Richter *et al*. 2007) for 28S rDNA. PCR amplification programs comprised an initial denaturation step at 94°C for 1 min, followed by 40 amplification cycles (94°C for 30 s, 50°C for 30 s, 72°C for 60 s) for COI, 38 amplification cycles (94°C for 30 s, 48°C for 30 s, 72°C for 60 s) for 16S, 35 amplification cycles (94°C for 30 s, 55°C for 30 s, 72°C for 60 s) for 28S, and a final elongation step at 72°C for 5 min. All PCR reactions were performed with a Mastercycler gradient (Eppendorf). PCR products were visualised by gel electrophoresis, using 5 µL of the PCR product with 1.5 µL loading buffer DNA b II (AppliChem) on a 1.2% agarose/TAE gel stained with 5 µL Rotisafe (Carl Roth). PCR products were purified using paramagnetic beads (High Prep PCR, Magbio) following the manufacturer's instruction with a finale volume of 25 µL. Sequencing of PCR products was performed in Lightrun96 well plates by the company Eurofins Genomics as well as using the dideoxy chain termination method and cycle sequencing using an ABI Prism® Big Dye® Terminator V.1.1 Cycle Sequencing Kit. Cycle sequencing products were analysed by using capillary separation on an ABI Genetic Analyzer 3130 xl (Applied Biosystems/Hitachi). The resulting chromatograms were manually checked and adjusted with Geneious 2019.1.3 (Biomatters Limited). All sequences were deposited in GenBank (Benson *et al*. 2003) (accession numbers: MW584899–MW584904, MW581074–MW581077, MW581544–MW581580).

The sequences of all three gene fragments were separately aligned using ClustalW (Thompson *et al*. 1994) implemented in Geneious Prime 2019.1.3 (Biomatters Limited). Pairwise distances were calculated using MEGA X (Kumar *et al*. 2018). For pairwise distance analyses the uncorrected p-distances were calculated. Phylogenetic networks were calculated with Network 5.0.1.1 (Fluxus Technologies) separately for COI, 16S, and 28S alignments by using the median-joining method with the parameter epsilon set to 10.

Results

We found *Anaspides tasmaniae* at three different localities east and south-east of Mt Wellington, within the known range of the species: at a small runnel near The Chalet, Mt Wellington (970 m asl); the Browns River at Silver Falls (520 m asl); and Fern Tree Bower (470 m asl) (Figs 1 and 2). Extensive searches of the Mt Wellington plateau in the head waters of North West Bay River, where *Anaspides* has been historically reported to occur (Ahyong 2016), recovered no evidence of *Anaspides*. Also considering the records in Ahyong (2016), true *A. tasmaniae* has been confirmed only from three different drainages in the east and south-east of Mt Wellington: the catchments of the New Town Rivulet, the Guy Fawkes Rivulet and the Browns River (Fig. 2). The neighbouring drainages, all in Wellington Park, i.e. North West Bay River catchment, Knights Creek catchment and Myrtle Forest Creek/Sorell Creek catchment, are inhabited by *Anaspides swaini* (form 3 of Ahyong 2016) (Figs 1 and 2).

Anaspides tasmaniae, however, was discovered within and near the Mt Field National Park. In Mt Field National Park, we recorded four species of *Anaspides*: *A. richardsoni*, *A. eberhardi*, *A. swaini* (supporting the general distribution shown in Ahyong 2016) as well as *A. tasmaniae*. *Anaspides richardsoni* inhabits the tarns and runnels on the plateau from Wombat Moor and the north side of the Mawson Plateau over the tarn shelf, Newdegate Pass and K Col to the waters of the Mt Field West plateau (Figs 1 and 3). The troglobitic species, *A. eberhardi*, occurs only in caves of the Junee–Florentine Karst at the edges of the Mt Field National Park and Junee Cave State Reserve. We observed *A. eberhardi* in Niggly Cave, Khazad Dum, Porcupine Pot and Junee Cave. Further records of *A. eberhardi* are from cave JF-104, Welcome Stranger Cave, Gormenghast Cave, Pendant Pot, Growling



Fig. 1. Hydrological map of Tasmania showing the Derwent River drainage systems (red outlines), the borders of Mt Field National Park and Wellington Park (black outlines) and collection sites of *Anaspides tasmaniae* (blue dots). Modified after the Tasmanian catchment map, Tasmanian Government, Department of Primary Industries, Parks, Water and Environment, 13.09.2016.

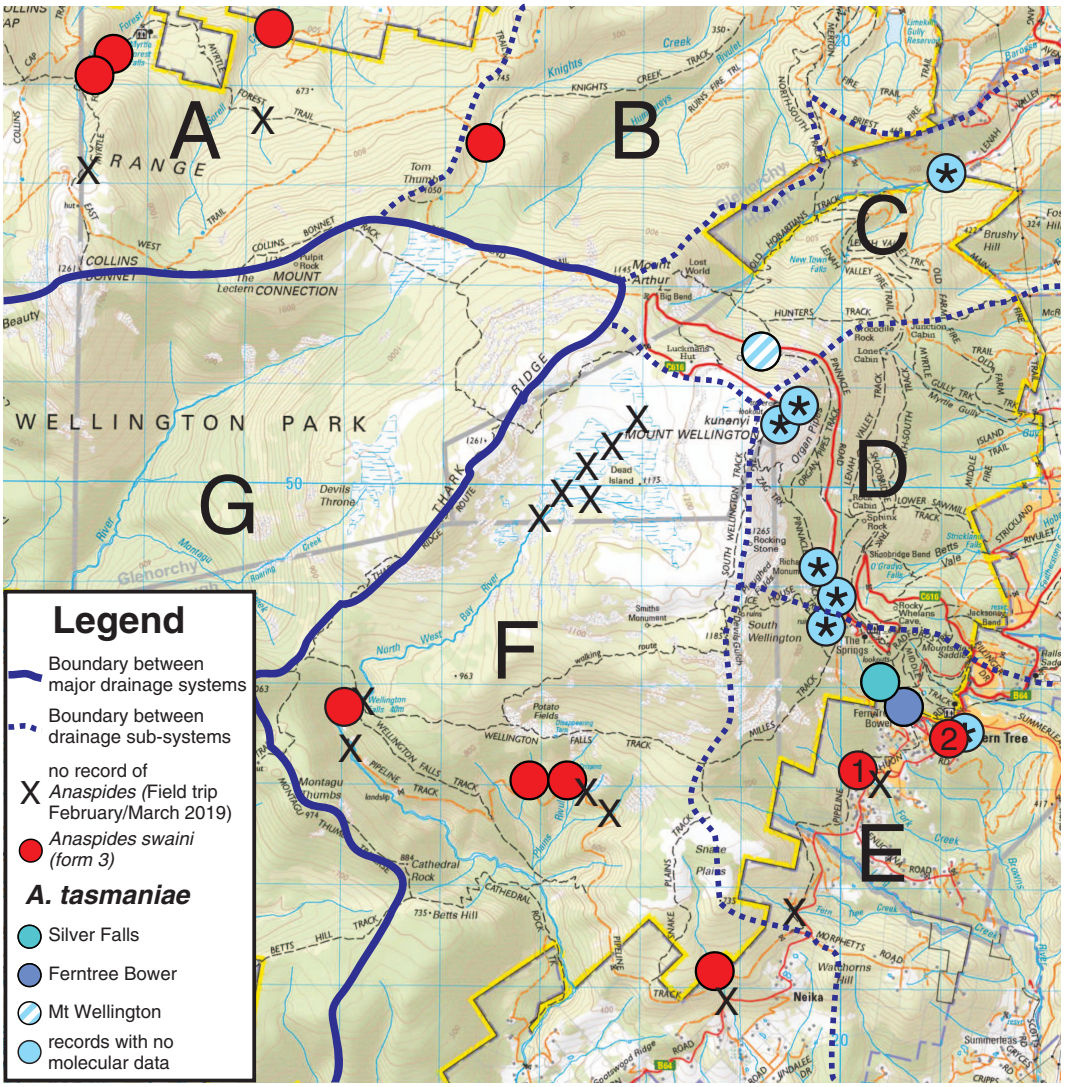


Fig. 2. Topographical map of eastern Wellington Park with drainage and subdrainage systems, as well as known collection sites of *Anaspides* from Ahyong (2016) and collection sites from this study. Subdrainage systems A–F drain into the Derwent River drainage system: A: Myrtle Forest Creek/Sorell Creek drainage system; B: Knights Creek drainage system; C: New Town Rivulet drainage system; D: Guy Fawkes drainage system; E: Browns River drainage system; F: North West Bay River drainage system, whereas subdrainage system G drains into the Huon River drainage system: G: Mountain River drainage system. Red circles with 1 and 2 refer to two locations that are considered to be accidental translocations of *A. swaini* form 3 by an aqueduct that drew water from the west to the east side of Mt Wellington. Base image by TASMAP (www.tasmap.tas.gov.au) © State of Tasmania.

Swallet and Settlement Cave (Ahyong 2016). *Anaspides swaini* occurs in the inflow creeks of Growling Swallet (Garths Creek) and Khazad Dum. Although, *A. swaini* has been recorded from Robert Tarn and the Mawson Plateau in the past (1970, 1975; see Ahyong 2016), *Anaspides swaini* is apparently now absent on the plateaus of the Mt Field National Park. Although Robert Tarn is currently inhabited by *A. richardsoni* only, our searches on the Mawson Plateau in March 2019 revealed no signs of any *Anaspides*, with the tarns being completely dried out.

Anaspides tasmaniae was found at four separate localities. Three of these localities lie outside the Mt Field National Park, alongside the Florentine Road, with two creeks draining from Nicholls Spur and one creek draining from Tyenna Peak. All of these three creeks are direct tributaries of the Tyenna River (Fig. 3). These creeks were situated in a tree fern rainforest, with low to no water flow at the time of sampling; *Anaspides* were mainly found in small seemingly isolated pools. All of these sites are in low-altitude areas at 320–340 m asl. The creek drainages (Tributary to Tyenna River I and II) originate

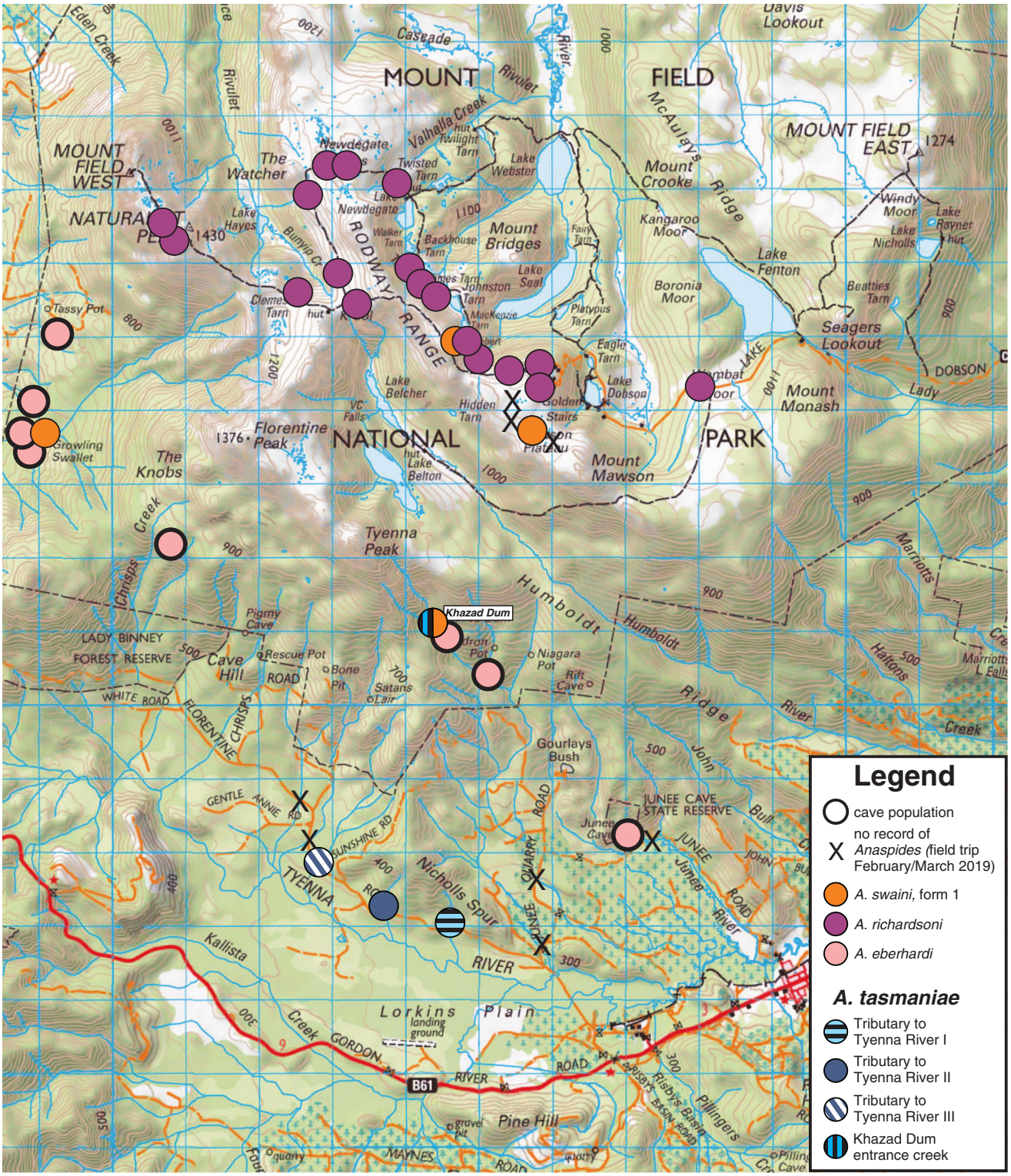


Fig. 3. Topographical map of Mt Field National Park to Gordon River Road with known collection sites of *Anaspides* from Ahyong (2016) and collection sites from this study. Base image by TASMAP (www.tasmap.tas.gov.au) © State of Tasmania.

Table 1. Water quality parameters for four different collection sites of *A. tasmaniae*

Locality	Date	Water temperature (°C)	pH	Conductivity (µS/cm)	Salinity (psu)
The Chalet, Mt Wellington	19.02.2019	6.6	8.8	39.6	0.0
Khazad Dum entrance	22.02.2019	–	7.75	74.9	0.0
Tributary to Tyenna River I	22.02.2019	10.5	7.6	365.0	0.1
Tributary to Tyenna River III	01.03.2019	11.1	6.47	90.5	0.0

at Nichols Spur with a maximum altitude of 515 m asl, but how far upstream *Anaspides* occurs is unknown. The neighbouring two tributaries to the Tyenna River crossing the Florentine Road as well as two tributaries to the Tyenna River crossing the Junee Quarry Road had no *A. tasmaniae* (see Fig. 3). The fourth locality is within the Mt Field National Park, where *A. tasmaniae* occurs in the inflow creek to the Khazad Dum cave (760 m asl) (Fig. 3). Here, *A. tasmaniae* was found sympatrically with *A. swaini* (form 1) and although *A. tasmaniae* and *A. swaini* were found outside the cave entrance, as well as in the twilight zone (up to 30 m inside the cave), both species showed no signs of cave adaptation.

Water quality parameters were taken from four different collection sites of *A. tasmaniae*: The Chalet, Mt Wellington; Khazad Dum cave; Tributary to the Tyenna River I and III (Table 1). The water temperatures ranged from 6.6°C at Mt Wellington to 10.5–11.1°C at the other collection sides. The pH ranged from slightly acidic (6.47 at Tributary to the Tyenna River III) to alkaline (8.8 at Mt Wellington, 7.75 at Khazad Dum cave and 7.6 at Tributary to the Tyenna River I). The conductivity within the localities was always low, ranging from 39.6 µS/cm at Mt Wellington over 74.9 µS/cm at Khazad Dum and 90.5 µS/cm at Tributary to the Tyenna River I to 365 µS/cm at Tributary to the Tyenna River III. The salinity ranged in all localities between 0.0 and 0.1 psu.

Analyses of COI and 16S sequences of *Anaspides tasmaniae* from each of the studied localities recovered three haplotype lineages with six different haplotypes in COI and three haplotypes in 16S (Fig. 4). The first lineage comprises specimens found on the east and south-east side of Mt Wellington, whereas the specimens of the remaining two lineages are from within and adjacent to the Mt Field National Park. Specimens of the second lineage are from the entrance creek of Khazad Dum and specimens of the third lineage are from tributaries of the Tyenna River I, II and III draining from Nicholls Spur and Tyenna Peak (Fig. 3). Between the lineages we found only slight genetic differentiation (uncorrected p-distances: COI: 1.1–1.6%, 16S: 0.3–0.6%). In 28S, individuals of all three lineages share the same haplotype (Fig. 4).

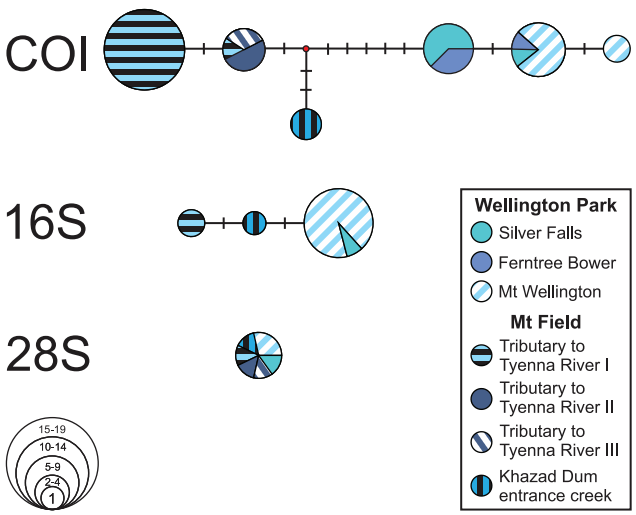


Fig. 4. COI, 16S and 28S median joining haplotype networks of *Anaspides tasmaniae*. Colours correspond to figure legend. The size of each haplotype corresponds to the number of individuals sharing that specific haplotype (see scale). Each dash corresponds to one mutation. The collection sites Silver Falls, Ferntree Bower and Mt Wellington are situated in Wellington Park, and Tributary to Tyenna River I–III and Khazad Dum entrance creek are located in and near Mt Field National Park.

Discussion

After the revision of *Anaspides* by Ahyong (2016), the type species of the genus, *A. tasmaniae*, was shown not to be widespread throughout Tasmania, as had long been believed. It has a much more restricted range, confirmed by Ahyong (2016) only from the east and south-east side of Mt Wellington. We now provide the first records of true *A. tasmaniae* from outside of Mt Wellington. *Anaspides tasmaniae* is present in three tributaries of the Tyenna River near Mt Field National Park as well as in the inflow waters of Khazad Dum (Fig. 5*b*, *g*). These localities are more than 50 km from the localities at which *A. tasmaniae* occurs at Mt Wellington and the water bodies are connected only via the Tyenna and Derwent rivers, in which *Anaspides*, however, does not occur (Fig. 1). Notably, *A. tasmaniae* occurs together with *A. swaini* (form 1) in the inflow creek of Khazad Dum, which is one of the few documented instances of sympatry in *Anaspides* and the only known locality where two *Anaspides* species actually occur in syntopy. There is no evidence for gene flow between these two species (unpubl. data).

Ahyong (2016) reported specimens from Khazad Dum cave (Ahyong 2016, fig. 34E–H) with a more rounded posterior telson margin as in *A. tasmaniae*, armed pleonite 5–6 terga and usually armed pleura as well, but tentatively considered these specimens to be aberrant *A. swaini*. We now reidentify these specimens as *A. tasmaniae*. Our specimens showed no apparent cave adaptations, which was also noted by Ahyong



Fig. 5. Typical habitats and appearance of *A. tasmaniae*: (*a*) small residual pool of a runnel near Florentine Road (Tributary to Tyenna River III), Markus Grams measuring water parameters; (*b*) inflow creek to Khazad Dum cave; (*c*) small pool in runnel at Mt Wellington; (*d*) male, Creek on Junee Florentine Road from Nicholls Spur (Tributary to Tyenna River I); (*e*) female, creek on Junee Florentine Road from Nicholls Spur (Tributary to Tyenna River I); (*f*) female, small pool at Mt Wellington, the Chalet; (*g*) inflow creek and twilight zone of Khazad Dum cave; (*h*) adult specimens in a small pool at The Chalet, Mt Wellington.

(2016). Interestingly, Ahyong (2016) mentioned also anomalous specimens similar to those from Khazad Dum from Risby Basin cave (located at the foot of the Maydena Range south of Gordon River Road, 8 km from Khazad Dum and draining as well into the Tyenna River), which potentially could also represent *A. tasmaniae*.

Furthermore, our searches 'confirmed' the absence of *Anaspides* on the Wellington Plateau. *Anaspides* was historically recorded from tarns on the plateau but has not been recorded there since major bushfires swept the area in the 1930s, permanently altering the habitat, resulting in the loss of tarns and swamp flora (O'Brien 1990). Ahyong (2016) also mentioned that Manton (1930) observed two colour forms in *Anaspides* on Mt Wellington: a dark brown to olive-green form found on the Mt Wellington plateau, and a light brown form occurring on the slopes. Manton's dark form probably refers to *Anaspides swaini* (form 3), and the light brown form, to *A. tasmaniae*. Our observations support these hypotheses with *A. tasmaniae* ranging from light to medium brown (Fig. 5*d–f*, *h*) and *Anaspides swaini* (form 3) being much darker, ranging from dark brown to dark olive green. In the Browns River catchment, we found only *A. tasmaniae*, although specimens of *A. swaini* (form 3) were collected there in the early 20th century, having presumably been translocated from the North-west Bay catchment via a now defunct aqueduct (Ahyong 2016). Evidently, the translocated *A. swaini* population has not survived.

The discovery of *A. tasmaniae* at independent localities around Mt Field, all distant from Mt Wellington, begs the question of whether the observed distribution is artificial or natural. Although *A. swaini* appears to have been translocated as a result of water-supply engineering in the early 20th century, no similar activities have occurred between Mt Wellington and Mt Field, nor are the localities in question subject to fishery stocking or other plausible interventions. Either way, if the Mt Field populations of *A. tasmaniae* were the result of artificial translocation from Mt Wellington, shared haplotypes would be expected. However, the genetic divergence between Mt Wellington and Mt Field populations indicates that the disjunct distribution is more likely to be natural, and we hypothesise that it relates to glacial events. The main limiting factor for the distribution of *Anaspides* appears to be water temperature (Williams 1965*a*; Swain and Reid 1983; O'Brien 1990). The species prefer cold water, although they are able to temporarily tolerate elevated water temperatures (Williams 1965*a*; Swain and Reid 1983). Also, the concentration of dissolved solids and turbidity could play a role in their distribution (Williams 1965*a*; Swain and Reid 1983; O'Brien 1990). Smith (1908) described the waters in which *Anaspides* occurs as 'ice-cold waters of absolute clarity', which is consistent with our field observations. Considering this, and that temperatures during glacial periods in the Pleistocene were 6–10°C lower than today, in combination with a lowered snowline (~1000–1500 m lower than current) and a lowered sea level (~120 m, 25 000 years ago) (Colhoun 1985; Lambeck and Chappell 2001; Thrush 2008; Colhoun *et al*. 2010), the Tyenna and Derwent rivers were potentially favourable habitats at that time. Thus, during glacial periods, *A. tasmaniae* may have occupied a wider range including lower altitudes that encompassed the Tyenna and Derwent River catchments during the Pleistocene glaciations. The top of the mountains might not have been inhabited during glaciations although it is not clear whether the plateau of Mt Wellington had an ice cap (Davies 1958) whereas the plateaus of the Mt Field National Park were glaciated several times (Kiernan 1990; Mackintosh *et al*. 2006; Colhoun *et al*. 2010). The increasing interglacial temperatures would have led to contractions of suitable *Anaspides* habitat throughout Tasmania. In the case of *A. tasmaniae*, we suggest it occupied a wider continuous range during the Pleistocene glacials, and with postglacial warming became restricted to the higher and colder areas at Mt Wellington and in the Mt Field area, where they are relictual today.

Conservation

Although our research extends the known distribution (four new collection sites) of *A. tasmaniae* as well as its known genetic diversity through discovery of three distinct haplotype clusters in COI and 16S, the overall geographic range is still limited and the populations are vulnerable. This is especially the case for the three tributaries of the Tyenna River, which are outside the protected area of the Mt Field National Park in low-altitude areas. Additionally, the presence of *Anaspides swaini* (form 3) in adjacent drainages at Mt Wellington suggests that *A. tasmaniae* is indeed limited to the three water catchments at the east and south-east side of Mt Wellington. As Ahyong (2016) stated, its conservation status requires reassessment to precisely determine its current distribution and population size, especially within the Mt Field National Park.

The Mt Field National Park and the Junee–Florentine Karst area can be considered as a hotspot of *Anaspides* diversity, with four species and several different genetic lineages occurring in that area. Furthermore, Mt Field National Park and the adjacent landscapes have great importance for the populations of *A. tasmaniae*, which is found only in a small range at the east and south-east of Mt Wellington and in four different localities in and alongside the Mt Field National Park. Current climatic trends will probably see further contraction of suitable habitats of *Anaspides* to higher altitudes in the future, making conservation planning even more poignant. It is uncertain if the Mawson Plateau or Mount Wellington Plateau will again become suitable habitats for *Anaspides* in the future. For the protection of this iconic species we suggest formal protection of the habitat of *A. tasmaniae* in the Mt Field area, perhaps by extension of the Mt Field National Park south over the Nicholls Spur to the Florentine Road between Junee Quarry Road and Drewhurst Road.

Conflicts of interest

The authors declare no conflicts of interest.

Declaration of funding

Collection of specimens in 2017 was funded by the German Science Foundation (DFG RI 837/22-1) and in 2019 was partly funded by the DAAD (Nr. 57438025, Kurzstipendien für

Doktoranden, 2019/2020) and the University of Rostock (Promotionsstipendienprogramm, 'Unsere Besten promovieren in Rostock'). The present project is funded by the German Science Foundation (DFG RI 837/22-2).

Acknowledgements

We are grateful to Alastair Richardson, Michael Driessen, Arthur Clarke, Cathy Plowman, David Butler, and Stefan Eberhard for enthusiastic support of our *Anaspides* research. We further thank the University of Tasmania, Institute for Zoology, especially David Green, for providing us with scientific equipment for our field trips. We are thankful to Markus Grams and Marian Reinhardt for assistance in the field and to Andrew Palfreyman for providing a new record on Mt Wellington. Specimens were collected under Tasmanian Department of Primary Industries, Parks, Water and Environment permit nos TFA16347 and FA18250. Ralf Bastrop (University of Rostock) provided the infrastructure for sequencing some of the data. We are grateful to the reviewers for their comments and suggestions.

References

Ahyong, S. T. (2015). Preliminary diagnoses of three new species of Tasmanian mountain shrimps, *Anaspides* Thomson, 1894 (Syncarida, Anaspidacea, Anaspididae). *Zootaxa* **3957**, 596–599. doi:10.11646/zootaxa.3957.5.8

Ahyong, S. T. (2016). The Tasmanian mountain shrimps, *Anaspides* Thomson, 1894 (Crustacea, Syncarida, Anaspididae). *Records of the Australian Museum* **68**, 313–364. doi:10.3853/j.2201-4349.68.2016.1669

Ahyong, S. T., and Alonso-Zarazaga, M. A. (2017). Anaspidesidae, a new family for syncarid crustaceans formerly placed in Anaspididae Thomson, 1893. *Records of the Australian Museum* **69**, 257–258. doi:10.3853/j.2201-4349.69.2017.1680

Benson, D. A., Karsch-Mizrachi, I., Lipman, D. J., Ostell, J., and Wheeler, D. L. (2003). GenBank. *Nucleic Acids Research* **31**, 23–27. doi:10.1093/nar/gkg057

Colhoun, E. A. (1985). Glaciations of the west coast range, Tasmania. *Quaternary Research* **24**, 39–59. doi:10.1016/0033-5894(85)90082-1

Colhoun, E. A., Kiernan, K., Barrows, T. T., and Goede, A. (2010). Advances in Quaternary studies in Tasmania. In 'Australian Landscapes'. (Eds P. Bishop, and B. Pillans.) pp. 165–183. (Geological Society: London.)

Davies, J. L. (1958). The cryoplanation of Mount Wellington. *Papers and Proceedings of the Royal Society of Tasmania* **92**, 151–154.

Folmer, O., Black, M., Hoeh, W., Lutz, R., and Vrijenhoek, R. (1994). DNA primers for amplification of mitochondrial cytochrome oxidase subunit I from diverse metazoan invertebrates. *Molecular Marine Biology and Biotechnology* **3**, 294–299.

Goede, A (1967). Tasmanian cave fauna: character and distribution. *Helictite* **5**, 71–86.

Jarman, S. N., and Elliott, N. G. (2000). DNA evidence for morphological and cryptic Cenozoic speciations in the Anaspididae, 'living fossils' from the Triassic. *Journal of Evolutionary Biology* **13**, 624–633. doi:10.1046/j.1420-9101.2000.00207.x

Kiernan, K. (1990). The extent of late Cenozoic glaciation in the Central Highlands of Tasmania, Australia. *Arctic and Alpine Research* **22**, 341–354. doi:10.2307/1551459

Kumar, S., Stecher, G., Li, M., Knyaz, C., and Tamura, K. (2018). MEGA X: molecular evolutionary genetics analysis across computing platforms. *Molecular Biology and Evolution* **35**, 1547–1549. doi:10.1093/molbev/msy096

Lake, P. S., and Coleman, D. J. (1977). On the subterranean syncarids of Tasmania. *Helictite* **15**, 12–17.

Lambeck, K., and Chappell, J. (2001). Sea level change through the last glacial cycle. *Science* **292**, 679–686. doi:10.1126/science.1059549

Mackintosh, A. N., Barrows, T. T., Colhoun, E. A., and Fifield, L. K. (2006). Exposure dating and glacial reconstruction at Mt. Field, Tasmania, Australia, identifies MIS 3 and MIS 2 glacial advances and climatic variability. *Journal of Quaternary Science* **21**, 363–376. doi:10.1002/jqs.989

Manton, S. M. (1930). 36. Notes on the habits and feeding mechanisms of *Anaspides* and *Paranaspides* (Crustacea, Syncarida). *Proceedings of the Zoological Society of London* **100**, 791–800. doi:10.1111/j.1096-3642.1930.tb00998.x

O'Brien, D. P. (1990). The conservation status of the mountain shrimp (*Anaspides tasmaniae* and *Anaspides spinulae*): a report on its distribution, ecology and taxonomy, including recommendations for management. Department of Parks, Wildlife and Heritage, Hobart.

Richter, S., Olesen, J., and Wheeler, W. C. (2007). Phylogeny of Branchiopoda (Crustacea) based on a combined analysis of morphological data and six molecular loci. *Cladistics* **23**, 301–336. doi:10.1111/j.1096-0031.2007.00148.x

Richter, S., Schwentner, M., Wirkner, C. S., and Ahyong, S. T. (2018). Phylogeny and species diversity of Tasmanian mountain shrimps and their relatives (Crustacea, Anaspidesidae). *Zoologica Scripta* **47**, 84–105. doi:10.1111/zsc.12263

Smith, G. W. (1908). Preliminary account of the habits and structure of the Anaspididae, with remarks on some other fresh-water Crustacea from Tasmania. *Proceedings of the Royal Society of London* **80**, 465–473.

Swain, R., and Reid, C. I. (1983). Observations on the life history and ecology of *Anaspides tasmaniae* (Thomson) (Syncarida: Anaspididae). *Journal of Crustacean Biology* **3**, 163–172. doi:10.2307/1548252

Thompson, J. D., Higgins, D. G., and Gibson, T. J. (1994). CLUSTAL W: improving the sensitivity of progressive multiple sequence alignment through sequence weighting, position-specific gap penalties and weight matrix choice. *Nucleic Acids Research* **22**, 4673–4680. doi:10.1093/nar/22.22.4673

Thomson, G. M. (1893). Notes on Tasmanian Crustacea, with descriptions of new species. *Papers & Proceedings of the Royal Society of Tasmania* 45–76.

Thomson, G. M. (1894). III. On a freshwater schizopod from Tasmania. *Transactions of the Linnean Society of London, 2nd Series. Zoology* **6**, 285–303.

Thrush, M. N. (2008). The Pleistocene glaciations of the Cradle Mountain region, Tasmania. Ph.D. Thesis, University of Newcastle, Newcastle.

Williams, W. D. (1965*a*). Ecological notes on Tasmanian Syncarida (Crustacea: Malacostraca), with a description of a new species of *Anaspides*. *Internationale Revue der Gesamten Hydrobiologie und Hydrographie* **50**, 95–126. doi:10.1002/iroh.19650500109

Williams, W. D. (1965*b*). Subterranean occurrence of *Anaspides tasmaniae* (Thomson) (Crustacea, Syncarida). *International Journal of Speleology* **1**, 333–337. doi:10.5038/1827-806X.1.3.7

Xiong, B., and Kocher, T. D. (1991). Comparison of mitochondrial DNA sequences of seven morphospecies of black flies (Diptera: Simuliidae). *Genome* **34**, 306–311. doi:10.1139/g91-050

Handling Editor: Steven Cooper

3 Höpel, C. G., Richter, S., & Ahyong, S. T. (2023). A new species of Tasmanian mountain shrimp, *Anaspides driesseni* sp. nov. (Malacostraca, Anaspidacea, Anaspidesidae). Records of the Australian Museum, 75(1), 25-43.

Records of the Australian Museum (2023)
vol. 75, issue no. 1, pp. 25–43
https://doi.org/10.3853/j.2201-4349.75.2023.1829

Records of the Australian Museum
a peer-reviewed open-access journal
published by the Australian Museum, Sydney
communicating knowledge derived from our collections
ISSN 0067-1975 (print), 2201-4349 (online)

A New Species of Tasmanian Mountain Shrimp, *Anaspides driesseni* sp. nov. (Malacostraca, Anaspidacea, Anaspidesidae)

Christoph G. Höpel[1], Stefan Richter[1], and Shane T. Ahyong[2]

[1] Allgemeine & Spezielle Zoologie, Institut für Biowissenschaften, Universität Rostock, Universitätsplatz 2, 18055 Rostock, Germany

[2] Australian Museum Research Institute, Australian Museum, 1 William Street, Sydney NSW 2010, Australia, and

[2] School of Biological, Earth & Environmental Sciences, University of New South Wales, Kensington NSW 2052, Australia

Abstract. Species of the genus *Anaspides*, known as mountain shrimps, are endemic to Tasmania and inhabit a variety of freshwater habitats such as mountain tarns, pools, creeks and runnels, as well as caves. Until 2015 only two species of Tasmanian mountain shrimps were recognized, *A. tasmaniae* (Thomson, 1893), which was believed to be widespread all over the island and *A. spinulae* from Lake St. Clair. Revision of the genus by Ahyong in 2016 recognized 7 species, most having narrow geographic distributions. Only two widespread species remained: *A. richardsoni,* occurring mainly on the Central Plateau and its margins, and *A. swaini*, occurring largely in south-western Tasmania. Notably, within *A. swaini*, three geographically correlated morphological forms were observed. We re-evaluated all three forms of *A. swaini* and herein describe one of the forms as a new species, *A. driesseni*, on the basis of morphological and molecular data. *Anaspides driesseni* corresponds to *A. swaini* form 3 and occurs mainly in south-eastern Tasmania from the Hartz Mountains over the Snowy Mountains to the Wellington Range. Telson structure, spination and male secondary sexual characters proved taxonomically instrumental.

Introduction

The investigations of Ahyong (2015, 2016) significantly expanded our taxonomic knowledge of *Anaspides* leading to the morphological description of five new species, *A. clarkei* Ahyong, 2015*, A. jarmani* Ahyong, 2015*, A. swaini* Ahyong, 2015*, A. eberhardi* Ahyong, 2016 and *A. richardsoni* Ahyong, 2016, bringing the known fauna to seven species. Ahyong (2016), however, observed geographically correlated morphological variation in some species (e.g., *A. swaini, A. richardsoni*) suggesting additional unrealized taxonomic diversity. *Anaspides swaini* is notable, having the widest putative distribution, ranging from southern Tasmania from the Weld River, Snowy Mountains region, Mt Field and Mt Wellington (North West Bay River catchment) to the Western Arthurs Range, throughout the Franklin-Gordon drainage, north to Lake Rhona and Frenchmans Cap, Mt Rufus and the vicinity of Lake St. Clair on the Central Plateau. Ahyong (2016) observed three morphologically different forms occurring in different areas and drainages. Form 1 corresponds to *A. swaini sensu stricto* and has a south-western range, essentially around the periphery of

Keywords: Crustacea, Anaspidacea, *Anaspides*, Tasmania, freshwater, shrimp
ZooBank registration: urn:lsid:zoobank.org:pub:21FA515F-B0F6-4455-BE03-B8A8745E107D
ORCID: Christof G. Höpel 0000-0001-6827-3767, Stefan Richter 0000-0002-2865-2751, and Shane T. Ahyong, 0000-0002-2820-4158
Corresponding author: Christoph G. Höpel christoph.hoepel@uni-rostock.de
Received: 20 October 2022 **Accepted**: 5 February 2023 **Published**: 15 March 2023 (in print and online simultaneously)
Publisher: The Australian Museum, Sydney, Australia (a statutory authority of, and principally funded by, the NSW State Government)
Citation: Höpel, Christoph G., Stefan Richter, and Shane T. Ahyong. 2023. A new species of Tasmanian mountain shrimp, *Anaspides driesseni* sp. nov. (Malacostraca, Anaspidacea, Anaspidesidae). *Records of the Australian Museum* 75(1): 25–43.
https://doi.org/10.3853/j.2201-4349.75.2023.1829
Copyright: © 2023 Höpel, Richter, Ahyong. This is an open access article licensed under a Creative Commons Attribution 4.0 International License (CC BY 4.0), which permits unrestricted use, distribution, and reproduction in any medium, provided the original authors and source are credited.

Lake Gordon and Lake Pedder, from Lake Rhona to Mt Field and Mt Mueller to the Snowy Mountains, Federation Peak, the Arthur Ranges and at least as far north as Coronation Peak on the south-western side of Lake Pedder. It is usually more spinose than form 2 and 3. *Anaspides swaini* form 1 was also included in the molecular study of Richter *et al*. (2018) where they found high intraspecific distances (especially within COI) between specimens that were collected alongside the Mueller Road occurring sympatrically in the sampled rivers. Form 2 has a northern range beyond Lakes Gordon and Pedder, from the southern part of the Central Plateau, where it ranges from the western vicinity of Lake St. Clair including the Cuvier Valley and Mt Rufus south to Butlers Gorge and Wentworth Hills and Frenchmans Cap; it continues further south in caves in the Nicholls Range karst (Bill Nielson) and Franklin River karst (Kutikina), where it is apparently isolated from surface forms (Eberhard *et al*., 1991). Form 3 has a south-eastern distribution; it occurs east of Tyler's Line, ranging from the western and northern Wellington Range, including the North West Bay River catchment of Mt Wellington, to at least the Huonville area.

The taxonomic status of *A. swaini* form 2 is currently subject to ongoing study, but herein, we formally recognize *A. swaini* form 3 as new to science.

Material and methods

Collection, identification of specimens and morphological methods

Morphological terminology follows Ahyong (2015, 2016). Measurements of specimens are of total body length, measured from the apex of the rostrum to the tip of the telson. Abbreviations: above sea-level (*asl*); feet (*ft*); indeterminate (*indet*); juvenile (*juv.*).

For the taxonomic descriptions, ethanol preserved specimens were softened in glycerol for 1–2 days before dissection of appendages along the left side of the body. Illustrations were produced using a drawing tube attached to a Nikon Eclipse 80i or Leica M165C stereomicroscope.

Specimens are deposited in the collections of the Australian Museum, Sydney (AM); South Australian Museum, Adelaide (SAMA); Tasmanian Museum and Art Gallery, Hobart (TMAG); National Museum of Natural History, Smithsonian Institution, Washington DC (USNM); Western Australian Museum (WAM); and Zoological Collection, Universität Rostock (ZSRO).

A total of 94 specimens of *A. swaini* and *A. driesseni* sp. nov. were collected and newly sequenced for this study (Table 1). In addition, a total of 47 COI, 57 16S rRNA and 30 28S sequences from the study by Richter *et al*. (2018) were included to calculate genetic distances.

Molecular methods

Tissue was removed from thoracopod 8 or from the pleopods. The DNA extraction was performed with the innuPrep Forensic Kit (Analytik Jena) and the DNeasy Blood and Tissue Kit (Qiagen), following the manufacturer´s instruction. Three different markers were partially sequenced: mitochondrial cytochrome c oxidase subunit I (COI) and 16S rRNA as well as the nuclear 28S rRNA. The polymerase chain reaction (PCR) had a total volume of 30 µl which contained 3 µl of each primer (each 10 µM), 3 µl 10× buffer (Sigma Aldrich), 3 µl dNTP mix (2 mM, Biozym), 2.58 µl $MgCl_2$ (25 mM, Sigma Aldrich), 0.12 µl Taq-polymerase (Sigma Aldrich), 10.71 µl ultrapure water and 4.5 µl of the DNA extract. Primers were LCO2 5'-TCN ACH AAY CAT AAA GAY ATT GGA AC-3' (Richter *et al*., 2018), HCO2198 5'-TAA ACT TCA GGG TGA CCA AAA AAT CA-3' (Folmer *et al*., 1994) for COI, 16Sa 5'-CGC CTG TTT ATC AAA AAC AT-3', 16Sb 5'-CTC CGG TTT GAA CTC AGA TCA-3' (Xiong & Kocher, 1991) for 16S and rd4.8a 5'-ACC TAT TCT CAA ACT TTA AAT GG-3', rd7b1 5'-GAC TTC CCT TAC CTA CAT-3' (Richter *et al*., 2007) for 28S rRNA. PCR amplification programs comprised an initial denaturation step at 94°C for 1 min, followed by 40 amplification cycles (94°C for 30 s, 50°C for 30 s, 72°C for 60 s) for COI, 38 amplification cycles (94°C for 30 s, 48°C for 30 s, 72°C for 60 s) for 16S, 35 amplification cycles (94°C for 30 s, 55°C for 30 s, 72°C for 60 s) for 28S and a final elongation step at 72°C for 5 min.

All PCR reactions were performed with a Mastercycler gradient (Eppendorf). PCR products were visualized by gel electrophoresis, using 5 µl of the PCR product with 1.5 µl loading buffer DNA b II (AppliChem) on a 1.2 % agarose/TAE gel stained with 5 µl Rotisafe (Carl Roth). PCR products were purified using paramagnetic beads (High Prep PCR, Magbio) following the manufacturer's instruction with a final volume of 25 µl. Sequencing of PCR products was performed in Lightrun 96 well plates by the company, Eurofins Genomics, as well as using the dideoxy chain termination method and cycle sequencing using an ABI Prism® Big Dye® Terminator V.1.1 Cycle Sequencing Kit. Cycle sequencing products were analysed by using capillary separation on an ABI Genetic Analyzer 3130 xl (Applied Biosystems/Hitachi). The resulting chromatograms were manually checked and adjusted with Geneious 2021.0.3 (Biomatters Limited). The sequences of all three gene fragments were separately aligned using Consensus Align implemented in Geneious Prime 2021.0.3 (Biomatters Limited) with default parameters. All sequences were deposited at GenBank (Benson *et al*., 2005) (accession numbers: OP684680–684764, OP686521–686535, OP686545–686569, OQ158727–OQ158764, OQ160856–OQ160881, OQ160958–OQ160970). Pairwise distances were calculated using MEGA X (Kumar *et al*., 2018). For pairwise distance analyses the uncorrected p-distance was calculated. Phylogenetic networks were calculated with Network 10.2.0.0. (Fluxus Technologies) separately for COI, 16S, and 28S alignments by using the median-joining method with the parameter epsilon set to 10.

Table 1. List of individuals newly sequenced for this study. For each specimen, ID, species, locality details, deposition and GenBank accession numbers are provided. Abbreviations: *(P)* denotes paratype; collectors: *SA*, S. Ahyong; *MD*, M. Driessen; *MG*, M. Grams; *CH*, C. Höpel; *AP*, A. Palfreyman; *MR*, M. Reinhardt; *SR*, S. Richter; and *MW*, M. Weiler. GenBank registrations listed under *28S, 16S* and *COI*.

ID	species	locality	latitude longitude	date	collectors	deposition	28S	16S	COI
Ana 143	*A. swaini*	Growling Swallet cave, "entrance hall"	-42.68974° 146.49950°	17.03.2017	CH, MR, SR	ZSRO CR69	—	—	OP684680
Ana 144	*A. swaini*	Growling Swallet cave, "entrance hall"	-42.68974° 146.49950°	17.03.2017	CH, MR, SR	ZSRO CR69	—	OP686521	OP684681
Ana 145	*A. swaini*	Growling Swallet cave, "entrance hall"	-42.68974° 146.49950°	17.03.2017	CH, MR, SR	ZSRO CR69	—	OP686522	OP684682
Ana 146	*A. driesseni* (P)	Myrtle Forest Creek MF 2	-42.86028° 147.15222°	28.02.2017	SA, CH, MR, SR	ZSRO CR67	OP686545	—	OP684728
Ana 147	*A. driesseni* (P)	Myrtle Forest Creek MF 2	-42.86028° 147.15222°	28.02.2017	SA, CH, MR, SR	ZSRO CR67	—	—	OP684729
Ana 148	*A. driesseni* (P)	Myrtle Forest Creek MF 2	-42.86028° 147.15222°	28.02.2017	SA, CH, MR, SR	ZSRO CR67	—	OP686534	OP684730
Ana 149	*A. swaini*	Garths Creek, Growling Swallet Cave	-42.68883° 146.50125°	17.03.2017	CH, MR, SR	ZSRO CR70	—	—	OP684683
Ana 150	*A. swaini*	Garths Creek, Growling Swallet Cave	-42.68883° 146.50125°	17.03.2017	CH, MR, SR	ZSRO CR70	—	—	OP684684
Ana 151	*A. swaini*	Garths Creek, Growling Swallet Cave	-42.68883° 146.50125°	17.03.2017	CH, MR, SR	ZSRO CR70	—	—	OP684685
Ana 152	*A. swaini*	Tributary of Weld Rv, Mueller Rd, 2 km behind west gate	-42.81269° 146.40881°	18.03.2017	CH, MR, SR	ZSRO CR73	—	OP686523	OP684686
Ana 153	*A. swaini*	Tributary of Weld Rv, Mueller Rd, 2 km behind west gate	-42.81269° 146.40881°	18.03.2017	CH, MR, SR	ZSRO CR73	OP686546	—	OP684687
Ana 154	*A. swaini*	Tributary of Weld Rv, Mueller Rd, 2 km behind west gate	-42.81269° 146.40881°	18.03.2017	CH, MR, SR	ZSRO CR73	—	OP686524	OP684688
Ana 155	*A. swaini*	Mueller Rd, 3.8 km behind west gate	-42.81069° 146.42728°	18.03.2017	CH, MR, SR	ZSRO CR74	—	—	OP684689
Ana 156	*A. swaini*	Mueller Rd, 3.8 km behind west gate	-42.81069° 146.42728°	18.03.2017	CH, MR, SR	ZSRO CR74	—	—	OP684690
Ana 157	*A. swaini*	Mueller Rd, 3.8 km behind west gate	-42.81069° 146.42728°	18.03.2017	CH, MR, SR	ZSRO CR74	—	—	OP684691
Ana 158	*A. swaini*	Mueller Rd, 4.4 km behind west gate	-42.81047° 146.43333°	18.03.2017	CH, MR, SR	ZSRO CR75	—	—	OP684692
Ana 159	*A. swaini*	Mueller Rd, 4.4 km behind west gate	-42.81047° 146.43333°	18.03.2017	CH, MR, SR	ZSRO CR75	—	—	OP684693
Ana 160	*A. swaini*	Mueller Rd, 4.4 km behind west gate	-42.81047° 146.43333°	18.03.2017	CH, MR, SR	ZSRO CR75	—	—	OP684694
Ana 161	*A. swaini*	Tributary of Weld Rv, Müller Rd, 5.1 km behind west gate	-42.81194° 146.44100°	18.03.2017	CH, MR, SR	ZSRO CR76	—	—	OP684695
Ana 162	*A. swaini*	Tributary of Weld Rv, Müller Rd, 5.1 km behind west gate	-42.81194° 146.44100°	18.03.2017	CH, MR, SR	ZSRO CR76	—	OP686525	OP684696
Ana 163	*A. swaini*	Tributary of Weld Rv, Müller Rd, 5.1 km behind west gate	-42.81194° 146.44100°	18.03.2017	CH, MR, SR	ZSRO CR76	—	—	OP684697
Ana 164	*A. swaini*	Tributary of Weld Rv, Müller Rd, 5.1 km behind west gate	-42.81011° 146.46025°	18.03.2017	CH, MR, SR	ZSRO CR77	—	—	OP684698
Ana 165	*A. swaini*	Tributary of Weld Rv, Müller Rd, 5.1 km behind west gate	-42.81011° 146.46025°	18.03.2017	CH, MR, SR	ZSRO CR77	—	—	OP684699
Ana 166	*A. swaini*	Tributary of Weld Rv, Müller Rd, 5.1 km behind west gate	-42.81011° 146.46025°	18.03.2017	CH, MR, SR	ZSRO CR77	—	OP686526	OP684700
Ana 167	*A. swaini*	Tributary of Weld Rv, Müller Rd, 5.1 km behind west gate	-42.81011° 146.46025°	18.03.2017	CH, MR, SR	ZSRO CR77	OP686547	—	OP684701
Ana 168	*A. swaini*	Styx River, Mueller Rd, 11.5 km behind west gate	-42.80467° 146.49436°	18.03.2017	CH, MR, SR	ZSRO CR78	—	—	OP684702
Ana 169	*A. swaini*	Styx River, Mueller Rd, 11.5 km behind west gate	-42.80467° 146.49436°	18.03.2017	CH, MR, SR	ZSRO CR78	—	—	OP684703
Ana 170	*A. driesseni*	Tributary of South Styx River, (Nevada Peak)	-42.84225° 146.61978°	18.03.2017	CH, MR, SR	ZSRO CR79	OP686548	OP686531	OP684731
Ana 310	*A. driesseni* (P)	Myrtle Forest Creek MF 1	-42.85944° 147.15917°	28.02.2017	SA, CH, MR, SR	ZSRO CR66	—	—	OP684732
Ana 311	*A. driesseni* (P)	Myrtle Forest Creek MF 1	-42.85944° 147.15917°	28.02.2017	SA, CH, MR, SR	ZSRO CR66	—	—	OP684733
Ana 312	*A. driesseni* (P)	Myrtle Forest Creek MF 1	-42.85944° 147.15917°	28.02.2017	SA, CH, MR, SR	ZSRO CR66	—	—	OP684734
Ana 313	*A. driesseni* (P)	Myrtle Forest Creek MF2	-42.86028° 147.15222°	28.02.2017	SA, CH, MR, SR	ZSRO CR67	—	—	OP684735
Ana 314	*A. driesseni* (P)	Myrtle Forest Creek MF2	-42.86028° 147.15222°	28.02.2017	SA, CH, MR, SR	ZSRO CR67	—	—	OP684736
Ana 315	*A. swaini*	Growling Swallet cave, "entrance hall"	-42.68974° 146.49950°	17.03.2017	CH, MR, SR	ZSRO CR69	—	—	OP684704
Ana 316	*A. swaini*	Growling Swallet cave, "entrance hall"	-42.68974° 146.49950°	17.03.2017	CH, MR, SR	ZSRO CR69	—	—	OP684705
Ana 317	*A. swaini*	Growling Swallet cave, "entrance hall"	-42.68974° 146.49950°	17.03.2017	CH, MR, SR	ZSRO CR69	—	—	OP684706
Ana 318	*A. swaini*	Garths Creek, Growling Swallet Cave	-42.68931° 146.49833°	17.03.2017	CH, MR, SR	ZSRO CR71	—	—	OP684707
Ana 319	*A. swaini*	Garths Creek, Growling Swallet Cave	-42.68931° 146.49833°	17.03.2017	CH, MR, SR	ZSRO CR71	OP686549	—	OP684708
Ana 320	*A. swaini*	Garths Creek, Growling Swallet Cave	-42.68931° 146.49833°	17.03.2017	CH, MR, SR	ZSRO CR71	—	—	OP684709
Ana 321	*A. swaini*	Garths Creek, Growling Swallet Cave	-42.68931° 146.49833°	17.03.2017	CH, MR, SR	ZSRO CR71	—	—	OP684710
Ana 322	*A. swaini*	Garths Creek, Growling Swallet Cave	-42.68931° 146.49833°	17.03.2017	CH, MR, SR	ZSRO CR71	—	—	OP684711
Ana 323	*A. swaini*	Tributary of Weld Rv, Mueller Rd, 2 km behind west gate	-42.81269° 146.40881°	18.03.2017	CH, MR, SR	ZSRO CR73	—	—	OP684712

Table 1 continued.

ID	species	locality	latitude longitude	date	collectors	deposition	28S	16S	COI
Ana 324	*A. swaini*	Tributary of Weld Rv, Mueller Rd, 2 km behind west gate	-42.81269° 146.40881°	18.03.2017	CH, MR, SR	ZSRO CR73	—	—	OP684713
Ana 325	*A. swaini*	Tributary of Weld Rv, Mueller Rd, 2 km behind west gate	-42.81269° 146.40881°	18.03.2017	CH, MR, SR	ZSRO CR73	—	—	OP684714
Ana 326	*A. swaini*	Tributary of Weld Rv, Mueller Rd, 4.4 km behind west gate	-42.81047° 146.43333°	18.03.2017	CH, MR, SR	ZSRO CR75	—	—	OP684715
Ana 327	*A. swaini*	Tributary of Weld Rv, Mueller Rd, 4.4 km behind west gate	-42.81047° 146.43333°	18.03.2017	CH, MR, SR	ZSRO CR75	—	—	OP684716
Ana 328	*A. swaini*	Tributary of Weld Rv, Mueller Rd, 4.4 km behind west gate	-42.81047° 146.43333°	18.03.2017	CH, MR, SR	ZSRO CR75	—	—	OP684717
Ana 329	*A. swaini*	Tributary of Weld Rv, Mueller Rd, 5.1 km behind west gate	-42.81194° 146.44100°	18.03.2017	CH, MR, SR	ZSRO CR76	—	—	OP684718
Ana 330	*A. swaini*	Tributary of Weld Rv, Mueller Rd, 5.1 km behind west gate	-42.81194° 146.44100°	18.03.2017	CH, MR, SR	ZSRO CR76	—	—	OP684719
Ana 331	*A. swaini*	Tributary of Weld Rv, Mueller Rd, 5.1 km behind west gate	-42.81194° 146.44100°	18.03.2017	CH, MR, SR	ZSRO CR76	—	—	OP684720
Ana 332	*A. swaini*	Tributary of Weld Rv, Mueller Rd, 7.1 km behind west gate	-42.81011° 146.46025°	18.03.2017	CH, MR, SR	ZSRO CR77	—	—	OP684721
Ana 333	*A. swaini*	Tributary of Weld Rv, Mueller Rd, 7.1 km behind west gate	-42.81011° 146.46025°	18.03.2017	CH, MR, SR	ZSRO CR77	—	—	OP684722
Ana 334	*A. swaini*	Tributary of Weld Rv, Mueller Rd, 7.1 km behind west gate	-42.81011° 146.46025°	18.03.2017	CH, MR, SR	ZSRO CR77	—	—	OP684723
Ana 335	*A. swaini*	Tributary of Styx Rv, Mueller Rd, 11.5 km behind west gate	-42.80467° 146.49436°	18.03.2017	CH, MR, SR	ZSRO CR78	OP686550	—	OP684724
Ana 489	*A. swaini*	Sanctuary Lake, Frankland Range	-42.93235° 146.03179°	13.02.2018	MD	ZSRO CR172	OP686551	—	—
Ana 490	*A. swaini*	Sanctuary Lake, Frankland Range	-42.93235° 146.03179°	13.02.2018	MD	AM P106566	OP686552	OP686527	—
Ana 491	*A. swaini*	Lake Sirona	-43.16481° 146.33769°	13.02.2018	MD	ZSRO CR173	OP686553	OP686528	OP684725
Ana 492	*A. swaini*	Lake Sirona	-43.16481° 146.33769°	13.02.2018	MD	ZSRO CR173	OP686554	OP686529	—
Ana 493	*A. swaini*	Lake Sirona	-43.16481° 146.33769°	13.02.2018	MD	AM P106567	OP686555	—	—
Ana 494	*A. swaini*	Lake Cygnus	-43.12971° 146.23611°	13.02.2018	MD	ZSRO CR174	OP686556	—	—
Ana 495	*A. swaini*	Lake Cygnus	-43.12971° 146.23611°	13.02.2018	MD	AM P106568	OP686557	—	—
Ana 496	*A. driesseni*	unnamed creek on Pipeline track	-42.95144° 147.23047°	19.02.2019	SA, MG, CH, SR	ZSRO CR175	—	—	OP684737
Ana 497	*A. driesseni*	unnamed creek on Pipeline track	-42.95144° 147.23047°	19.02.2019	SA, MG, CH, SR	ZSRO CR175	OP686558	—	OP684738
Ana 498	*A. driesseni*	unnamed creek on Pipeline track	-42.95144° 147.23047°	19.02.2019	SA, MG, CH, SR	ZSRO CR175	—	OP686532	OP684739
Ana 499	*A. driesseni*	unnamed creek on Pipeline track	-42.95144° 147.23047°	19.02.2019	SA, MG, CH, SR	ZSRO CR175	OP686559	—	OP684740
Ana 500	*A. driesseni*	Levert Rivulet	-42.94593° 147.23030°	19.02.2019	SA, MG, CH, SR	ZSRO CR176	—	—	OP684741
Ana 501	*A. driesseni*	Levert Rivulet	-42.94593° 147.23030°	19.02.2019	SA, MG, CH, SR	ZSRO CR176	OP686560	—	OP684742
Ana 502	*A. driesseni*	Levert Rivulet	-42.94593° 147.23030°	19.02.2019	SA, MG, CH, SR	ZSRO CR176	OP686561	—	OP684743
Ana 503	*A. driesseni*	Levert Rivulet	-42.94593° 147.23030°	19.02.2019	SA, MG, CH, SR	ZSRO CR176	—	—	OP684744
Ana 504	*A. driesseni*	St. Crispins Well	-42.94583° 147.23000°	19.02.2019	SA, MG, CH, SR	ZSRO CR177	OP686562	—	OP684745
Ana 505	*A. driesseni*	St. Crispins Well	-42.94583° 147.23000°	19.02.2019	SA, MG, CH, SR	ZSRO CR177	—	—	OP684746
Ana 508	*A. driesseni*	East-West track, roadside ditch	-42.87389° 147.14333°	20.02.2019	SA, MG, CH, SR	ZSRO CR178	OP686563	—	OP684747
Ana 509	*A. driesseni*	East-West track, roadside ditch	-42.87389° 147.14333°	20.02.2019	SA, MG, CH, SR	ZSRO CR178	—	—	OP684748
Ana 510	*A. driesseni*	East-West track, roadside ditch	-42.87389° 147.14333°	20.02.2019	SA, MG, CH, SR	ZSRO CR178	—	—	OP684749
Ana 511	*A. driesseni*	East-West track, roadside ditch	-42.87389° 147.14333°	20.02.2019	SA, MG, CH, SR	ZSRO CR178	—	—	OP684750
Ana 512	*A. driesseni*	Knights Creek	-42.88111° 147.13639°	20.02.2019	SA, MG, CH, SR	ZSRO CR179	—	—	OP684751
Ana 513	*A. driesseni*	Knights Creek	-42.88111° 147.13639°	20.02.2019	SA, MG, CH, SR	ZSRO CR179	—	—	OP684752
Ana 514	*A. driesseni*	Knights Creek	-42.88111° 147.13639°	20.02.2019	SA, MG, CH, SR	ZSRO CR179	—	—	OP684753
Ana 515	*A. driesseni*	Knights Creek	-42.88111° 147.13639°	20.02.2019	SA, MG, CH, SR	ZSRO CR179	OP686564	OP686533	OP684754
Ana 517	*A. driesseni*	Glen Dhu Creek	-42.88111° 147.13639°	20.02.2019	SA, MG, CH, SR	ZSRO CR180	OP686565	—	OP684755
Ana 518	*A. driesseni*	Glen Dhu Creek	-42.88111° 147.13639°	20.02.2019	SA, MG, CH, SR	ZSRO CR180	—	—	OP684756
Ana 519	*A. driesseni*	silted pool near creek feeding Glen Dhu Creek	-42.88222° 147.13472°	20.02.2019	SA, MG, CH, SR	ZSRO CR181	OP686566	—	OP684757
Ana 523	*A. swaini*	Khazad Dum entrance creek	-42.71428° 146.56731°	22.02.2019	SA, MG, CH, SR	ZSRO CR182	OP686567	—	OP684726
Ana 524	*A. swaini*	Khazad Dum entrance creek	-42.71428° 146.56731°	22.02.2019	SA, MG, CH, SR	ZSRO CR182	—	OP686530	OP684727
Ana 525	*A. driesseni*	road off Waterfall Creek Rd, unnamed creek	-42.75364° 146.62361°	23.02.2019	SA, MG, CH, SR	ZSRO CR183	—	—	OP684758
Ana 526	*A. driesseni*	road off Waterfall Creek Rd, unnamed creek	-42.75364° 146.62361°	23.02.2019	SA, MG, CH, SR	ZSRO CR183	OP686568	—	OP684759

Table 1 continued.

ID	species	locality	latitude longitude	date	collectors	deposition	28S	16S	COI
Ana 527	*A. driesseni*	road off Waterfall Creek Rd, unnamed creek	-42.75364° 146.62361°	23.02.2019	SA, MG, CH, SR	ZSRO CR183	—	—	OP684760
Ana 528	*A. driesseni*	road off Waterfall Creek Rd, unnamed creek	-42.75364° 146.62361°	23.02.2019	SA, MG, CH, SR	ZSRO CR183	—	—	OP684761
Ana 529	*A. driesseni*	road off Waterfall Creek Rd, unnamed creek	-42.75364° 146.62361°	23.02.2019	SA, MG, CH, SR	ZSRO CR183	OP686569	—	OP684762
Ana 530	*A. driesseni*	road off Waterfall Creek Rd, unnamed creek	-42.75364° 146.62361°	23.02.2019	SA, MG, CH, SR	ZSRO CR183	—	OP686535	OP684763
Ana 560	*A. driesseni*	road off Waterfall Creek Rd, unnamed creek	-42.75364° 146.62361°	23.02.2019	SA, MG, CH, SR	ZSRO CR183	—	—	OP684764
Ana 710	*A. driesseni* (P)	Myrtle Forest Creek	-42.86392° 147.15313°	08.11.2021	AP	ZSRO CR202	OQ160970	OQ160856	OQ158727
Ana 711	*A. driesseni* (P)	Myrtle Forest Creek	-42.86392° 147.15313°	08.11.2021	AP	ZSRO CR202	—	OQ160857	OQ158728
Ana 712	*A. driesseni* (P)	Myrtle Forest Creek	-42.86392° 147.15313°	08.11.2021	AP	ZSRO CR202	—	OQ160858	OQ158729
Ana 713	*A. driesseni*	Trestle Creek	-42.90022° 147.13638°	12.11.2021	AP	ZSRO CR204	OQ160969	OQ160859	OQ158730
Ana 714	*A. driesseni*	Billy Brown River	-42.91558° 146.98708°	21.01.2022	AP	ZSRO CR203	OQ160968	OQ160860	OQ158731
Ana 715	*A. driesseni*	Billy Brown River	-42.91558° 146.98708°	21.01.2022	AP	ZSRO CR203	—	OQ160861	OQ158732
Ana 716	*A. driesseni*	Billy Brown River	-42.91558° 146.98708°	21.01.2022	AP	ZSRO CR203	OQ160967	OQ160862	OQ158733
Ana 717	*A. driesseni*	Billy Brown River	-42.91558° 146.98708°	21.01.2022	AP	ZSRO CR203	OQ160966	OQ160863	OQ158734
Ana 718	*A. driesseni*	Billy Brown River	-42.91558° 146.98708°	21.01.2022	AP	ZSRO CR203	—	OQ160864	OQ158735
Ana 719	*A. driesseni*	Billy Brown River	-42.91558° 146.98708°	21.01.2022	AP	ZSRO CR203	OQ160965	OQ160865	OQ158736
Ana 747	*A. driesseni*	Trestle Creek	-42.90022° 147.13638°	02.11.2022	SA, MG, CH, AP, SR, MW	ZSRO CR205	OQ160964	OQ160866	OQ158737
Ana 748	*A. driesseni*	Trestle Creek	-42.90022° 147.13638°	02.11.2022	SA, MG, CH, AP, SR, MW	ZSRO CR205	—	OQ160867	OQ158738
Ana 749	*A. driesseni*	Trestle Creek	-42.90022° 147.13638°	02.11.2022	SA, MG, CH, AP, SR, MW	ZSRO CR205	—	OQ160868	OQ158739
Ana 750	*A. driesseni*	Trestle Creek	-42.90022° 147.13638°	02.11.2022	SA, MG, CH, AP, SR, MW	ZSRO CR205	OQ160963	OQ160869	OQ158740
Ana 751	*A. driesseni*	Trestle Creek	-42.90022° 147.13638°	02.11.2022	SA, MG, CH, AP, SR, MW	ZSRO CR205	—	—	OQ158741
Ana 752	*A. driesseni*	Trestle Creek	-42.90022° 147.13638°	02.11.2022	SA, MG, CH, AP, SR, MW	ZSRO CR205	—	—	OQ158742
Ana 753	*A. driesseni*	Trestle Creek	-42.90022° 147.13638°	02.11.2022	SA, MG, CH, AP, SR, MW	ZSRO CR205	—	—	OQ158743
Ana 754	*A. driesseni*	Trestle Creek	-42.90022° 147.13638°	02.11.2022	SA, MG, CH, AP, SR, MW	ZSRO CR205	—	—	OQ158744
Ana 755	*A. driesseni*	Trestle Creek	-42.90022° 147.13638°	02.11.2022	SA, MG, CH, AP, SR, MW	ZSRO CR205	—	—	OQ158745
Ana 756	*A. driesseni*	Trestle Creek	-42.90022° 147.13638°	02.11.2022	SA, MG, CH, AP, SR, MW	ZSRO CR205	—	—	OQ158746
Ana 762	*A. driesseni*	Lake Skinner	-42.94036° 146.67886°	02.12.2022	MG, CH, AP, SR, MW	ZSRO CR206	OQ301631	—	OQ158747
Ana 765	*A. driesseni*	Lake Skinner	-42.94036° 146.67886°	02.12.2022	MG, CH, AP, SR, MW	ZSRO CR206	OQ301632	—	OQ158748
Ana 767	*A. driesseni*	Lake Skinner	-42.94036° 146.67886°	02.12.2022	MG, CH, AP, SR, MW	ZSRO CR206	OQ301633	—	OQ158749
Ana 769	*A. driesseni*	Lake Skinner	-42.94036° 146.67886°	02.12.2022	MG, CH, AP, SR, MW	ZSRO CR206	OQ301634	—	OQ158750
Ana 772	*A. driesseni*	unnamed tarn near summit of Snowy South	-42.94047° 146.66472°	02.12.2022	AP	ZSRO CR207	OQ160962	OQ160870	OQ158751
Ana 773	*A. driesseni*	unnamed tarn near summit of Snowy South	-42.94047° 146.66472°	02.12.2022	AP	ZSRO CR207	—	OQ160871	OQ158752
Ana 774	*A. driesseni*	unnamed tarn near summit of Snowy South	-42.94047° 146.66472°	02.12.2022	AP	ZSRO CR207	—	OQ160872	OQ158753
Ana 775	*A. driesseni*	unnamed tarn near summit of Snowy South	-42.94047° 146.66472°	02.12.2022	AP	ZSRO CR207	OQ160961	OQ160873	OQ158754
Ana 776	*A. driesseni*	unnamed tarn near summit of Snowy South	-42.94047° 146.66472°	02.12.2022	AP	ZSRO CR207	—	—	OQ158755
Ana 777	*A. driesseni* (P)	Myrtle Forest Creek	-42.85944° 146.15917°	08.12.2022	MG, CH, SR	ZSRO CR208	OQ160960	OQ160874	OQ158756
Ana 778	*A. driesseni* (P)	Myrtle Forest Creek	-42.85944° 146.15917°	08.12.2022	MG, CH, SR	ZSRO CR208	—	OQ160875	OQ158757
Ana 779	*A. driesseni* (P)	Myrtle Forest Creek	-42.85944° 146.15917°	08.12.2022	MG, CH, SR	ZSRO CR208	—	OQ160876	OQ158758
Ana 780	*A. driesseni* (P)	Myrtle Forest Creek	-42.85944° 146.15917°	08.12.2022	MG, CH, SR	ZSRO CR208	OQ160959	OQ160877	OQ158759
Ana 781	*A. driesseni*	Sorell Creek	-42.86835° 147.16942°	08.12.2022	MG, CH, SR	ZSRO CR209	OQ160958	OQ160878	OQ158760
Ana 782	*A. driesseni*	Sorell Creek	-42.86835° 147.16942°	08.12.2022	MG, CH, SR	ZSRO CR209	—	OQ160879	OQ158761
Ana 783	*A. driesseni*	Sorell Creek	-42.86835° 147.16942°	08.12.2022	MG, CH, SR	ZSRO CR209	—	OQ160880	OQ158762
Ana 784	*A. driesseni*	Sorell Creek	-42.86835° 147.16942°	08.12.2022	MG, CH, SR	ZSRO CR209	—	OQ160881	OQ158763
Ana 785	*A. driesseni*	Sorell Creek	-42.86835° 147.16942°	08.12.2022	MG, CH, SR	ZSRO CR209	—	—	OQ158764

Systematics

Syncarida Packard, 1885

Anaspidacea Calman, 1904

Anaspidesidae Ahyong & Alonso-Zarazaga, 2017

Anaspides Thomson, 1894

Anaspis Thomson, 1893: 7 (preoccupied, *Anaspis* Geoffroy, 1762 [Coleoptera]; type species: *Anaspis tasmaniae* Thomson, 1893).

Anaspides Thomson, 1894: 285, 286 (replacement name for *Anaspis* Thomson, 1892, preoccupied).

Diagnosis. See Ahyong (2016).

Species composition. *Anaspides tasmaniae* (Thomson, 1894) (type species), *A. clarkei* Ahyong, 2015, *A. driesseni* sp. nov., *A. eberhardi* Ahyong, 2016, *A. jarmani* Ahyong, 2015, *A. richardsoni* Ahyong, 2016, *A. spinulae* Williams, 1965, and *A. swaini* Ahyong, 2015.

Anaspides driesseni sp. nov.

urn:lsid:zoobank.org:act:555CA468-CCA2-42FC-8985-239C251CFCCF

Figs 1–5, 10E–F

Anaspides tasmaniae.—Smith, 1909a: 64, 70 (North West Bay River).—Manton, 1930: pl. 2, 3 (dark form).—Tjønneland *et al*., 1984: 226, figs. 1–10 (heart ultrastructure).

Anaspides swaini.—Ahyong, 2016: 352, 353, 359: fig. 32 G–J, 33A–J.—Höpel *et al*., 2021: 47, 52, fig. 2 [in part, form 3].

Holotype: TMAG G9228, ♂ (32 mm), Myrtle Forest Creek, Wellington Range, 42°51.6'S 147°10.3'E, 440 m asl, coll. R. Swain, Jun 1969. **Paratypes**: TMAG G6403, 4 ♂♂ (28–33 mm), 14 juv. ♂♂ (17–26 mm), 17 ♀♀ (24–38 mm), 3 juv. ♀♀ (18–21 mm), collected with holotype; ZSRO CR208, Ana777–Ana780 (sequenced), 1 juv. ♂ (23 mm), 3 juv. ♀♀ (21–23 mm), Myrtle Forest Creek, 42°51'34"S 147°09'33"E, 553 m asl, coll. M. Grams, C. Höpel & S. Richter, 08 Dec 2022; ZSRO CR202, Ana710-712 (sequenced) 1 ♂ (34 mm), 1 juv. ♂ (21 mm), 1 juv. ♀ (22 mm), Myrtle Forest Creek, 42°51'50.1012"S 147°09'11.2788"E, 676 m asl, coll. A. Palfreyman, 8 Nov 2021; ZSRO CR66, Ana310–Ana312 (sequenced), 3 juv. ♀♀ (8–11 mm), Myrtle Forest Creek, 42°51'34"S 147°09'33"E, 553 m asl, coll. S. Ahyong, C. Höpel, M. Reinhardt & S. Richter, 28 Feb 2017; ZSRO CR67, Ana146–148 (sequenced), Ana313–314 (sequenced), 2 juv. ♂♂ (13–15 mm), 3 juv. ♀♀ (12–15 mm), Myrtle Forest Creek, 42°51'37"S 147°09'08"E, 734 m asl, coll. S. Ahyong, C. Höpel, M. Reinhardt & S. Richter, 28 Feb 2017; AM P106558, 5 juv. ♂♂ (9–29 mm), 2 juv. ♀♀ (14–16 mm), Myrtle Forest Creek, 42°51'37"S 147°09'08"E, 734 m asl, coll. S. Ahyong, C. Höpel, M. Reinhardt & S. Richter, 28 Feb 2017; TMAG G6402, 4 ♂♂ (26–31 mm), 1 juv. ♂ (22 mm), 10 ♀♀ (27–34 mm), Myrtle Forest Creek, 42°51.6'S 147°10.3'E, 440 m asl, coll. R. Swain, Jun 1969; TMAG G983, 19 juv. ♂♂ (18–25 mm), 12 juv. ♀♀ (14–26 mm), Sorell Creek, Myrtle Gully [Myrtle Forest], Collinsvale, 42°53.8'S 147°15.4'E, 400 m asl, coll. museum staff, 9 Dec 1964; TMAG G6315, 4 ♂♂ (24–28 mm), 6 ♀♀ (25–32 mm), Myrtle Forest, Collinsvale, 42°51.6'S 147°10.3'E, 440 m asl, coll. R. Swain, Sep 1969.

Other material examined. *Southwest National Park, Snowy Mountains*: ZSRO CR183, 6 ♂♂ (29–35 mm), 3 juv. ♂♂ (15–16 mm), 3 ♀♀ (32–35 mm), 7 juv. ♀♀ (12–20 mm), Snowy North, road off Waterfall Creek Road, unnamed creek, tributary of Styx River, 42°49'39.03"S 146°39'41.70"E, 521 m asl, coll. S. Ahyong, M. Grams, C. Höpel, S. Richter, 23 Feb 2019; AM P106559, 2 ♂♂ (29–34 mm), 2 juv. ♂♂ (13–17 mm), 6 ♀♀ (31–35 mm), 7 juv. ♀♀ (12–16 mm), Snowy North, logging road off Waterfall Creek Road, unnamed creek, tributary of Styx River, 42°45'13.1"S 146°37'25"E, 521 m asl, coll. S. Ahyong, M. Grams, C. Höpel, S. Richter, 23 Feb 2019; ZSRO CR79, 1 juv. ♀ (9 mm), Snowy North, tributary of South Styx River, 42°50'32.1"S 146°37'11.2"E, 439 m asl, coll. C. Höpel, M. Reinhardt & S. Richter, 18 Mar 2017; TMAG 14369/G113, 2 ♂♂ (29 mm), 2 juv. ♂♂ (24–25 mm), 5 ♀♀ (24–34 mm), 1 juv. ♀ (23 mm) Snowy Mountains, 42°53.4'S 146°39'E, 2000 ft asl [600 m], coll. C.D. King, 20 Feb 1939; TMAG 14373/G117, 3 ♂♂ (29–32 mm), 2 juv. ♂♂ (25–26 mm), 3 ♀♀ (26–33 mm), 2 juv. ♀♀ (19–24 mm), Snowy Mountains, 42°55.5'S 146°40.5'E, 3000 ft asl [900 m], small Lake, coll. C.D. King, Feb 1939; AM P56374, 2 juv. ♂♂ (22–29 mm), Lake Skinner, Snowy Mountains, 42°57'S 146°41'E, C.62T, small stream at end of track to Lake, coll. W. Ponder *et al*., 15 Jan 1982; AM P73044, 2 juv. ♂♂ (17–28 mm), 3 juv. ♀♀ (10–25 mm), Snowy North, stream flowing into Styx River, 42°53.26'S 146°39.30'E, 590 m asl, coll. S. Jarman; TMAG G397, 1 ♀ (40 mm), plateau on summit of Mt Snowy, small pool 3 inches deep, 3500 ft asl [1050 m], coll. J.F. Thompson, 31 Jan 1962; ZSRO CR207, 2 ♂♂ (40 mm), 2 juv. ♂♂ (28–29 mm), 1 ♀ (41 mm), nameless tarn near summit of Snowy South, Snowy Mountains, 42°56'25.7"S 146°39'53.0"E, 1260 m asl, coll. A. Palfreyman, 02 Dec 2022; ZSRO CR206, 3 juv. ♂♂ (21–23 mm), 2 ♀♀ (27–31 mm), 2 juv. ♀♀ (22 mm), Lake Skinner, Snowy Mountains, 42°56'25.3"S 146°40'43.9"E, 980 m asl, coll. M. Grams, C. Höpel, A. Palfreyman, S. Richter, & M. Weiler, 02 Dec 2022; TMAG G3432, 4 ♀♀ (25–33 mm), 1 juv. ♀ (24 mm), Lake Skinner, Snowy Mountains, 42°56.8'S 146°40.5'E, 970 m asl], coll. D. Farnell, 28 Jan 1962; TMAG G130, 2 ♂♂ (32–34 mm), 1 juv. ♂ (25 mm), 3 ♀♀ (32–35 mm), 2 juv. ♀♀ (17–22 mm), Lake Denison, 42°57.4'S 146°41.0'E, 1900 ft asl [570 m], coll. C. King, Feb 1936; TMAG G127, 1 juv. ♂ (25 mm), 5 juv. ♀♀ (13–20 mm), Lake Denison, 42°57.4'S 146°41.0'E, 1900 ft asl [570 m], coll. C. King, Feb 1939; TMAG G112, 1 ♂ (28 mm), 2 juv. ♂♂ (23–25 mm), 7 ♀♀ (26–31 mm), 2 juv. ♀♀ (22–25 mm), Lake Skinner, Snowy Mountains, 42°56.8'S 146°40.1'E, c. 3000 ft asl [970 m], coll. C.D. King, Feb 1939; TMAG G6407, 2 ♂♂ (28–29 mm), 6 juv. ♂♂ (20–22 mm), 10 ♀♀ (23–26 mm), 9 juv. ♀♀ (8–14 mm), Snowy Mountains, 42°54'S 146°42'E, tarn, coll. M. Fenton, 19 Nov 1970; TMAG G6361, 1 juv. ♂ (12 mm), Snowy South, 42°56.7'S 146°39.4'E, small Lake on slope, 1340 m asl, coll. P. Davies, Apr 1986; AM P99308, 1 ♂ (damaged), Lake Picton, 43°09.56'S 146°38.23'E, coll. S. Jarman; TMAG G6317, 10 juv. ♂♂ (15–28 mm), 20 ♀♀ (24–33 mm), 11 juv. ♀♀ (14–21), Lake Picton, 43°09.5'S 146°38.3'E, 900 m asl, 23 Jan 1969; TMAG G6424, 1 ♂ (24 mm), 2 juv. ♂♂ (26–28 mm), 25 ♀♀ (23–36 mm), Lake Picton, 43°09.5'S 146°38.2'E, 900 m asl, coll. P. Tyler, Jan 1969.

Arve Valley, Hartz: TMG G2214, 1 ♀ (25 mm), Arve Loop Road, Arve Valley, 43°07.7'S 146°44.9'E, from creek, 390 m asl, coll. R. Shoobridge, 14 Feb 1980; TMAG G6382, 24 juv. ♂♂ (13–28 mm), 8 ♀♀ (26–32 mm), 39 juv. ♀♀ (8–24 mm), 1 indet juv. (7 mm), Hartz Mountains [almost certainly from northern Hartz], coll. R. Swain & G. Bert, Feb 1970.

Wellington Range: ZSRO CR209, 1 ♂ (35 mm), 7 juv. ♂♂ (16–25 mm), 1 ♀ (37 mm), 5 juv. ♀♀ (13–24 mm), 3 indet juv. (5–7 mm), Sorell Creek, 42°52'6.0492"S 147°10'9.9084"E, 600 m asl, coll. M. Grams, C. Höpel, & S. Richter, 08 Dec 2022; ZSRO CR178, 5 indet juv. (6–11 mm), East-West track, roadside ditch, 42°52'26"S 147°08'36"E, 961 m asl, coll. S. Ahyong, M. Grams, C. Höpel, S. Richter, 20 Feb 2019; AM P106563, 1 juv. ♂ (24 mm), 2 ♀♀ (33–34 mm), 1 indet juv. (7 mm), East-West track, roadside ditch, 42°52'26"S 147°08'36"E, 961 m asl, coll. S. Ahyong, M. Grams, C. Höpel, S. Richter, 20 Feb 2019; ZSRO CR181, 1 ♀ (38 mm), silted pool near creek feeding Glen Dhu Creek, 42°52'56"S 147°08'05"E, 946 m asl, coll. S. Ahyong, M. Grams, C. Höpel, S. Richter, 20 Feb 2019; ZSRO CR180, 3 juv. ♀♀ (16–21 mm), 2 indet (9 mm), Glen Dhu Creek, 42°52'52"S 147°08'11"E, 930 m asl, coll. S. Ahyong, M. Grams, C. Höpel, S. Richter, 20 Feb 2019; AM P106564, 1 ♂ (30 mm), 3 ♀♀ (27–40 mm), Glen Dhu Creek, 42°52'52"S 147°08'11"E, 930 m asl, coll. S. Ahyong, M. Grams, C. Höpel, S. Richter, 20 Feb 2019; ZSRO CR179, 3 juv. ♂♂ (22–29 mm), 1 ♀ (33 mm) Knights Creek, 42°52'08"S 147°12'02"E, 687 m asl, coll. S. Ahyong, M. Grams, C. Höpel, S. Richter, 20 Feb 2019; AM P106565, 1 juv. ♂ (24 mm), 3 ♀♀ (35–39 mm), Knights Creek, 42°52'08"S 147°12'02"E, 687 m asl, coll. S. Ahyong, M. Grams, C. Höpel, S. Richter, 20 Feb 2019; AM P106780, 1 ♂ (34 mm), 1 juv. ♂ (15 mm), 1 juv. ♀ (21 mm), 3 ♀♀ (33–40 mm), Trestle Creek, 42°54'0.7812"S 147°08'10.9788"E, 480 m asl, coll. S. Ahyong, M. Grams, C. Höpel, A. Palfreyman, S. Richter & M. Weiler, 02 Nov 2022; ZSRO CR205, 1 ♂ (30 mm), 2 juv. ♂♂ (18–21 mm), 9 ♀♀ (32–36 mm), 3 juv. ♀♀ (18–21 mm), Trestle Creek, 42°54'0.7812"S 147°08'10.9788"E, 480 m asl, coll. S. Ahyong, M. Grams, C. Höpel, A. Palfreyman, S. Richter & M. Weiler, 02 Nov 2022; ZSRO CR204, 1 juv. ♀ (16 mm), Trestle Creek, 42°54'0.7812"S 147°08'10.9788"E, 480 m asl, coll. A. Palfreyman, 12 Nov 2021; AM P4143, 1 ♂ (32 mm), 1 ♀ (34 mm), Mt Wellington, 42°53.8'S 147°14.5'E, coll. E.A. Briggs, pre 1918; AM P14772, 2 ♂♂ (24–26 mm), 1 juv. ♂ (19 mm), 1 juv. ♀ (21 mm), Mt Wellington, 42°54'S 147°14'E, from University of Sydney Biology Dept,

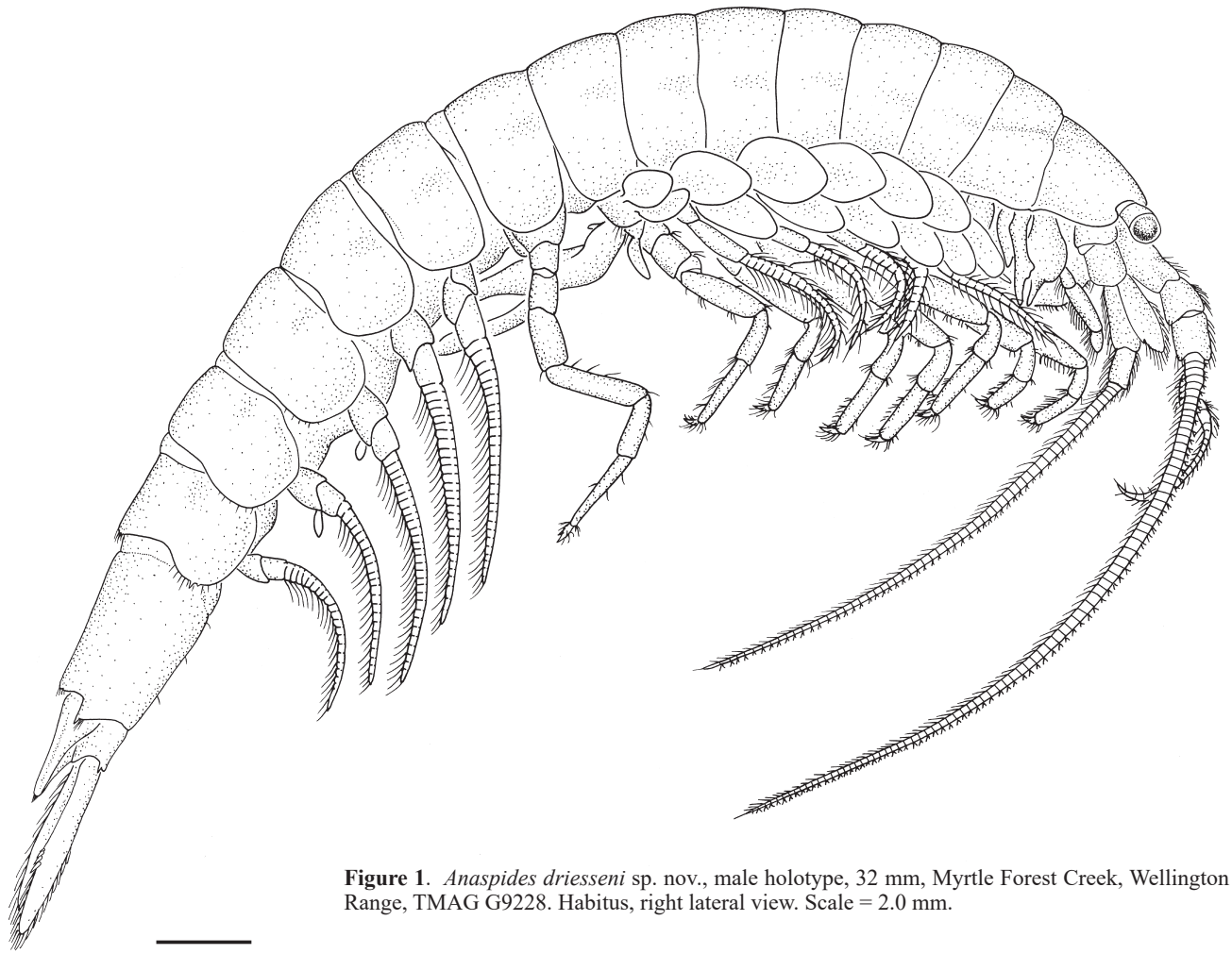


Figure 1. *Anaspides driesseni* sp. nov., male holotype, 32 mm, Myrtle Forest Creek, Wellington Range, TMAG G9228. Habitus, right lateral view. Scale = 2.0 mm.

1964; AM P14773, 1 ♂ (36 mm), Mt Wellington, from University of Sydney Biology Dept in 1964, possible Haswell label; AM G1779, 1 ♂ (24 mm), 3 ♀♀ (24–27 mm), 5 juv. ♀♀ (14–20 mm), summit of Mt Wellington, 42°54'S 147°14'E, pres. C. Hedley, pre 1898; AM P2266, 1 ♂ (34 mm), Mt Wellington, 42°54'S 147°14'E, pres. E.G. Goddard; AM P2551, 1 ♂ (32 mm), 4 juv. ♂♂ (19–22 mm), 3 ♀♀ (23–24 mm), 4 juv. ♀♀ (12–20 mm), Mt Wellington, 42°54'S 147°14'E, coll. T.T. Flynn; USNM 59126 (ex AM P2551), 2 ♂♂ (24–25 mm), Mt Wellington, coll. T.T. Flynn; USNM 78433, 1 ♂ (29 mm), Mt Wellington, snow pools in swamp, coll. Mel Ward; USNM 25030, 1 ♂ (27 mm), 1 ♀ (25 mm), "Lakes (4000 ft) Tasmania", G.M. Thomson; AM P9217, 11 juv. ♂♂ (18–29 mm), 12 juv. ♀♀ (19–27 mm), Wishing Well, Mt Wellington, 42°55.67'S 147°14.76'E, 1450 feet asl [442 m], coll. C. Anderson, A. Musgrave, G.P. Whitley, 23 Jan 1928; AM P10724, 8 juv. ♂♂ (16–22 mm), 3 ♀♀ (26–37 mm), 15 juv. ♀♀ (8–24 mm), Mt Wellington, 42°54'S 147°14'E, coll. F.D. Manning, Jan 1935; AM P56375, 1 ♂ (32 mm), 3 juv. ♂♂ (14–18 mm), 7 juv. ♀♀ (12–20 mm), Mt Wellington, small pools (running water) 2500 ft [750 m], coll. J.W. Evans, Dec 1938; AM P82859, 1 ♂ (24 mm), 2 juv. ♂♂ (9–11 mm), 1 ♀ (23 mm), 15 juv. ♀♀ (8–12 mm), Mt Wellington, 12 Mar 1997; TMAG G794, 1 ♂ (23 mm), back of Mt Wellington, coll. G.E. Nicholls, 16 Dec 1933; WAM C58162, 2 ♀♀ (29–34 mm), Mt Wellington, coll. J. Searle; WAM C367 (ex No. 6613), 3 juv. ♀♀ (16–17 mm), Mt Wellington, coll. J. Searle, 29 Jan 1913; SAMA C473, 2 ♀♀ (shrivelled, previously dried; c. 25–26 mm), 2 juv. ♀♀ (9–13 mm), 2 indet juv. (6 mm), North West Bay River, Mt Wellington, 42°55.3'S 147°11.2'E, 2700 ft [810 m], coll. Prof. Osborn; ZSRO CR203, 3 ♂♂ (29–31 mm), 1 juv. ♂ (22 mm), 2 ♀♀ (30–32 mm), Billy Brown River, 42°54'56.0988"S 146°59'13.4988"E, 580 m asl, coll. A. Palfreyman, 21 Jan 2022; AM P9218, 2 ♂♂ (30–32 mm), 3 juv. ♂♂ (20–22 mm), 5 ♀♀ (28–34 mm), 7 juv. ♀♀ (15–23 mm), Fern Tree Glen, Mt Wellington, 42°55.5'S 147°15.7'E, coll. C. Anderson, A. Musgrave, G.P. Whitley, 23 Jan 1928; TMAG G6450, 3 ♂♂ (30–33 mm), 3 juv. ♂♂ (16–22 mm), 6 ♀♀ (26–40 mm), 4 juv. ♀♀ (18–23 mm), St. Crispins Well, Mt Wellington, 42°55.76'S 147°12.57'E, 640 m asl, coll. R. Swain, 14 Feb 1971; ZSRO CR177, 1 juv. ♂ (25 mm), 1 juv. ♀ (16 mm), 3 indet juv. (7–10 mm), St. Crispins Well, 42°55'39.73"S 147°12'42.48"E, 750 m asl, coll. S. Ahyong, M. Grams, C. Höpel & S. Richter, 19 Feb 2019; AM P106560, 1 juv. ♂ (24 mm), 2 juv. ♀♀ (13–20 mm), 1 indet juv. (7 mm), St. Crispins Well, 42°55'39.73"S 147°12'42.48"E, 750 m asl, coll. S. Ahyong, M. Grams, C. Höpel & S. Richter, 19 Feb 2019; ZSRO CR176, 1 juv. ♀ (12 mm), 3 indet juv. (7–9 mm), Levert Rivulet, 42°56'45.33"S 147°13'49.08"E, 524 m asl, coll. S. Ahyong, M. Grams, C. Höpel & S. Richter, 19 Feb 2019; AM P106561, 1 juv. ♀ (26 mm), Levert Rivulet, 42°56'45.33"S 147°13'49.08"E, 524 m asl, coll. S. Ahyong, M. Grams, C. Höpel & S. Richter, 19 Feb 2019; ZSRO CR175, 2 juv. ♂♂ (10–13 mm), 1 juv. ♀ (13 mm), 2 indet juv. (9 mm), unnamed creek on Pipeline track, 42°57'05.2"S 147°13'49.7"E, 716 m asl, coll. S. Ahyong, M. Grams, C. Höpel & S. Richter, 19 Feb 2019; AM P106562, 1 juv. ♀ (12 mm), 1 indet juv. (7 mm), unnamed creek on Pipeline track, 42°57'05.2"S 147°13'49.7"E, 716 m asl, coll. S. Ahyong, M. Grams, C. Höpel & S. Richter, 19 Feb 2019; SAMA C8445, 1 juv. ♂ (21 mm), 1 ♀ (28 mm), 1 juv. ♀ (22 mm), Huonville, creeks, coll. R.T.T.

Description. Eyes with well-developed cornea, pigmented, wider than and longer than half length of stalk; stalk with subparallel margins. Rostrum narrow in adults, apex blunt.

Pleonites with pleura sparsely setose, rounded; pleura 1–3 unarmed; pleuron 4 usually unarmed (rarely with 1 small spine on one side); pleuron 5 with 0–3 small spines (usually unarmed or with 1 spine). Pleonite 5 posterior tergal margin setose, unarmed or with 1–4 small spines either side of midline. Pleonite 6 tergal posterior margin with 0–11 spines in juveniles and 0–15 in adults, setose; posterolateral margin setose, rounded, with or without minute denticles. Pleonal sternites 3–4 with distinctly bilobed median processes between pleopod bases, widest on sternite 3; sternite 5 with narrow, weakly emarginate lobe.

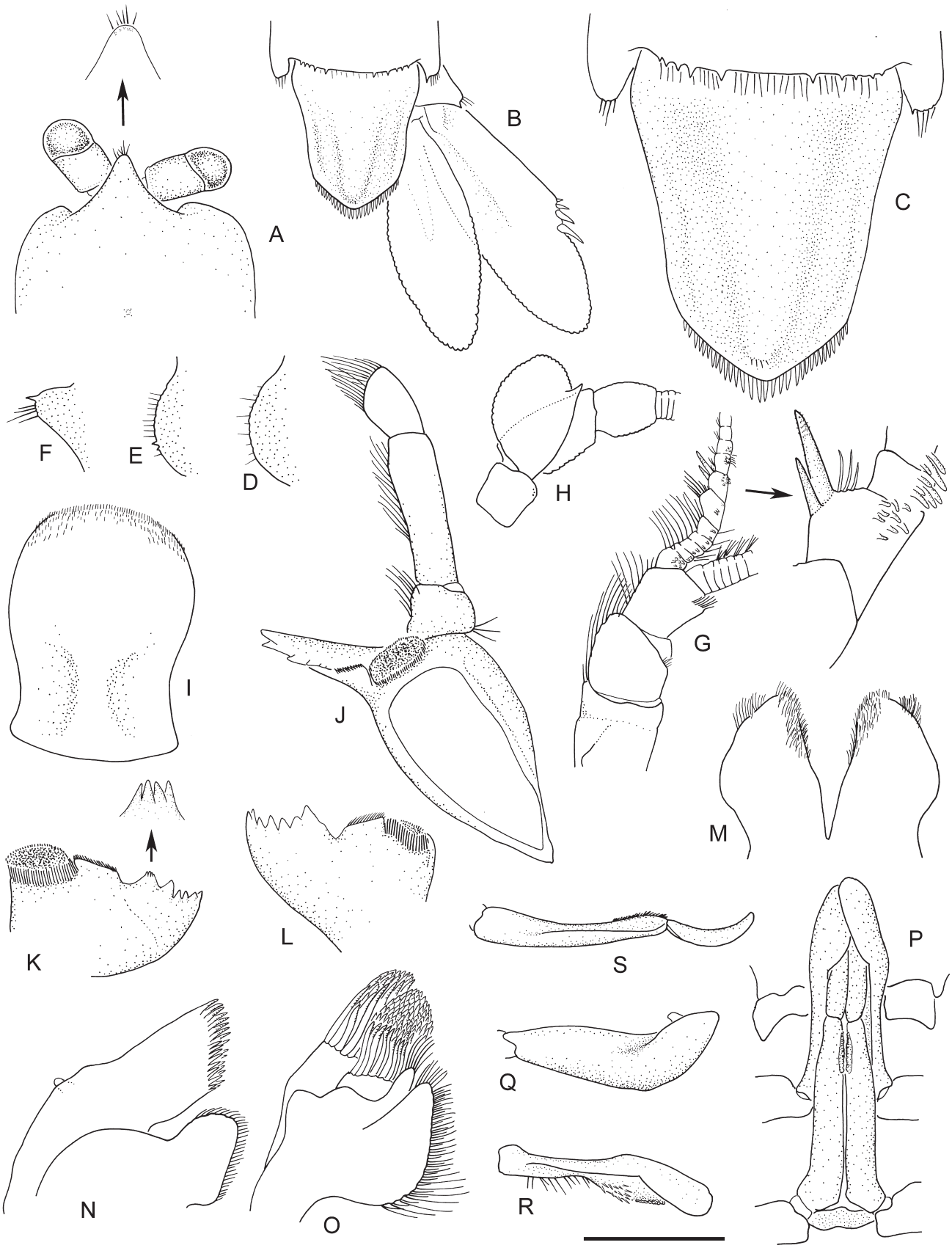


Figure 2. *Anaspides driesseni* sp. nov., male holotype, 32 mm, Myrtle Forest Creek, Wellington Range, TMAG G9228. (*A*) anterior cephalothorax, dorsal view; (*B*) pleonite 6, telson and right uropod; (*C*) pleonite 6 and telson; (*D–F*) pleonites 4–6 pleura, right lateral view; (*G*) right antennule; (*H*) right antenna; (*I*) labrum, anterior view; (*J*) right mandible; (*K*) right mandible incisor process; (*L*) left mandible incisor process; (*M*) paragnaths, anterior view; (*N*) right maxillule; (*O*) right maxilla; (*P*) pleopods 1–2, in-situ, ventral view; (*Q–R*) right pleopod 1 endopod, lateral view and dorsal view, respectively; (*S*) right pleopod 2 endopod, lateral view. Scale: A, B, D–H, P–S = 2.0 mm, C, I–O = 1.0 mm.

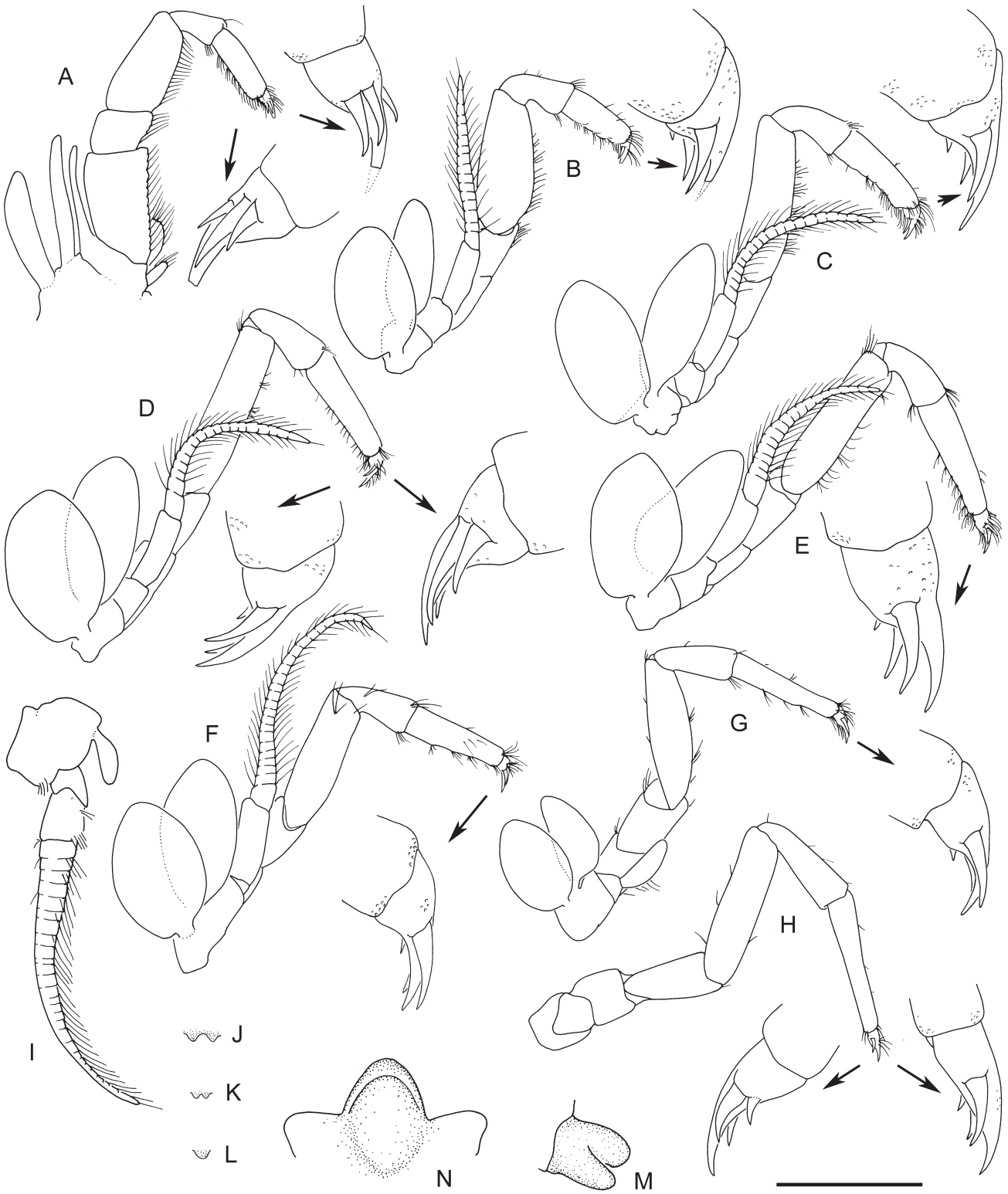


Figure 3. *Anaspides driesseni* sp. nov., (*A–L*) male holotype, 32 mm, Myrtle Forest Creek, Wellington Range, TMAG G6403; (*M–N*), female, 34 mm, Mount Wellington, AM P9218. (*A*) right thoracopod 1 (maxilliped); (*B–H*) right thoracopods 2–8, respectively; (I) right pleopod 4, anterior view; (*J–L*) pleonites 3–5 median sternal processes, respectively; (*M, N*) female gonopore, right lateral and ventral views, respectively. Scale 2.0 mm.

Telson slightly wider than long to longer than wide (usually equal to slightly wider than long), pentagonal, widest proximally; lateral margins slightly sinuous to nearly parallel in dorsal outline, transition from lateral to posterior margin obtusely angular; posterior margin slightly angular, apex bluntly rounded medially; posterior spine row with 14–53 (juveniles) or 24–54 (adults) slender, evenly graded, closely spaced spines, longest medially.

Antennule inner flagellum about 0.2× body length (22–23 annulations in holotype); in adult males articles 1–5 wider

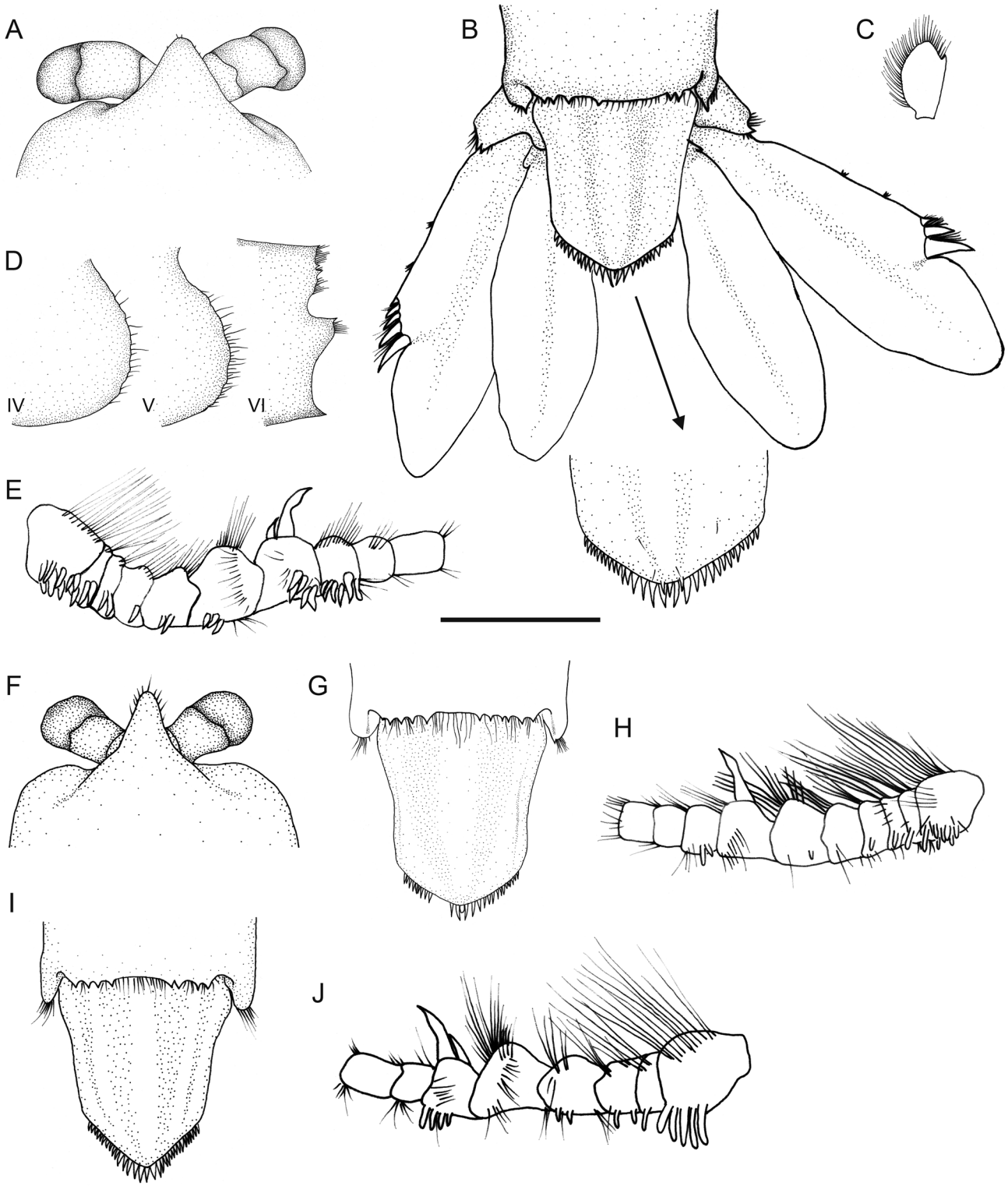


Figure 4. *Anaspides driesseni* sp. nov. selected features. (*A–E*) juv. male, 28 mm, Myrtle Forest, AM P106558; (*F–H*) juv. male, 29 mm, Myrtle Forest, AM P106558 (*I–J*) male, 28 mm, Mt Fenton, TMAG G6407. (*A*, *F*) anterior cephalothorax. (*B*) telson with uropods. (*C*) scaphocerite. (*G, I*) telson. (*D*) pleonal pleura. (*E*) right antennule with clasping spines. (*H*, *J*) left antennule with clasping spines. Scale: A–D, F, G, I = 2.0 mm, E, H, J = 1.0 mm.

than long, articles 6–7 as wide as long, article 8 wider than long, articles 1–6 densely setose on lateral inner margin, articles 1–8 with small spines on the outer lateral margin, longest on article 1, article 4–7 obtusely angled inner margin, article 7 usually with 2 small, clasping spines proximally (rarely 3 or 4 clasping spines on one site), directed distally, distal clasping spines equal to slightly longer than width of article 7, proximal clasping spine equal to slightly shorter than width of article 7; outer flagellum 0.5–0.9× body length (usually 0.5–0.7) (77–85 annulations in holotype).

Antennal flagellum 0.3–0.4× body length (55–58 annulations in holotype); scaphocerite elongate, ovate, lateral

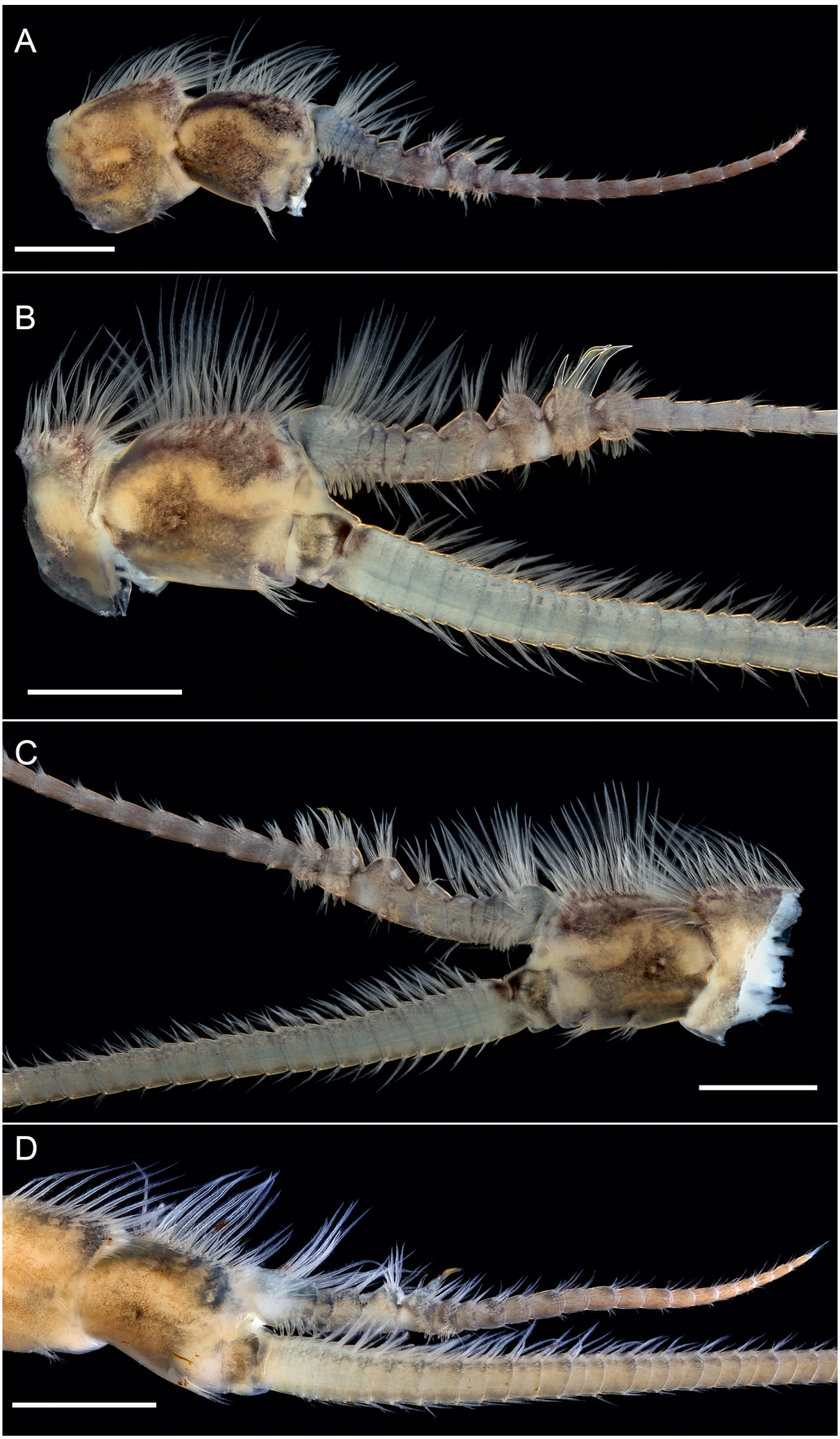


Figure 5. Dorsal view on the antenna of male *A. driesseni* sp. nov. (*A–C*) Snowy North, unnamed tributary of Styx River crossing the road off Waterfall Creek Road, ZSRO CR183; (*A*) 35 mm, right antenna; (*B*) Ana 560, 35 mm, right antenna, with 4 abnormal clasping spines, highlighted with white outlines; (*C*) Ana 560, 35 mm, left antenna; (*D*) right antenna, 29 mm, Knights Creek, Wellington Range, ZSRO CR179. Scale bars: 1 mm.

spine slightly distal to midlength; apex reaching as far as midlength of distal peduncular article.

Right mandibular incisor process with proximal tooth distally bifid to quadrifid, usually trifid.

Pleopods 1–4 (rarely on pleopod 5 on one side) each with endopod in adults. Adult male pleopod 1 distally widened, scoop-like, lateral margins expanded, obscuring retinacular lobe in lateral view.

Uropodal protopod dorsally unarmed or with 1–3 small spines; exopod with 2–5 movable spines on outer margin near position of partial diaeresis; exopod length about 2.5–3.0× width, slightly wider than endopod, apex rounded, narrow to relatively broad.

Measurements. Adult male (n = 62) 24–40 mm, juvenile male (n = 165) 9–29 mm, adult female (n = 187) 23–41 mm, juvenile female (n = 214) 8–27 mm, sex indeterminate (n = 24) 5–11 mm.

Distribution. South-eastern Tasmania from the Arve Valley and Hartz Mountains area over the Mt Picton area and Snowy Mountains to the Wellington Range and western to north-western Mt Wellington (Collinsvale and North West Bay River catchment); Southern-Derwent and Huon drainage system (Figs 7–10); 390–1260 m asl.

Etymology. Named in honour of Michael Driessen PhD, for his many contributions to the conservation of Tasmanian Wildlife, especially of our knowledge of *Allanaspides,* and for his facilitation of our research in Tasmania.

Remarks. Of the three morphological forms of *Anaspides swaini* recognized by Ahyong (2016), *A. driesseni* sp. nov. corresponds to form 3. *Anaspides driesseni* sp. nov. differs from form 1 through the reduced pleonal spination (except for some specimens from the Arthurs Range and Frankland Range), the less narrowed lateral margins of the telson, which are more parallel and narrows just to the end, the shape of the antennule inner flagellum with the highly setose lateral inner margins on article 1–6, the proportions of article 5–6 (in *A. swaini* form 1, article 5 is as wide as long to slightly longer than wide and article 6 is always longer than wide), the obtusely angled inner margin of article 4–7 and the presence of two short clasping spines, with the distal clasping spine being equal to slightly longer than the width of article 7 and the proximal clasping spine being equal to slightly shorter than the width of article 7 (Figs 2G, 4E,H,M, 5). In contrast, both clasping spines of *A. swaini* form 1 are always longer than the width of article 7 (1.3–2.0× longer than the width) (Fig. 11A,B). *Anaspides swaini* form 2 has reduced pleonal spination as in *A. driesseni*, but differs in the shape of the telson, resembling that of form 1, the presence of pleopodal endopod 1–5 and the shape of the antennule inner flagellum. As in *A. swaini* form 1, both clasping spines are longer than the width of article 7 (1.1–1.8× longer than the width of article 7), only article 6 is obtusely angled and articles 5–6 are longer than wide (Fig. 11C). Also *A. swaini* form 2 shows less setation on articles 1–6, similar to that of *A. swaini* form 1.

Anaspides driesseni sp. nov. is distinguished from other congeners by the combination of the angular posterior margin of the telson, the presence of pleopodal endopod 1–4, the greater size at maturity (23–29 mm, usually 26–28 mm), the shape of the antennule inner flagellum in adult males (Figs 2G, 4E,H,J, 5) and the presence of two small clasping spines (Figs 2G, 4E,J, 5).

Sexual maturation at a larger body size (indicated by the full development of secondary sexual features) is noticeable and separates *A. driesseni* from all other species of the genus. In *A. driesseni*, sexual maturity is reached by 23–29 mm, usually at 26–28 mm body length, while other species reach maturity at 18–23 mm (usually 20–21 mm), respectively 14–15 mm in *A. spinulae* (Ahyong, 2016). In *A. driesseni*, the endopod of pleopod 4 is not developed (occasionally on one side) before reaching a size of about 11 mm.

Overall, *A. driesseni* is morphologically rather consistent, with only slight variation evident. The specimens from the Snowy Range region, except those from the unnamed creek crossing the road off Waterfall Creek Road (tributary of Styx River) (ZSRO CR183, AM P106559), some specimens from Lake Skinner and one specimen from Lake Picton (TMAG G6424), lack the denticle on the uropodal protopod and show no pleural spination of the pleon. Furthermore, the antennular outer flagellum is elongated, ranging from 0.7–0.9× of the body length in comparison to specimens from the Wellington Range and the tributary of Styx River (0.4–0.8× of the body length, usually 0.4–0.6). The Arve-Valley-Hartz populations similarly lack the denticle on the uropodal protopod, but in the remaining characters, resemble the populations from the Wellington Range. Only in three aberrant specimens from Snowy North (ZSRO CR183) and one specimen from a nameless tarn near the summit of Snowy South, an abnormal number of clasping spines on one side was observed. Three specimens had 3 clasping spines (2x Snowy North, 1x Snowy South) on one side rather than the usual 2, and one specimen had 4 clasping spines (Fig. 5B). In these specimens the additional spines were not in a row as in "normal" males, but instead they stand disorderly in a second row, forming a kind of cluster. These cases appear to be the result of abnormal development of the clasping spines, which typically develop in a single row along the article axis.

Anaspides driesseni the species with the largest known males, with two males from an unnamed tarn near the summit of Snowy South reaching 40 mm total length. The largest known male so far is one male of *A. richardsoni* from Honeycomb Cave in the Mole Creek karst system reaching 37 mm. The largest epigean males apart *A. driesseni* are recorded with 33 mm in *A. richardsoni* and *A. tasmaniae* (Ahyong, 2016).

Why epigean *A. driesseni* attains such a large maximum body size compared to congeners might be related to the onset of maturity at a larger body size.

To date, there are no known subterranean occurrences of *A. driesseni*.

Molecular data. Maximum intraspecific uncorrected p-distances for *A. driesseni* were 2.2% in COI, 0.6% in 16S and 0.3% in 28S, while interspecific distances to other congeners of the genus *Anaspides* were 8.4–14.2% in COI, 1.2–7.1% in 16S and 0.6–3.5% in 28S (Table 2). In COI we uncovered 11 different haplotypes in 4 distinct haplotype clusters for *Anaspides driesseni* (Fig. 6). The first cluster comprises specimens from an unnamed creek crossing the road off Waterfall Creek Road, the tributary of South Styx River, a nameless tarn near Snowy South, Billy Brown River, Glen Dhu Creek and a roadside ditch near the East-West track. The second cluster comprises specimens from Lake Skinner, while the third cluster comprises specimens from St. Crispins Well and an unnamed creek crossing the Pipeline Track. The fourth cluster comprises specimens from Myrtle

Table 2. Inter- and intraspecific uncorrected p-distances for COI, 16S and 28S of *Anaspides spp.*

		A. swaini (form 1)	*A. driesseni*	*A. richardsoni*	*A. spinulae*	*A. tasmaniae*	*A. clarkei*	*A. jarmani*
A. swaini (form 1)	COI	0.0–10.2						
	16S	0.0–2.8						
	28S	0.0–0.2						
A. driesseni	COI	8.4–11.1	0.0–2.2					
	16S	1.2–3.1	0.0–0.6					
	28S	0.6–1.0	0.0–0.3					
A. richardsoni	COI	11.1–14.4	12.0–14.2	0.0–6.2				
	16S	3.1–4.3	4.0–5.3	0.0–1.2				
	28S	2.6–2.9	3.4–3.5	0.0–0.2				
A. spinulae	COI	12.0–14.2	13.3–14.0	0.5–5.6	0.0–1.6			
	16S	3.4–4.3	4.3–5.0	0.0–1.5	0.0–0.6			
	28S	—	—	—	—			
A. tasmaniae	COI	12.2–14.2	10.7–11.5	9.3–10.6	9.5–9.8	0		
	16S	2.8–4.0	4.0–4.6	2.8–3.4	2.8–3.1	0		
	28S	2.0–2.1	2.4–2.6	1.3–1.5	—	0		
A. clarkei	COI	11.3–14.4	10.7–12.8	11.7–13.3	11.5–12.9	11.7–12.9	0.0–2.6	
	16S	4.0–6.5	5.3–6.8	3.7–5.3	3.7–4.3	2.8–4.3	0.0–2.5	
	28S	2.7–2.8	2.8–3.0	2.9–3.0	—	2.5	0	
A. jarmani	COI	12.0–14.8	11.5–13.1	12.4–13.8	12.9–13.5	12.8–12.9	5.3–6.0	0.0–0.4
	16S	4.7–7.2	5.9–7.1	4.7–6.2	4.3–5.6	4	1.5–2.8	0.0–1.9
	28S	2.5–2.7	2.7–2.8	2.3–2.5	—	2.2	1.2	0

Forest Creek, Sorell Creek, Trestle Creek and Levert Rivulet. In 16S, three haplotypes were found each separated by one mutation. One haplotype comprises specimens from Myrtle Forest Creek and Sorell Creek, one comprises specimens from Trestle Creek and Knights Creek and the last one comprises specimens from Billy Brown River, a tributary of the South Styx River and a nameless tarn near the summit of Snowy South. In 28S, we found 4 haplotypes, each separated by one mutation respectively one indel (compared with 6 nucleotide positions in the other two haplotypes). The first haplotype comprises specimens from Billy Brown River, Levert Rivulet, Glen Dhu Creek and the roadside ditch at the East-West track. The second haplotype comprises specimens from Trestle Creek, Billy Brown River, St. Crispins Well, an unnamed creek crossing the Pipeline Track, the tributary to South Styx River, an unnamed creek crossing the road off Waterfall Creek Road, Lake Skinner and a nameless tarn near the summit of Snowy South. The third haplotype comprises specimens from Lake Skinner, while the fourth haplotypes comprises specimens from Myrtle Forest Creek (Fig. 6).

Discussion

Our results support the findings of Ahyong (2016) that *A. swaini* is a diverse species clade, now comprising two named species (*A. swaini* and *A. driesseni*). This expands the genus *Anaspides* to eight species. As with other species of *Anaspides*, the secondary sexual characters of the male antennules, especially the shape of the antennule inner flagellum (articles, setation and clasping spines) and presence of pleopodal endopods proved instrumental in taxonomic delineations. Furthermore, the onset of sexual maturity (indicated by the development of secondary sexual features) appears to be a valuable character in *A. driesseni*.

Of the three morphological forms of *A. swaini* recognized by Ahyong (2016) *A. driesseni* corresponds to form 3. The geographic distribution of *A. driesseni* as determined by present results, however, is extended slightly from that originally reported for *A. swaini* form 3, which now includes the Arve Valley and Hartz Mountains area, over the Snowy Mountains to the Wellington Range and western to north-western Mt Wellington (Collinsvale and North West Bay River catchment). To date there are no known sympatric occurrences of *A. driesseni* with other species of *Anaspides*, although it is parapatric with *A. tasmaniae* at Wellington Park (*A. swaini* (form 3) in Ahyong, 2016 and Höpel *et al*., 2021).

Ahyong (2016) pointed out that *Anaspides driesseni* was previously recorded from the plateau near the summit of Mt Wellington in tarns and creeks by Manton (1930) under the name *A. tasmaniae*. The current absence of *Anaspides* from the summit of Mt Wellington is probably a result of major bushfires that swept across the top of Mt Wellington in 1930s (Swain pers. com. in O'Brien, 1990). A detailed search in 2019 in tarns and creeks across the plateau "confirmed" the absence of *Anaspides* in this area (Höpel *et al*., 2021).

The low intraspecific and high interspecific genetic distances support the delimitation of *Anaspides driesseni* as a separate species. Moreover, the monophyly of *A. driesseni* and its position as sister species to *A. swaini* form 1 are supported by mitogenomic analysis of the genus (Höpel *et al*., unpublished). On the other hand, in *A. swaini* form 1 as now restricted, the high intraspecific distances (up to 10.3 % in COI) are striking, especially between the lineages found in tributaries of the Weld River (Richter *et al*., 2018). Nevertheless, these lineages are sympatric and no significant morphological differences between these lineages were detectable. Only specimens from the Arthur Range and Frankland Range differ to some degree

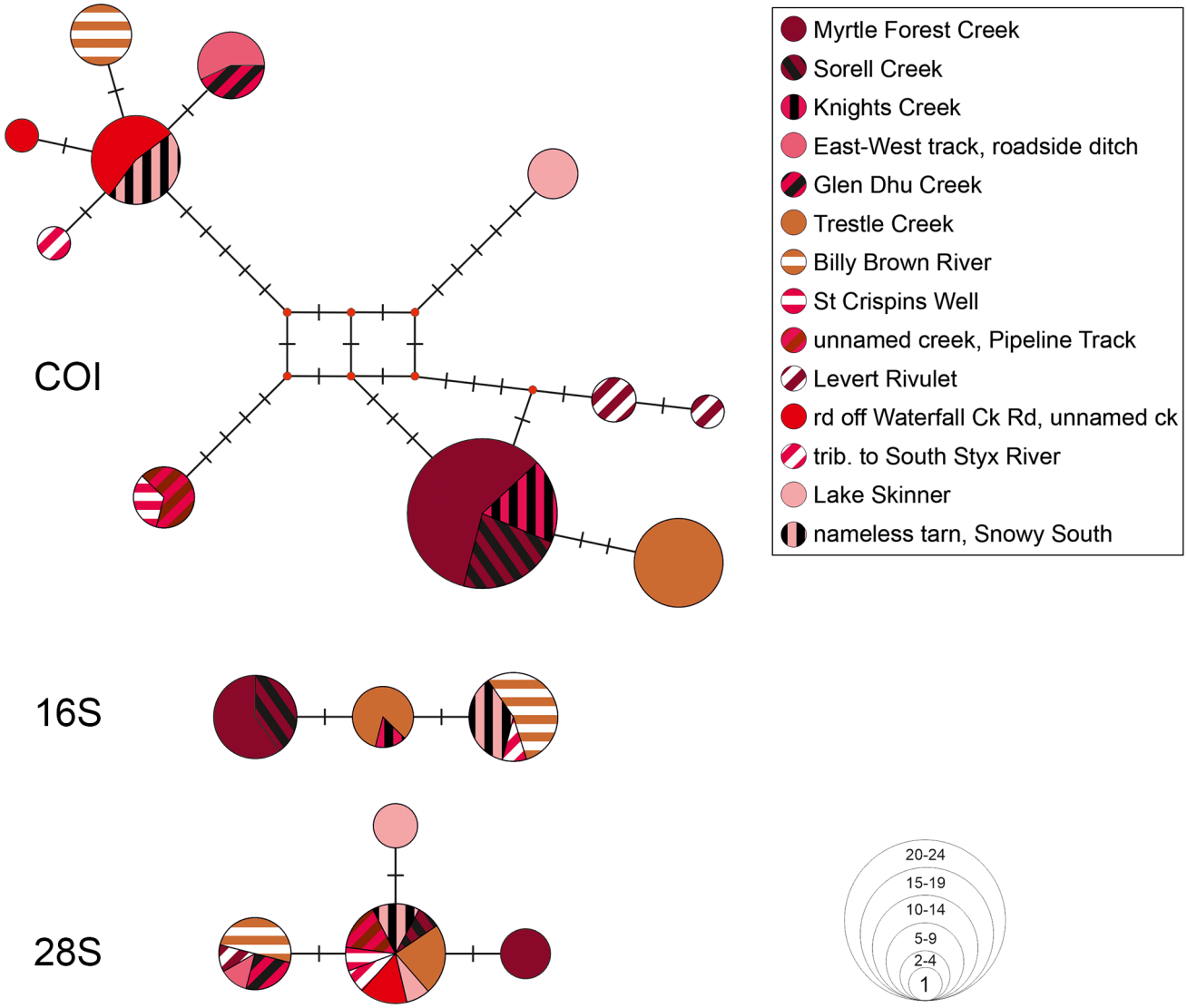


Figure 6. COI, 16S and 28S median joining haplotype networks of *Anaspides driesseni*. Colours correspond to figure legend. The size of each haplotype corresponds to the number of individuals sharing that specific haplotype (see scale). Each dash corresponds to one mutation respectively indel.

morphologically, being less spinose than their more easterly occurring conspecifics. Until more detailed population data are available, they are considered to represent a single species (*A. swaini*).

Comparable to *Anaspides tasmaniae* (Höpel *et al*., 2021), in *A. driesseni* a disjunct distribution between Wellington Park and areas in the south-western wilderness is present (25 km apart, Billy Brown River–Lake Skinner, Figs 7–9), which might be due to a current lack of suitable habitats in the lower areas between the two mountain ranges with the main limiting factors being the water temperature, dissolved solids and turbidity (Williams, 1965; Swain and Reid, 1983; O'Brien, 1990). It should also be noted that we see no signs of artificial translocation as shared haplotypes in COI between Snowy Range and Wellington Range as well as between major drainage systems at Wellington Range (Figs 6, 8–9) do not occur. Therefore, we are likely witnessing the same phenomenon as observed in *A. tasmaniae*, namely that during glacial periods (6–10°C colder than today, Colhoun *et al*., 2010), *A. driesseni* may have occupied a wider geographic range including lower altitudes that includes the Styx and Derwent River as well as the Weld and Huon Rivers; localities at Snowy Range and Wellington Park might have been connected for *Anaspides* during these periods. In contrast to *A. tasmaniae*, however, the genetic difference between these haplotypes is lower (Höpel *et al*., 2021) (see Fig. 6, separation in COI between the haplotype incorporates the unnamed creek crossing the road off Waterfall Creek Road and nameless tarn near the summit of Snowy South and the two haplotypes representing localities at western Wellington Park, Billy Brown River and Glen Dhu Creek catchment), with just one mutation difference and might indicate a more recent connection of these habitats, maybe during the Last Glacial Maximum.

Interestingly, we detected one shared haplotype in COI between two locations at the Snowy Range, which belong to two different major drainage systems (Derwent and Huon River catchment) (Figs 6, 8). We suggest that this shared haplotype is explained by colonization of neighbouring drainages over mountain plateaus via floodplains, swamps or

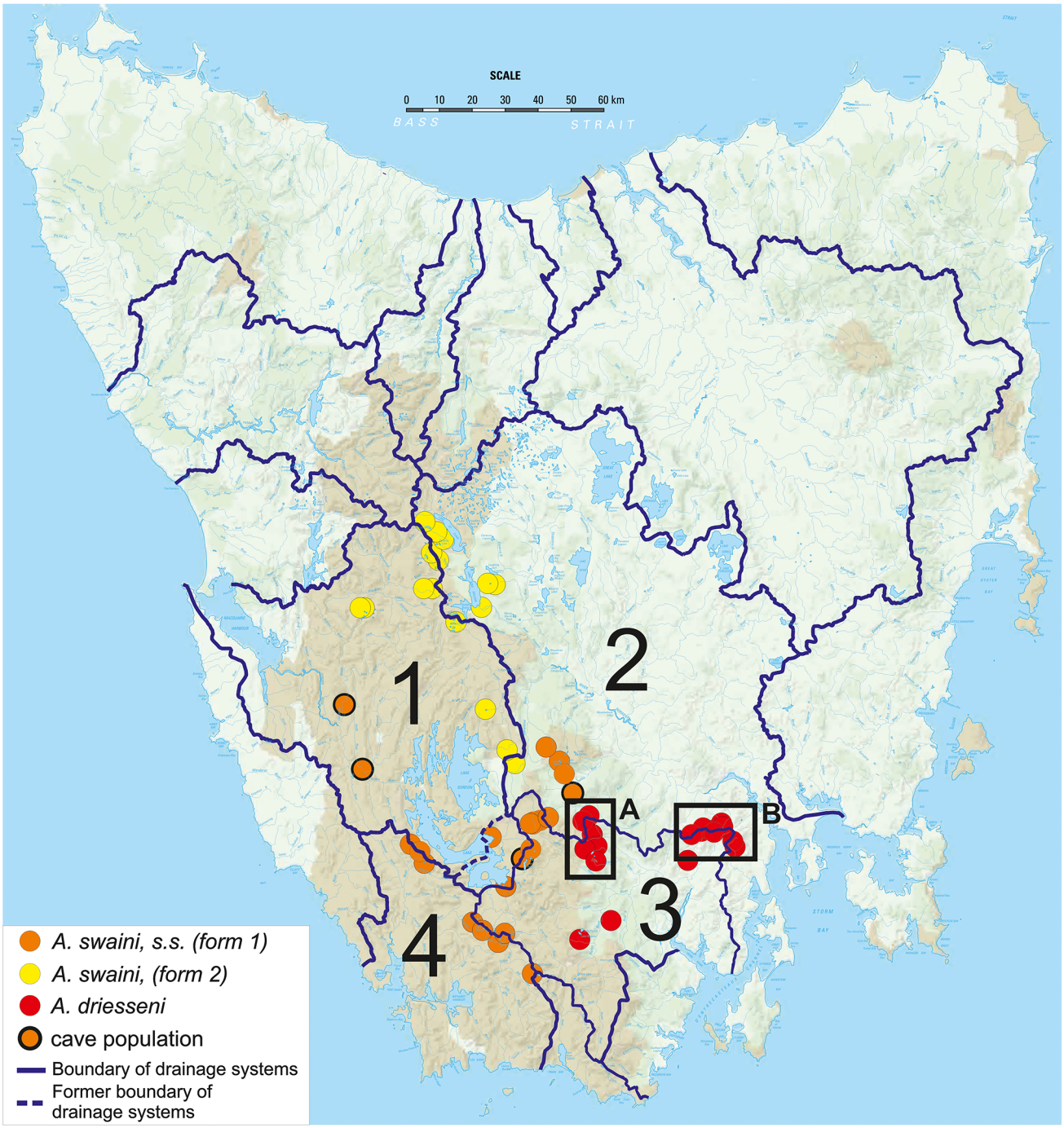


Figure 7. Distribution map of *A. swaini* and *A. driesseni* with important drainage divides (*1*) Franklin-Gordon; (*2*) Derwent; (*3*) Huon; (*4*) Port Davey; and (*5*) North West Bay River. Light brownish background colour indicates National Parks. (*A*) detailed view of Snowy Range, see Fig. 8; (*B*) detailed view of Wellington Park, see Fig. 9. Modified after the Tasmania catchments map. https://dpipwe.tas.gov.au/Documents/Tasmania-Catchment-Map.pdf

snow and snowmelt channels, connecting temporarily different water systems (e.g., at Nevada Peak) (Fig. 8). Interestingly, specimens from a nameless tarn near the summit of Snowy South and Lake Skinner belong to different haplotype clusters in COI (Fig. 6) despite being only 800 m horizontally and 300 m in altitude apart. A similar case of potential crossing of watersheds is found at Wellington Park, where we have two closely related haplotypes in COI and even a shared one in 16S (Fig. 6), between the Myrtle Forest Creek/Sorell Creek (Fig. 9, subdrainage system 3) + Knights Creek systems (Fig. 9, subdrainage system) (all Derwent River catchment) and the Mountain River catchment (Fig. 9, subdrainage system 9, Huon River catchment). A potential crossing area could be the floodplains, swampy area near todays Big Bend Trail. This model of phylogeographic pattering corresponds largely to the Headwater Model (HM) proposed by Finn *et al*. (2007) (waterbug *Abedus herberti*, limited overland dispersal), extended by temporarily connections due to flooded tarn shelfs or swamps or snow and snow melt. *Anaspides* probably also has a limited overland dispersal ability, having been previously observed to sometimes crawl out of the water and being able to survive several days on land (Swain & Reid, 1983).

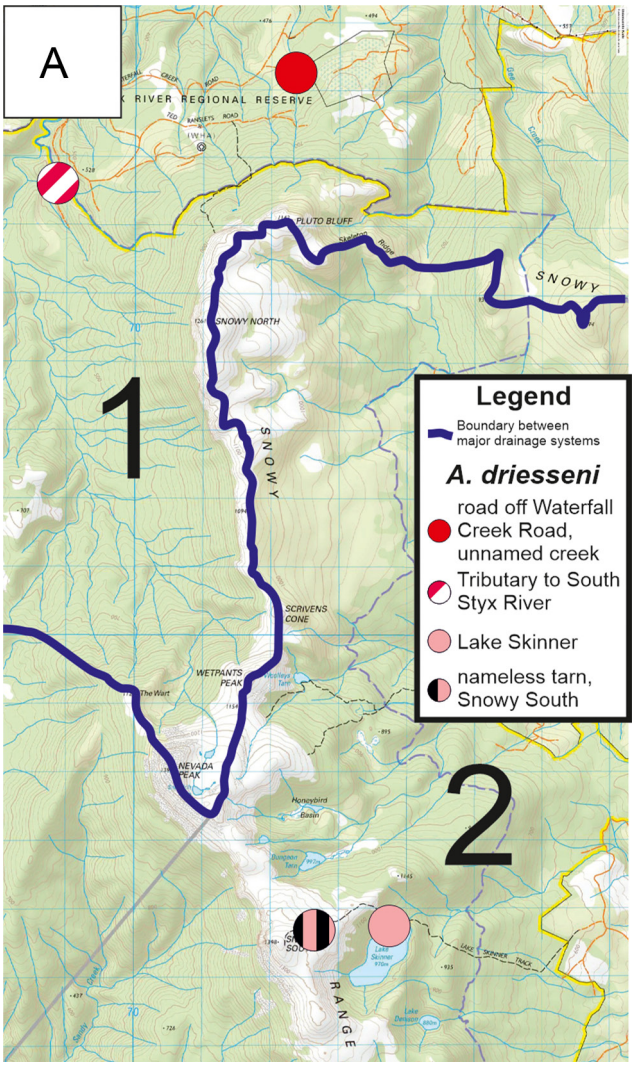


Figure 8. Topographical map of Snowy Range with major drainage systems, as well as collection sites with genetically analysed individuals from this study. 1 corresponds to the Derwent River drainage system, while 2 corresponds to the Huon River drainage systems. Base image by TASMAP© (www.tasmap.tas.gov.au) State of Tasmania.

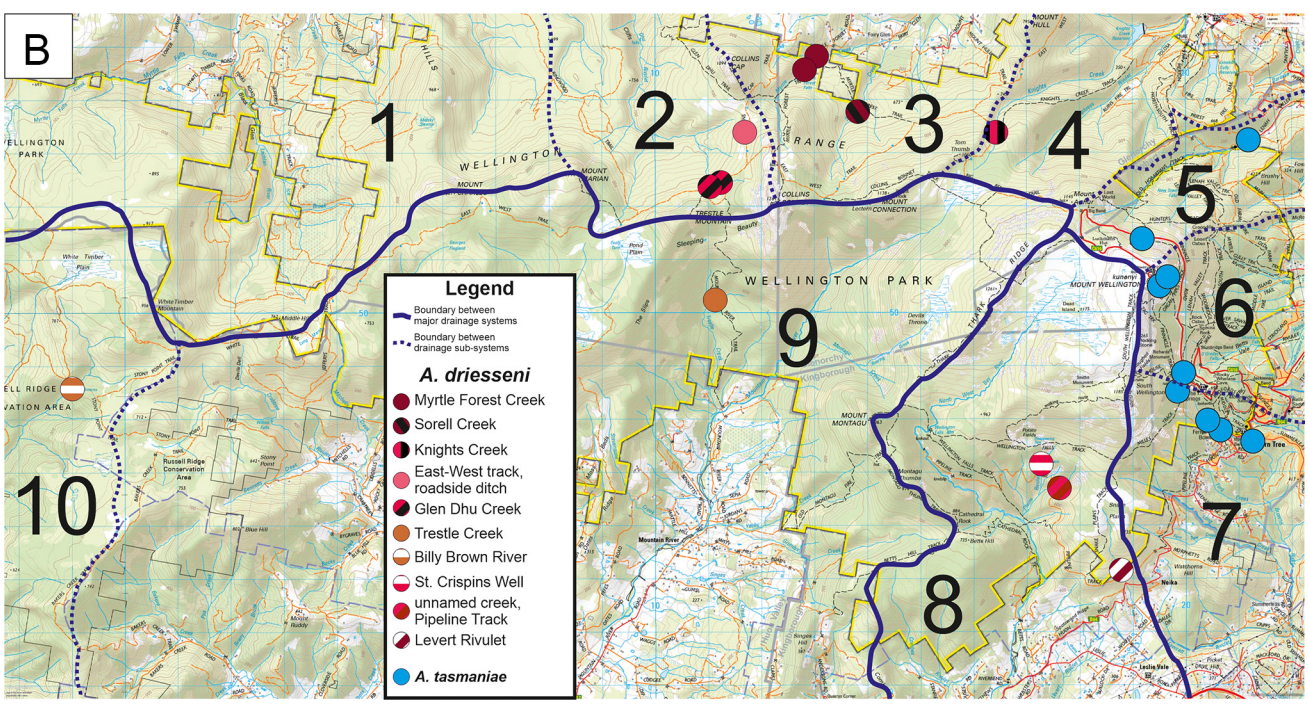


Figure 9. Topographical map of Wellington Park with drainage and sub-drainage systems, as well as collection sites with genetically analysed individuals from this study. Subdrainage systems 1–7 drain into the Derwent River drainage system: (*1*) Lachlan River/Myrtle Falls Creek; (*2*) Glen Dhu Creek; (*3*) Myrtle Forest Creek/Sorell Creek; (*4*) Knights Creek; (*5*) New Town Rivulet; (*6*) Guy Fawkes; (*7*) Browns River; (*8*) corresponds to the Noth West Bay River drainage system; whereas subdrainage system 9–10 drain into the Huon River drainage system; (*9*) Mountain River; (*10*) Judds Creek. Base image by TASMAP© (www.tasmap.tas.gov.au). State of Tasmania.



Figure 10. Typical habitats and colour-in-life of *A. driesseni*: (*A*) Glen Dhu Creek (*B*) Knights Creek at Knights Creek Track (*C*) small trickle fed road side ditch, next to Collins Cap Trail (*D*) unnamed creek, tributary of Styx River, crossing the road off Waterfall Creek Road (*E*) adult male, 35 mm, Ana560, unnamed creek, tributary of Styx River, crossing the road off Waterfall Creek Road. (*F*) adult male, 29 mm, AM P106559, unnamed creek, tributary of Styx River, crossing the road off Waterfall Creek Road.



Figure 11. Dorsal view on the antenna of male *A. swaini* form 1 and 2: (*A*) *A. swaini* form 1, 28 mm, tributary of Weld River, Mueller Road, 5.1 km behind west gate, ZSRO CR76, Ana329, right antenna; (*B*) *A. swaini* form 1, 23 mm, tributary of Weld River, Mueller Road, 4.4 km behind west gate, ZSRO CR75, Ana 655, right antenna; (*C*) *A. swaini* form 2, 29 mm, Lake Oenone, ZSRO CR206, Ana621, left antenna (mirrored view). Scale bars: 1 mm.

Acknowledgements. We are grateful to Cathy Plowman, David Butler, Alastair Richardson, Arthur Clarke, Stefan Eberhard, Andrew Palfreyman, Jenny Sprent, Ben Masterman, and Michael Driessen for advice and helping us to collect various specimens in Tasmania. We further thank the University of Tasmania, Institute for Zoology, especially David Green, for providing us with scientific equipment for our field trips. We are thankful to the Department of Natural Resources and Environment Tasmania (NRE), the Parks and Wildlife Service Tasmania and the Wellington Park Management Trust for supporting and facilitating our research. Specimens were collected in 2017, 2019 and 2022 (Permits of the Tasmanian Government, Department of Primary Industries, Parks, Water & Environment, nos. FA16347, FA18250, FA21214 and FA22411, respectively). We also thank Christian Wirkner, Marian Reinhardt, Malte Weiler, Fabio Oliveira and Markus Grams (all Universität Rostock) for assistance in the field. Collecting in 2017 was funded by the German Science Foundation (DFG RI 837/22-1). Advanced education and collecting in 2019 was partly funded by the DAAD (Nr. 57438025, Kurzstipendien für Doktoranden, 2019/2020). Ralf Bastrop (University of Rostock) provided the infrastructure for sequencing some of the data. We thank Peter Michalik, Lara Lopardo and Tim Dederichs (all University of Greifswald) for taking the high resolution pictures of the antenna. The present project is funded by the Deutsche Forschungsgemeinschaft (DFG RI 837/22-2).

References

Ahyong, S. T. 2015. Preliminary diagnoses of three new species of Tasmanian mountain shrimps, *Anaspides* Thomson, 1894 (Syncarida, Anaspidacea, Anaspididae). *Zootaxa* 3957(5): 596–599.
https://doi.org/10.11646/zootaxa.3957.5.8

Ahyong, S. T. 2016. The Tasmanian mountain shrimps, *Anaspides* Thomson, 1894 (Crustacea, Syncarida, Anaspididae). *Records of the Australian Museum* 68(7): 313–364.
https://doi.org/10.3853/j.2201-4349.68.2016.1669

Ahyong, S. T., and M. A. Alonso-Zarazaga. 2017. Anaspidesidae, a new family for syncarid crustaceans formerly placed in Anaspididae Thomson, 1893. *Records of the Australian Museum* 69(4): 257–258.
https://doi.org/10.3853/j.2201-4349.69.2017.1680

Benson, D. A., I. Karsch-Mizrachi, D. J. Lipman, J. Ostell, and D. L. Wheeler. 2003. GenBank. *Nucleic Acids Research* 31(1): 23–27.
https://doi.org/10.1093/nar/gkg057

Calman, W. T. 1904. On the classification of the Crustacea: Malacostraca. *Annals and Magazine of Natural History* 12: 144–158.
https://doi.org/10.1080/00222930408562451

Colhoun, E. A., K. Kiernan, T. T. Barrows, and A. Goede. 2010. Advances in Quaternary studies in Tasmania. Geological Society, London, Special Publications 346(1): 165–183.
https://doi.org/10.1144/SP346.10

Eberhard, S., A. M. M. Richardson, and R. Swain. 1991. *The Invertebrate Cave Fauna of Tasmania*. Zoology Department, University of Tasmania, 174 pp.

Finn, D. S., M. S. Blouin, and D. A. Lytle. 2007. Population genetic structure reveals terrestrial affinities for a headwater stream insect. *Freshwater Biology* 52(10): 1881–1897.
https://doi.org/10.1111/j.1365-2427.2007.01813.x

Folmer, O., M. Black, W. Hoeh, R. Lutz, and R. Vrijenhoek. 1994. DNA primers for amplification of mitochondrial cytochrome oxidase subunit I from diverse metazoan invertebrates. *Molecular Marine Biology and Biotechnology* 3: 294–299.

Höpel, C. G., S. T. Ahyong, and S. Richter. 2021. Genetic structure and new occurrence records of the iconic Tasmanian mountain shrimp *Anaspides tasmaniae* (Thomson, 1893) (Anaspidesidae: Anaspidacea) reveal relictual distribution in southern Tasmania. *Australian Journal of Zoology* 68(1): 45–53.
https://doi.org/10.1071/ZO20100

Kumar, S., G. Stecher, M. Li, C. Knyaz, and K. Tamura. 2018. MEGA X: molecular evolutionary genetics analysis across computing platforms. *Molecular Biology and Evolution* 35(6): 1547–1549.
https://doi.org/10.1093/molbev/msy096

Manton, S. M. 1930. 36. Notes on the habits and feeding mechanisms of *Anaspides* and *Paranaspides* (Crustacea, Syncarida). *Proceedings of the Zoological Society of London* 100(3): 791–800, pl. 1–4.
https://doi.org/10.1111/j.1096-3642.1930.tb00998.x

O'Brien, D. P. 1990. *The Conservation Status of the Mountain Shrimp (Anaspides tasmaniae and Anaspides spinulae): A Report on its Distribution, Ecology and Taxonomy, Including Recommendations for Management*. Department of Parks, Wildlife and Heritage, Tasmania, 46 pp.

Packard, A. S. 1885. The Syncarida, a group of Carboniferous Crustacea. *American Naturalist* 19: 700–703.
https://doi.org/10.1086/274094

Richter, S., J. Olesen, and W. C. Wheeler. 2007. Phylogeny of Branchiopoda (Crustacea) based on a combined analysis of morphological data and six molecular loci. *Cladistics* 23(4): 301–336.
https://doi.org/10.1111/j.1096-0031.2007.00148.x

Richter, S., M. Schwentner, C. S. Wirkner, and S. T. Ahyong. 2018. Phylogeny and species diversity of Tasmanian mountain shrimps and their relatives (Crustacea, Anaspidesidae). *Zoologica Scripta* 47(1): 84–105.
https://doi.org/10.1111/zsc.12263

Smith, G. 1909. On the Anaspidacea, living and fossil. *Journal of Cell Science* 2(211): 489–578.
https://doi.org/10.1242/jcs.s2-53.211.489

Swain, R., and C. I. Reid. 1983. Observations on the life history and ecology of *Anaspides tasmaniae* (Thomson) (Syncarida: Anaspididae). *Journal of Crustacean Biology* 3(2): 163–172.
https://doi.org/10.2307/1548252

Thomson, G. M. 1893. Notes on Tasmanian Crustacea, with descriptions of new species. *Papers & Proceedings of the Royal Society of Tasmania* 1892: 45–76.

Thomson, G. M. 1894. III. On a Freshwater Schizopod from Tasmania. *Transactions of the Linnean Society of London. 2nd Series. Zoology* 6(3): 285–303.
https://doi.org/10.1111/j.1096-3642.1894.tb00482.x

Tjønneland, A., S. Økland, A. Bruserud, and A. Nylund. 1984. Heart ultrastructure of *Anaspides tasmaniae* Thomson (Crustacea, Syncarida). *Journal of Crustacean Biology* 4: 226–232.
https://doi.org/10.2307/1548019

Williams, W. D. 1965. Ecological notes on Tasmanian Syncarida (Crustacea: Malacostraca). with a description of a new species of *Anaspides*. *Internationale Revue der gesamten Hydrobiologie und Hydrographie* 50(1): 95–126.
https://doi.org/10.1002/iroh.19650500109

Xiong, B., and T. D. Kocher. 1991. Comparison of mitochondrial DNA sequences of seven morphospecies of black flies (Diptera: Simuliidae). *Genome* 34(2): 306–311.
https://doi.org/10.1139/g91-050

4 **Höpel, C. G., Yeo, D., Ahyong, S. T., Meier, R., & Richter, S. (2023). First mitochondrial genomes of Anaspidacea (Malacostraca, Crustacea) and the phylogenetic relationships of mountain shrimps (*Anaspides* Thomson, 1894) and their relatives within Anaspidesidae. Journal of Crustacean Biology, 43(2), ruad028.**

Journal of Crustacean Biology, 2023, **23**, 1–10
https://doi.org/10.1093/jcbiol/ruad028
Advance access publication 5 June 2023
Research Article

The Crustacean Society

OXFORD

First mitochondrial genomes of Anaspidacea (Malacostraca, Crustacea) and the phylogenetic relationships of mountain shrimps (*Anaspides* Thomson, 1894) and their relatives within Anaspidesidae

Christoph G. Höpel[1], Darren Yeo[2], Shane T. Ahyong[3], Rudolf Meier[4] and Stefan Richter[1]

[1]Allgemeine & Spezielle Zoologie, Institut für Biowissenschaften, Universität Rostock, 18055 Rostock, Germany
[2]Centre for Wildlife Forensics, Animal and Plant Health Centre, National Parks Board, Singapore 718827
[3]Australian Museum Research Institute, Australian Museum, Sydney NSW 2010, Australia and School of Biological, Earth & Environmental Sciences, University of New South Wales, Kensington, NSW 2052, Australia
[4]Museum für Naturkunde, Leibniz-Institut für Evolutions- und Biodiversitätsforschung, 10115 Berlin, Germany

Correspondence: C.G. Höpel: e-mail: christoph.hoepel@uni-rostock.de

ABSTRACT

We present the first complete mitochondrial genomes for Anaspidacea by sequencing 24 specimens from 12 different species in four genera (*Anaspides* Thomson, 1894; *Paranaspides* Smith, 1908; *Allanaspides* Swain, Wilson, Hickman & Ong, 1970; and *Micraspides* Nicholls, 1931). We recovered 20 complete (13 protein coding genes, two ribosomal RNA genes, 22 transfer RNAs), and four partial mitogenomes. The full mitogenomes range in length from 15,213 bp to 17,962 bp. We found five different gene orders and reconstruct the ground pattern of Anaspidacea, which differs from the hypothetical pancrustacean ground pattern by the translocation and reversal of tRNA-L1. The same translocation is also found in Euphausiacea and could represent a synapomorphy of these two taxa. Moreover, we reconstruct the phylogenetic relationships of the Anaspidesidae using a data set consisting of the mitochondrial protein coding genes, the two ribosomal RNAs as well as nuclear 18S and 28S rRNA. Our results strongly corroborate the monophyly of all three anaspidesiid genera, with *Paranaspides* as the sister group to *Anaspides*, which together, are sister to *Allanaspides*. Lastly, we resolve the main phylogenetic relationships within *Anaspides*.

KEY WORDS: Australia, Crustacea, gene pattern, ground pattern, mitogenome, phylogeny, Tasmania

INTRODUCTION

Modern-day Anaspidacea is a freshwater malacostracan taxon with a Gondwanan distribution, occurring in mainland Australia, Tasmania, New Zealand, and South America. They are often referred to as living fossils because of their presumably plesiomorphic character traits (within Malacostraca) and the striking similarities between the Triassic *Anaspidites antiquus* Chilton, 1929 from the Hawkesbury sandstone (Brookvale, Australia) and the extant *Anaspides* Thomson, 1894 (Brooks, 1962). Additional fossils convincingly allied to extant Anaspidacea are only known from Cretaceous Lagerstätten in Australia, indicating that Anaspidacea inhabited surfaces waters on Australian mainland in the Mesozoic. The relationship with the morphologically similar fossil group, Palaeocaridacea, which inhabited brackish to freshwater habitats in North America and Europe is not yet resolved (Schram & Koenemann, 2021). Moreover, the phylogenetic position of Anaspidacea within the malacostracans remains unresolved. The most recent molecular results place Anaspidacea as the sister group of the Euphausiacea (Schwentner *et al.*, 2018), but a sister group relationship with Decapoda (Siewing, 1956) or Euphausiacea + Peracarida (Xenommacarida-concept; Richter & Scholtz, 2001) has been suggested.

Among the five recognised families within Anaspidacea, Anaspidesidae Ahyong & Alonso-Zarazaga, 2017 is the largest and best studied, comprising the Tasmanian mountain shrimps of the genus *Anaspides* Thomson, 1894 with eight species, the lake-shrimps *Paranaspides* Smith, 1908, and the swamp shrimps *Allanaspides* Swain, Wilson, Hickman & Ong, 1970 [Swain *et al.*, 1970], each with two species. The

Received 15 December 2022; Accepted 16 May 2023
© The Author(s) 2023. Published by Oxford University Press on behalf of The Crustacean Society. All rights reserved. For permissions, please e-mail: journals.permissions@oup.com

Downloaded from https://academic.oup.com/jcb/article/43/2/ruad028/7190409 by Universitaetsbibliothek Rostock user on 07 June 2023

mentioned similarity of *Anaspides* to *Anaspidites antiquus* might also imply that Anaspidesidae already existed in the Triassic and that the current distribution in Tasmania represents a relict endemism.

The iconic mountain shrimps of the genus *Anaspides* (Fig. 1A) occur mainly in high-altitude lakes, tarns, pools, rivers, and runnels as well as caves all over Tasmania. Only two species were formally recognized until the taxonomic revision by Ahyong (2015, 2016), although earlier studies of cave and surface water *Anaspides* had already revealed high morphological and genetic variability (Goede, 1967; Lake & Coleman, 1977; O'Brien, 1990, Jarman & Elliott, 2000). One species, *Anaspides tasmaniae* (Thompson, 1893), was believed to be widespread all over the island, whereas *A. spinulae* Williams, 1965 was restricted to Lake St. Clair. Ahyong (2015, 2016) described five new species and showed that most of the species have restricted distributions. Only *A. richardsoni* Ahyong, 2016 and *A. swaini* Ahyong, 2015 were accorded wide distributions, but both species show morphological variation that might indicate species flocks (Ahyong, 2016). *Anaspides eberhardi* Ahyong, 2016 is a troglodytic species of the Junee-Florentine karst, probably closely related to *A. richardsoni* from the Mt. Field plateau. Ahyong (2016) found three different, geographically correlated morphological forms within *A. swaini*. Morphological and genetic reexamination of *A. swaini* led to a recognition of 'form 3' as a distinct species, *A. driesseni* Höpel, Richter & Ahyong, 2023 [Höpel *et al.*, 2023]. Another species group was found in southeastern Tasmania, comprising *A. jarmani* Ahyong, 2015 and *A. clarkei* Ahyong, 2015. While *A. jarmani* inhabits surface waters as well as caves, *A. clarkei* is a troglodytic species only found in caves of the Ida Bay and Hastings karst. Richter *et al.* (2018) recovered, depending on the analyses, either of the species as paraphyletic or even polyphyletic with respect to the other species.

The second anaspidesiid genus, *Paranaspides* Smith, 1908 (Fig. 1B), has bentho-pelagic rather than benthic habits. *Paranaspides* is restricted to a few large lakes on the Central Plateau. While *P. lacustris* Smith, 1908 inhabits Great Lake and adjacent lagoons, *P. williamsi* Ahyong, Schwentner & Richter, 2017 [Ahyong *et al.*, 2017]is restricted to Arthurs and Woods lakes. Although Great and Arthurs lakes are artificially connected via a hydrological aqueduct, Ahyong *et al.* (2017) found no evidence of translocation and sympatric occurrence of these two species. Morphologically, *Paranaspides* is more slender but considerably more spinose than *Anaspides*. The most important distinguishing features are the distinct pleonal flexure at pleonite 1 (superficially resembling some decapod caridean shrimps) and the absence of sexually dimorphic antennules (Ahyong *et al.*, 2017). Moreover, species of *Paranaspides* are frequently natatory and occur only in association with aquatic vegetation, amongst and above which they freely swim (Ahyong *et al.*, 2017). The phylogenetic position of *Paranaspides* is currently unresolved. Using 16S sequences, Jarman & Elliott (2000) found *Paranaspides* to be of uncertain position within a clade comprising two lineages of *Anaspides*. Richter *et al.* (2018), using three genetic markers (COI, 16S, and 28S) recovered *Paranaspides* as either the sister group to all *Anaspides* or nested within *Anaspides* as sister group to a clade comprising *A. jarmani* and *A. clarkei.* In the latter case, *Anaspides* was paraphyletic, which would have significant implications for the accuracy of molecular divergence estimates. This would change the interpretation of geological events in the formation of species clades and population divergence in Anaspidesidae, as already shown by Richter *et al.* (2018) in regards to the molecular clock dating.

Allanaspides differs from all other anaspidesiids through the absence of an exopod on thoracopod 7, absence of epipods on the first thoracic appendages, endopods on the pleopods (except for the male petasma), and the presence of a fenestra dorsalis, which is thought to have a function in ion transport and excretion (Fig. 1C) (Lake *et al.*, 1974; McConnell, 1987). The two species of *Allanaspides*, *A. helonomus* Swain, Wilson, Hickman & Ong, 1970 [Swain *et al.*, 1970] and *A. hickmani*

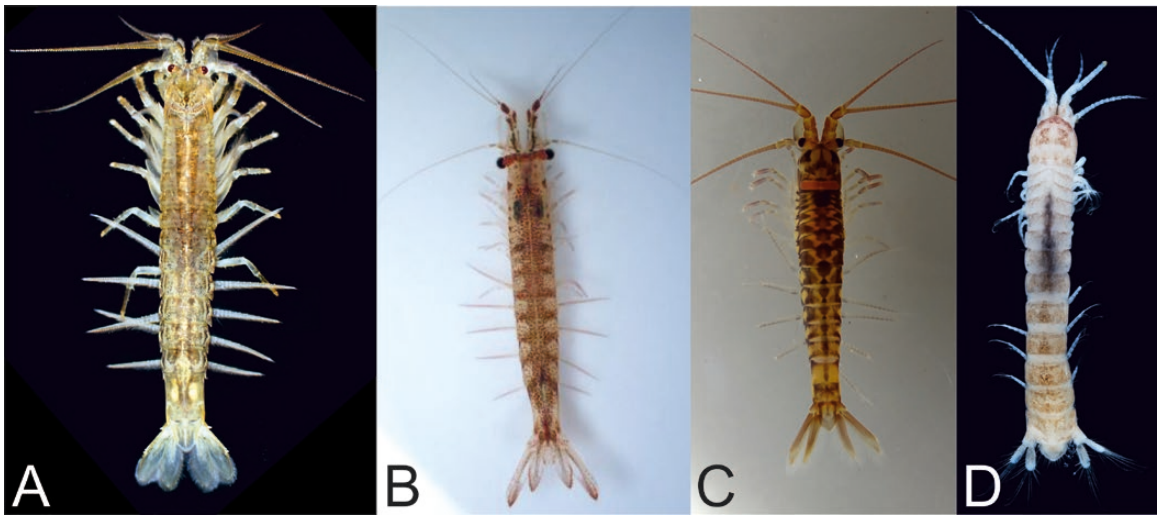


Figure 1. Habitus of four representatives of Anaspidacea: *Anaspides swaini* Ahyong 2015, female, inflow creek to Khazad Dum Cave, Tasmania (**A**); *Paranaspides lacustris* Smith, 1908, female, 18 mm, Tods Corner, Great Lake, AM P100410, Tasmania (modified from Ahyong *et al.* 2017) (**B**); *Allanaspides hickmani* Swain, Wilson & Ong, 1971, female, Lake Pedder edge, Coronation Bay, Tasmania (**C**); *Micraspides sp.*, male, 4.8 mm, crayfish burrow in buttongras moorland, near Zeehan Highway, Tasmania (**D**).

Downloaded from https://academic.oup.com/jcb/article/43/2/ruad028/7190409 by Universitaetsbibliothek Rostock user on 07 June 2023

Swain, Wilson & Ong, 1971 [Swain *et al.*, 1971], primarily inhabit small acidic pools and crayfish burrows (pH 4) in buttongrass moorland swamps around the margins of Lake Pedder and Lake Gordon. Here they can be found in sympatry (Driessen *et al.*, 2014).

A second family within Anaspidacea, Koonungidae Sayce, 1908, includes two genera: *Koonunga* Sayce, 1908 (six species) and *Micraspides* Nicholls, 1931 (one species) (Fig. 1D). While *Koonunga* inhabits small runnels, pools, moorland, and interstitial waters at scattered sites across southeastern Australia (South Australia, Victoria, New South Wales, and Tasmania), *Micraspides calmani* Nicholls, 1931 is currently known only from western Tasmania in buttongrass moorland pools, muddy waters, beneath sphagnum as well as in the diatom-loaded ooze of moss-grown puddles or in burrows of the crayfish *Engaeus* Erichson, 1846 (Nicholls, 1931). It is eyeless and about 8 mm in length.

More and more complete mitochondrial genomes of crustaceans have been published and used in phylogenetic analyses within the last decades (Shen *et al.*, 2015; Tan *et al.*, 2019, González-Castellano *et al.*, 2020; Zhang *et al.*, 2020, Höpel *et al.*, 2022). In particular, some malacostracan groups such as Decapoda, Stomatopoda, Isopoda, and Amphipoda are well represented in mt-genome studies. The gene order of the mitochondrial genome was originally described as highly conserved and thus well suited for resolving phylogenetic relationships between higher taxa (Boore *et al.*, 1998), but it was later revealed to be highly variable in certain taxa, e.g. Isopoda (Kilpert *et al.*, 2012). Nothing is unfortunately known about the gene order of the mitochondrial genome of the enigmatic Anaspidacea, because the mt genome is unknown.

To resolve the phylogenetic relationships of Anaspidacea within Malacostraca as well as the disputed phylogenetic relationships within the anaspidacean family Anaspidesidae, we here report the first mitochondrial genomes of Anaspidacea belonging to Anaspidesidae and Koonungidae. We obtained mitochondrial data from 24 specimens of 12 species in four genera and infer the phylogenetic relationships within Anaspidesidae using mitochondrial as well as nuclear data. We also provide evidence for a potential sister group relationship between Anaspidacea and Euphausiacea.

MATERIAL AND METHODS

Specimens and species delimitation

Specimens were collected during four field surveys in Tasmania in 2006, 2013, 2017, and 2019. A total of 24 specimens from 12 species in four genera (Fig. 1) were newly sequenced for this study (Supplementary material Table S6). The specimens were collected using hand nets and preserved directly in 80–95% ethanol. Specimens of *Anaspides* and *Paranaspides* were identified based on morphology following Ahyong (2015, 2016), Ahyong *et al.* (2017), and Höpel *et al.* (2023). Specimens of *A. swaini* were assigned to morphological 'form 1' or 'form 2' following Ahyong (2016). Specimens of *Allanaspides* were identified following the descriptions of Swain *et al.* (1970, 1971). Sequenceable material of *Micraspides calmani* was unavailable for the present study, so an undescribed species of *Micraspides* (Koonungidae) collected by us from Tasmania was used as an outgroup for the reconstruction of the phylogeny of Anaspidesidae.

DNA extraction, amplification, and sanger sequencing

The DNA extraction was performed with the DNeasy Blood and Tissue Kit (Qiagen, Hilden, Germany), following the manufacturer´s instructions. The two nuclear markers 18S rDNA and 28S rDNA were completely sequenced using different sets of primers (Supplementary material Table S3). The fragment of 18S rRNA was amplified in three overlapping segments, using the following primer pairs: 18S1F/18S5R, 18S3F/18Sbi, 18Sa2.0/18S9R (Giribet *et al.*, 1996; Whiting *et al.*, 1997). The 28S rRNA fragment was amplified using different overlapping sets of primer pairs depending on the species: 28Srd1a/28Sb, 28Sa/28Srd5b, 28Srd4.8a/28Srd7b1, 28Srd1a/28Srd4b, 28Sa/28SBout, and 28Srd3a/28Sb (Schwendinger & Giribet, 2005; Edgecombe & Giribet, 2006; Richter *et al.*, 2007). The polymerase chain reaction (PCR) had a total volume of 30 µl containing 3 µl of each primer (each 10 µM), 3 µl 10× buffer (Sigma Aldrich, St. Louis, MO, USA), 3 µl dNTP mix (2 mM, Biozym, Hessisch Oldendorf, Germany), 2.58 µl MgCl2 (25 mM; Sigma Aldrich), 0.12 µl Taq-polymerase (Sigma Aldrich), 10.71 µl ultrapure water and 4.5 µl of the DNA extract. PCR amplification programs comprised an initial denaturation step at 94 °C for 1 min, followed by 35 amplification cycles (94 °C for 30 s, 55 °C for 30 s, 72 °C for 60 s) and a final elongation step at 72°C for 8 min. All PCR reactions were performed with a Mastercycler gradient (Eppendorf, Hamburg, Germany). PCR products were visualized by gel electrophoresis, using 5 µl of the PCR product with 1.5 µl loading buffer DNA b II (AppliChem, Darmstadt, Deutschland) on a 1.2 % agarose/TAE gel stained with 5 µl Rotisafe (Carl Roth, Karlsruhe, Deutschland). PCR products were purified using paramagnetic beads (High Prep PCR, Magbio, Lausanne, Schweiz) following the manufacturer's instructions with a final volume of 25 µl. Sequencing of PCR products was performed in Lightrun96 well plates by Eurofins Genomics (Ebersberg, Germany). The resulting chromatograms were manually checked and adjusted with Geneious 2021.0.3 (Biomatters Ltd., Auckland, New Zealand). We obtained the complete 18S sequence from all and the complete 28S sequence from 18 specimens. From 5 specimens we obtained the partial 28S sequence and no 28S sequence was obtained for Ana561 (*Micraspides* sp.) (Supplementary material Table S5). All sequences were deposited in GenBank (Benson *et al.*, 2003) (accession numbers: OQ818832 - OQ818854, OQ820201–OQ820224).

Mitogenome sequencing and assembly

The DNA extraction was performed with the DNeasy Blood and Tissue Kit (Qiagen), following the manufacturer's instruction. The extracted DNA was quantified with a Qubit 2.0 Fluorometer (Thermo Fisher, Waltham, MA, USA) and pooled in separate libraries such that closely related species (< 5% *cox1* p-distance) were never in the same pool (Supplementary material Table S7). The pools were then sent to AIT Novogene (Singapore) for Illumina library preparation with NEBNext Ultra II Kits (New England Biolabs, Ipswich, MA, USA) and 150-bp paired-end sequencing on Hiseq 4000 and Novaseq 6000 platforms (Illumina, San Diego, CA, USA).

Downloaded from https://academic.oup.com/jcb/article/43/2/ruad028/7190409 by Universitaetsbibliothek Rostock user on 07 June 2023

The reads were processed following a modified mitochondrial metagenomics pipeline outlined in Crampton-Platt *et al.* (2016). Adapter trimming was first performed on the raw reads with Trimmomatic v0.36 (Bolger *et al.*, 2014). A BLAST search was then performed against a reference database of full Malacostraca mitogenomes downloaded from NCBI Genbank (accessed 8 May 2020) to retain only 'mitochondrial gene-like' reads. The filtered reads were then assembled using four different assemblers: 1) Qiagen CLC Genomics Workbench [*de novo* assembly, create simple contig sequences], 2) SPAdes [-meta, -k 21,33,55,77] (Bankevich *et al.*, 2012), 3) Ray [-k 61, -minimumseedlength 100, -minimumcontiglength 1000] (Boisvert *et al.*, 2010) and 4) IDBA-UD [–mink 60, -axk 150] (Peng *et al.*, 2012). For IDBA, an additional quality filtering step was performed prior to assembly using PRINSEQ [-min_len 150 -min_qual_mean 25 -ns_max_n 0 -trim_qual_right 20] (Schmieder & Edwards, 2011).

The assembled contigs were checked for anomalies with an additional BLAST search against the same reference. Contigs < 1,000-bp were discarded while the remaining contigs were assembled into supercontigs in Geneious R7 (1,000-bp minimum overlap, 1% maximum mismatches per read) (Kearse *et al.*, 2012). Cox1 and 16S fragments obtained via Sanger sequencing of the target species were used as mitochondrial gene baits to assign the supercontigs to species. The baiting was performed via similarity-based mapping in Geneious R7 (100-bp minimum overlap, 0% maximum mismatches per read) (Kearse *et al.*, 2012).

Mitogenome annotation and nucleotide composition analysis

The rRNAs and protein-coding genes were annotated using MITOS2 WebServer (Donath *et al.*, 2019) as well as the Annotate and Predict function in Geneious Prime 2021.0.3 (Biomatters Ltd.) using various malacostracan mitogenomes available on NCBI as reference. The boundaries of protein-coding genes were then manually checked and adjusted if necessary by searching for their start and stop codons and with direct comparison with other malacostracan genes annotated in GenBank.

The tRNA genes were identified and checked by using the MITOS2 WebServer, ARWEN (Laslett & Canbäck, 2008), tRNAscan-SE 2.0 (Chan & Lowe, 2019), and the Annotate and Predict function in Geneious Prime 2021.0.3. The AT and GC skews were analysed using the formulas of Perna & Kocher (1995): AT skew = (A − T)/(A + T) and GC skew = (G − C)/(G + C). The annotated full and partly genome sequences were finally deposited in GenBank under the accession numbers: OQ721873–OQ721896).

Phylogenetic analyses

We separately aligned each protein coding gene (PCG) using Translation Align implemented in Geneious Prime 2021.0.3 (Biomatters Ltd.) with default parameters (Genetic Code: Invertebrate Mitochondrial). Each rRNA gene (12S, 16S, 18S, 28S) was separately aligned using Clustal Omega with default parameters, implemented in Geneious Prime® 2021.0.3 (Biomatters Ltd.). All individual alignments were combined into a single data set comprising 17,543 characters.

Phylogenetic relationships were inferred by Bayesian Inference (BI), Maximum-Likelihood and Maximum-Parsimony (MP) analyses. For the BI and ML analyses the best fit model of evolution was determined by the implemented model test in raxmlGUI 2.0.8 (Darriba *et al.*, 2020). Bayesian-inference analyses were performed with MrBayes 3.2.7a (Ronquist *et al.*, 2012) on CIPRES Science Gateway (Miller *et al.*, 2010). Each Bayesian analyses included four runs with four differentially heated chains and the analysis was run for 30×10^6 generations, sampled every 3,000 generations. The first 10% were discarded as burn-in. All parameters were checked with Tracer version 1.7 (Rambaut *et al.*, 2018). Maximum-Likelihood analyses were performed using RAxML v2.0 (Stamatakis, 2014). The data were unpartitioned and the analysis was performed with a random seed, the GTRGAMMA model and 1,000 thorough bootstraps. Maximum-Parsimony analyses were conducted with the console version of TNT v1.5, June 2021 (Goloboff & Catalano, 2016) using New Technology (Torres *et al.*, 2021). The script PhylogenomicSearch.run (Torres *et al.*, 2021) was applied with the following arguments specified: search nt level 5 hits 5 weights equal gaps miss output newick outgroup Ana561. Bootstrap values were calculated using the script PhylogenomicSupport.run (Torres *et al.*, 2021). The applied arguments were: format tnt sites boot gaps miss replic 1,000 search nt level 5 weights equal output newick. Resulting trees were visualised with FigTree v.1.4.2 (Rambaut, 2014) and Corel Draw 2020.

RESULTS

Genomic characters, genes, and gene order

From 24 studied specimens we obtained the complete circular mitochondrial genome for 20 specimens and a partial mitochondrial genome for four specimens (Supplementary material Table S4). The complete mitochondrial genomes range in size from 15,213 bp (*Anaspides clarkei*, Ana11) up to 17,962 bp (*A. jarmani*, Ana246). Within the 20 complete mitogenomes we could identify all typical 37 metazoan genes (13 protein-coding, 22 tRNA, and 2 rRNA genes) (Fig. 2). We were still able to identify all 37 genes of the partial mitogenome of Ana332; here only parts of 12S rRNA and the non-coding region were missing. The 12S rRNA was missing in Ana378, both rRNA genes were missing in Ana468, whereas both rRNA genes and nad2 were missing in Ana543. We found 38 genes in Ana138 and Ana141 (both *Allanaspides hickmani*). Here we identified a second tRNA-L1 gene located next to the other tRNA-L1 gene. Both were situated between COI and tRNA-L2 (Fig. 3). We identified 40 genes in *Micraspides* sp., with four tRNA-L2 genes, all situated next to each other and located between tRNA-L1 and CO2 (Fig. 3). The overall A+T content regarding the complete mitogenomes ranges from 69% (*Allanaspides helonomus*, Ana127) to 75.5 % (*Micraspides* sp., Ana561) (Supplementary material Table S4). We discovered six different start codons for the 24 examined specimens: ATG, ATT, ACG, ATA, ATC, and GTG, as well as three different stop codons: TAA, TAG, and the incomplete T– The mitogenome of all examined species showed a negative AT and GC skew. The AT skew ranged from –0.051 (Ana120, *P. lacustris*) to –0.134 (Ana154, *A. swaini* form 1) and the GC skew ranges from –0.217 (Ana154, *A. swaini* form 1 and Ana553, *P. williamsi*) to –0.310 (Ana128, *Allanaspides helonomus*). Nine protein coding genes (cox1, cox2, cox3, cob, nad2, nad3, nad6, atp6, atp8)were encoded on the heavy strand, whereas the others (nad1, nad4, nad4L, nad5) were encoded

Downloaded from https://academic.oup.com/jcb/article/43/2/ruad028/7190409 by Universitaetsbibliothek Rostock user on 07 June 2023

on the light strand (Fig. 2). We recovered two reading-frame overlaps on the same strand, between atp6/atp8 and nad4/nad4L, overlapping by seven nucleotides.

We discovered five different gene order patterns (Fig. 3). All species of *Anaspides* share the same gene order (Figs. 2, 3). The two species of *Paranaspides* differ in the translocation of tRNA-W from the pattern of *Anaspides* (Fig. 3; difference no. 2). Here tRNA-W is situated between tRNA-C and tRNA-Y. Both species of *Allanaspides* also show a translocation of tRNA-W, but in contrast to *Paranaspides,* tRNA-W is situated between tRNA-Q and tRNA-I in *Allanaspides* (Fig. 3; difference no. 3). In addition, *A. hickmani* has a duplication of the tRNA-L1 gene (Fig. 3; difference no. 4). Both tRNA-L1 genes are situated next to each other. These two tRNA-L1 genes have 80.7% similarity. Furthermore, the tRNA-L1 gene directly next to cox1 has 80.7–87.7% similarity with other Anaspidacea tRNA-L1 genes, whereas the other has a slightly higher similarity (86–94.7%) compared with other Anaspidacea tRNA-L1 genes. The t-RNA-L1 gene with the higher similarity is therefore considered to represent the original copy (Fig. 3). *Micraspides* sp. differs in gene order from *Anaspides* only in the presence of 4 tRNA-L2 genes, which are located directly next to each other (Fig. 3; difference no. 5). These genes have a 95.1–100% similarity. Two of these genes are identical, whereas the others differ in one and two base pairs, respectively.

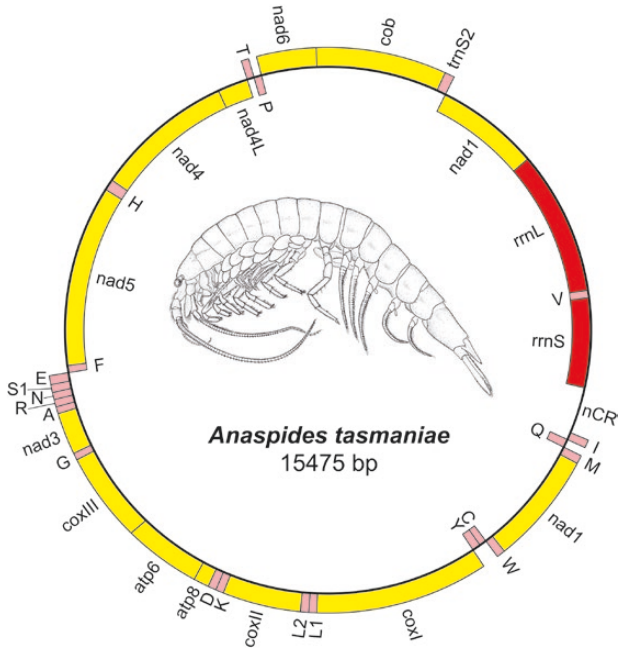


Figure 2. Map of the mitochondrial genome of *Anaspides tasmaniae* (Ana535). PCGs are yellow, rRNAs red, and tRNAs pink. Genes encoded on the heavy and light strands are shown outside and inside the circular gene map. Transfer RNA genes are labelled with their one-letter amino acid codes. Image of *A. tasmaniae* modified after Ahyong (2016: fig. 1).

Phylogeny of Anaspidesidae

The resulting phylogenetic trees of MP and BI show identical topologies, while in the ML analyses the position of Ana473 (*A. richardsoni*) differs slightly within the central clade with only low bootstrap support of 66 in the ML analyses (98 bootstrap support in MP and posterior probability of 1 in BI), although not affecting any of the other phylogenetic relationships (Fig. 4, Supplementary material Figs. S1, S2). *Allanaspides* is recovered as monophyletic in all analyses, and is sister group to the clade comprising reciprocally monophyletic *Anaspides* and *Paranaspides* (MP, ML: 100 bootstrap support, BI posterior probability 1). *Paranaspides* is always recovered as sister group

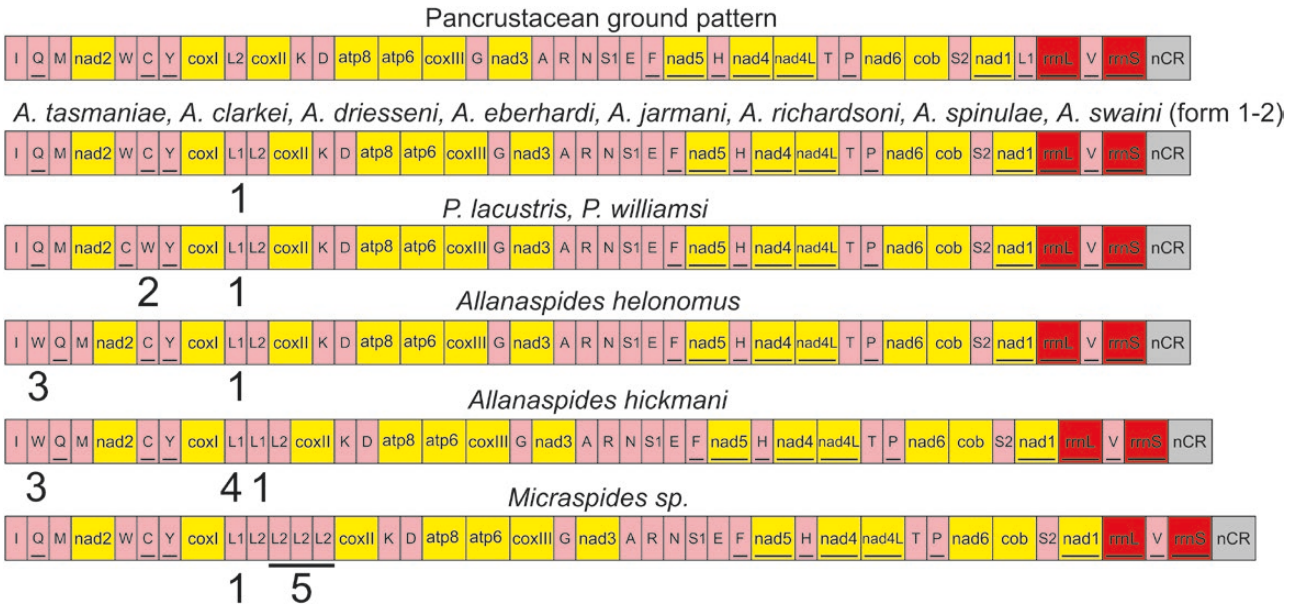


Figure 3. Gene order pattern of the 12 anaspidacean species and the hypothetical pancrustacean groundpattern. Genes encoded on the light strand are underlined. PCGs are yellow, rRNAs red, and tRNAs pink. Transfer RNA genes are labelled with their one-letter amino acid codes. Differences in gene pattern to the pancrustacean ground pattern (translocations, duplications) are indicated with numbers under the corresponding genes; 1 = translocation and reversal of tRNA-L1, 2 = translocation of tRNA-W, 3 = translocation of tRNA-W, 4 = duplication of tRNA-L1, 5 = duplications of tRNA-L2.

Downloaded from https://academic.oup.com/jeb/article/43/2/ruad028/7190409 by Universitaetsbibliothek Rostock user on 07 June 2023

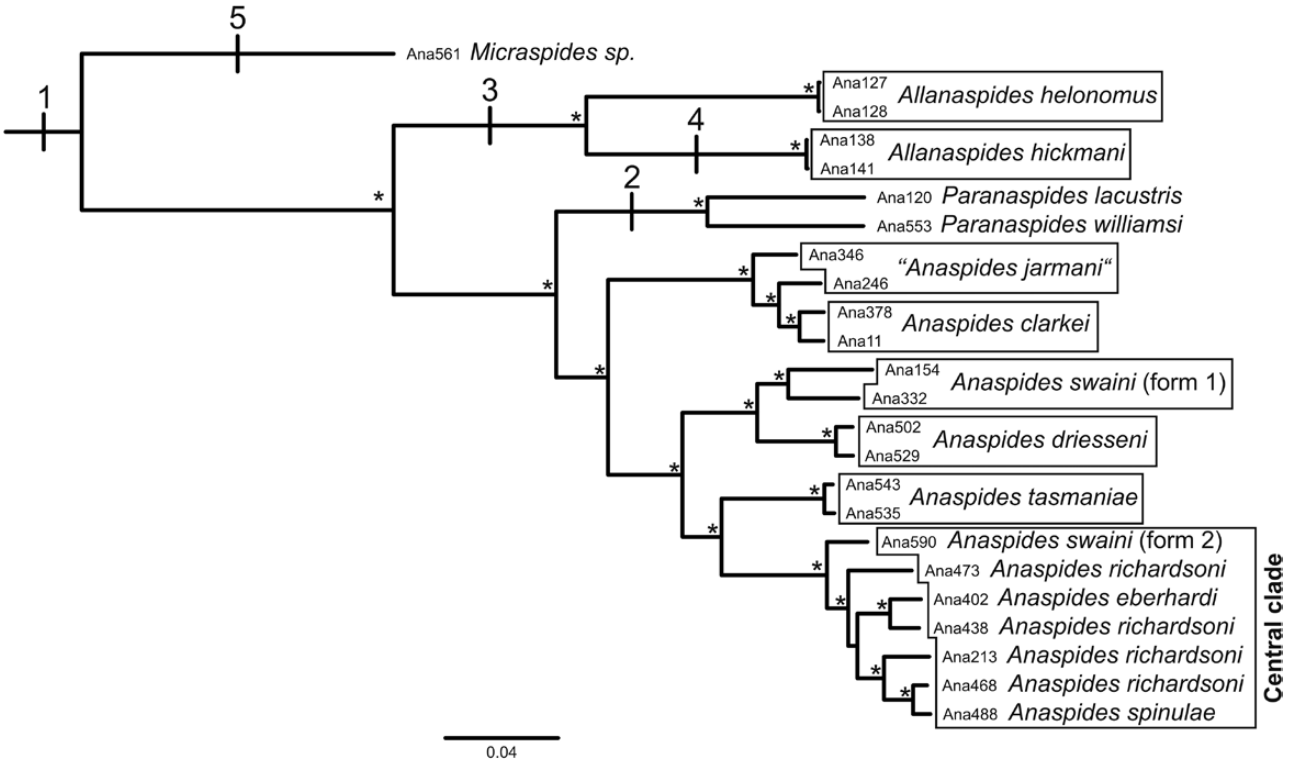


Figure 4. Bayesian inference phylogram calculated with MrBayes 3.2.7a, with their corresponding Ana number and species. The concatenated dataset (PCGs + 12S + 16S + 18S + 28S) includes 17543 characters. *Micraspides* sp. was set as outgroup. Posterior probabilities (*) are 1 for every node. Differences in gene pattern to the pancrustacean ground pattern (translocations, duplications) are indicated by vertical lines and numbers corresponding to Figure 3.

to *Anaspides* (MP, ML: 100 bootstrap support, BI posterior probability 1). Within *Anaspides*, a species clade comprising *A. jarmani* and *A. clarkei*, is sister group to the remaining species of *Anaspides* (MP: 96 bootstrap support, ML: 88 bootstrap support, BI posterior probability 1). *Anaspides clarkei* is recovered within a paraphyletic *A. jarmani*. *Anaspides swaini* form 1 (= *A. swaini* sensu stricto) is sister group to *A. driesseni*, which together form a clade that is sister group to larger clade containing *A. tasmaniae*, *A. eberhardi* Ahyong, 2016, *A. richardsoni*, *A. spinulae*, and *A. swaini* (form 2) (MP, ML: 100 bootstrap support, BI posterior probability 1). This species clade (with exception of *A. tasmaniae*) is called herein 'central clade' following Richter *et al.* (2018) but expanded by inclusion of *A. swaini* form 2 (Fig. 4). *Anaspides tasmaniae* is sister species to the central clade (MP, ML: 100 bootstrap support, BI posterior probability 1). Within the central clade, *A. swaini* form 2 (Ana590) is sister group to the remaining representatives of the central clade. Moreover, we recovered a paraphyletic *A. richardsoni*, with *A. spinulae* closest to Ana468 (*A. richardsoni*, tributary of Travellers Rest River) and *A. eberhardi* closest to Ana438 (*A. richardsoni*, Robert Tarn).

DISCUSSION

Phylogenetic relationships: the position of *Paranaspides*

Similar to Jarman & Elliott (2000) and Richter *et al.* (2018), we recover a monophyletic *Allanaspides* as sister group to *Anaspides* + *Paranaspides*. Unlike previous studies, however, we robustly determine the phylogenetic position of the Lake Shrimps (*Paranaspides* spp.). All our analyses recovered *Paranaspides* as sister group to *Anaspides* in contrast to the uncertain position in Jarman & Elliott (2000) and Richter *et al.* (2018). Our result is similar to what was previously reported based on an analysis of 16S (Richter *et al.*, 2018). *Anaspides jarmani* and *A. clarkei* form a clade, the latter species nested within a paraphyletic *A. jarmani*. This species clade was also uncovered by Jarman & Elliott (2000) (labelled as *A. tasmaniae*, fig. 4 node D) and Richter *et al.* (2018) with different internal relationships depending on the analysed gene. In our analyses the *A. jarmani* + *A clarkei* clade is sister group to all remaining *Anaspides*. This is the first phylogenetic analysis to include specimens of all three forms of *A. swaini* delineated by Ahyong (2016) (of which form 1 corresponds to *A. swaini* sensu stricto and form 3 to *A. driesseni*). Our results always show a sister group relationship between *A. driesseni* and *A. swaini* form 1. Richter *et al.* (2018) recovered three distinct genetic lineages within *A. swaini* form 1 (labelled *A. swaini* 1–3) when examining specimens from Mueller Road, all unfortunately juveniles. We obtained results for two of the three lineages (Ana154, lineage 2; Ana 332, lineage 1). As in Richter *et al.* (2018), the two lineages had higher intraspecific distances in comparison to lineages within other species of *Anaspides*. Further sampling within the range of *A. swaini* form 1 is required to better evaluate the taxonomic implications of our observations.

Our analyses also include for the first time specimens of *A. swaini* form 2 (Ana590). It is noteworthy that *A. swaini* form 2 is neither closely related to *A. swaini* sensu stricto (form 1) nor

Downloaded from https://academic.oup.com/jcb/article/43/2/ruad028/7190409 by Universitaetsbibliothek Rostock user on 07 June 2023

A. driesseni (formerly *A. swaini* form 3), but is recovered as sister group to a species group comprising *A. richardsoni*, *A. eberhardi*, and *A. spinulae*. Moreover, Ana590 has the same 28S and 18S sequence as Ana473 (*A. richardsoni*) and Ana402 (*A. eberhardi*). Populations of *A. swaini* form 2 also occur in the same drainage system as *A. richardsoni* (Derwent River water system) and some are parapatric (possibly sympatric) with *A. spinulae* (Lake St. Clair) (Ahyong, 2016). Therefore, *A. swaini* form 2 is considered to be part of the 'central clade' of Richter *et al.* (2018). Although the position of *A. swaini* form 2 is perhaps unexpected, it having been previously considered part of *A. swaini* by having two antennular clasping spines in males, the sister group position is, nevertheless, recovered in all of our analyses. Given the phylogenetic position of *A. swaini* sensu stricto, *A. driesseni* and *A. tasmaniae* and common presence of two antennular clasping spines, the presence of one antennular clasping spine is best interpreted as a derived state in the species of the 'central clade' (except *A. spinulae*, with two spines). The presence of two clasping spines in *A. swaini* form 2 simply reflects retention of the plesiomorphic state as exhibited also by *A. driesseni*, *A. swaini* sensu stricto, and *A. tasmaniae*. While the phylogenetic position of *A. tasmaniae* varied between analyses in Richter *et al.* (2018), it is always recovered as the sister group to the 'central clade' in our analyses.

We found several lineages of *A. richardsoni* and the lineages of *A. eberhardi* (Ana402) within the central clade, as well as *A. spinulae* (Ana488), which are nested within *A. richardsoni*. *Anaspides eberhardi* is recovered as sister taxon to *A. richardsoni* from Robert Tarn, Mt. Field (Ana438). The populations at the top of Mt. Field, such as Robert Tarn, are the geographically closest known *A. richardsoni* populations to *A. eberhardi*, which only inhabits the caves of the Junee Florentine karst system in and around the Mt. Field National Park. Nevertheless, there are no known incidences of sympatry between these two species (Ahyong, 2016; Höpel *et al.*, 2021). A similar situation is also present in *A. spinulae*, which is closely related to *A. richardsoni* from a tributary of the Travellers Rest River (Ana468). Again, this population of *A. richardsoni* is the geographically nearest known to *A. spinulae*, with the Travellers Rest River draining into the Derwent River, as with Lake St. Clair. The evolutionary dynamics in the 'central clade' is evidently more complex than in other clades of *Anaspides*, but the current state of knowledge limits our interpretation of the phylogenetic patterns. Further population genetic analyses, comprising more specimens and locations are needed to clarify the phylogenetic relationships within these species clades.

Gene order

The Pancrustacea/Tetraconata ground pattern has been originally described as highly conservative (Boore *et al.*, 1998), but subsequent studies have uncovered a greater variability, especially in certain taxa (Kilpert *et al.*, 2012; Tan *et al.*, 2019; Moreno-Carmona *et al.*, 2021). For example, Hexapoda can be considered as a highly variable group because of the high level of reorganization (47%), although this variability is unevenly distributed among higher taxonomic units. Many higher taxa of Hexapoda still retain the pancrustacean ground pattern (11 taxonomic groups) or have only a low percentage of rearrangements (0.1–10%, 15 taxonomic orders), whereas three insect orders show a more substantial percentage (24–40%) and three taxa a high percentage (> 70%) of rearrangements (Moreno-Carmona *et al.*, 2021). Moreover, 80% (86.4% in Hexapoda) of the rearrangements affecting mitogenome architecture involve tRNAs (Bernt *et al.*, 2013) and it has been observed that different tRNAs move at different rates (Moritz *et al.*, 1987). For example, one of the most mobile regions within the mitogenomes is the region comprising trnI, trnQ, and trnM.

The same phenomenon can also be observed within crustaceans. Rearrangements are unevenly distributed and while some taxa show none (e.g. Stomatopoda, Spinicaudata), or only few (Notostraca, Anonstraca, Euphausiacea, Pentastomida), certain other taxa show higher variability, e.g. Decapoda, Amphipoda, Cladocera, Copepoda, or Ostracoda (Tan *et al.*, 2019, Castellucci *et al.*, 2022) (Fig. 5). In most of these higher taxonomic units, however, basal branching taxa often retain the pancrustacean ground pattern or differ only slightly. For instance, the pancrustacean ground pattern is dominant in the most basal branching taxa in Decapoda (e.g. Dendrobranchiata, Caridea, Achelata, and Glypheidea), whereas only a few taxa show high variability, such as Anomura and Gebiidea. Some of these gene rearrangements, however, are informative synapomorphies for some taxonomic groups providing strong independent support for certain phylogenetic relationships (Tan *et al.*, 2019). In contrast to Decapoda, no taxa within Peracarida retained the pancrustacean ground pattern and many taxa have a high percentage of rearrangements (Fig. 5) (Kilpert *et al.*, 2012; Krebes & Bastrop, 2012; Pons *et al.*, 2014; Stokkan *et al.*, 2016). For most higher taxa, however, it was possible to deduce a ground pattern and to find autapomorphic translocations, respectively gene patterns as in Isopoda or Amphipoda (Fig. 5) (Kilpert *et al.*, 2012; Krebes & Bastrop, 2012). Moreover, it is possible to find certain autapomorphic patterns for different subgroups. Gene translocation

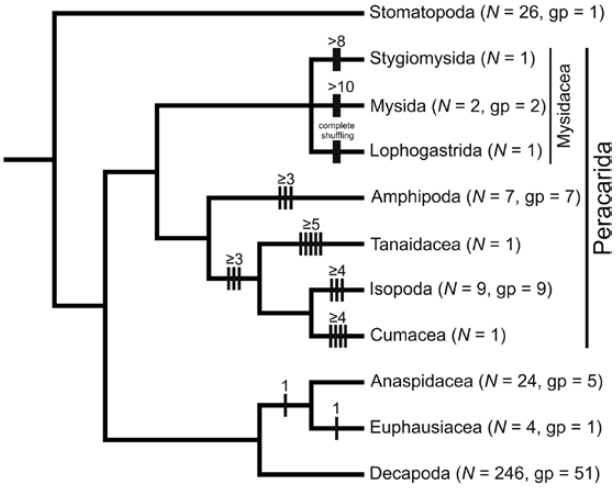


Figure 5. Cladogram of malacostracan crustaceans with higher classification and the numbers of differences of the taxa ground pattern from the pancrustacean ground pattern (translocations, duplications) indicated by vertical lines. Phylogeny modified after Schwentner *et al.*, 2018. Included species (*N*) and number of different gene pattern (gp) indicated in brackets after the taxon name. Taxa ground pattern and number of included species deduced for: Amphipoda: Krebes *et al.*, 2012; Decapoda: Tan *et al.*, 2019; Isopoda: Kilpert *et al.*, 2012.

Downloaded from https://academic.oup.com/jcb/article/43/2/ruad028/7190409 by Universitaetsbibliothek Rostock user on 07 June 2023

events leading to gene rearrangements could therefore be valuable in phylogenetic analyses. The only exception is Mysidacea, where no shared, derived translocations were detected between Mysida, Lophogastrida, and Stygiomysida (Fig. 5). Moreover, all taxa have distinctly different gene orders and only few ancestral clusters (Höpel *et al.*, 2022).

In comparison to the ground pattern of Pancrustacea/Tetraconata, which is also the ground pattern for the eumalacostracans, all Anaspidacea show one difference, namely, the translocation and reversion of tRNA-L1. The tRNA-L1 is situated between cox1 and tRNA-L2 (Figs. 3, 4; difference no. 1). We consider the most parsimonious explanation is that this pattern represents the potential ground pattern of the Anaspidacea (with the obvious caveat that several families within Anaspidacea are yet to be studied) (Figs. 3, 4). This translocation and reversion of tRNA-L1 is present in all examined specimens of Anaspidacea and also in Euphausiacea, so it could represent a synapomorphy uniting Euphausiacea and Anaspidacea as potential sister groups, as uncovered in the analyses of Schwentner *et al.* (2018) (Fig. 5). The two species of *Paranaspides* diverge from the anaspidacean ground pattern in the translocation of tRNA-W, being now situated between tRNA-C and tRNA-Y (Figs. 3, 4; difference no. 2), representing an autapomorphic translocation for *Paranaspides*. tRNA-W is translocated and situated between tRNA-Q and tRNA-I in both species of *Allanaspides*, which represents an autapomorphy for *Allanaspides*. Moreover, we found two tRNA-L1 genes situated next to each other in *A. hickmani*. We uncovered the presence of four tRNA-L2 genes in *Micraspides* sp., which are directly adjacent. Two of these tRNA-L2 are even identical, whereas the other differs in 1 and 2 base pairs, respectively. The high similarity of the tRNA genes and their positions in both species (*Allanaspides hickmani*, *Micraspides* sp.) suggest that these are duplications. All of these duplications form stable secondary structures and are therefore considered to be functional. Such a duplication of a tRNA gene, in combination with maintaining its function, was also observed in the freshwater crab *Geothelphusa dehaani* (White, 1847) (Segawa & Aotsuka, 2005). In this case, the tRNA-L gene was duplicated. We can also find tRNA duplication in the non-malacostracan species, *Epopella plicata* (Gray, 1843) (Cirripedia), where an entire tRNA pattern (S2-C-Y) was duplicated and the two tRNA-C genes have a 100% similarity (Shen *et al.*, 2017).

Our mitogenomic analyses resolved the phylogenetic relationships within the Anaspidesidae and provided valid autapomorphies for certain lower taxa such as *Allanaspides* and *Paranaspides*, showing again that mitogenomic rearrangement can provide a promising tool to infer phylogenetic relationships, including at a smaller scale. Additionally, all of the differences between the gene order were related to translocation/duplications of tRNAs genes (Bernt *et al.*, 2013; Moreno-Carmona *et al.*, 2021). The monophyly of all three anaspadesiid genera is strongly corroborated.

This approach was cost-effective due to the now low cost of high-throughput sequencing. This makes genome skimming an increasingly attractive option for obtaining full-length mt genome for many species. This is particularly cost-effective for the naturally enriched DNA of plastomes. The multiplexing of multiple species per library (as long as they are genetically distinct) (Supplementary material Table S7) is also facilitated by mitochondrial 'baits,' which can be sequenced in a cost-effective manner (see Srivathsan *et al.*, 2021). We find that 1 Gb per species is often sufficient to recover full-mitochondrial genomes for crustaceans, even where mitochondrial gene rearrangements are present (see Gan *et al.*, 2016; Tan *et al.*, 2019, 2021; Höpel *et al.*, 2022). In cases where the starting material is degraded, greater sequencing depth and a larger number of 'baits' might be required. this, however, is likely not much more expensive given the low per Gb costs of Illumina sequencers. We hope that this genome skimming approach provides more crustacean researchers the tools for more cost-effective mitochondrial genome sequencing for phylogenetic reconstruction.

SUPPLEMENTARY MATERIAL

Supplementary material is available at *Journal of Crustacean Biology* online.

S1 Figure. Maximum-Likelihood phylogram calculated with RAxML v2.0, with their corresponding Ana number and species.

S2 Figure. Maximum-Parsimony phylogram calculated with TNT v1.5, with their corresponding Ana number and species.

S3 Table. List of 28S rRNA and 18S rRNA primers used.

S4 Table. Selected genomic characters of the examined species.

S5 Table. Length of the 18S rrnA and 28S rrnA fragment newly sequenced.

S6 Table. List of individuals used for this study.

S7 Table. Sequencing effort for the analysed specimens.

ACKNOWLEDGEMENTS

We are grateful to Alastair Richardson, Michael Driessen, Arthur Clarke, Cathy Plowman, David Butler, Ben Masterman, Andrew Palfreyman, and Stefan Eberhard for enthusiastic support of our research and collecting. We further thank the Institute for Zoology, University of Tasmania, especially David Green, for providing scientific equipment for our field trips. We are thankful to the Department of Natural Resources and Environment Tasmania (NRE), the Parks and Wildlife Service Tasmania, and the Wellington Park Management Trust for supporting and facilitating our research. We are also thankful to Christian Wirkner, Markus Grams, Jonas Keiler and Marian Reinhardt for assistance in the field. We want to thank Petr Smejkal and Serena Benjamin for collecting *Anaspides* in Khazad Dum Cave and Bradley Smith leading us to Lake Pedder collecting the lake population of *Allananspides helonomus*. We are grateful to the reviewers for their comments and suggestions. Specimens were collected under Tasmanian Department of Primary Industries, Parks, Water and Environment permit TFA17038, TFA16347 and FA18250. Collection of specimens in 2017 was funded by the German Science Foundation (DFG RI 837/22-1) and in 2019 was partly funded by the German Academic Exchange Service (57438025, Kurzstipendien für Doktoranden, 2019/2020) and the University of Rostock (Promotionsstipendienprogramm, 'Unsere Besten promovieren in Rostock'). The present

Downloaded from https://academic.oup.com/jcb/article/43/2/ruad028/7190409 by Universitaetsbibliothek Rostock user on 07 June 2023

project was funded by the German Science Foundation (DFG RI 837/22-2).

REFERENCES

Ahyong, S.T. 2015. Preliminary diagnoses of three new species of Tasmanian mountain shrimps, *Anaspides* Thomson, 1894 (Syncarida, Anaspidacea, Anaspididae). *Zootaxa*, **3957**: 596–599.

Ahyong, S.T. 2016. The Tasmanian mountain shrimps, *Anaspides* Thomson, 1894 (Crustacea, Syncarida, Anaspididae). *Records of the Australian Museum*, **68**: 313–364.

Ahyong, S.T. & Alonso-Zarazaga, M.A. 2017. Anaspidesidae, a new family for syncarid crustaceans formerly placed in Anaspididae Thomson, 1893. *Records of the Australian Museum*, **69**: 257–258.

Ahyong, S.T., Schwentner, M. & Richter, S. 2017. The Tasmanian Lake Shrimps, *Paranaspides* Smith 1908 (Crustacea, Syncarida, Anaspididae). *Records of the Australian Museum*, **69**: 259–275.

Bankevich, A., Nurk, S., Antipov, D., Gurevich, A.A., Dvorkin, M., Kulikov, A.S., Lesin, V.M., Nikolenko, A.I., Pham, S., Prjibelski, A.D., Pyshkin, A.V., Sirotkin, A.V., Vyahhi, N., Tesler, G., Alekseyev, M.A. & Pevzner, P.A. 2012. SPAdes: a new genome assembly algorithm and its applications to single-cell sequencing. *Journal of Computational Biology*, **19**: 455–477.

Benson, D.A., Karsch-Mizrachi, I., Lipman, D.J. & Ostell, J. & Wheeler, D.L. 2003 Genbank. *Nucleic Acids Research*, **31**: 23–27.

Bernt, M., Braband, A., Schierwater, B. & Stadler, P. F. 2013. Genetic aspects of mitochondrial genome evolution. *Molecular Phylogenetics and Evolution*, **69**: 328–338.

Boisvert, S., Laviolette, F. & Corbeil, J. 2010. Ray: simultaneous assembly of reads from a mix of high-throughput sequencing technologies. *Journal of Computational Biology*, **17**: 1519–1533.

Bolger, A.M., Lohse, M. & Usadel, B. 2014. Trimmomatic: a flexible trimmer for Illumina sequence data. *Bioinformatics*, **30**: 2114–2120.

Boore, J.L., Lavrov, D.V. & Brown, W.M. 1998. Gene translocation links insects and crustaceans. *Nature*, **392**: 667–668.

Brooks, H.K. 1962. On the fossil Anaspidacea, with a revision of the classification of the Syncarida. *Crustaceana*, **4**: 229–242.

Castellucci, F., Luchetti, A. & Mantovani, B. 2022. Exploring mitogenome evolution in Branchiopoda (Crustacea) lineages reveals gene order rearrangements in Cladocera. *Scientific Reports*, **12**: 1–10 [https://doi.org/10.1038/s41598-022-08873-y].

Chan, P.P. & Lowe, T.M. 2019. tRNAscan-SE: searching for tRNA genes in genomic sequences. In: *Gene prediction*, pp. 1–14. Humana, New York.

Chilton, C. 1929. Note on a fossil shrimp from Hawkesbury sandstones. *Journal of the Royal Society of New South Wales*, **62**: 366–368.

Crampton-Platt, A., Yu, D.W., Zhou, X. & Vogler, A. P. 2016. Mitochondrial metagenomics: letting the genes out of the bottle. *GigaScience*, **5**: s13742–016 [https://doi.org/10.1186/s13742-016-0120-y].

Darriba, D., Posada, D., Kozlov, A.M., Stamatakis, A., Morel, B. & Flouri, T. 2020. ModelTest-NG: a new and scalable tool for the selection of DNA and protein evolutionary models. *Molecular Biology and Evolution*, **37**: 291–294.

Donath, A., Jühling, F., Al-Arab, M., Bernhart, S.H., Reinhardt, F., Stadler, P.F. & Bernt, M. 2019. Improved annotation of protein-coding genes boundaries in metazoan mitochondrial genomes. *Nucleic Acids Research*, **47**: 10543–10552.

Driessen, M.M., Mallick, S.A., Thurstans, S., Smith, B. & Brereton, R.N. 2014. Distribution and conservation status of two endemic Tasmanian crustaceans, *Allanaspides hickmani* and *Allanaspides helonomus* (Syncarida: Anaspididae). *Papers and Proceedings of the Royal Society of Tasmania*, **148**: 1–9.

Edgecombe, G.D. & Giribet, G. 2006. A century later–a total evidence re-evaluation of the phylogeny of scutigeromorph centipedes (Myriapoda: Chilopoda). *Invertebrate Systematics*, **20**: 503–525.

Erichson, W.F. 1846. Uebersicht der Arten der Gattung *Astacus*. *Archiv für Naturgeschichte*, **12**: 86–103.

Gan, H.Y., Gan, H.M., Tan, M.H., Lee, Y.P. & Austin, C.M. 2016. The complete mitogenome of the hermit crab *Clibanarius infraspinatus* (Hilgendorf, 1869), (Crustacea; Decapoda; Diogenidae) – a new gene order for the Decapoda. *Mitochondrial DNA Part A*, **27**: 4099–4100.

Giribet, G., Carranza, S., Baguna, J., Riutort, M. & Ribera, C. 1996. First molecular evidence for the existence of a Tardigrada + Arthropoda clade. *Molecular Biology and Evolution*, **13**: 76–84.

Goede, A. 1967. Tasmanian cave fauna: character and distribution. *Helictite*, **5**: 71–85.

Goloboff, P.A. & Catalano, S.A. 2016. TNT version 1.5, including a full implementation of phylogenetic morphometrics. *Cladistics*, **32**: 221–238.

González-Castellano, I., Pons, J., González-Ortegón, E. & Martínez-Lage, A. 2020. Mitogenome phylogenetics in the genus *Palaemon* (Crustacea: Decapoda) sheds light on species crypticism in the rockpool shrimp *P. elegans*. *PLoS ONE*, **15**: e0237037 [https://doi.org/10.1371/journal.pone.0237037].

Gray, J.E. 1843. Chapter 10. Fauna of New Zealand. In: *Travels in New Zealand; with contributions to the geography, geology, botany, and natural history of that country*. Vol. **2**, (E. Dieffenbach, ed.), pp. 177–296, John Murray, London.

Höpel, C.G., Ahyong, S.T. & Richter, S. 2021. Genetic structure and new occurrence records of the iconic Tasmanian mountain shrimp *Anaspides tasmaniae* (Thomson, 1893) (Anaspidesidae: Anaspidacea) reveal relictual distribution in southern Tasmania. *Australian Journal of Zoology*, **68**: 45–53.

Höpel, C.G., Richter, S. & Ahyong, S.T. 2023. A new species of Tasmanian Mountain Shrimp, *Anaspides driesseni* sp. nov. (Malacostraca, Anaspidacea, Anaspidesidae). *Records of the Australian Museum*, **75**: 25–43.

Höpel, C.G., Yeo, D., Grams, M., Meier, R. & Richter, S. 2022. Mitogenomics supports the monophyly of Mysidacea and Peracarida (Malacostraca). *Zoologica Scripta*, **51**: 603–613.

Jarman, S.N. & Elliott, N.G. 2000. DNA evidence for morphological and cryptic Cenozoic speciations in the Anaspididae, 'living fossils' from the Triassic. *Journal of Evolutionary Biology*, **13**: 624–633.

Kearse, M., Moir, R., Wilson, A., Stones-Havas, S., Cheung, M., Sturrock, S., Buxton, S., Cooper, A., Markowitz, A., Duran, C., Thierer, T., Ashton, B., Meintjes, P. & Drummond, A. 2012. Geneious Basic: an integrated and extendable desktop software platform for the organization and analysis of sequence data. *Bioinformatics*, **28**: 1647–1649.

Kilpert, F., Held, C. & Podsiadlowski, L. 2012. Multiple rearrangements in mitochondrial genomes of Isopoda and phylogenetic implications. *Molecular Phylogenetics and Evolution*, **64**: 106–117.

Krebes, L. & Bastrop, R. 2012. The mitogenome of *Gammarus duebeni* (Crustacea Amphipoda): A new gene order and non-neutral sequence evolution of tandem repeats in the control region. *Comparative Biochemistry and Physiology Part D: Genomics and Proteomics*, **7**: 201–211.

Lake, P.S. & Coleman, D.J. 1977. On the subterranean syncarids of Tasmania. *Helictite*, **15**: 12–17.

Lake, P.S., Swain, R. & Ong, J.E. 1974. The ultrastructure of the fenestra dorsalis of the syncarid crustaceans *Allanaspides helonomus* and *Allanaspides hickmani*. *Zeitschrift für Zellforschung und Mikroskopische Anatomie*, **147**: 335–351.

Laslett, D. & Canbäck, B. 2008. ARWEN: a program to detect tRNA genes in metazoan mitochondrial nucleotide sequences. *Bioinformatics*, **24**: 172–175.

McConnell, F. M. 1987. Morphometry of transport tissues in a freshwater crustacean. *Tissue and Cell*, **19**: 319–349.

Miller, M.A., Pfeiffer W. & Schwartz T. 2010. Creating the CIPRES Science Gateway for inference of large phylogenetic trees. Gateway Computing Environments Workshop (GCE), New Orleans, LA, USA, pp. 1-8 [https://doi.org/10.1109/GCE.2010.5676129].

Moreno-Carmona, M., Cameron, S.L. & Quiroga, C.F.P. 2021. How are the mitochondrial genomes reorganized in Hexapoda? Differential evolution and the first report of convergences within Hexapoda. *Gene*, **791**: 145719 [https://doi.org/10.1016/j.gene.2021.145719].

Downloaded from https://academic.oup.com/jeb/article/43/2/ruad028/7190409 by Universitaetsbibliothek Rostock user on 07 June 2023

Moritz, C.T.E.D., Dowling, T.E. & Brown, W.M. 1987. Evolution of animal mitochondrial DNA: relevance for population biology and systematics. *Annual Review of Ecology and Systematics*, **18**: 269–292.

Nicholls, G.E. 1931. *Micraspides calmani*, a new Syncaridan from the West Coast of Tasmania. *Journal of the Linnean Society of London, Zoology*, **37**: 473–488.

O'Brien, D.P. 1990. *The conservation status of the mountain shrimp (Anaspides tasmaniae and Anaspides spinulae): a report on its distribution, ecology and taxonomy, including recommendations for management*. Department of Parks, Wildlife and Heritage, Hobart, Tasmania, Australia.

Peng, Y., Leung, H.C., Yiu, S.M. & Chin, F.Y. 2012. IDBA-UD: a de novo assembler for single-cell and metagenomic sequencing data with highly uneven depth. *Bioinformatics*, **28**: 1420–1428.

Perna, N.T. & Kocher, T.D. 1995. Patterns of nucleotide composition at fourfold degenerate sites of animal mitochondrial genomes. *Journal of Molecular Evolution*, **41**: 353–358.

Pons, J., Bauzà-Ribot, M.M., Jaume, D. & Juan, C. 2014. Next-generation sequencing, phylogenetic signal and comparative mitogenomic analyses in Metacrangonyctidae (Amphipoda: Crustacea). *BMC Genomics*, **15**: 1–16 [https://doi.org/10.1186/1471-2164-15-566].

Rambaut, A. 2014. *FigTree: Tree figure drawing tool version 1.4.2*. Institute of Evolutionary Biology, University of Edinburgh, Edinburgh, UK.

Rambaut, A., Drummond, A.J., Xie, D., Baele, G. & Suchard, M.A. 2018. Posterior summarization in Bayesian phylogenetics using Tracer 1.7. *Systematic Biology*, **67**: 901–904.

Richter, S. & Scholtz, G. 2001. Phylogenetic analysis of the Malacostraca (Crustacea). *Journal of Zoological Systematics and Evolutionary Research*, **39**: 113–136.

Richter, S., Olesen, J. & Wheeler, W.C. 2007. Phylogeny of Branchiopoda (Crustacea) based on a combined analysis of morphological data and six molecular loci. *Cladistics*, **23**: 301–336.

Richter, S., Schwentner, M., Wirkner, C.S. & Ahyong, S.T. 2018. Phylogeny and species diversity of Tasmanian mountain shrimps and their relatives (Crustacea, Anaspidesidae). *Zoologica Scripta*, **47**: 84–105.

Ronquist, F., Teslenko, M., Van der Mark, P., Ayres, D.L., Darling, A., Höhna, S., … Huelsenbeck, J.P. 2012. MrBayes 3.2: Efficient Bayesian phylogenetic inference and model choice across a large model space. *Systematic Biology*, **61**: 539–542.

Sayce, O.A. 1908. On *Koonunga cursor*: a remarkable new type of malacostracous Crustaceans. *Transactions of the Linnean Society of London* (Series 2, Zoology), **11**: 1–16, pl. 1, 2.

Schmieder, R. & Edwards, R. 2011. Quality control and preprocessing of metagenomic datasets. *Bioinformatics*, **27**: 863–864.

Schram, F.R., & Koenemann, S. 2021. *Evolution and Phylogeny of Pancrustacea: A Story of Scientific Method*. Oxford University Press, Oxford.

Schwendinger, P.J. & Giribet, G. 2005. The systematics of the southeast Asian genus *Fangensis* Rambla (Opiliones: Cyphophthalmi: Stylocellidae). *Invertebrate Systematics*, **19**: 297–323.

Schwentner, M., Richter, S., Rogers, D.C. & Giribet, G. 2018. Tetraconatan phylogeny with special focus on Malacostraca and Branchiopoda: highlighting the strength of taxon-specific matrices in phylogenomics. *Proceedings of the Royal Society B: Biological Sciences*, **285**: 20181524 [https://doi.org/10.1098/rspb.2018.1524].

Segawa, R.D. & Aotsuka, T. 2005. The mitochondrial genome of the Japanese freshwater crab, *Geothelphusa dehaani* (Crustacea: Brachyura): evidence for its evolution via gene duplication. *Gene*, **355**: 28–39.

Shen, X., Tian, M., Yan, B. & Chu, K. 2015. Phylomitogenomics of Malacostraca (Arthropoda: Crustacea). *Acta Oceanologica Sinica*, **34**: 84–92.

Shen, X., Tsang, L.M., Chu, K.H. & Chan, B.K.K. 2017. A unique duplication of gene cluster (S2–C–Y) in *Epopella plicata* (Crustacea) mitochondrial genome and phylogeny within Cirripedia. *Mitochondrial DNA, Part A*, **28**: 285–287.

Siewing, R. 1956. Untersuchungen zur Morphologie der Malacostraca (Crustacea). *Zoologische Jahrbücher, Abteilung für Anatomie und Ontogenie der Tiere*, **75**: 39–176.

Smith, G.W. 1908. Preliminary account of the habits and structure of the Anaspididae, with remarks on some other fresh-water Crustacea from Tasmania. *Proceedings of the Royal Society of London*, Series B, **80**, 465–473.

Srivathsan, A., Lee, L., Katoh, K., Hartop, E., Kutty, S.N., Wong, J., Yeo, D. & Meier, R. 2021. ONTbarcoder and MinION barcodes aid biodiversity discovery and identification by everyone, for everyone. *BMC Biology*, **19**: 1–21 [https://doi.org/10.1186/s12915-021-01141-x].

Stamatakis, A. 2014. RAxML version 8: a tool for phylogenetic analysis and post-analysis of large phylogenies. *Bioinformatics*, **30**: 1312–1313.

Stokkan, M., Jurado-Rivera, J.A., Juan, C., Jaume, D. & Pons, J. 2016. Mitochondrial genome rearrangements at low taxonomic levels: three distinct mitogenome gene orders in the genus *Pseudoniphargus* (Crustacea: Amphipoda). *Mitochondrial DNA, Part A*, **27**: 3579–3589.

Swain, R., Wilson, I.S. & Ong, J.E. 1971. A new species of *Allanaspides* (Syncarida, Anaspididae) from south-western Tasmania. *Crustaceana*, **21**: 196–202.

Swain, R., Wilson, I.S., Hickman, J.L. & Ong, J.E. 1970. *Allanaspides helonomus* gen. et sp. nov. (Crustacea: Syncarida) from Tasmania. *Records of the Queen Victoria Museum*, **35**: 1–13.

Tan, M.H., Gan, H.M., Bracken-Grissom, H., Chan, T.Y., Grandjean, F. & Austin, C.M. 2021. More from less: Genome skimming for nuclear markers for animal phylogenomics, a case study using decapod crustaceans. *Journal of Crustacean Biology*, **41**: ruab009 [https://doi.org/10.1093/jcbiol/ruab009].

Tan, M.H., Gan, H.M., Lee, Y.P., Bracken-Grissom, H., Chan, T.Y., Miller, A.D. & Austin, C.M. 2019. Comparative mitogenomics of the Decapoda reveals evolutionary heterogeneity in architecture and composition. *Scientific Reports*, **9**: 1–16 [https://doi.org/10.1038/s41598-019-47145-0].

Thompson, G.M. 1893. Notes on Tasmania crustacea, with description of new species. *Papers and Proceedings of the Royal Society of Tasmania*, **1892**: 45–76.

Thomson, G.M. 1894. III. On a freshwater schizopod from Tasmania. *Transactions of the Linnean Society of London* (Series 2, Zoology), **6**: 285–303.

Torres, A., Goloboff, P.A. & Catalano, S.A. 2021. Parsimony analysis of phylogenomic datasets (I): scripts and guidelines for using TNT (Tree Analysis using New Technology). *Cladistics*, **38**: 103–125.

White, A. 1847. *List of the specimens of Crustacea in the collection of the British Museum*. British Museum, London.

Whiting, M.F., Carpenter, J.C., Wheeler, Q.D. & Wheeler, W.C. 1997. The Strepsiptera problem: phylogeny of the holometabolous insect orders inferred from 18S and 28S ribosomal DNA sequences and morphology. *Systematic Biology*, **46**: 1–68.

Williams, W.D. 1965. Ecological notes on Tasmanian Syncarida (Crustacea: Malacostraca) with a description of a new species of *Anaspides*. *Internationale Revue der gesamten Hydrobiologie und Hydrographie*, **50**: 95–126.

Zhang, Y., Bi, Y. & Feng, M. 2020. The complete mitochondrial genome of *Lophosquillia costata* (Malacostraca: Stomatopoda) from China and phylogeny of stomatopods. *Mitochondrial DNA Part B*, **5**: 2495–2497.

Downloaded from https://academic.oup.com/jcb/article/43/2/ruad028/7190409 by Universitaetsbibliothek Rostock user on 07 June 2023

5 Höpel, C. G., Ahyong, S. T., Kapun, M., Schwentner, M., & Richter, S. (2025). Phylogeography of the *Anaspides richardsoni* species clade (Anaspidacea, Anaspidesidae): glaciation and recolonization of the Central Plateau and the question of paraphyletic species. Cladistics. (https://doi.org/10.1111/cla.70005)

Check for updates

WILEY

Cladistics

Cladistics (2025) 1–23

doi: 10.1111/cla.70005

Phylogeography of the *Anaspides richardsoni* species clade (Anaspidacea, Anaspidesidae): glaciation and recolonization of the Tasmanian Central Plateau and the question of paraphyletic species

Christoph G. Höpel[a,*], Shane T. Ahyong[b,c], Martin Kapun[d], Martin Schwentner[d] and Stefan Richter[a,*]

[a]*Allgemeine & Spezielle Zoologie, Institut für Biowissenschaften, Universität Rostock, Universitätsplatz 2, 18055 Rostock, Germany;* [b]*Australian Museum Research Institute, Australian Museum, 1 William Street, Sydney, NSW 2010, Australia;* [c]*School of Biological, Earth & Environmental Sciences, University of New South Wales, Kensington, NSW 2052, Australia;* [d]*Naturhistorisches Museum Wien, Burgring 7, 1010 Wien, Austria*

Received 30 December 2024; Revised 19 June 2025; Accepted 30 June 2025

Abstract

We herein present a phylogenetic and population genetic analysis of a Tasmanian Mountain Shrimp clade, based on ddRAD and cytochrome oxidase subunit-1 data sets. Our data show that the morphologically well-delineated and widespread *Anaspides richardsoni* Ahyong, 2016 is paraphyletic with respect to four other species (*A. eberhardi* Ahyong, 2016, *A. spinulae* Williams, 1965 and two undescribed species). These four species all form discrete (monophyletic) lineages and exhibit clear morphological distinctions in relation to *A. richardsoni* and to one another. However, we detect signals of introgression between some populations of *A. richardsoni*, *A. spinulae* and an undescribed species. We also find two instances of syntopic occurrences without evidence for interbreeding. Also, *A. richardsoni* is split into several allopatric and comparably old lineages. *Anaspides spinulae* from Lake St. Clair, however, seems to be a young species that might have differentiated only after the last glacial maximum of central Tasmania (22 000–17 000 years ago). Moreover, we analyse the present population structure and recolonization of the Central Plateau and Western Mountain Ranges in regard to their glacial history. We distinguish several glacial refugia and show that the recolonization most likely occurred only from one or two of these.

© 2025 The Author(s). *Cladistics* published by John Wiley & Sons Ltd on behalf of Willi Hennig Society.

Introduction

The mountain shrimps of the genus *Anaspides* are endemic to Tasmania and represent one of the most "iconic" freshwater invertebrates of the island. Since their discovery more than a century ago (Thomson, 1893), they have attracted significant scientific interest as a kind of "living fossil" (closely resembling their Triassic ancestors/relatives; Brooks, 1962). For most of the time since its discovery, *Anaspides* was assumed to include only a single species, *A. tasmaniae* (Thomson, 1893), that was widespread over most parts of Tasmania in various freshwater bodies such as streams, tarns, lagoons, lakes and caves. Based on distinct but variable morphological characters and being apparently reproductively isolated from nearby populations of *A. tasmaniae*, a second species, named *A. spinulae* Williams, 1965, was described only in 1965 from Lake St. Clair at the edges of the Central Plateau.

To date, eight species of *Anaspides* are recognized (Ahyong, 2015, 2016; Höpel et al., 2023a), of which two are obligate cave dwellers (*A. clarkei* Ahyong, 2015, *A. eberhardi* Ahyong, 2016) and three have surface as well as cave populations (*A. jarmani* Ahyong, 2015, *A. richardsoni* Ahyong, 2016, *A. swaini* Ahyong, 2015). The three remaining species (*A. driesseni* Höpel et al., 2023a, *A. spinulae*, *A. tasmaniae*) are only known from surface habitats. According to Richter et al. (2018) and Höpel

*Corresponding author:
E-mail address: c.hoepel@melica-mv.de (C.G.H.); stefan.richter@uni-rostock.de (S.R.)

© 2025 The Author(s). *Cladistics* published by John Wiley & Sons Ltd on behalf of Willi Hennig Society.
This is an open access article under the terms of the Creative Commons Attribution License, which permits use, distribution and reproduction in any medium, provided the original work is properly cited.

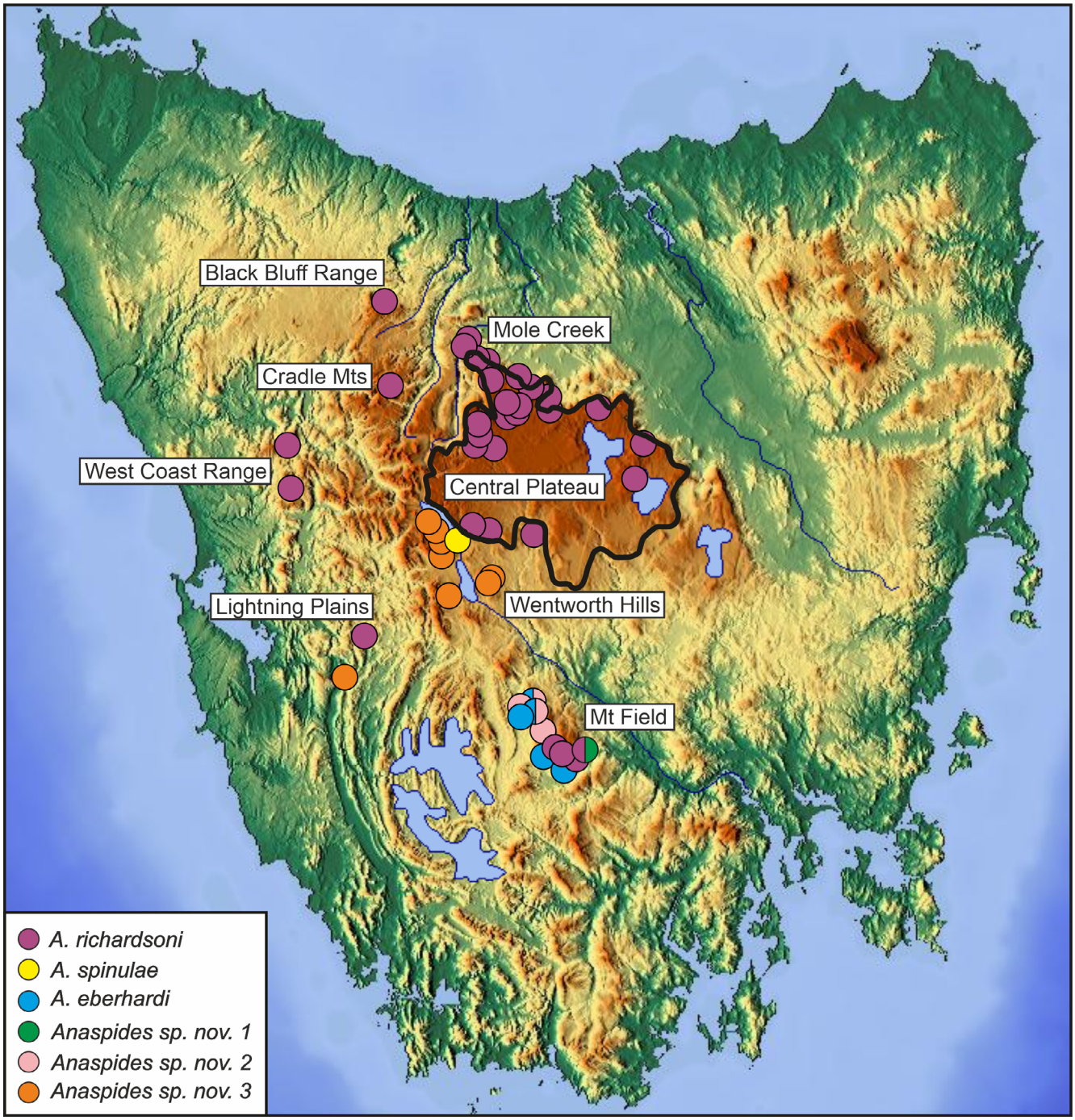


Fig. 1. Topographical map of Tasmania with collection sites of the six species of *Anaspides* (forming the "central clade") examined in this study. Central Plateau marked with a black line (after Corbett, 2019). Purple: *A. richardsoni*, Yellow: *A. spinulae*, Blue: *A. eberhardi*, Green: *Anaspides* sp. nov. 1 from Lake Nicholls, Pink: *Anaspides* sp. nov. 2 from the Florentine Valley, Orange: *Anaspides* sp. nov. 3. Halved circles indicate syntopic occurrence of different species. Modified after the topographic map from Wikipedia (https://upload.wikimedia.org/wikipedia/commons/2/21/Topography_of_Tasmania.jpg, common licence under Creative Commons Attribution-ShareAlike 3.0 Unported).

et al. (2023b), the widespread *A. richardsoni* and the more narrowly distributed species, *A. eberhardi* (Junee-Florentine karst at Mt. Field) and *A. spinulae* (Lake St. Clair), form a species group, therein called the "central clade," alluding to its central Tasmanian distribution (Fig. 1). The distribution of the "central clade" includes the Central Plateau, a highland area mostly above 1000 m with ridges that steeply drop 500–700 m

10960031, 0, Downloaded from https://onlinelibrary.wiley.com/doi/10.1111/cla.70005 by Christoph Höpel - University Rostock Universitätsbibliothek , Wiley Online Library on [30/07/2025]. See the Terms and Conditions (https://onlinelibrary.wiley.com/terms-and-conditions) on Wiley Online Library for rules of use; OA articles are governed by the applicable Creative Commons License

to the west and north, which slopes more gently to the south (Corbett, 2019), but also the Western Mountain Ranges (e.g. West Coast Range, Cradle Mountains, Black Bluff Range) as well as Mt. Field plateau in central Tasmania. The Central Plateau and the Mt. Field plateau are composed of Jurassic dolorite as the uppermost layer.

Phylogenetic analyses based on data from the mitochondrial (mt) cytochrome oxidase subunit-1 (COI) marker (Richter et al., 2018) and from mt genomes (Höpel et al., 2023b) indicate that *A. richardsoni* is paraphyletic with *A. eberhardi* and *A. spinulae* nested within. Höpel et al. (2023b) also showed that the species identified by Ahyong (2016) as "*A. swaini*, form 2" belongs to the central clade as well (herein *Anaspides* sp. nov. 3). The molecular clock analysis based on COI data in Richter et al. (2018) suggested that the initial split in the central clade occurred 4 Mya, but that most subsequent splits are younger and might have indeed appeared during the Pleistocene. Because most surface species of *Anaspides* live at high altitudes, the distribution of extant *Anaspides* in Tasmania has been heavily influenced by glaciation during the Pleistocene (e.g. Kiernan, 1990; Kiernan et al., 2001). For example, the previously glaciated parts of the Central Plateau and Mt. Field were re-colonized after glaciation.

During the Early Pleistocene, vast areas of Tasmania were covered with thick glaciers (Colhoun et al., 2010). The largest were present during the multi-phased Linda Glaciations, which covered huge areas of the Central Plateau and spanned most of the western mountain regions (Fig. 11). A total area of approximately 7000 km^2 was covered with a maximum ice thickness of 500–800 m. The outlet glaciers in the valleys still had a thickness of 150–350 m. However, the exact age of this glacial maximum is uncertain. Because of reversed magnetic polarity in varved clays in lake deposits, these glaciations are older than 0.785 Mya (Barbetti and Colhoun, 1988) and, with little doubt, some of these ice advances are up to 2.5 million years old. There is even evidence for glaciations between the Oligocene and Pliocene, which is consistent with glaciations in Patagonia and New Zealand; however, without any dating (Macphail et al., 1993; Augustinus and Idnurm, 1993). The mid-Pleistocene glaciations (at least three) were less extensive (Colhoun et al., 2010). The last glacial maximum (LGM) occurred from 22 000 to 7000 years ago during marine isotope stage 2. There is again evidence for a couple of succeeding glaciations (e.g. Mackintosh et al., 2006). The LGM glaciations had an extent of 1100 km^2, a thickness of 250 m and covered the Central Plateau, the Western Mountain Ranges and several mountain ranges in the south and south-west of Tasmania (Fig. 11).

Species concepts and phylogeography

The dominant species concept at present is the general lineage species concept (De Queiroz, 1998), where species correspond to segments of population lineages with (definitely) independent trajectories (Vences et al., 2024). The other species "concepts" are suggested as operational "criteria" that emerge gradually during speciation (De Queiroz, 1998, 2007). During speciation, there is a transition from a single population lineage with reticulating relationships among individuals towards bifurcating relationships between two population lineages with progressively reduced gene flow and finally reproductive isolation between these lineages (De Queiroz, 1998). Full reproductive isolation corresponds to the Biological Species Concept (BSC; Mayr, 1942) or to the Hennigian Species Concept (HSC; Meier and Willmann, 2000). In general, de Queiroz' concept is quite close to Hennig's (1966) concept on speciation as "dissolving tokogenetic relationships" *within* species and the origin of phylogenetic relationships *between* species (and higher taxa). Delimiting lineages into species has often relied on quantifying their genetic divergences, for example, by sequencing the "barcoding gene" COI (Hebert et al., 2003). It is now well known, however, that this is often misleading when hybridization and/or ancestral polymorphism result in mitonuclear discordance (Bonnet et al., 2017). High-throughput sequencing now allows combining thousands of markers from both the mitochondrial and the nuclear genomes, which obviously allows a much more nuanced analysis of divergences between lineages than the use of a few (or only a single) barcoding genes (Vences et al., 2024).

One important aspect of species delimitation is the integration of biogeographical criteria. If two lineages occur in sympatry without genetic admixture, they conclusively fulfil the biological species criterion (Vences et al., 2022, 2024). Much more challenging are allopatric lineages, where genetic differentiation inferred from SNPs might reflect old phylogeographical structure driven by allopatric evolution (Vences et al., 2024). Dufresnes et al. (2024) suggested a workflow to delimit "phylogeographic lineages" into species and subspecies.

The question, however, is if species must be monophyletic or whether species might also be paraphyletic ("paraspecies" *sensu* Ackery and Vane-Wright, 1984) (Crisp and Chandler, 1996). In a strict sense, Hennig (1966) applied the term monophyletic and paraphyletic only for taxa above the species-level because within the conceptual framework of Hennig's argumentation the stem species becomes extinct during the process of speciation, which formally excludes the possibility of paraphyletic species (see also Meier and Willmann, 2000). However, if the focus is placed on the speciation process itself (instead of its formalized outcome), it is quite obvious that if new species arise by a gradual

10960031, 0, Downloaded from https://onlinelibrary.wiley.com/doi/10.1111/cla.70005 by Christoph Höpel - University Rostock Universitätsbibliothek , Wiley Online Library on [30/07/2025]. See the Terms and Conditions (https://onlinelibrary.wiley.com/terms-and-conditions) on Wiley Online Library for rules of use; OA articles are governed by the applicable Creative Commons License

process (e.g. by evolving ecological differentiation and isolating mechanisms) from an allopatric population within a wide-spread species, the "remainders" of the original species would not necessarily evolve in the same timeframe and manner. These "remainders" then might still consist of various (allopatric) populations (Barraclough, 2019) as, for example, found for the island endemic *Aphelocoma insularis*, which arose from the Western scrub-jay (*Aphelocoma californica*), a widely distributed mainland bird species in the USA (Delayne, 2014). This would most probably result in what could be considered a paraphyletic species (if no isolating mechanisms arise between these "remaining" populations). Interestingly, this might not only be the outcome of allopatric speciation but also of sympatric speciation (e.g. Barluenga et al., 2006), which is in good concordance with the so-called Phylogenetic Species Concept (PSC), where species are "the smallest diagnosable cluster of self-perpetuating organisms that have unique sets of [morphological] characters" (Nelson and Platnick, 1981; see also Nixon and Wheeler, 1990, 1992). This includes the possibility that a species might be characterized only by plesiomorphic characters which would be expected for paraphyletic species.

Coyne and Orr (2004) in their book on "Speciation" discuss the problem of paraphyletic species in the light of the Biological Species Concept (which in our view can be adopted to the General Lineage Concept, GLC). They suggest that most cases of reported "paraphyletic species" are an analytical artefact of the use of only a few (mostly) mitochondrial genes. The main problem they describe is the supposed ongoing gene flow between the population of the "paraphyletic species" which might not be correctly discovered by analyses using only a few genes. They recognize, however, that "it is likely that some multi-gene phylogenies may show biological species to be truly paraphyletic, and that the relatedness of populations and individuals may not always be concordant with their assignment to biological species" (Coyne and Orr, 2004).

Herein, we present a new analysis of the "central clade" *Anaspides* using ddRAD data as well as COI. The ddRAD data allow a remarkable population-level resolution. Populations are first characterized by the collecting locality that, in the case of the surface populations, are (mostly) (micro)allopatric water bodies such as tarns and lakes. We discuss the geographic separation of these habitats in correlation with the genetic isolation of the inhabitants (a case of "reciprocal illumination").

This study has two major aims. Based on the relationships of the populations, we aim for a causal understanding of species differentiation and speciation in terms of allopatric lineages and the acquisition of new morphological characters. The second aim is to correlate population differentiation with paleoecological events, namely glaciation, in order to develop our causal understanding of the observed pattern.

Materials and methods

Specimens were identified using the morphological descriptions of Ahyong (2015, 2016). The three as yet undescribed species can also be diagnosed by morphological characters used by Ahyong (2015, 2016) and Höpel et al. (2023a).

Specimens for this study were collected during five field trips in 2017, 2019, 2022, 2023 and 2024. A total of 347 specimens from 48 localities were examined and newly sequenced for this study (Table S1). All sequences were deposited at GenBank (Benson et al., 2003) (COI: PV780789–PV781115; ddRAD: SAMN49064136–SAMN49064398, BioProject ID: PRJNA1276447).

The DNA extraction was performed with the DNeasy Blood and Tissue Kit (Qiagen, Hilden, Germany), following the manufacturer's instructions. Mitochondrial cytochrome c oxidase subunit I (COI) was partially sequenced. The polymerase chain reaction (PCR) had a total volume of 30 µL containing 3 µL of each primer, 3 µL 10× PCR buffer (Sigma-Aldrich, St. Louis, MO, USA), 3 µL dNTP mix (Biozym, Hessisch Oldendorf, Germany), 2.58 µL $MgCl_2$ (Sigma-Aldrich), 0.12 µL Taq-polymerase (Sigma-Aldrich), 10.71 µL ultrapure water, and 4.5 µL of the DNA extract. Primers were LCO2 (50-TCN ACH AAY CAT AAA GAY ATT GGA AC-30) (Richter et al., 2018), HCO2198 (50-TAA ACT TCA GGG TGA CCA AAA AAT CA-30) (Folmer et al., 1994). PCR amplification programs comprised an initial denaturation step at 94 °C for 1 min, followed by 40 amplification cycles (94 °C for 30 s, 50 °C for 30 s, 72 °C for 60 s) and a final elongation step at 72 °C for 5 min. All PCR reactions were performed with a Mastercycler gradient (Eppendorf, Hamburg, Germany). PCR products were visualized by gel electrophoresis, using 5 µL of the PCR product with 1.5 µL loading buffer DNA b II (AppliChem) on a 1.2% agarose/TAE gel stained with 5 µL Rotisafe (Carl Roth, Karlsruhe, Deutschland). PCR products were purified using paramagnetic beads (High Prep PCR; Magbio, Lausanne, Schweiz) following the manufacturer's instructions with a final volume of 25 µL. Sequencing of PCR products was performed in Lightrun96 well plates by the company Eurofins Genomics. The resulting chromatograms were manually checked and adjusted with Geneious 2019.1.3 (Biomatters Limited, Auckland, New Zealand). The sequences of the COI gene fragment were aligned using Geneious Align. Haplotype networks were calculated with Network 5.0.1.1 (Fluxus Technologies, Stanway, UK) by using the median-joining method. A maximum likelihood phylogeny was calculated using the RaxML GUI (Darriba et al., 2020) with the best model (HKY + G + I) determined by the implemented model test. The calculation was run using the thorough bootstrap analysis for 1000 bootstraps.

Molecular clock analyses were performed in BEAST 2.4.6 (Bouckaert et al., 2014). The input files for BEAST were created with Beauti as part of the BEAST package. Mutation rates for COI were based on averages of reported mutation rates for Crustacea: 1.4% per million years (Knowlton and Weigt, 1998), 1.66% per million years (Schubart et al., 1998) and 2.33% per million years (Schubart et al., 1998) for COI (average per lineage 0.9% per million years). In addition to setting the mean rates, the original rates were set as maximum or minimum rate constraints, respectively. A strict clock with a Yule tree prior with standard parameters was employed as well as the GTR + I + G nucleotide substitution model. BEAST was run for 110 mio generations, saving every 10 000th tree. Stable likelihood plateaus and convergence were assessed with Tracer v1.7.1 (Rambaut et al., 2018). The first 20% of trees were discarded as burn-in, and the posterior probability limit was set to 0.5 in TreeAnnotator 2.4.6 (Bouckaert et al., 2014).

ddRAD data analyses

For ddRAd analyses, we largely followed the protocol by Schwentner and Lörz (2021). For example, we added four random nucleotides in one adapter to allow the downstream detection and removal of

10960031, 0, Downloaded from https://onlinelibrary.wiley.com/doi/10.1111/cla.70005 by Christoph Höpel - University Rostock Universitatsbibliothek , Wiley Online Library on [30/07/2025]. See the Terms and Conditions (https://onlinelibrary.wiley.com/terms-and-conditions) on Wiley Online Library for rules of use; OA articles are governed by the applicable Creative Commons License

PCR duplicates (similar to Franchini et al., 2017). The DNA concentration of each DNA extract was quantified on a Qubit 3.0 (Invitrogen). Of each DNA extract, 150–250 ng DNA was diluted in 24 μL with H_2O. Samples were always processed in batches of eight, which were pooled prior to PCR amplification (all of these eight share the index added by PCR but received individual barcodes during adapter ligation; Table S1) and which always had the same DNA concentration. 1.5 μL fastdigest MspI, 1.5 μL fastdigest EcoRI and 3 μL 10× buffer (all Thermo Fisher) were added to each DNA sample and incubated for at least 4 h at 37 °C. Digested DNA was cleaned with 45 μL magnetic beads (AmpliClean Cleanup Kit, Nimagen) following the manufacturer's recommendations and eluted with 21 μL H_2O, of which 19 μL were transferred for adapter ligation. The above-mentioned steps were repeated for a few samples as internal technical replicates to ascertain reproducibility of the results. These samples were digested twice and each of these replicates was treated like an independent sample (e.g. receiving its own barcode/index combination, etc.). All adapters were diluted in annealing buffer (10× annealing buffer comprises 500 mM NaCl, 100 mM Tris-Cl, 10 mM EDTA) to 2 μM (EcoRI adapters) or 31.6 μL (MspI adapters), respectively (following Peterson et al., 2012). Sixteen EcoRI and 8 MspI adapter variations with unique barcodes (MspI adapters with additionally four random nucleotides following the barcode: Franchini et al., 2017) were used to tag each library with a unique adapter combination within each batch of eight samples. Barcode sequences were derived from Peterson et al. (2012). Ligation reactions comprised 19 μL digested DNA, 3 μL EcoRI adapter, 3 μL MspI adapter, 2 μL T4 Ligase (2 Weiss units; Thermo Fisher Scientific, Waltham, MA, USA) and 3 μL 10× T4 ligase buffer and was incubated at 22 °C for 1 h and then heat killed at 65 °C for 10 min. Subsequently, the eight samples of each batch were pooled and each pool cleaned with 360 μL magnetic beads, eluting in 32 μL TE buffer. Size selection was carried out on a BluePippin (1.5% dye free cassettes with marker L; Biozym) for each pool independently, selecting the "tight" option with a mean size of 300 bp (range 261–339 bp). To reduce amplification biases during PCR, four PCR replicates were run for each pool. Each PCR comprised 0.3 μL (10 nM) of each primer, 5 μL 2× Kappa HIFI HotStart ReadyMix (Roche, Basel, Switzerland) and 4.4 μL of a pool after size selection. A two-step PCR program of 95 °C initial denaturation and 12–15 cycles of 98 °C for 20 s and 72 °C for 25 s plus a final elongation step of 1 min at 72 °C was run. Forward and reverse primers were available with eight different 8 bp indices each and combined to add a unique index combination for each pool (Table S1). After PCR, the four PCR replicates of each pool were mixed and cleaned with 40 μL magnetic beads (eluting in 20 μL H_2O). Concentrations of all cleaned pools were measured with Qubit 3.0, and correct fragment size length (~350 bp) was assessed on a Tapestation (D1000 ScreenTape; Agilent, Santa Clara, CA, USA). All libraries were mixed at equal molarity into a final pool of 20 nM in 60 μL. Paired-end sequencing with 100 bp each was carried out on one Illumina HiSeq4000 lane by Macrogen (Seoul, South Korea). Upon sequencing, Macrogen pre-demultiplexed the data into the respective pools (based on provided index combinations).

Using STACKS v2.59 (Rochette et al., 2019), PCR duplicates were removed using the clone_filter program, and subsequently, the process_radtags program was used to demultiplex, these pools into the individuals by their unique barcodes. The program denovo_map.pl was then used to create a catalogue of loci (parameters: -m 3, -M 7, -n 7).

Four data sets were generated using the populations program of STACKS v2.59 (Rochette et al., 2019) with the parameter -R set to 0.89 (Table 1). The first and second data sets comprised 261 and 260 specimens, respectively, with data set 1 including one specimen of *A. tasmaniae* which was used as an outgroup in the subsequent tree analyses. Specimens with more than 30% missing loci were excluded from the analyses (except for the outgroup). The third data set comprised 177 specimens of the more derived lineages (based on the previous tree analyses of the first data set, see Fig. 2). Again, specimens with more than 30% missing loci were excluded. In this data set, we could more than double the number of polymorphic loci in comparison to data sets 1 and 2. This allows us to analyse the population structure, admixture and potential introgression within these derived lineages at much higher resolution and detail. It is also necessary to facilitate a detailed analysis of potential glacial refuges and recolonization paths. We also generated a fourth data set including only specimens from Clarence Lagoon, Tributary to Travellers Rest River (both *A. richardsoni*) and Lake St. Clair (*A. spinulae*) to get a fine-scale resolution of this group.

Table 1
Data sets with number of specimens, loci, polymorphic loci and sites analysed

Data set	Specimen	Loci	Polymorphic loci	Variable sites (SNPs)
1	261	1963	1945	38 926
2	260	1981	1963	38 290
3	177	4024	3976	54 396
4	23	6385	5379	24 633

Phylogenetic relationships between the species, populations and lineages were inferred by maximum likelihood (ML) and maximum parsimony (MP) analyses using the .var.phy file generated by the populations program using STACKS as well as an unrooted phylogenetic network calculated using SplitsTree4 v4.19.2 (Huson and Bryant, 2006) with the Neighbor-Net algorithm and uncorrected *p*-distances. We used IQ-TREE 2 (Minh et al., 2020) to infer the ML tree using the TVM + G + I model and 1000 bootstraps. The best-fit model of evolution was determined by the implemented model test in RaxML GUI 2.0.8 (Darriba et al., 2020). Maximum-parsimony analyses were conducted with the console version of TNT v1.6, June 2021 (Goloboff and Catalano, 2016) using New Technology (Torres et al., 2022). The script PhylogenomicSearch.run (Torres et al., 2022) was applied with the following arguments specified: search, nt; level, 10; hits, 5; output, newick; outgroup Ana1375. *Anaspides tasmaniae* (Ana1375) was used as outgroup. Resulting trees were visualized with FigTree v.1.4.2 (Rambaut, 2014) and Corel Draw 2020. The Script PhylogenomicSupport.run was used to obtain support values with the following argument specified: reftree, StrictConsensus_tnt.tre; format, tnt; sites, boot; replic, 1000; search, nt; level, 5; output, newick.

To infer population structure, ancestry and admixture we used fineRADstructure (Malinsky et al., 2018), principal component analysis (PCA) following the ipyrad workflow and analyses of population structure and grouping using STRUCTURE 2.3.4 (Pritchard et al., 2000). The fineRADstructure is a high-resolution method, which was specifically designed to deal with a very large number of populations. It utilizes haplotype linkage information and constructs a coancestry matrix (a summary of nearest neighbour haplotype relationships; Malinsky et al., 2018). The fineRADstructure analyses were run with default parameters (as suggested by the developers) and results were plotted with the fineRADstructure GUI. STRUCTURE and PCA are also using these multi-locus genotype data to determine distinct populations and can be used to identify and study hybrid zones as well as for identifying migrants and admixed individuals (Pritchard et al., 2000). Both analyses are only using one randomly chosen SNP per locus to minimize the effect of linkage between neighbouring SNPs, which may bias the analyses. For the STRUCTURE analyses, we tested *k* values, that is, the putative number of ancestral groups, from 1 to 30 and conducted 20 replicate runs for each *k* value. Based on these calculations, we selected the optimal number of clusters using the StructureSelector website (Li and Liu, 2018). We only report the first four PC axes of the PCA as the remaining axes cumulatively only explained less than 3.5% of the total genetic variation. To

10960031, 0, Downloaded from https://onlinelibrary.wiley.com/doi/10.1111/cla.70005 by Christoph Höpel - University Rostock Universitatsbibliothek , Wiley Online Library on [30/07/2025]. See the Terms and Conditions (https://onlinelibrary.wiley.com/terms-and-conditions) on Wiley Online Library for rules of use; OA articles are governed by the applicable Creative Commons License

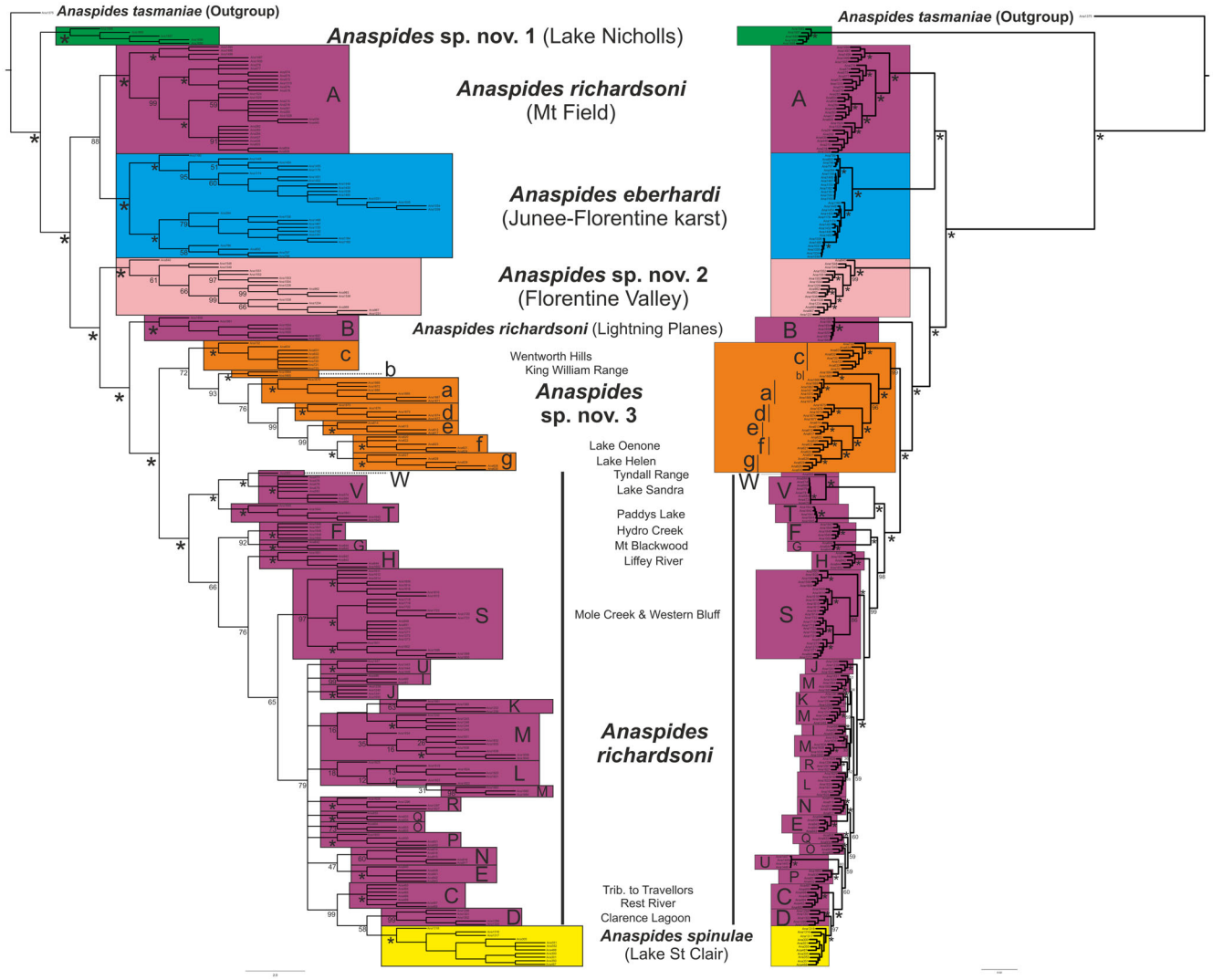


Fig. 2. Strict consensus tree of 1000 most parsimonious trees calculated with TNT V1.6 using the script PhylogenomicSupport.run (Torres et al., 2022) (left) and maximum-likelihood phylogeny calculated with IQ-Tree 2.3.6 (TVM + G + I, 1000 iterations) of ddRAD data set 1 using *Anaspides tasmaniae* as outgroup (261 individuals, 1945 polymorphic loci with 38 926 variable sites). The letters correspond to the populations/metapopulations in Fig. 11. Support values are only shown for the deep branches and major lineages. Support values for MP analysis were calculated using the PhylogenomicsSupport.run script (Torres et al., 2022). Best score for MP analysis was 48 021. An asterisk (*) indicates support value of 100. Coloured boxes correspond to morphologically delineated species (based on Ahyong, 2015, 2016; Höpel et al., 2023a). Green: *Anaspides* sp. nov. 1, Purple: *A. richardsoni*, Blue: *A. eberhardi*, Light Pink: *Anaspides* sp. nov. 2, Orange: *Anaspides* sp. nov. 3, Yellow: *A. spinulae*. Most localities mentioned in the text are given for the respective clade.

quantify genetic differentiation among the populations we calculated the F_{ST} and d_{xy} values using the program populations in STACKS v2.59 for all clusters recovered in the fineRADstructure.

To further test for historical gene flow, we calculated *D*-statistics/ABBA-BABA test statistics using DSuite (Malinsky et al., 2021) and estimated introgression events using the program TreeMix (Pickrell and Pritchard, 2012). We tested for historical gene flow between the lineages uncovered in the fineRADstructure analyses. DSuite analyses were carried out using the Dtrios method for all possible population trios with *Anaspides* sp. nov. 1 (data set 2) and *Anaspides richardsoni* (B) (data set 3) set as outgroups. The TreeMix analysis was run for *m* values, that is, the number of independent migration events, ranging from 1 to 10 with 10 replicate runs per *m* value. The optimal number of migration events was calculated with the OptM package (Fitak, 2021) in R.

All resulting trees, plots, statistics and figures were post-processed with Corel Draw 2020. The complete and well-documented bioinformatic analysis pipeline including custom scripts and the commands for third-party programs can be found at Github (https://github.com/ch515/Hoepel_paraphyletic_species).

Results

Morphological data

Using the taxonomic/diagnostic morphological characters described/delineated by Ahyong (2016) and

10960031, 0, Downloaded from https://onlinelibrary.wiley.com/doi/10.1111/cla.70005 by Christoph Höpel - University Rostock Universitatsbibliothek , Wiley Online Library on [30/07/2025]. See the Terms and Conditions (https://onlinelibrary.wiley.com/terms-and-conditions) on Wiley Online Library for rules of use; OA articles are governed by the applicable Creative Commons License

Höpel et al. (2023a), we can *a priori* distinguish six species (not including *A. tasmaniae,* which is used as outgroup), of which three are formally described (*A. spinulae*, *A. richardsoni* and *A. eberhardi*) and three are as yet undescribed species (*Anaspides* sp. nov. 1, 2, 3). *Anaspides* sp. nov. 3 was identified by Ahyong (2016) as *A. swaini*, form 2.

Anaspides richardsoni and *Anaspides* sp. nov. 1 (so far only known from Lake Nicholls on the east side of Mt. Field) are syntopic, as are *A. eberhardi* and *Anaspides* sp. nov. 2, which co-occur in two caves in the Florentine Valley.

The number and arrangement of antennular clasping spines in adult males is diagnostic in species of *Anaspides* (Ahyong, 2016; Höpel et al., 2023a). *Anaspides richardsoni* and *A. eberhardi* possess only a single antennular clasping spine in adult males, whereas *A. spinulae* and all three undescribed species have two clasping spines. However, in *Anaspides* sp. nov. 1, these two spines are in a dorso-ventral plane, instead of an anterior–posterior plane as in all other *Anaspides* with more than one clasping spine. For the "central clade" the presence of two clasping spines is the plesiomorphic condition, being present also in *A. tasmaniae* (but also in the more distantly related *A. swaini* and *A. driesseni*). Clasping spines might play a role in reproductive isolation between species (Ahyong, 2016).

Anaspides sp. nov. 1 and *A. eberhardi* have pleopodal endopods only on pleonites 1–4, whereas *A. richardsoni*, *A. spinulae*, *Anaspides* sp. nov. 2 and *Anaspides* sp. nov. 3 have pleopodal endopods also on pleonite 5. Both *Anaspides* sp. nov. 1 and *A. spinulae* mature at a smaller size than their congeners (14–15 mm body length in *A. spinulae*). *Anaspides spinulae* is also characterized by having a telson with a spine row of slender, uneven, closely spaced spines, with several longer spines. Moreover, this species shows pronounced spination of the pleural margins (usually starting on pleuron 1) and the tergal margin 5–6, a characteristic also found in *Anaspides* sp. nov. 2 (starting on pleuron 3–4) and rarely in some populations of *A. richardsoni* (e.g. small pool near Little Throne, some specimens from Clarence Lagoon).

ddRAD data

Both the analysis of population structure with fineRADstructure and the phylogenetic analyses of the ddRAD data (see below, Figs 2 and 5) reveal a strong correlation between locality and lineages. Therefore, we assume that all conspecific specimens from a certain locality belong to the same population. For simplicity, we further combined (some) populations into metapopulations (Figs 2–7, Figs S1 and S2, A, S and M).

Both phylogenetic analysis approaches (MP and ML) result in identical topologies with regard to the deep nodes and basal branching clades (*A. richardsoni* populations and metapopulations A, B, F, G, H, S, T, V, W, *A. eberhardi*, *Anaspides* sp. nov. 1, 2, 3) with high support values. All morphologically distinguished species, with the exception of *A. richardsoni*, represent discrete, monophyletic lineages. The same applies to phylogenetic networks reconstructed with SplitsTree. However, these analyses differ with respect to resolution and relationships among the more derived lineages (*A. richardsoni* C, D, E, I–R, U, *A. spinulae*). Especially in the MP consensus tree, these derived lineages were recovered as a polytomy. However, certain clades and lineages were recovered in both analyses. These clades were *A. richardsoni* C + D + *A. spinulae*, *A. richardsoni* N + E and several populations as discrete groups, *A. richardsoni*: U, I, J, O, P, Q, R. These results are also supported by the SplitsTree analyses (Fig. S1).

Our data show that *Anaspides* sp. nov. 1 is the most basal branching clade. Its genetically separate position is well supported by the PCA, STRUCTURE, fineRADstructure and SplitsTree analyses (Figs 2–5, Fig. S1). This species is currently only known from a single lake on the eastern side of Mt. Field (Lake Nicholls) where it is syntopic with *A. richardsoni* A. Our data show no evidence of interbreeding between this species and *A. richardsoni* A, and no signs of shared genetic signal with any other herein studied species or population. This species can be readily separated from the remaining species and is sister group to what we herein refer to as the *A. richardsoni* species complex.

The major split of the *A. richardsoni* species complex shows *A. richardsoni* (A) and *A. eberhardi* from Mt. Field/Junee-Florentine as the sister group to the remaining populations and species. The second clade consists of *Anaspides* sp. nov. 2 as the sister species to the remaining taxa. This species is found in and near cave waters in the Florentine Valley (Figs 1 and 11, pink-coloured circles). The next lineage branching off is represented by an isolated population of *A. richardsoni* found in a cave at Lightning Plains (location B, exhibiting very slight cave adaptation, such as slight depigmentation, slight elongation of antenna, slight reduction of telson spines) followed by *Anaspides* sp. nov. 3. The latter species has been found in alpine tarns, lakes and caves to the south and south-west of Lake St. Clair and the Franklin-Gordon Wild Rivers National Park.

The remaining clade consists of several lineages of *A. richardsoni* as well as *A. spinulae*. Some of these lineages are further split into subgroups/sublineages mainly corresponding to certain localities that are important for understanding recolonisation of the

10960031, 0, Downloaded from https://onlinelibrary.wiley.com/doi/10.1111/cla.70005 by Christoph Höpel - University Rostock Universitatsbibliothek , Wiley Online Library on [30/07/2025]. See the Terms and Conditions (https://onlinelibrary.wiley.com/terms-and-conditions) on Wiley Online Library for rules of use; OA articles are governed by the applicable Creative Commons License

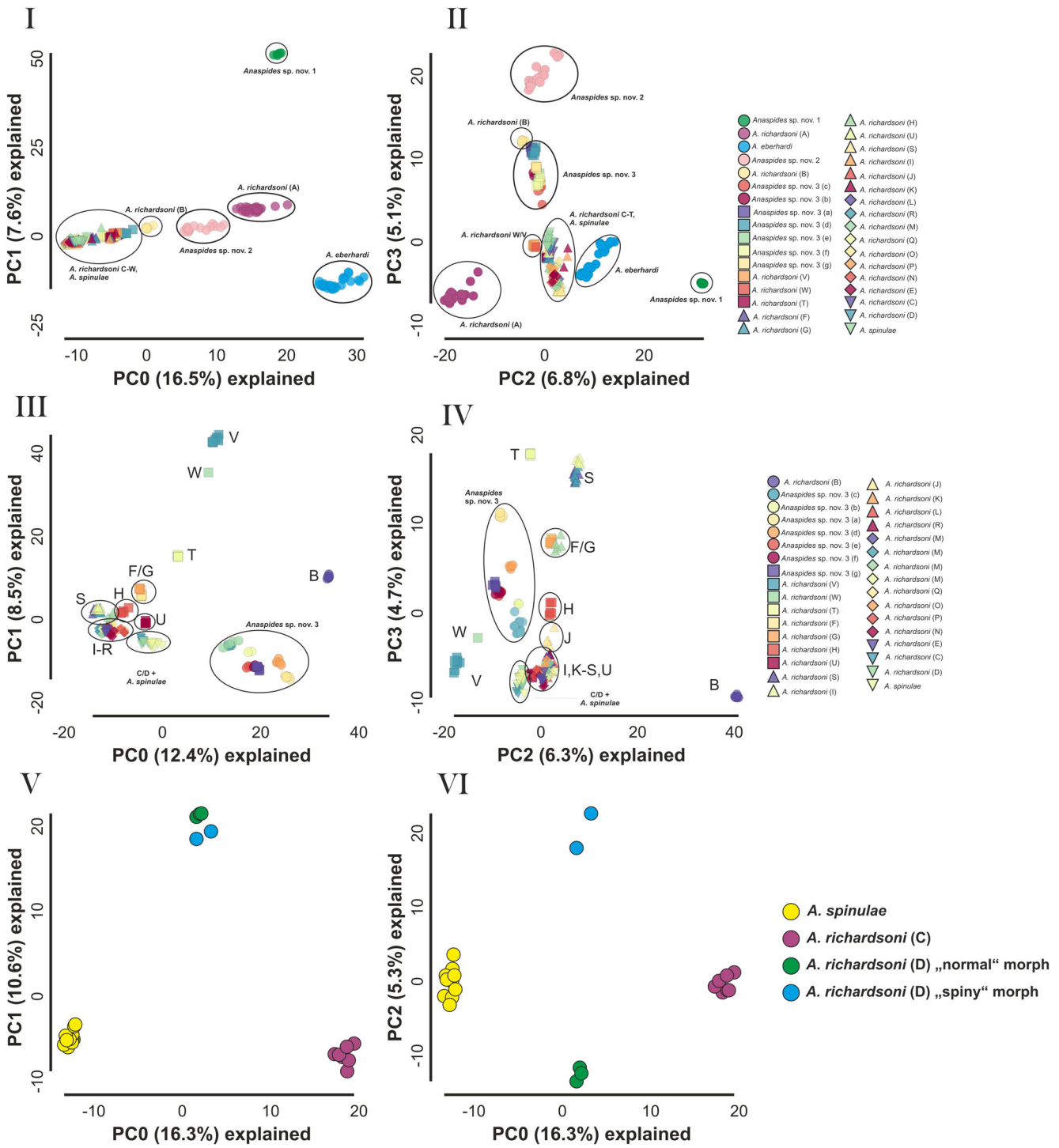


Fig. 3. Principal component analyses using data sets 2, 3 and 4. Data set 2: (I) PC0/PC1 and (II) PC2/3; data set 3: (III) PC0/PC1 and (IV) PC2/3; data set 4: (V) PC0/PC1 and (VI) PC0/PC2. The following PCs for data sets 2 and 3 explain less than 3.5% and less than 4.5% for data set 4 and are not shown here. The letters correspond to the populations/metapopulations in Fig. 11.

central plateau (see below). With the exception of metapopulation M, each lineage represents a discrete locality (and also population, see Fig. 2). In the ML tree we distinguish 12 lineages of *A. richardsoni* (in the order: T/V/W, F/G, H, S, J, I/K/L/M/R, E/N, Q, O, P/U, C, D) that are gradually related to *A. spinulae*, with the basal branching clades (up to J) showing very high support values (>98) (Fig. 2). Note that the

10960031, 0, Downloaded from https://onlinelibrary.wiley.com/doi/10.1111/cla.70005 by Christoph Höpel - University Rostock Universitätsbibliothek , Wiley Online Library on [30/07/2025]. See the Terms and Conditions (https://onlinelibrary.wiley.com/terms-and-conditions) on Wiley Online Library for rules of use; OA articles are governed by the applicable Creative Commons License

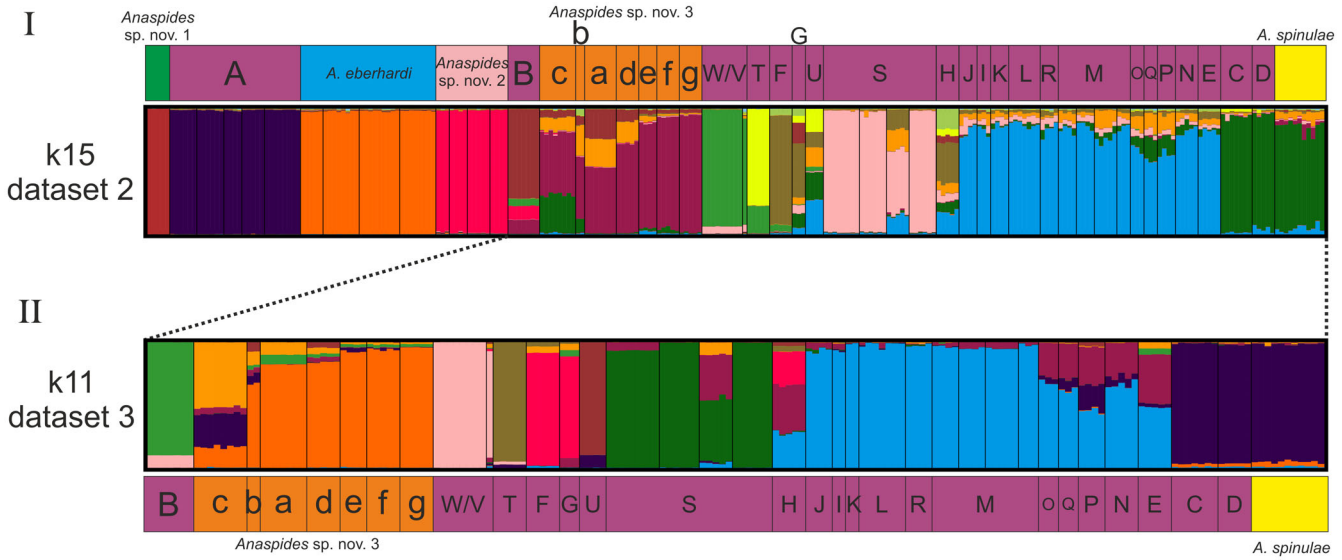


Fig. 4. STRUCTURE analysis using data set 2 (I) and data set 3 (II) of the six species analysed in this study. Plots for the best *k* values for each data set are shown (data set 2: k15, data set 3: k11). The letters correspond to the populations/metapopulations in Fig. 11. Coloured boxes correspond to morphologically delineated species (based on Ahyong, 2015, 2016; Höpel et al., 2023a). Green: *Anaspides* sp. nov. 1, Purple: *A. richardsoni*, Blue: *A. eberhardi*, Light Pink: *Anaspides* sp. nov. 2, Orange: *Anaspides* sp. nov. 3, Yellow: *A. spinulae*. Note colours for population structure plots do not match between data sets 2 and 3.

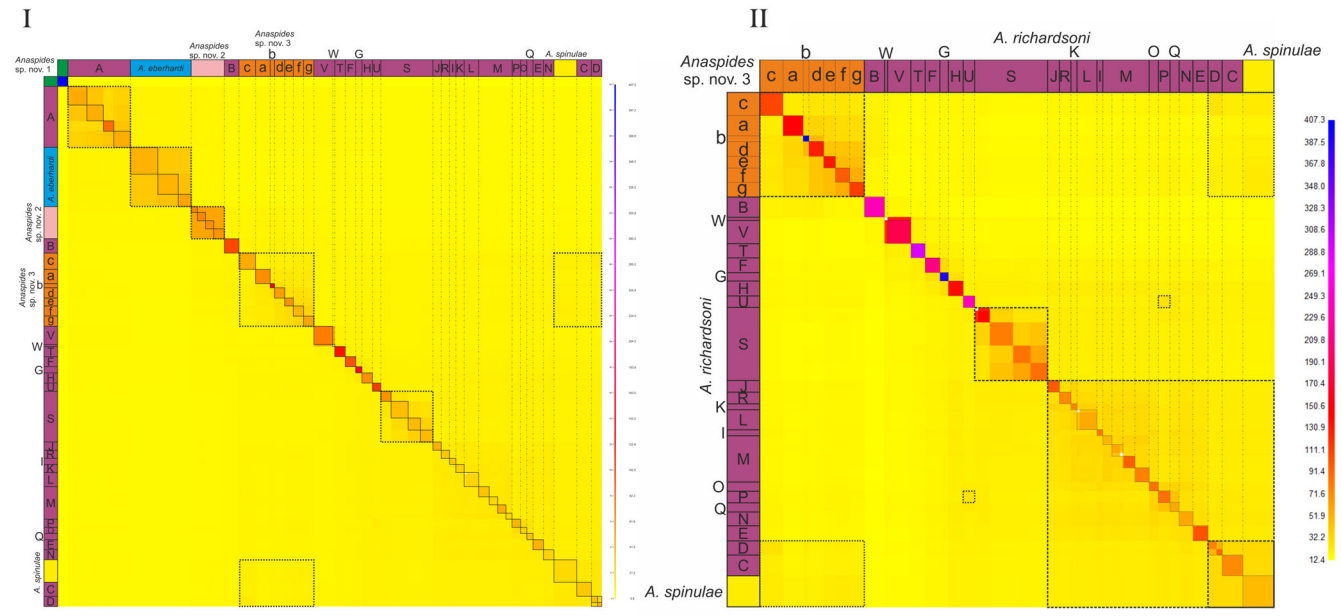


Fig. 5. FineRADstructure analyses of the six species analyses in this study for (I) data set 2 and (II) data set 3. Darker colours (range: blue–>yellow) indicate higher shared coancestry. The letters correspond to populations/metapopulations in Fig. 11. Coloured boxes on sides correspond to morphologically delineated species (based on Ahyong, 2015, 2016; Höpel et al., 2023a). Green: *Anaspides* sp. nov. 1, Purple: *A. richardsoni*, Blue: *A. eberhardi*, Light Pink: *Anaspides* sp. nov. 2, Orange: *Anaspides* sp. nov. 3, Yellow: *A. spinulae*. Black closed lined boxes were manually added for better visibility of clusters with higher coancestry representing populations. Dashed broken lines were manually added for better assignment of coloured boxes (letters) with the genetic clusters. Black broken lined boxes were manually added to highlight some areas with increased coancestry.

support values of all other nodes still exceed 59. The MP consensus tree is less resolved, but still recovered at least six lineages that are gradually related to *A. spinulae* (T/V/W, F/G, H, S, C, D) and several lineages (comprising the populations from E, I–R, U) with unresolved (polytomy) relationships with regard to

10960031, 0, Downloaded from https://onlinelibrary.wiley.com/doi/10.1111/cla.70005 by Christoph Höpel - University Rostock Universitatsbibliothek , Wiley Online Library on [30/07/2025]. See the Terms and Conditions (https://onlinelibrary.wiley.com/terms-and-conditions) on Wiley Online Library for rules of use; OA articles are governed by the applicable Creative Commons License

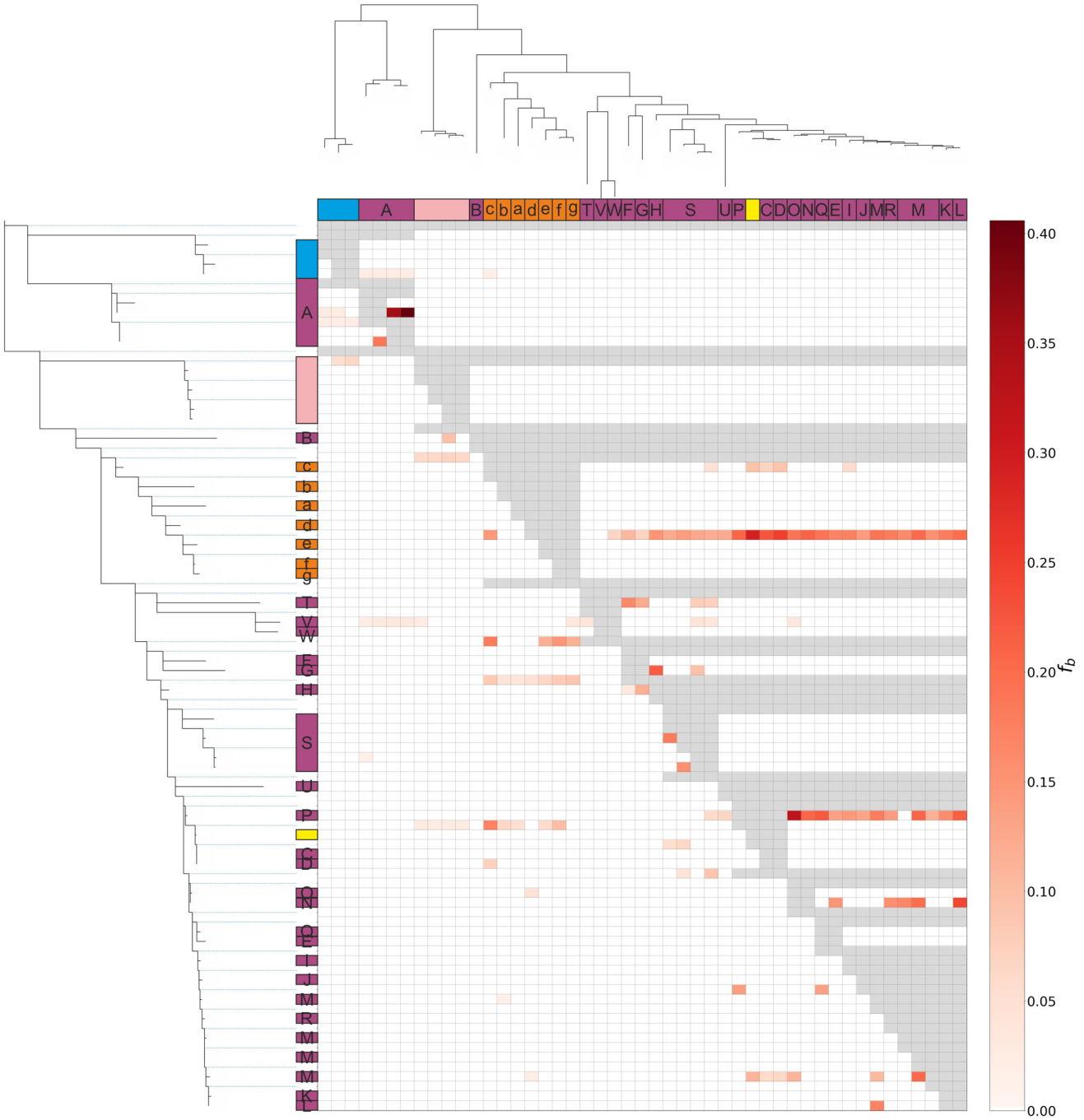


Fig. 6. DSuite analysis of ddRAD data set 2 (260 individuals, 1945 polymorphic loci with 38 926 variable sites). *Anaspides* sp. nov. 1 was used as an outgroup. Grey boxes are impossible combinations for Dtrios calculation. The letters correspond to the populations/metapopulations in Fig. 11. Coloured boxes correspond to morphologically delineated species (based on Ahyong, 2015, 2016; Höpel et al., 2023a). Green: *Anaspides* sp. nov. 1, Purple: *A. richardsoni*, Blue: *A. eberhardi*, Light Pink: *Anaspides* sp. nov. 2, Orange: *Anaspides* sp. nov. 3.

A. spinulae + C + D. The bootstrap support values for the resolved lineages all exceed 65 (Fig. 2). The topology of the basal branching lineages in this clade is in both trees the same. The first lineage to branch off comprises populations found in the west and north-west edge of the known distribution range, populations V (Lake Sandra), W (Tyndall Range) and T (Paddys Lake, Black Bluff Range) with the first two being sister groups (both West Coast Range). The following lineage shows populations F (Hydro Creek) and G (Mt Blackwood) as sister groups that are found on the eastern border of the range (eastern part of the

10960031, 0, Downloaded from https://onlinelibrary.wiley.com/doi/10.1111/cla.70005 by Christoph Höpel - University Rostock Universitätsbibliothek , Wiley Online Library on [30/07/2025]. See the Terms and Conditions (https://onlinelibrary.wiley.com/terms-and-conditions) on Wiley Online Library for rules of use; OA articles are governed by the applicable Creative Commons License

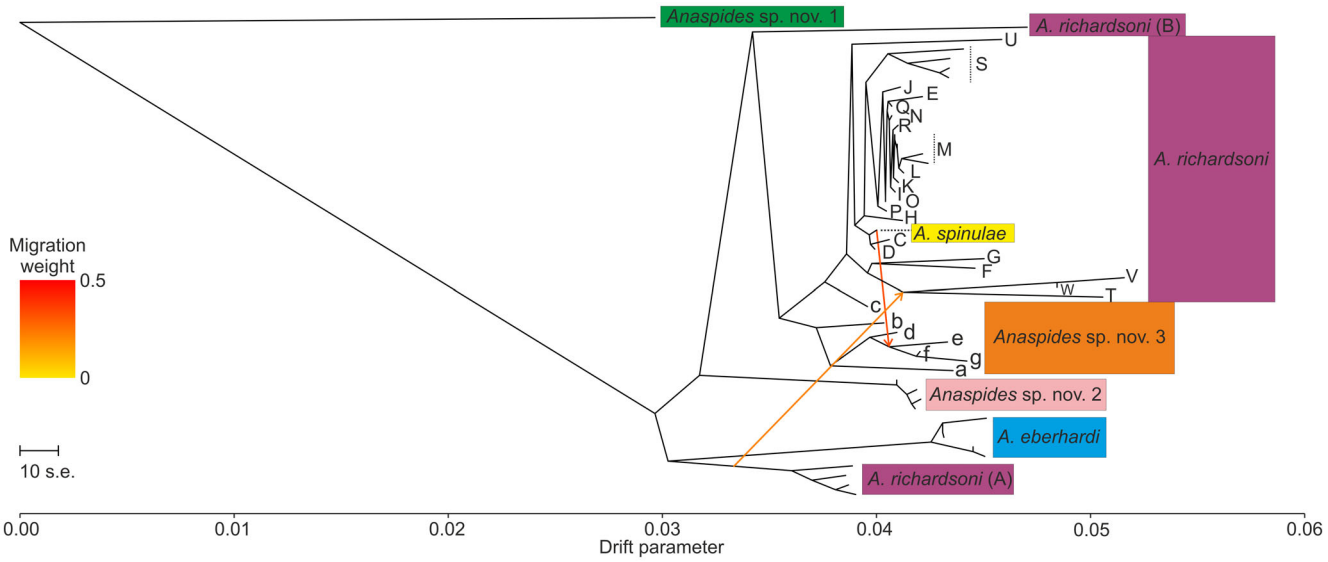


Fig. 7. TreeMix analyses of data set 2 with *Anaspides* sp. nov. 1 set as outgroup (best parameter $m = 2$). Arrows correspond to possible gene flow events and colour to weight of the migration. Letters correspond to populations/metapopulations in Fig. 11. Coloured boxes on sides correspond to morphologically delineated species (based on Ahyong, 2015, 2016; Höpel et al., 2023a). Green: *Anaspides* sp. nov. 1, Purple: *A. richardsoni*, Blue: *A. eberhardi*, Light Pink: *Anaspides* sp. nov. 2, Orange: *Anaspides* sp. nov. 3, Yellow: *A. spinulae*. The phylogram was calculated with IQ-Tree 2.3.6., Yellow: A. spinulae. The phylogram was calculated with IQ-Tree 2.3.6.

Central Plateau). The next lineage comprises the specimens from population H (Liffey River) followed by the lineage comprising the populations of metapopulation S (Mole Creek).

The PCA (PC0-1, PC2-3) based on data set 2 of the *A. richardsoni* species complex reveals distinct genetic clusters for *A.* sp. nov. 1, *A.* sp. nov. 2, *A.* sp. nov. 3, *A. eberhardi* as well as *A. richardsoni* from Mt. Field (A), Lightning Plains (B), West Coast Range (W/V), whereas the remaining populations, all from the Central Plateau and Western Mountain Ranges (*A. richardsoni* C–U + *A. spinulae*) cluster together (Fig. 3I/II). Finally, data set 3 represents a subset of all samples that excludes *A.* sp. nov. 1, *A.* sp. nov. 2, *A. eberhardi* as well as *A. richardsoni* from Mt. Field (A) and is comprised of twice as many loci as the former data set. PCA analyses of this data set, which benefits from a higher genetic resolution for PCA due to the surplus of loci, show a clear-cut separation of *A. richardsoni* populations/metapopulations C/D/*A. spinulae*, F/G, H, J, U, V, W (Fig. 3III/IV). Using data set 4, we can clearly separate *A. richardsoni* populations C, D and *A. spinulae* (Fig. 3V/VI), and in PC2, even the two morphological forms of *A. richardsoni* occurring in Clarence Lagoon (genetic lineage D, Figs 3 and 4).

We likewise carried out STRUCTURE analyses for data sets 2 and 3. For data set 2, 15 clusters were determined as best-fitting to explain the genetic structure, while for data set 3, the best-fitting *k*-value was 11. Again *A.* sp. nov. 1, *A.* sp. nov. 2, *A. eberhardi* as well as *A. richardsoni* from Mt. Field (A) were uncovered as distinct clusters showing no sign of shared genetic coancestry (Fig. 4I). Also *A. richardsoni* from Lightning Plains (B) and *Anaspides* sp. nov. 3 form distinct clusters, but *A. richardsoni* from Lightning Plains (B) shows signals of minor genetic coancestry with *A.* sp. nov. 2 and *A.* sp. nov. 3. Moreover, *Anaspides* sp. nov. 3, especially population c, shares genetic ancestry with a group consisting of *A. richardsoni* populations C, D and *A. spinulae* (Fig. 4I/II). Regarding the *A. richardsoni* populations/metapopulations and *A. spinulae* from the Central Plateau/Western Mountain regions we can detect eight major groups having a distinct genetic signal. These groups are W/V, T, F/G, U, S, I–M/R, E/N–Q and the aforementioned clade comprising C/D/*A. spinulae*. However, we have detected shared genetic ancestry between some of those groups. The highest degree of shared genetic variation was found between I–M/R and E/N–Q. H is the only population that cannot be assigned to any of the other groups but seems to be composed of three shared ancestral components all at more or less similar ratios (F/G, E/N–Q, I–M/R). Moreover, the following groups also share some genetic signal: F/G + H, H + E–R, E/N–Q + H + S (one population), U + E/N–Q + C/D/*A. spinulae* (Fig. 4II).

In the fineRADstructure analysis of data set 2, we could detect 49 discrete genetic clusters corresponding largely to sampling localities (Fig. 5I, black boxes), with basically each sampling locality representing a separate cluster. The only exceptions to this are four

10960031, 0, Downloaded from https://onlinelibrary.wiley.com/doi/10.1111/cla.70005 by Christoph Höpel - University Rostock Universitatsbibliothek , Wiley Online Library on [30/07/2025]. See the Terms and Conditions (https://onlinelibrary.wiley.com/terms-and-conditions) on Wiley Online Library for rules of use; OA articles are governed by the applicable Creative Commons License

sampling sites for *A. eberhardi*. The sampling sites "Nameless Spring" and "Settlement" (F_{ST} values 0.017, d_{xy} 0.0037, Figs S3 and S4) were recovered as one cluster, as also for the locations "Junee Cave" and "Gormenghast Cave" (F_{ST} value, 0.048, d_{xy} 0.0037, Figs S3 and S4). The sampling site "Clarence Lagoon" (genetic group D) shows two discrete clusters. Interestingly, these clusters correspond to two different morphological variations of *A. richardsoni* within the lagoon, with one exhibiting an overall higher degree of pleonal spination. However, as there were only five specimens examined that are most closely related to one another, have no other morphological differences and were found together at the same location, they are considered in the following as a single population.

The fineRADstructure analysis of data set 2 likewise supports the separation of the species, respectively lineages, of *A.* sp. nov. 1, *A.* sp. nov. 2, *A. eberhardi* as well as *A. richardsoni* from Mt. Field (A) and Lightning Plains (B). All are uncovered as discrete clusters with higher coancestry, and we did not detect any significant shared genetic variation between them. Both analyses (of data sets 2 and 3) also show both the separation of the populations of *Anaspides* sp. nov. 3 as well as of *A. richardsoni* (C–V) and *A. spinulae* from the Central Plateau (and adjacent mountain ranges; West Coast Range, Black Bluff Range, Cradle Mts). Moreover, particularly data set 3 allows us to distinguish groups that have a higher degree of shared coancestry such as *A. richardsoni* W/V, metapopulation S or *A. richardsoni* U/N. However, the shared coancestry between populations D, C and *A. spinulae* most likely represents common ancestry and not later introgression (particularly considering the phylogeny Fig. 2; also shown in the STRUCTURE analysis Fig. 4). Interestingly, there is also a signal of coancestry between *Anaspides* sp. nov. 3 population c and the group comprising *A. richardsoni* population C, D and *A. spinulae*, with the strongest signal to *A. richardsoni* population D. These populations all occur in close proximity. Furthermore, we detected slightly increased coancestry between the nearest populations to Lake St. Clair of *Anaspides* nov. sp. 3 (e, f and g) and *A. spinulae*.

The DSuite analyses uncover signals of historical gene flow, albeit most of these instances being found between populations of the same species. In *A. richardsoni* we can find strong signals of gene flow between some populations of metapopulation A, S and M as well as between populations P/O, N/L, H/G, L/M, T/F or J/P. In *Anaspides* sp. nov. 3, we could detect such gene flow between c and e/f/g. However, we can also find two instances of gene flow between species. One signal is between *Anaspides* sp. nov. 3 population c and the group/ancestral lineage comprising *A. richardsoni* C + D + *A. spinulae*. The second strong signal is between *A. spinulae* and the group comprising population e, f and g of *Anaspides* sp. nov. 3. While the first signal is found on both axes of the matrix, the second signal is only found on the *x*-axis indicating probable introgression of *A. spinulae* into *Anaspides* sp. nov. 3 (Fig. 6, Fig. S2).

Using the OptM package, the best number of migration edges was $m = 2$. The first migration edge was found between the stem of *A. richardsoni* metapopulation A and the lineage comprising *A. richardsoni* populations T, V, and W. This gene flow event might indicate ancestral gene flow, respectively shared ancestry, between those two groups. The second migration event was detected between *A. spinulae* and the lineage comprising *Anaspides* sp. nov. 3 populations e, f and g and might indicate interbreeding between these two lineages, with introgression of *A. spinulae* into *Anaspides* sp. nov. 3 population e–g (Fig. 7).

COI data

Anaspides sp. nov. 1 is not shown here, as it has a distinctly different cluster and 7.6–9.8% pairwise distance to all remaining species and populations examined in this study (all other species, respectively, populations have pairwise distances <7.3%).

In the COI haplotype network, seven major clusters (>3% pairwise distance) are present (Fig. 8). Cluster 1 comprises *A. richardsoni* from the Mt. Field area (metapopulation A), *A. eberhardi* and *Anaspides* sp. nov. 2, showing a complex structure with potential introgression, which will not be discussed in detail here. Cluster 2 comprises specimens from the West Coast Range (W/V), cluster 3 from the Black Bluff Range (T) and cluster 4 comprises one specimen from Liffey River (H). Population H (Liffey River) has also a second small cluster of haplotypes grouped within cluster 7. Cluster 5 comprises *Anaspides* sp. nov. 3 from populations a–e and *A. richardsoni*, population B. *Anaspides* sp. nov. 3 population c and *A. richardsoni* population B, however, show long branches within this cluster (>2% difference). Cluster 6 includes *A. richardsoni* from location F, and Cluster 7 comprises *A. richardsoni* from the Central Plateau and Cradle Mts (C–G, I–U), *A. spinulae*, and *Anaspides* sp. nov. 3 from populations f and g. Again, the presence of *Anaspides* sp. nov. 3 (f and g) in cluster 7 might indicate mitochondrial introgression into these two populations. Moreover, some populations/metapopulations have shared haplotypes such as the *A. richardsoni* populations I/K/M, E/N, M/R, O/P, P/Q, R/S as well as *A. spinulae*/*A. richardsoni* C and *A. spinulae*/*A. richardsoni* D. Moreover, *A. spinulae* together with *A. richardsoni* D have two distinct subclusters. The two subclusters in *A. richardsoni*

10960031, 0, Downloaded from https://onlinelibrary.wiley.com/doi/10.1111/cla.70005 by Christoph Höpel - University Rostock Universitätsbibliothek , Wiley Online Library on [30/07/2025]. See the Terms and Conditions (https://onlinelibrary.wiley.com/terms-and-conditions) on Wiley Online Library for rules of use; OA articles are governed by the applicable Creative Commons License

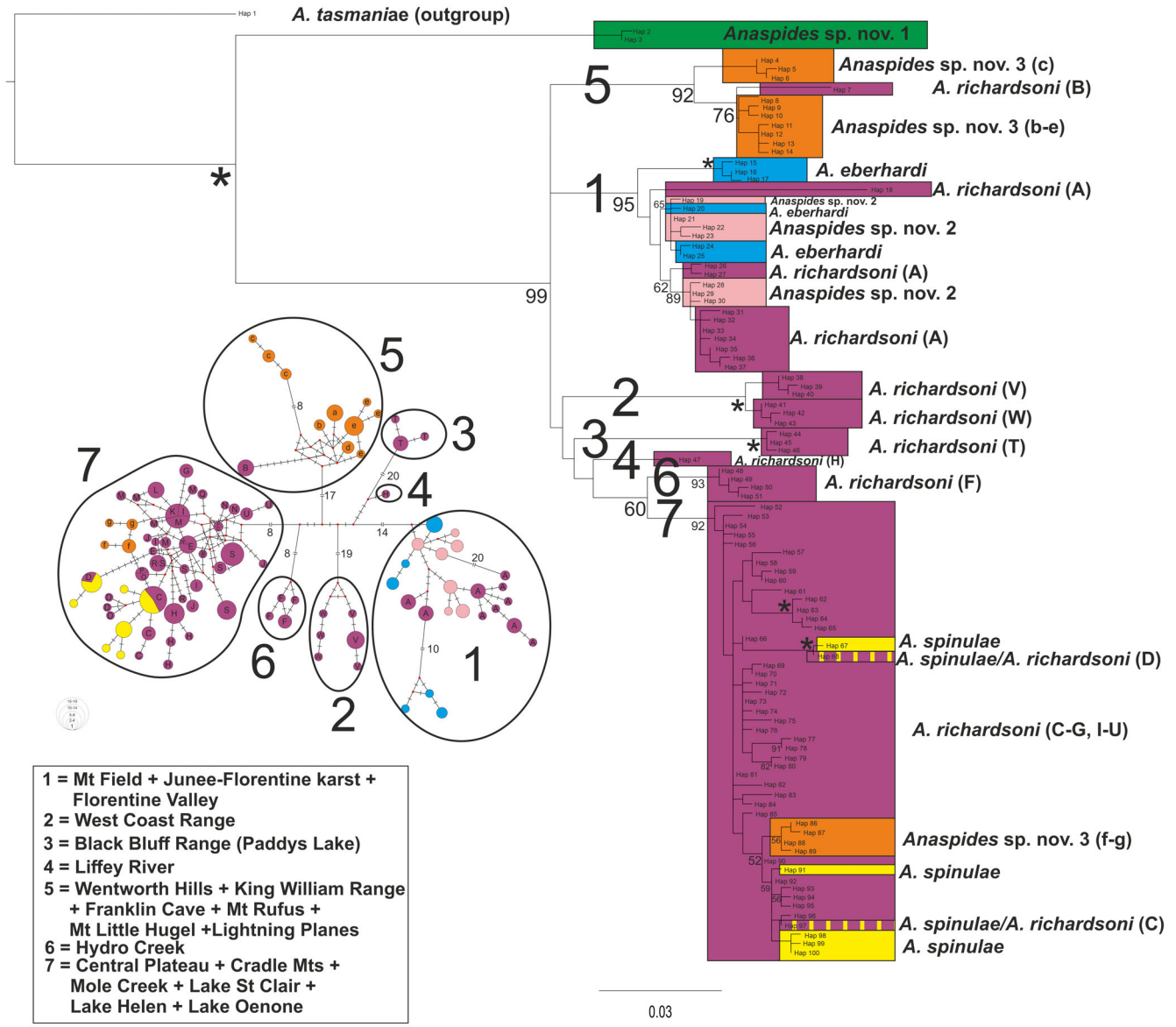


Fig. 8. Maximum Likelihood phylogeny and median joining haplotype network of COI of the six species analysed in this study (323 individuals, 560 bp). The phylogeny was calculated with RaxML and *Anaspides tasmaniae* was used as an outgroup (HKY + G + I, 1000 iterations). The haplotype network was calculated with NETWORK 10.2.0.0 (Fluxus Technology Ltd.). Colours correspond to morphologically delineated species (based on Ahyong, 2015, 2016; Höpel et al., 2023a). Purple: *A. richardsoni*, Blue: *A. eberhardi*, Light Pink: *Anaspides* sp. nov. 2, Orange: *Anaspides* sp. nov. 3, Yellow: *A. spinulae*. Letters correspond to population/metapopulation in Fig. 11. Numbers correspond to major cluster (>3% pairwise distance).

D also correspond to the two morphological forms found in this habitat.

The phylogenetic analysis shows seven lineages corresponding to the seven clusters of the network (Fig. 8). At the base a polytomy between clusters 1, 5 and the rest (*A. richardsoni* C–W, *A. spinulae*, *Anaspides* sp. nov. 3 f–g) was recovered. The next off-branching cluster is 2 (*A. richardsoni* V/W), followed by 3 (*A. richardsoni* T), 4 (*A. richardsoni* H), 6 (*A. richardsoni* F) and 7 (*A. richardsoni* C–G, I–U, *A. spinulae* and *Anaspides* sp. nov. 3 f–g). Within cluster 7, we find nested *A. spinulae* and *Anaspides* sp. nov. 3 (f–g). We can also distinguish one subcluster within cluster 7 comprising specimens belonging to *A. richardsoni* C, D, P, O, *A. spinulae* and *Anaspides* sp. nov. 3 (f–g). These areas (except O, P) are in close geographical proximity, belong to the same water system and were influenced by Pleistocene glaciation.

Because of the insufficient resolution in COI, paired with the multiple potential introgressions and nested

10960031, 0, Downloaded from https://onlinelibrary.wiley.com/doi/10.1111/cla.70005 by Christoph Höpel - University Rostock Universitatsbibliothek , Wiley Online Library on [30/07/2025]. See the Terms and Conditions (https://onlinelibrary.wiley.com/terms-and-conditions) on Wiley Online Library for rules of use; OA articles are governed by the applicable Creative Commons License

position of some of the species, we do not apply an automatic species delimitation method for the COI data set.

Discussion

The ddRAD data provide remarkable genetic resolution for most populations, where (almost) each sampling site represents an independent population (i.e. with higher genetic similarity of the individuals within the sampling site than with individuals from other sampling sites). There are few exceptions, and for the sake of simplicity, we summarized and collapsed some populations into metapopulations. The ddRAD data also indicate a limited dispersal potential of the individuals. This is particularly true for those specimens living in tarns and lakes but might be less strict for those individuals living in streams and creeks. The COI data are mostly concordant with the ddRAD data but provide less resolution, which might be due to substantially different evolutionary rates between mitochondrial and nuclear markers, incomplete lineage sorting and introgression. However, some of the lineages of the *A. richardsoni* species complex are well separated, indicating relatively old separation of the basal lineages. Both data sets also show more recent introgression of what is considered herein as separate species.

Species delimitation and the case of A. richardsoni *as a paraphyletic species*

One of the currently undescribed species, herein called *Anaspides* sp. nov. 1, emerges as the sister species to all species of the *A. richardsoni* species complex (Fig. 2) in our analyses. *Anaspides* sp. nov. 1 is syntopic with *A. richardsoni* in Lake Nicholls (Mt. Field). Our genetic data (nuclear and COI) show no evidence of interbreeding between these two species, and they are morphologically distinct. *Anaspides* sp. nov. 1 clearly represents a separate species.

Anaspides richardsoni, as currently morphologically delineated (see diagnosis of Ahyong, 2016), represents a "paraphyletic" species relative to the remaining species in the species complex (*A. eberhardi*, *Anaspides* sp. nov. 2, *Anaspides* sp. nov. 3, *A. spinulae*) (Fig. 10). This formal description, however, does *not necessarily* represent biological reality but needs further consideration.

Anaspides eberhardi, *Anaspides* sp. nov. 2 and *Anaspides* sp. nov. 3 are well characterized by morphologically discrete characters, which, in our opinion, demonstrate ecological adaptations (*A. eberhardi*) and reproductive isolating mechanisms (*Anaspides* sp. nov. 2 and *Anaspides* sp. nov. 3). They are all monophyletic in the ddRAD data set. We consider the number of clasping spines as particularly important although we are aware that these differences alone might not result in a perfect (prezygotic) isolating mechanism. Differences also occur in the shape and length of the telson spines as well as the shape and setation of the inner antennular flagellum. We contend that the presence of only one clasping spine is the apomorphic condition for the *A. richardsoni* species complex, with three reversals to the plesiomorphic condition of two clasping spines, characterizing *Anaspides* sp. nov. 2, *Anaspides* sp. nov. 3 and *A. spinulae* (Fig. 10). The convergent reduction to one clasping spine in three *A. richardsoni* lineages (Mt. Field, Lightning Plains, Central Plateau/Western Mountain Ranges) would still require the reversal to two clasping spines in *A. spinulae*. We consider the convergent reduction to one clasping spine also as less plausible considering the high morphological similarity of all *A. richardsoni* lineages. In any case, *A. eberhardi*, *Anaspides* sp. nov. 2 and *Anaspides* sp. nov. 3 are "good" species according to the GLC.

For *A. richardsoni*, one could also argue for recognition to (at least) three "cryptic" species, "Mt. Field" (type locality, population A), "Lightning Plains" (population B) and "Central Plateau/Western Mountain Ranges/Mole Creek" (populations C to W), the latter potentially including *A. spinulae*. These (at least) three putative species are clearly allopatric, genetically distinct both in the ddRAD and the COI data sets. The split between "Mt. Field" and "Central Plateau" appears also to be relatively old (4.25 Mya, Fig. 9). Following this argument, each of the lineages (at least those six recognized in both phylogenetic analyses) grading towards *A. spinulae* might also be argued to represent separate species. For clarity, we deal with *A. spinulae* separately below. However, we hesitate to follow this approach for the following reasons. First, there are no diagnostic morphological differences between *A. richardsoni* populations A and C–W based on the careful and detailed study by Ahyong (2016), nor are there any known behavioural or ecological differences. The situation may be slightly different for population B from Lightning Plains because it shows slight troglomorphy. Only one of the "species criteria" from De Queiroz (1998, 2007) is fulfilled, which is being allopatric and reciprocally monophyletic. However, we cannot exclude the possibility of incipient speciation—not necessarily because of divergent ecological adaptation but long-term genetic isolation. This may lead to post-zygotic reproductive isolation owing to the emergence of Muller-Dobzhansky incompatibilities in the form of incompatible novel mutations in the allopatric populations (Orr and Turelli, 2001).

The other more practical reason favouring treatment of *A. richardsoni* as a "paraphyletic" species for now is that separation of three or more species would lead to

10960031, 0, Downloaded from https://onlinelibrary.wiley.com/doi/10.1111/cla.70005 by Christoph Höpel - University Rostock Universitätsbibliothek , Wiley Online Library on [30/07/2025]. See the Terms and Conditions (https://onlinelibrary.wiley.com/terms-and-conditions) on Wiley Online Library for rules of use; OA articles are governed by the applicable Creative Commons License

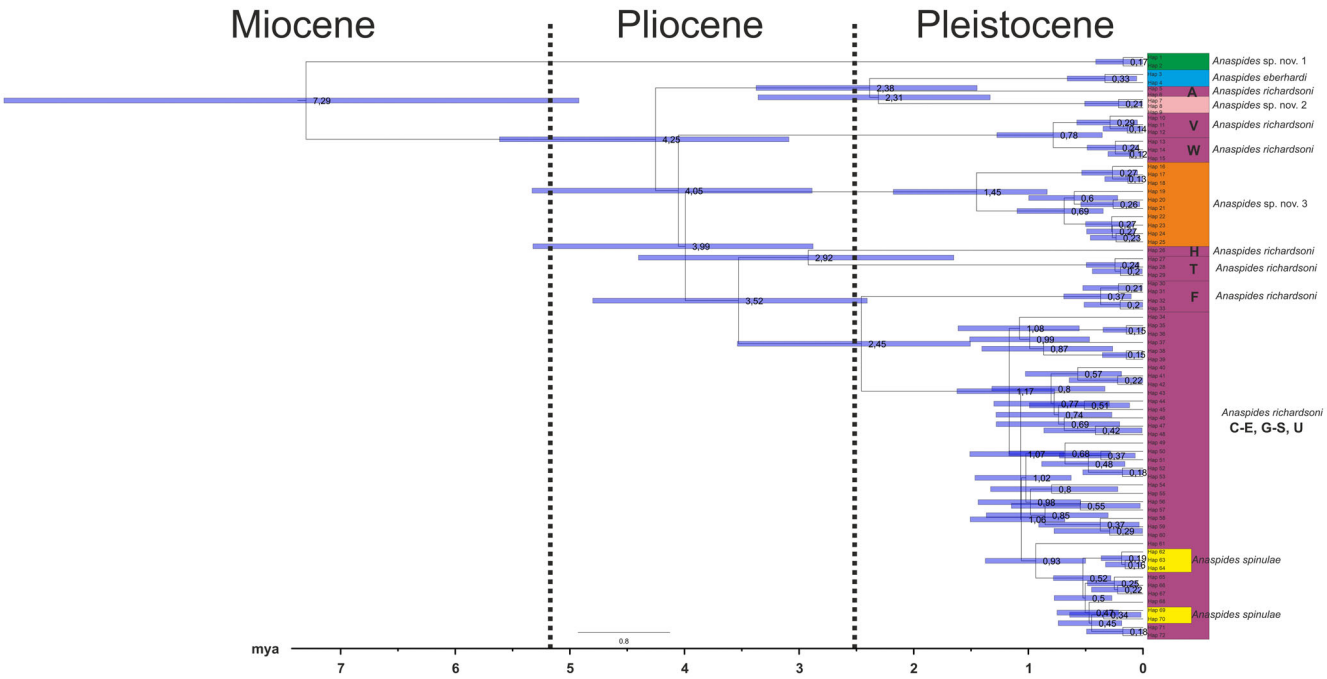


Fig. 9. Strict molecular clock calculated with Beast V2 of COI of the six species analyses in this study (323 individuals, 560 bp). Letters correspond to populations/metapopulations in Fig. 11. We excluded lineages/haplotypes where we expect introgression and/or incomplete lineage sorting to have occurred (e.g. *Anaspides* sp. nov. 3 f-g or *A. richardsoni* B). The split between the Mt. Field/Junee Florentine clade and the Central Plateau/Western Mountain Ranges clade has a median age of 4.25 Mya, and the split between the *Anaspides* sp. nov. 3 and those of the supposed refugial areas are only slightly younger (4.05 Mya) meaning that the same paleoclimatic event might have caused separation of the lineages.

a great taxonomic and diagnostic instability—they are morphologically and ecologically indistinguishable. Recognition of three (or more) *subspecies* would be in the vein of Dufresnes et al. (2024) but still remain problematic because, although "inhabiting a geographic subdivision of the species", they are not "differing taxonomically" (see Mayr, 1969). Notwithstanding that species delimitations represent hypotheses (Fitzhugh, 2009) and future analyses of more data might lead to different taxonomic conclusions, the recognition of new species within *A. richardsoni* should be done cautiously (Fig. 10).

The case of the *Anaspides* "central clade" is evolutionarily interesting as adaptive and non-adaptive processes played crucial roles. On the one hand, the plesiomorphic morphology and absence of morphological differences, especially between the Mt. Field (A) and Central Plateau/Western Mountain Ranges (C–W) and among the C–W populations of *A. richardsoni*, are remarkable and seem to have prevailed over long evolutionary times (and potentially multiple speciation events). This suggests that this morphology is highly conserved and well adapted to the prevailing ecological conditions. This is sometimes referred to as "non-adaptive radiation" (Gittenberger, 1991) but the question remains if this radiation necessarily leads to speciation. Our study also corresponds to the theory of allopatric speciation, where from several populations of originally one widespread species, some speciate (by sexual or ecological selection) and others do not (Mayr, 1942; Baker, 2005). On the other hand, several (good) species in our data set have evolved new morphological traits. In most cases, this involves a shift in the number of clasping spines that are assumed to play a role in mate recognition (Ahyong, 2015, 2016) and may thus contribute to prezygotic reproductive isolation. Such shifts can be observed in *A.* sp. nov. 2 and 3 and *A. spinulae*. They either occur syntopically with a single-spined species (*A.* sp. nov. 2 and *A. eberhardi*) or show genetic evidence for past hybridization with such a single-spined species (*A. spinulae* and *A. richardsoni* C/D; *A.* sp. nov. 3 and *A. richardsoni* C/D) and also often go hand in hand with a shift in habitats (surface to cave or lake). It seems plausible that in these cases, the secondary contact between young, recently diverging lineages leads to reinforcement through accelerated adaptive and segregating evolution (Noor, 1999). If the hybrids are less well adapted, the evolution of diverging mate recognition mechanisms (here the evolution of a second clasping spine) would increase the species fitness and reduce hybridization.

10960031, 0, Downloaded from https://onlinelibrary.wiley.com/doi/10.1111/cla.70005 by Christoph Höpel - University Rostock Universitätsbibliothek , Wiley Online Library on [30/07/2025]. See the Terms and Conditions (https://onlinelibrary.wiley.com/terms-and-conditions) on Wiley Online Library for rules of use; OA articles are governed by the applicable Creative Commons License

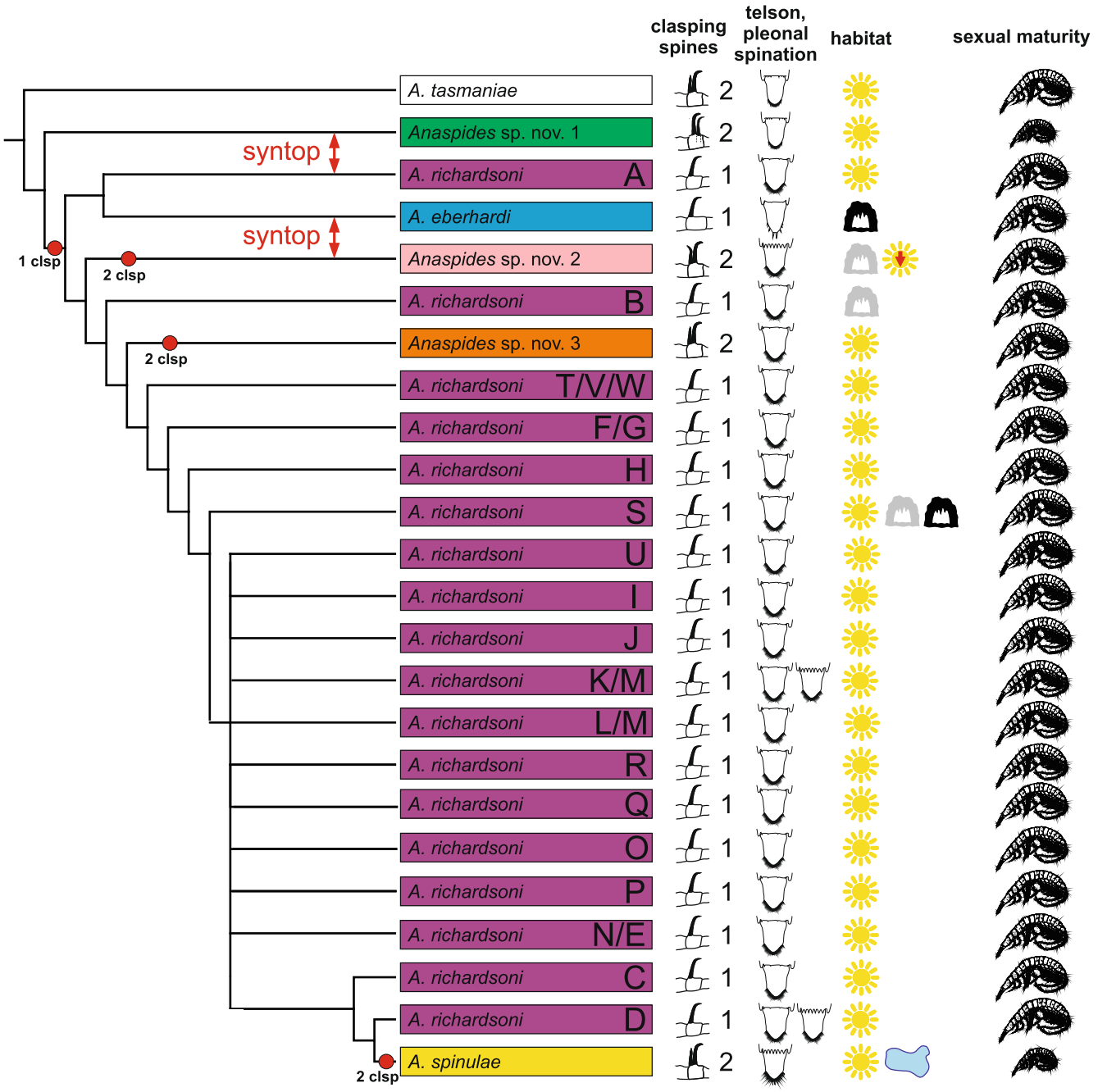


Fig. 10. Scheme showing the relationships of the species of *Anaspides* which belong to the *Anaspides richardsoni* species complex with the two nearest outgroups (*A. tasmaniae* and *Anaspides* sp. nov. 1) and important morphological characters (number and position of clasping spines [clsp]., telson shape and spination of the telson and the tergal margins of pleonite 6, size of reaching sexual maturity) and habitat (sun = surface; red arrow = lowland >450 m, black cave = troglodytic, grey cave = cave inhabiting with slight cave adaptations, lake = big lake inhabiting).

Anaspides spinulae *as a separate species*

Probably, the most interesting case is that of *A. spinulae*. Our data indicate that several lineages of *A. richardsoni* from the Central Plateau/Western Mountain Ranges (Fig. 2) are successively related to *A. spinulae* in a grade. If considering *A. spinulae* a valid species, this again supports the paraphyly of *A. richardsoni* (as formally described). The minimum number of separate lineages gradually related to *A. spinulae* supported by our phylogenetic analyses is six (W/V/T, F/G, H, S, C, D, Fig. 2), depending on the analytical method. Even more striking is the very high genetic similarity between *A. spinulae* and *A. richardsoni* C + D (PCA,

10960031, 0, Downloaded from https://onlinelibrary.wiley.com/doi/10.1111/cla.70005 by Christoph Höpel - University Rostock Universitätsbibliothek , Wiley Online Library on [30/07/2025]. See the Terms and Conditions (https://onlinelibrary.wiley.com/terms-and-conditions) on Wiley Online Library for rules of use; OA articles are governed by the applicable Creative Commons License

STRUCTURE, FineRADstructure, F_{ST} 0.025, d_{xy} 0.0039), also reflected by the shared haplotypes in COI, which suggest very recent speciation and rapid evolution of the morphological differences between these species. As with most *A. richardsoni* lineages, *A. spinulae* is recovered as a discrete (monophyletic) lineage in the tree and a discrete population in fineRADstructure. However, in contrast to the discrete *A. richardsoni* lineages/populations, *A. spinulae* shows discrete morphological and ecological adaptations, that is, the presence of two clasping spines, the strong, uneven spination of the telson and earlier onset of sexual maturity, which also speaks against the "ecomorph hypothesis" discussed by Williams (1965) when formally describing *A. spinulae*. We do not think that morphological plasticity and the presence of fish predators (e.g. galaxiids), such as seen in *Daphnia* (Adler and Harvell, 1990), played a major role in acquiring pronounced spination in *A. spinulae* and some populations of *A. richardsoni* (e.g. some specimens from population D and metapopulation M). Spiny and non-spiny *A. richardsoni* sometimes occur syntopically (Clarence Lagoon), populations with pronounced spination occur in fishless waters (e.g. some locations in the Walls of Jerusalem, pool near Little Throne) and non-spiny *A. richardsoni* occur syntopically with galaxiid fish (e.g. Lake Nicholls, Little Pine Lagoon, Pine Lake). Also, other species of *Anaspides* have not acquired pronounced spination although inhabiting lakes and occurring syntopically with fish (e.g. Lake Skinner, Weld River). As Ahyong (2016) noted, the distribution of the "spinulae" form of *A. richardsoni* correlates more strongly with geography than ecology and might reflect phylogeographic genotypic variation.

However, hybridization has been observed between *A. spinulae* (or more precisely the *A. spinulae*/*A. richardsoni* C/D group) and *A.* sp. nov. 3. There is evidence for two introgression events between *Anaspides* sp. nov. 3 and *A. spinulae* (or the common ancestor of *A. spinulae* and *A. richardsoni* C + D). One is between *Anaspides* sp. nov. 3 (population c; Wentworth Hills) and the actual ancestral populations C, D and *A. spinulae* (see STRUCTURE analyses; Treemix; Dsuite), which is not reflected in the COI data. However, in the analyses of COI data, we found a haplotype cluster of *Anaspides* sp. nov. 3 from locations f and g (Lake Helen, Lake Oenone; the geographically closest populations to Lake St Clair), which is only four mutations different from the cluster comprising *A. spinulae* and lineage C of *A. richardsoni*, suggesting potential mitochondrial introgression into these populations of *Anaspides* sp. nov. 3. These hybridization events may have transgressed the phenotype of two clasping spines from *Anaspides* sp. nov. 3 into *A. spinulae*, which would have been reinforced by segregation (Rieseberg et al., 1999) due to secondary contact with *A. richardsoni*. This raises again the question of whether the pronounced spination of the tergal and pleural margins of the pleonites, and especially of the telson, in combination with the smaller size at sexual maturity might be related to the lacustrine habitat of Lake St. Clair. Alternatively, a convergent reversal to 2 clasping spines in *A. spinulae* could have facilitated the introgression. In any case, we consider the apparent introgressions as not contradicting the presence of separate species, only that the complete reproductive isolation criterion might not yet have been completely fulfilled. In summary, we recognize *A. spinulae* as a very young species.

Potentially, the two genetically slightly diverging and morphologically differing syntopic lineages of *A. richardson*i D are at an early stage of adaptive and segregating evolution where the reproductive isolating mechanisms (i.e. diverging number of clasping spines) have not yet been established.

In summary, our multi-gene analysis with well-separated, allopatric populations fulfils the criteria of Coyne and Orr (2004) implying that "*A. richardsoni*" might indeed represent a "paraphyletic" species, whether or not populations A and B are considered (we are aware that the name *A. richardsoni* is connected to population A, from which the holotype comes). Paraphyletic species are also recognized among freshwater fish (Barluenga et al., 2006; Secci-Petretto et al., 2023) and ground beetles (Fujisawa et al., 2019). Fujisawa et al. (2019) uncovered paraphyletic relationships for *Carabus maiyasanus* and *C. iwakanianus*, as well as *C. arrowianus* being paraphyletic in regard to three other species (all having parapatric boundaries with *C. arrowianus* being the central species sharing boundaries with all other species). Paraphyly also occurs within the *S. salamandra* species clade, which comprises over 12–17 subspecies, one sometimes being considered a separate species (mostly based on coloration patterns and geographic distribution). Burgon et al. (2021) suggest at least four instances of paraphyletic subspecies. Secci-Petretto et al. (2023) show that the grayling *Thymallus baicalensis* (widespread species in Siberia and Mongolia, mainly found in rivers and near outlets of lakes including the outlet of Lake Hovsgol) is paraphyletic with respect to *T. nigrescens* (only found in Lake Hovsgol, with different ecological adaptations). Roman et al. (2018) suggest a very recent divergence of *T. nigrescens* (32 kyr). This example is strikingly similar to the case of *A. spinulae*.

Paleoecological reconstruction of extant distribution of Central Plateau/Western Mountain Ranges Anaspides

The influence of the Pleistocene glacials and interglacials on the distribution of animals and plants has

10960031, 0, Downloaded from https://onlinelibrary.wiley.com/doi/10.1111/cla.70005 by Christoph Höpel - University Rostock Universitätsbibliothek , Wiley Online Library on [30/07/2025]. See the Terms and Conditions (https://onlinelibrary.wiley.com/terms-and-conditions) on Wiley Online Library for rules of use; OA articles are governed by the applicable Creative Commons License

been long discussed (e.g. de Lattin, 1967). In particular, higher elevations were covered with ice shields but also non-glaciated areas were influenced by changing climatic conditions. Individuals of mobile species (e.g. birds, many insects) might have dispersed to the refugial areas, whereas less mobile (e.g. soil animals, but probably also certain limnic taxa) might have become extinct in these areas. In the interglacials and after the LGM, these areas have become recolonized from so-called glacial refugia. Crustaceans are not well studied in terms of Pleistocene paleoclimate changes (e.g. Puli et al., 2024) and the "central clade" *Anaspides* might be an excellent system for such study.

Since the Early Miocene, Tasmania was carried north due to plate tectonics on the Australian Plate from 65° latitude and reaching its present position at 42° latitude around the Late Miocene (Gallagher et al., 2003; Corbett, 2019). Around this time, the Antarctic started to freeze over with the biggest fluctuation of glacial extent during the Pliocene (Warnke et al., 1992). This also led to variations in the relative dominance of rainforest and wet sclerophyll forests in south-eastern Australia through that time period (Macphail, 1997). Gallagher et al. (2003) showed that in the early Pliocene the climate was warm and wet with a peak in summer rainfall (mean annual temperature 2–4 °C higher than present, mean annual precipitation 50–70% higher than present), whereas the climate at the end of the Late Pliocene was drier and cooler with a winter rainfall peak (mean annual temperature 0–2 °C higher than present, mean annual precipitation 0–30% higher than present) We thus assume that *Anaspides* (specifically the *A. richardsoni* complex) inhabited a continuous range in Central Tasmania including Mt. Field, the Central Plateau, the Western Mountain Ranges and adjacent landscapes already during the Pliocene.

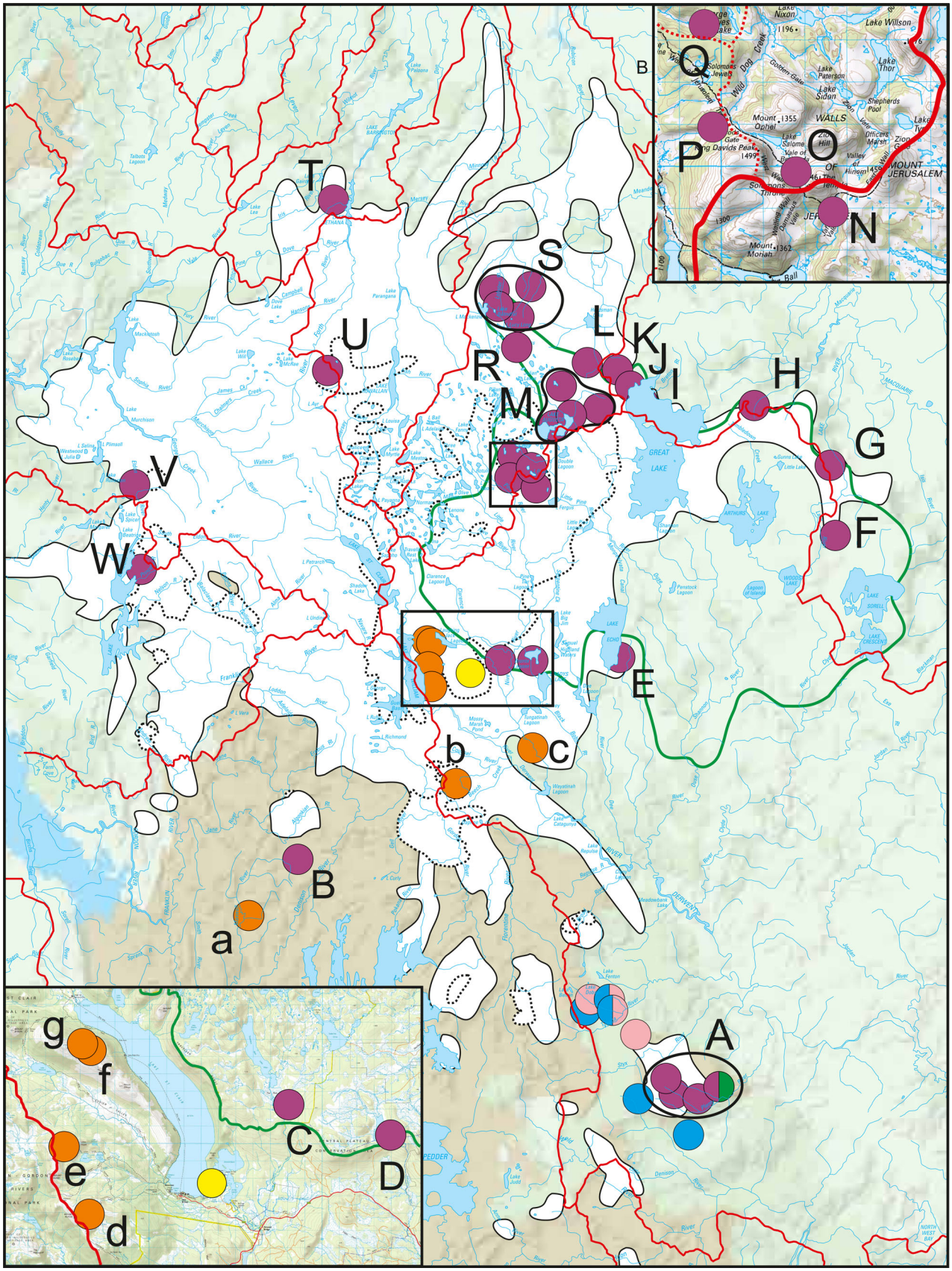
In the following, we will focus on the *A. richardsoni* populations from the Central Plateau/Western Mountain Ranges C–W as well as *A. spinulae*. Lineages T, U, V, and W belong to the Western Mountain Regions, while lineages C–S lie directly on or on the edges of the Central Plateau (Fig. 11, green outline). The locations on the edges are E, I, J, K, which are creeks draining from the Central Plateau (specimens in region K are found on the Plateau as well as on the slopes) as well as the caves which are found in region S.

We propose that Cenozoic glaciations (the latest being the so called Linda glaciations in the early Pleistocene; Colhoun et al., 2010) may have wiped out most of the populations on the western and northern part of Central Plateau and Western Mountain Ranges and left or forced *Anaspides* to regions at and/or beyond the ice margins. Subsequent glaciations are often referred to as being in general less extensive, giving the potential that habitats uninhabitable during previous glaciations may have served as new and additional refugia and subsequently as stepping stones and sources for recolonization, which may have been continuously inhabited throughout even during later glaciation events. It is likely that some of the diverging genetic lineages of *A. richardsoni* evolved and persisted in these refugial areas, though we do not know their exact localities. Other regions may have been (re-) colonized once or repeatedly from one or multiple refugia; the genetic differentiation of these recolonized populations is expected to be less pronounced than in the continuously inhabited regions and the chance for hybridization from different long-term refugia increases. In any case, the extant distribution at higher elevations is the result of a post-glacial recolonization. Lowland areas, which are not inhabited by *Anaspides* today, might have been suitable habitats during that time, as temperatures were 6–10 °C cooler than the present and the snowline was lower by 1000–1500 m (Colhoun et al., 2010); also the sea level was lowered by 130 m during the LGM (Morrison et al., 2023). An exception is *Anaspides* sp. nov. 2, which still occurs in lowland creeks (>450 m) near the outflow of caves, which supply cold and clear water.

With regard to the genetic clusters uncovered in the STRUCTURE analyses (k11), we have to assume several glacial refugia during the Pleistocene (or earlier) glaciations regarding *A. richardsoni* populations from the Central Plateau/Western Mountain Ranges C–W as well as *A. spinulae*. The exact area of the glacial refugia can only be determined vaguely. However, it is assumed to be at least in proximity to the ice margins and present-day areas, in adjacent landscapes, lowland areas and in some cases potentially even the same waters (e.g. F). These glacial refugia are mainly represented by the lineages comprising the basal branching populations and two groups containing the majority of populations in the central and western part of the Central Plateau. For the basal branching lineages, we assume glacial refugia to the west (lineage W/V),

Fig. 11. Distribution map of the six species of *Anaspides* examined in this study with watersheds (red lines) and maximum glaciated area of the Central Plateau (green line) during the Linda Glaciations (closed black lines, white) after Corbett (2019); Houshold and Jackson (2023) and during the Last Glacial Maximum (LGM, 22 000–17 000 Mya) (dotted black lines, white) after Colhoun et al. (1996). The Central Plateau is marked with a green outline (after Corbett, 2019). Purple: *A. richardsoni*; Yellow: *A. spinulae*; Blue: *A. eberhardi*; Green: *Anaspides* sp. nov. 1 from Lake Nicholls; Pink: *Anaspides* sp. nov. 2 from the Florentine Valley; Orange: *Anaspides* sp. nov. 3. Half-circles indicate syntopic.

10960031, 0, Downloaded from https://onlinelibrary.wiley.com/doi/10.1111/cla.70005 by Christoph Höpel - University Rostock Universitatsbibliothek , Wiley Online Library on [30/07/2025]. See the Terms and Conditions (https://onlinelibrary.wiley.com/terms-and-conditions) on Wiley Online Library for rules of use; OA articles are governed by the applicable Creative Commons License



10960031, 0, Downloaded from https://onlinelibrary.wiley.com/doi/10.1111/cla.70005 by Christoph Höpel - University Rostock Universitatsbibliothek , Wiley Online Library on [30/07/2025]. See the Terms and Conditions (https://onlinelibrary.wiley.com/terms-and-conditions) on Wiley Online Library for rules of use; OA articles are governed by the applicable Creative Commons License

north-west (lineage T) and east (lineage F/G) of the glaciated area. Our molecular clock analysis dates the separation of the basal branching lineages between 2.45 and 4.05 Mya, which is slightly older than early Pleistocene glaciations (Linda glaciations). This could either be a miscalibration of the molecular clock itself (no fossils or geological events were used for calibrating) or could indicate that these populations were already separated before the Linda glaciations. This could have been caused by a potential earlier glaciation during the Pliocene (Macphail et al., 1993; Augustinus and Idnurm, 1993). The Pleistocene glaciations then only reinforced a further separation of these populations. In any case, those populations geographically in-between the separated ones became entirely extinct.

The discrete cluster in the STRUCTURE analyses also indicates that the caves inhabited by metapopulation S could have acted as a separate refugium, which will be in the focus of another study. For group C–-E/I–R, the potential refugia could have been on the north-eastern (I–R) and south-eastern (C, D, *A. spinulae*) parts of the glaciation. The north-eastern refugium could have been situated near the areas of today's populations H–K. Our molecular clock also dates the first split of the clade comprising C–E/I–S to 1.17 Mya, which is substantially younger than the split of the basal branching lineages. This leads us to believe that the glacial refugia for the populations U, *A. richardsoni* C/D, and *A. spinulae* became only glacial refugia during the subsequent (mid-Pleistocene) glaciations. This is also in concordance with the heavy glaciation of these areas and adjacent landscapes during the Linda glaciations.

Our data give evidence that the main recolonization of the western and central parts of the Central Plateau (I–R) happened from the refugial area inhabited by the ancestors of H and, to a minor part, also from the refugium of *A. richardsoni* C/D and *A. spinulae*, seen by the shared genetic information in the STRUCTURE analyses (k11 light and dark blue colours). As the populations N–Q (Walls of Jerusalem) also exhibit a certain genetic cluster comprising two different genetic components, they could represent a separate glacial refugium during one of the later glaciation events, as the area was ice free during the LGM. Interestingly, population E, although located at the ice margins (south-east border), probably never acted as a refugial population because of the derived position in the tree and the close genetic proximity (sister groups in ddRAD, shared haplotype in COI) to population N in the northern part of the Plateau. This area must have been recolonized from the northern part of the Central Plateau (Walls of Jerusalem, populations N, O, P, Q), which is one of the only instances so far of "long distance" dispersal (for a small mountain shrimp) in *Anaspides*. This migration can be well explained through the fact that populations N and E belong to the same water system, even to the same river system (Pine River) with N being the headwaters region.

Despite substantial glaciation during the LGM (20000–12000 years ago) only a few of the herein studied populations and areas would have been directly affected by those glaciers (Fig. 11). These areas comprise the populations in and around the margins of Lake St Clair (*Anaspides* sp. nov. 3 d–g, *A. spinulae* and *A. richardsoni* C–D). Given that Lake St. Clair was glaciated during the LGM, this might indicate that *A. spinulae* would have evolved after that time. This is in contrast with the earlier views of Williams (1965) that *A. spinulae* survived the Pleistocene glaciation of Lake St. Clair in adjacent periglacial lakes or melt-waters and also with the hypothesized in situ refugium in deeper parts of the lake proposed by Ahyong (2016). Lake St Clair offers a very different environment than the substantially smaller mountain tarns, pools and runnels otherwise inhabited by *A. richardsoni*. Thus, after colonization of Lake St. Clair, probably from the refugial region of *A. richardsoni* C/D, the lake population quickly adapted to the new lacustrine environment. At that time, *A. richardsoni* may have dispersed more frequently to Lake St. Clair, favouring segregating mate recognition mechanisms. In fact, this may be a case of character displacement (Brown and Wilson, 1956). It might therefore represent an interesting case of parapatric or even sympatric speciation (Coyne and Orr, 2004; Barraclough, 2019) which needs further consideration. Such cases of speciation with gene flow are also known from *Heliconius* butterflies (Martin et al., 2013), *Myotis* bats (Morales et al., 2017) and ground beetles (Fujisawa et al., 2019). Moreover, Fujisawa et al. (2019) state that the genomic divergence pattern among *Carabus* (*Ohomopterus*) beetles demonstrates how divergence of a key trait for reproductive isolation (genital morphology) may result in increased species richness despite occasional gene flow due to hybridization.

Based on the COI molecular clock, it appears also reasonable to suggest that the same paleoclimatic event that was responsible for the separation of the basal branching lineages of the Central Plateau/Western Mountain Ranges (2.45–4.05 Mya) was also responsible for the earlier separation (4.25 Mya) between the Mt. Field/Junee-Florentine species group and the Central Plateau/Western Mountain Ranges species group. The glaciations certainly blocked the connection between north and south in what are today the Gordon and the Derwent Rivers. This event would also include the separation of *Anaspides* sp. nov. 3 from the other lineages. Given the deep nodes and clusters in the STRUCTURE analyses, *Anaspides* sp. nov. 3

10960031, 0, Downloaded from https://onlinelibrary.wiley.com/doi/10.1111/cla.70005 by Christoph Höpel - University Rostock Universitätsbibliothek , Wiley Online Library on [30/07/2025]. See the Terms and Conditions (https://onlinelibrary.wiley.com/terms-and-conditions) on Wiley Online Library for rules of use; OA articles are governed by the applicable Creative Commons License

(or its *A. richardsoni*-like progenitor) might have had its glacial refugium during the Linda glaciations in the south-eastern part of its distribution, close to the areas of population c (Wentworth Hills) and b (King William Range). From here it must have recolonized the areas in the north west of Lake St Clair comprising the populations d–g (all branching off in that order, which is also the specific geographical order from south to north).

Conclusion

Our data show a remarkable resolution on the population level with essentially each water body having its own distinct *Anaspides* population. This underlines the low dispersal ability of *Anaspides* and the high potential for allopatric speciation, especially in combination with different geomorphological processes, such as glaciation. We show that even these glaciations played a major role in shaping the current distribution of *Anaspides richardsoni* and *Anaspides spinulae* populations, with several glacial refugial areas. Most of these refugial populations might not have migrated very far (if at all), while the final recolonization of the western and central parts of the Central Plateau derived from two refugia to the north-east and south-east of the plateau, respectively. However, the question remains: do genetically distinct populations represent species or not? This has significant conservation implications. It is not only necessary to protect individual species but also to protect the many separate populations (which might represent incipient species) and areas where they exist.

Acknowledgements

We thank Cathy Plowman, David Butler, Alastair Richardson, Stefan Eberhard, Roland Eberhard, Chris Sharples, John Oxley, John Webb, Andrew Palfreyman and Michael Driessen for collecting various specimens in Tasmania as well as for their advice and guidance. We are grateful for the detailed review and comments of Chris Burridge. We thank Kevin Kiernan for his comments concerning Tasmanian geomorphology. We further thank the University of Tasmania, Institute for Zoology, especially David Green, for logistic support and providing us with scientific equipment for our field trips. We are thankful to the Department of Natural Resources and Environment Tasmania (NRE) and the Parks and Wildlife Service Tasmania for supporting and facilitating our research. We further thank the SFM Lenah Estate for granting us access to certain areas in the Florentine Valley which include Nameless Spring and Settlement Cave. Specimens were collected in 2017, 2019, 2022, 2023 and 2024 (Permits of the Tasmanian Government, Department of Primary Industries, Parks, Water & Environment, nos. FA16347, FA18250, FA21214, FA22411 and FA 23244, respectively). We also want to thank Christian Wirkner, Marian Reinhardt, Malte Weiler, Fabio Oliveira, Birk Rillich, Alexander Rixen and Markus Grams (all Universität Rostock) for assistance in the field. Collecting was funded by the German Science Foundation (DFG RI 837/22-1, 2). Advanced education and collecting in 2019 was partly funded by the DAAD (Nr. 57438025, Kurzstipendien für Doktoranden, 2019/2020). Ralf Bastrop (University of Rostock) provided the infrastructure for sequencing some of the data. The ddRAD library preparations were conducted in cooperation with the National History Museum Vienna. The present project is funded by the Deutsche Forschungsgemeinschaft (DFG RI 837/22-1, 2, 3). Open Access funding enabled and organized by Projekt DEAL.

Conflict of interest

None declared.

Data availability statement

The data that support the findings of this study are openly available in https://github.com/ch515/Hoepel_paraphyletic_species. All sequences and genetic data are uploaded to NCBI. COI: PV780789–PV781115; ddRAD: SAMN49064136–SAMN49064398, BioProject ID: PRJNA1276447.

References

Ackery, P.R. and Vane-Wright, R.I., 1984. Milkweed Butterflies, Their Cladistics and Biology. Cornell University Press, Ithaca.

Adler, F.R. and Harvell, C.D., 1990. Inducible defenses, phenotypic variability and biotic environments. Trends Ecol. Evol. 5, 407–410.

Ahyong, S.T., 2015. Preliminary diagnoses of three new species of Tasmanian mountain shrimps, *Anaspides* Thomson, 1894 (Syncarida, Anaspidacea, Anaspididae). Zootaxa 3957, 596–599.

Ahyong, S.T., 2016. The Tasmanian mountain shrimps, *Anaspides* Thomson, 1894 (Crustacea, Syncarida, Anaspididae). Rec. Aust. Mus. 68, 313–364.

Augustinus, P.C. and Idnurm, M., 1993. Palaeomagnetism of ferricrete from Vale of Belvoir, western Tasmania: implications for Tasmanian Cenozoic glacial history. Explor. Geophys. 24, 301–302.

Baker, J.M., 2005. Adaptive speciation: the role of natural selection in mechanisms of geographic and non-geographic speciation. Stud. Hist. Phil. Biol. Biomed. Sci. 36, 303–326.

Barbetti, M. and Colhoun, E.A., 1988. Reversed magnetization of glaciolacustrine sediments from western Tasmania. Search 19, 151–153.

Barluenga, M., Stölting, K.N., Salzburger, W., Muschick, M. and Meyer, A., 2006. Sympatric speciation in Nicaraguan crater lake cichlid fish. Nature 439, 719–723.

10960031, 0, Downloaded from https://onlinelibrary.wiley.com/doi/10.1111/cla.70005 by Christoph Höpel - University Rostock Universitätsbibliothek , Wiley Online Library on [30/07/2025]. See the Terms and Conditions (https://onlinelibrary.wiley.com/terms-and-conditions) on Wiley Online Library for rules of use; OA articles are governed by the applicable Creative Commons License

Barraclough, T.G., 2019. The Evolutionary Biology of Species. Oxford University Press, Oxford.
Benson, D.A., Karsch-Mizrachi, I., Lipman, D.J., Ostell, J. and Wheeler, D.L., 2003. Genbank. Nucleic Acids Res. 31, 23–27.
Bonnet, T., Leblois, R., Rousset, F. and Crochet, P.A., 2017. A reassessment of explanations for discordant introgressions of mitochondrial and nuclear genomes. Evolution 71, 2140–2158.
Bouckaert, R., Heled, J., Kühnert, D., Vaughan, T., Wu, C.H., Xie, D. and Drummond, A.J., 2014. BEAST 2: a software platform for Bayesian evolutionary analysis. PLoS Comput. Biol. 10, e1003537.
Brooks, H.K., 1962. On the fossil Anaspidacea, with a revision of the classification of the Syncarida. Crustaceana 4, 229–242.
Brown, W.L. and Wilson, E.O., 1956. Character displacement. Syst. Zool. 5, 49–64.
Burgon, J.D., Vences, M., Steinfartz, S., Bogaerts, S., Bonato, L., Donaire-Barroso, D., Martínez-Solano, I., Velo-Antón, G., Vieites, D.R., Mable, B.K. and Elmer, K.R., 2021. Phylogenomic inference of species and subspecies diversity in the Palearctic salamander genus *Salamandra*. Mol. Phylogenet. Evol. 157, 107063.
Colhoun, E.A., Hannan, D. and Kiernan, K., 1996. Late Wisconsin glaciation of Tasmania. Pap. Proc. R. Soc. Tasmania 130, 33–45.
Colhoun, E.A., Kiernan, K., Barrows, T.T. and Goede, A., 2010. Advances in Quaternary studies in Tasmania. Geol. Soc. Lond. Spec. Publ. 346, 165–183.
Corbett, K.D., 2019. Child of Gondwana: The Geological Making of Tasmania. Forty South Publishing Pty Limited, Hobart.
Coyne, J.A. and Orr, H.A., 2004. Speciation. Sinauer Associates, ENG, Sunderland, MA.
Crisp, M.D. and Chandler, G.T., 1996. Paraphyletic species. Telopea 6, 813–844.
Darriba, D., Posada, D., Kozlov, A.M., Stamatakis, A., Morel, B. and Flouri, T., 2020. ModelTest-NG: a new and scalable tool for the selection of DNA and protein evolutionary models. Mol. Biol. Evol. 37, 291–294.
De Queiroz, K., 1998. The general lineage concept of species, species criteria, and the process of speciation. In: Howard, D.J. and Berlocher, S.H. (Eds.), Endless Forms: Species and Speciation. Oxford University Press, Oxford.
De Queiroz, K., 2007. Species concepts and species delimitation. Syst. Biol. 56, 879–886.
Delaney, K.S., 2014. Landscape Genetics of Urban Bird Populations. Avian Urban Ecology. Oxford University Press, Oxford, pp. 143–154.
Dufresnes, C., Ambu, J., Galán, P., Sequeira, F., Viesca, L., Choda, M., Álvarez, D., Alard, B., Suchan, T., Künzel, S., Martínez-Solano, I., Vences, M. and Nicieza, A., 2024. Delimiting phylogeographic diversity in the genomic era: application to an Iberian endemic frog. Zool. J. Linnean Soc. 202, zlad170.
Fitak, R.R., 2021. OptM: estimating the optimal number of migration edges on population trees using Treemix. Biol. Methods Protoc. 6, bpab017.
Fitzhugh, K., 2009. Species as explanatory hypotheses: refinements and implications. Acta Biotheor. 57, 201–248.
Folmer, O., Black, M., Hoeh, W., Lutz, R. and Vrijenhoek, R., 1994. DNA primers for amplification of mitochondrial cytochrome c oxidase subunit I from diverse metazoan invertebrates. Mol. Mar. Biol. Biotechnol. 3, 294–299.
Franchini, P., Monné Parera, D., Kautt, A.F. and Meyer, A., 2017. quaddRAD: a new high-multiplexing and PCR duplicate removal ddRAD protocol produces novel evolutionary insights in a nonradiating cichlid lineage. Mol. Ecol. 26, 2783–2795.
Fujisawa, T., Sasabe, M., Nagata, N., Takami, Y. and Sota, T., 2019. Genetic basis of species-specific genitalia reveals role in species diversification. Sci. Adv. 5, eaav9939.
Gallagher, S.J., Greenwood, D.R., Taylor, D., Smith, A.J., Wallace, M.W. and Holdgate, G.R., 2003. The Pliocene climatic and environmental evolution of southeastern Australia: evidence from the marine and terrestrial realm. Palaeogeogr. Palaeoclimatol. Palaeoecol. 193, 349–382.
Gittenberger, E., 1991. What about non-adaptive radiation. Biol. J. Linn. Soc. 43, 263–272.
Goloboff, P.A. and Catalano, S.A., 2016. TNT version 1.5, including a full implementation of phylogenetic morphometrics. Cladistics 32, 221–238.
Hebert, P.D., Cywinska, A., Ball, S.L. and DeWaard, J.R., 2003. Biological identifications through DNA barcodes. Proc. R. Soc. Lond. B Biol. Sci. 270, 313–321.
Hennig, W., 1966. Phylogenetic Systematics. University of Illinois Press, Urbana, IL.
Höpel, C.G., Richter, S. and Ahyong, S.T., 2023a. A new species of Tasmanian mountain shrimp, *Anaspides driesseni* sp. nov. (Malacostraca, Anaspidacea, Anaspidesidae). Rec. Aust. Mus. 75, 25–43.
Höpel, C.G., Yeo, D., Ahyong, S.T., Meier, R. and Richter, S., 2023b. First mitochondrial genomes of Anaspidacea (Malacostraca, Crustacea) and the phylogenetic relationships of mountain shrimps (*Anaspides* Thomson, 1894) and their relatives within Anaspidesidae. J. Crustac. Biol. 43, ruad028.
Houshold, I. and Jackson, A., 2023. Tasmania. In: Australian Caves and Karst Systems. Springer International Publishing, Cham, pp. 43–73.
Huson, D.H. and Bryant, D., 2006. Application of phylogenetic networks in evolutionary studies. Mol. Biol. Evol. 23, 254–267.
Kiernan, K., 1990. The extent of late Cenozoic glaciation in the Central Highlands of Tasmania, Australia. Arct. Alp. Res. 22, 341–354.
Kiernan, K., Lauritzen, S.E. and Duhig, N., 2001. Glaciation and cave sediment aggradation around the margins of the Mt Field Plateau, Tasmania. Aust. J. Earth Sci. 48, 251–263.
Knowlton, N. and Weigt, L.A., 1998. New dates and new rates for divergence across the Isthmus of Panama. Proc. R. Soc. Lond. B Biol. Sci. 265, 2257–2263.
de Lattin, G., 1967. Grundriss der Zoogeographie, Vol. 12. Gustav Fischer Verlag, GER, Jena.
Li, Y.L. and Liu, J.X., 2018. StructureSelector: a web-based software to select and visualize the optimal number of clusters using multiple methods. Mol. Ecol. Resour. 18, 176–177.
Mackintosh, A.N., Barrows, T.T., Colhoun, E.A. and Fifield, L.K., 2006. Exposure dating and glacial reconstruction at Mt. Field, Tasmania, Australia, identifies MIS 3 and MIS 2 glacial advances and climatic variability. J. Quat. Sci. 21, 363–376.
Macphail, M.K., 1997. Late Neogene climates in Australia: fossil pollen-and spore-based estimates in retrospect and prospect. Aust. J. Bot. 45, 425–464.
Macphail, M.K., Colhoun, E.A., Kiernan, K. and Hannan, D., 1993. Glacial climates in the Antarctic region during the late Paleogene: evidence from northwest Tasmania, Australia. Geology 21, 145–148.
Malinsky, M., Trucchi, E., Lawson, D.J. and Falush, D., 2018. RADpainter and fineRADstructure: population inference from RADseq data. Mol. Biol. Evol. 35, 1284–1290.
Malinsky, M., Matschiner, M. and Svardal, H., 2021. Dsuite-Fast D-statistics and related admixture evidence from VCF files. Mol. Ecol. Resour. 21, 584–595.
Martin, S.H., Dasmahapatra, K.K., Nadeau, N.J., Salazar, C., Walters, J.R., Simpson, F., Blaxter, M., Manica, A., Mallet, J. and Jiggins, C.D., 2013. Genome-wide evidence for speciation with gene flow in *Heliconius* butterflies. Genome Res. 23, 1817–1828.
Mayr, E., 1942. Systematics and the Origin of Species. Columbia University Press, New York City.
Mayr, E., 1969. The biological meaning of species. Biol. J. Linn. Soc. 1, 311–320.
Meier, R. and Willmann, R., 2000. The Hennigian species concept. In: Wheeler, Q.D. and Meier, R. (Eds.), Species Concepts and Phylogenetic Theory: A Debate. Columbia University Press, New York, pp. 30–43.
Minh, B.Q., Schmidt, H.A., Chernomor, O., Schrempf, D., Woodhams, M.D., Von Haeseler, A. and Lanfear, R., 2020. IQ-TREE 2: new models and efficient methods for phylogenetic inference in the genomic era. Mol. Biol. Evol. 37, 1530–1534.

10960031, 0, Downloaded from https://onlinelibrary.wiley.com/doi/10.1111/cla.70005 by Christoph Höpel - University Rostock Universitätsbibliothek , Wiley Online Library on [30/07/2025]. See the Terms and Conditions (https://onlinelibrary.wiley.com/terms-and-conditions) on Wiley Online Library for rules of use; OA articles are governed by the applicable Creative Commons License

Morales, A.E., Jackson, N.D., Dewey, T.A., O'Meara, B.C. and Carstens, B.C., 2017. Speciation with gene flow in North American *Myotis* bats. Syst. Biol. 66, 440–452.
Morrison, P., O'Leary, M. and McDonald, J., 2023. The evolution of Australian Island geographies and the emergence and persistence of Indigenous maritime cultures. Quat. Sci. Rev. 308, 108071.
Nelson, G.J. and Platnick, N.I., 1981. Systematics and Biogeography: Cladistics and Vicariance. Columbia University Press, New York City.
Nixon, K.C. and Wheeler, Q.D., 1990. An amplification of the phylogenetic species concept. Cladistics 6, 211–223.
Nixon, K.C. and Wheeler, Q.D., 1992. Extinction and the origin of species. In: Novacek, M.J. and Wheeler, Q.D. (Eds.), Extinction and Phylogeny, Vol. 119. Columbia University Press, New York, p. 143.
Noor, M.A., 1999. Reinforcement and other consequences of sympatry. Heredity 83, 503–508.
Orr, H.A. and Turelli, M., 2001. The evolution of postzygotic isolation: accumulating Dobzhansky-Muller incompatibilities. Evolution 55, 1085–1094.
Peterson, B.K., Weber, J.N., Kay, E.H., Fisher, H.S. and Hoekstra, H.E., 2012. Double digest RADseq: an inexpensive method for de novo SNP discovery and genotyping in model and non-model species. PLoS One 7, e37135.
Pickrell, J. and Pritchard, J., 2012. Inference of population splits and mixtures from genome-wide allele frequency data. Nat. Prec., https://doi.org/10.1038/npre.2012.6956.1.
Pritchard, J.K., Stephens, M. and Donnelly, P., 2000. Inference of population structure using multilocus genotype data. Genetics 155, 945–959.
Puli, G., Santos, S., Zimmermann, B.L., Gonçalves, A.S. and Bartholomei-Santos, M.L., 2024. Impact of Pleistocene climate on diversification and distribution of congeneric freshwater crustacean species. J. Biogeogr. 52, 670–685.
Rambaut, A., 2014. Tree Figure Drawing Tool Version 1.4. Institute of Evolutionary Biology, University of Edinburgh, Edinburgh.
Rambaut, A., Drummond, A.J., Xie, D., Baele, G. and Suchard, M.A., 2018. Posterior summarization in Bayesian phylogenetics using Tracer 1.7. Syst. Biol. 67, 901–904.
Richter, S., Schwentner, M., Wirkner, C.S. and Ahyong, S.T., 2018. Phylogeny and species diversity of Tasmanian mountain shrimps and their relatives (Crustacea, Anaspidesidae). Zool. Scr. 47, 84–105.
Rieseberg, L.H., Archer, M.A. and Wayne, R.K., 1999. Transgressive segregation, adaptation and speciation. Heredity 83, 363–372.
Rochette, N.C., Rivera-Colón, A.G. and Catchen, J.M., 2019. Stacks 2: analytical methods for paired-end sequencing improve RADseq-based population genomics. Mol. Ecol. 28, 4737–4754.
Roman, I., Bourgeois, Y., Reyes-Velasco, J., Jensen, O.P., Waldman, J. and Boissinot, S., 2018. Contrasted patterns of divergence and gene flow among five fish species in a Mongolian rift lake following glaciation. Biol. J. Linn. Soc. 125, 115–125.
Schubart, C.D., Diesel, R. and Hedges, S.B., 1998. Rapid evolution to terrestrial life in Jamaican crabs. Nature 393, 363–365.
Schwentner, M. and Lörz, A.N., 2021. Population genetics of cold-water coral associated Pleustidae (Crustacea, Amphipoda) reveals cryptic diversity and recent expansion off Iceland. Mar. Ecol. 42, e12625.
Secci-Petretto, G., Englmaier, G.K., Weiss, S.J., Antonov, A., Persat, H., Denys, G.P., Denys, G.P.J., Schenekar, T., Romanov, V.I., Taylor, E.B. and Froufe, E., 2023. Evaluating a species phylogeny using ddRAD SNPs: Cyto-nuclear discordance and introgression in the salmonid genus *Thymallus* (Salmonidae). Mol. Phylogenet. Evol. 178, 107654.
Thomson, G.M., 1893. Notes on Tasmanian Crustacea, with descriptions of new species. Pap. Proc. R. Soc. Tasmania 1, 45–76.
Torres, A., Goloboff, P.A. and Catalano, S.A., 2022. Parsimony analysis of phylogenomic datasets (I): scripts and guidelines for using TNT (Tree Analysis using New Technology). Cladistics 38, 103–125.
Vences, M., Multzsch, M., Gippner, S., Miralles, A., Crottini, A., Gehring, P.S., Rakotoarison, A., Ratsoavina, F.M., Glaw, F. and Scherz, M.D., 2022. Integrative revision of the *Lygodactylus madagascariensis* group reveals an unexpected diversity of little brown geckos in Madagascar's rainforest. Zootaxa 5179, 1–61.
Vences, M., Miralles, A. and Dufresnes, C., 2024. Next-generation species delimitation and taxonomy: Implications for biogeography. J. Biogeogr. 51, 1709–1722.
Warnke, D.A., Allen, C.P., Muller, D.W., Hodell, D.A. and Brunner, C.A., 1992. Miocene-Pliocene Antarctic glacial evolution: a synthesis of ice-rafted debris, stable isotope, and planktonic foraminiferal indicators, ODP Leg 114. In: The Antarctic Paleoenvironment: A Perspective on Global Change: Part One. American Geophysical Union, Washington, Vol. 56, pp. 311–326.
Williams, W.D., 1965. Ecological notes on Tasmanian Syncarida (Crustacea: Malacostraca) with a description of a new species of *Anaspides*. Int. Rev. Gesamten Hydrobiol. 50, 95–126.

Supporting Information

Additional supporting information may be found online in the Supporting Information section at the end of the article.

Fig. S1. Unrooted phylogenetic network of ddRAD data set 1 (261 individuals, 1945 polymorphic loci with 38 926 variable sites, TVM + G + I, 1000 iterations) calculated with SplitsTree4 v4.19.2 (Huson & Bryant, 2006) with the Neighbor-Net algorithm and uncorrected *p*-distances.

Fig. S2. DSuite analysis of data set 3 with *Anaspides richardsoni* population B set as outgroup.

Fig. S3. F_{ST} values using data set 2.

Fig. S4. d_{xy} values using data set 2, (I) with *Anaspides* sp. nov. 1 and (II) without *Anaspides* sp. nov. 1.

Table S1. List of individuals used for this study.

Table S2. F_{ST} values using data set 2.

Table S3. d_{xy} values using data set 2.

10960031, 0, Downloaded from https://onlinelibrary.wiley.com/doi/10.1111/cla.70005 by Christoph Höpel - University Rostock Universitätsbibliothek , Wiley Online Library on [30/07/2025]. See the Terms and Conditions (https://onlinelibrary.wiley.com/terms-and-conditions) on Wiley Online Library for rules of use; OA articles are governed by the applicable Creative Commons License

6 Höpel, C. G., Ahyong, S. T., Eberhard, S., Fordyce, S., Kapun, M., Schwentner, M., & Richter, S. Comparative phylogeography and speciation in correlation with cave colonization in Tasmanian mountain shrimps (*Anaspides*, Anaspidacea, Crustacea). Zoological Journal of the Linnean Society. (Under review)

Comparative phylogeography and speciation in correlation with cave colonization in Tasmanian mountain shrimps (*Anaspides*, Anaspidacea, Crustacea)

Christoph G. Höpel[1], Shane T. Ahyong[2,3], Stefan M. Eberhard[4,5], Stephen Fordyce[6], Martin Kapun[7], Martin Schwentner[7], Stefan Richter[1]

[1]Allgemeine & Spezielle Zoologie, Institut für Biowissenschaften, Universität Rostock, Universitätsplatz 2, 18055 Rostock, Germany
[2]Australian Museum Research Institute, Australian Museum, 1 William Street, Sydney NSW 2010, Australia and School of Biological, Earth & Environmental Sciences, University of New South Wales, Kensington, NSW 2052, Australia
[3]School of Biological, Earth & Environmental Sciences, University of New South Wales, Kensington, NSW 2052, Australia
[4]Honorary Associate, Western Australian Museum, Francis Street, Perth WA 6000, Australia
[5]Adjunct Affiliate, Connected Waters Initiative Research Centre, University of New South Wales, Sydney, NSW 2093, Australia
[6]Southern Tasmanian Caverneers, PO Box 416, Sandy Bay, Tasmania, 7006, Australia
[7]Naturhistorisches Museum Wien, Burgring 7, 1010 Wien, Austria

Abstract

The Tasmanian mountain shrimps (*Anaspides:* Malacostraca) are enigmatic freshwater crustaceans that entered the subterranean habitat multiple times independently during Pleistocene times. Some lineages are exclusively stygomorphic species, such as *A. eberhardi* (Ahyong, 2016), while others, such as *A. richardsoni* (Ahyong, 2016), have surface and cave forms. Two different models for speciation have been suggested for recent colonization events of caves, the Climatic Relict Hypothesis (CRH) and the Adaptive Shift Hypothesis (ASH). The major difference is the absence (CRH) or presence (ASH) of gene flow during divergence, corresponding to allopatric and parapatric speciation.

We herein present a phylogenetic analysis of the obligate cave dwelling species *A. eberhardi* and two closely related species using ddRAD and COI datasets. Despite the detected mito-nuclear discordance, the extensive ddRAD datasets clearly support the monophyly of each species. However, we detected one instance of localized introgression into *A. eberhardi* from a surface population of *A. richardsoni*, whereas syntopically occurring populations with an undescribed species showed no evidence of interbreeding. Our data supports a single origin of *A. eberhardi* during the Pleistocene followed by underground dispersal, and extinction of surface populations, all in correlation with glacial events. This clearly favours the CRH as the mode of speciation.

Introduction

The processes and underlying mechanisms that result in the colonization of extreme habitats, such as caves and groundwater, are among the most fascinating topics in evolutionary biology. Special adaptations are necessary for surviving in caves and other subterranean habitats. Permanent darkness and low food availability present major challenges for new colonizers. Studying cave biodiversity allows answering questions about the interaction of adaptation, phylogeography and evolution. Phylogeographic and phylogenetic frameworks provide the basis for discriminating between whether cave forms derive from a single entry followed by subterranean dispersal, or from multiple independent colonization events into different subterranean habitats. This further allows assessment of whether stygomorphic features have a single origin or have evolved by evolutionary parallelism (Juan et al., 2010).

For recent (i.e. Pleistocene) cave colonization events two different models for speciation have been suggested. For temperate zones, the Climatic Relict Hypothesis (CRH) suggests that under certain climatically induced environmental changes (e.g. glaciation, deforestation, aridification) caves became passively colonized and served as refugia (Peck & Finston, 1993; Holsinger, 2000; Rivera et al., 2002). Initially, two-way migration occurs with sufficient frequency to prevent genetic divergence between the surface and cave populations. As the first neutral or regressive mutations (e.g. loss of pigmentation and vision) appear in the cave population, these mutations may or may not involve adaptive shifts in relation to reproductive isolation from the surface population. Important for this hypothesis is that the surface population becomes locally extinct owing to climatic or environmental changes (but may survive in other regions) and only the cave population survives. This corresponds to the classical allopatric speciation model. Conversely, the “adaptive shift hypothesis” (ASH), first proposed by Howarth (1980) to explain the non-relictual parapatric distribution patterns of troglobites in climatically stable tropical zones, differs from the CRH model by active colonization of caves. In other words, speciation is herein initiated by different selective regimes in surface and cave habitats. Reproductive isolation appears as a by-product of differential ecological adaptation or an adaptive-shift (Howarth, 1980; Peck & Finston, 1993; Desutter-Grandcolas & Grandcolas, 1996). Because adaptation might also play a role in the CRH, the key distinction is not adaptation but absence (CRH) or presence (ASH) of gene flow during divergence (Niemiller et al., 2008), which defines the models of allopatric and parapatric speciation (Baker, 2005; Wolf et al., 2010).

The “mountain shrimps” of the genus *Anaspides* (Anaspidesiidae Ahyong & Alonso-Zarazaga, 2017), endemic to Tasmania, are an ideal model system for studying cave adaptation and speciation because colonization of caves occurred several times independently at different karst localities on the island, with partly uncertain species status of some cave populations (Richter et al., 2018). They are not true shrimps (Decapoda) but belong to a different malacostracan order (i.e. Anaspidacea) with a relictual Gondwanan distribution and represent one of the most iconic freshwater invertebrates of Tasmania. Their current distribution is stenothermally restricted to cool freshwater habitats above 300m elevation, and caves and has been strongly influenced by the Pleistocene glaciations, as many of their alpine habitats,

such as mountain tarns and pools, creeks and runnels, have a glacial origin or were influenced by cold-climate geomorphic and hydrological processes. It has been previously hypothesized that *Anaspides* entered caves during the Pleistocene through opening of cave habitat through glaciation and meltwater (Richter et al., 2018), although most caves themselves were formed during late Mesozoic and early Cenozoic (Kiernan, 1996; Coulhoun et al., 2010).

The Junee–Florentine karst valleys and the abutting Mount Field plateau in Tasmania are an excellent study area for testing those speciation models and highly important in terms of conservation (Kiernan, 2018). The Mt Field National Park is located in central Tasmania (Fig. 1) and is Tasmania's oldest national park (since 1916), with peaks rising up to over 1,400 metres. During different periods of the Pleistocene, glaciers covered the mountain plateaus (Kiernan et al., 2001, Mackintosh et al., 2006, Kiernan, 2018). The adjacent Junee–Florentine karst area has developed in Ordovician Gordon Group limestone in the deeply dissected Florentine and Tyenna valleys (the Junee-Florentine area), with limestone plains in the upper Gordon valley to the west (the Vale of Rasselas; Corbett, 1964). This extensive limestone area and potentially karstic terrain spans over 18 500 ha with over 600 caves (Eberhard, 1998). The available relief in the Junee-Florentine karst is over 400 m, predominantly on the east side of the Florentine and north side of the Tyenna valleys. Streams draining the impermeable non–karstic rocks of the Mt Field plateau sink underground at or near the limestone contact, forming impressive dolines and stream sinks at cave entrances such as Growling Swallet, Cauldron Pot and Niagara Pot (Bunton & Eberhard, 1984).

As with many other Tasmanian karst systems, development of the Junee–Florentine karst was strongly influenced by ice and meltwater during Plio-Pleistocene glacial stages (Kiernan et al., 2001). Large inputs of glacio-fluvial, periglacial and alluvial sediments caused drainage modification through blockage of cave passages (Kiernan et al., 2001). As the distance from the ice margin increased, surface streams entrained increasing amounts of sediment, depositing it and choking many of the stream sinks and caves with outwash gravels, thus causing the streams to temporarily revert to a surface course (Goede, 1973; Goede & Harmon, 1983). Following deglaciation and landscape stabilisation, the fine-grained portions of the sediments blocking the caves have been gradually carried away by ongoing stream action and many stream sinks have been reactivated. These major changes in hydrology and sediment regimes, across glacial-interglacial cycles, may have significantly influenced the habitat conditions and habitat suitability for *Anaspides* populations in both surface and underground habitats. It is postulated that the plugging of stream sinks and caves with proglacial sediments may have rendered some parts of the underground drainage network temporarily uninhabitable during periods when the streams were diverted to a surface course.

Surface water bodies on the Mt. Field plateaus are inhabited by *Anaspides richardsoni* Ahyong 2016, while down-slope in the caves of the Junee–Florentine karst *A. eberhardi* Ahyong 2016, is present, the sister species to the *A. richardsoni* populations on the plateau. While *A. eberhardi* is only found in caves of this karst area, *A. richardsoni* has a wide distribution in central and northern Tasmania. *Anaspides richardsoni* represents a paraphyletic species, with *A. eberhardi* and three other species nested within *A. richardsoni* (see Höpel et al. 2025). In addition, *A. tasmaniae* (Thomson, 1893) and *A. swaini* Ahyong, 2015, as well as two

undescribed species (*Anaspides* sp. nov. 1 and 2) are present in the Mt Field/ Junee–Florentine area (Höpel et al., 2021, Höpel et al., 2025).

The present study analyses the relationships between the populations of *A. eberhardi, A. richardsoni* (Mt Field) and *Anaspides* sp. nov. 2 using molecular markers (ddRAD, COI) to understand the timing and mode of cave colonization. The speciation processes associated with it, as well as subterranean population structure and dispersal routes in relation to geomorphology and glaciation events are in the centre of the current study.

Materials & Methods

For the distribution of species, we focus only on those populations for which we have molecular data, mostly collected during our field trips in 2017, 2019, 2022, 2023 and 2024 (see Fig. 1) from 58 different localities. Some of the data are already published (Höpel et al., 2021, 2025). We used 69 COI sequences and 79 ddRAD sequenced specimens from Höpel et al. (2025). We newly sequenced 223 specimens for COI and 176 for ddRAD. We obtained adults and juveniles of both sexes from most of the sampling sites. We also re-sampled specific sites over several years, e.g. Robert Tarn, Wombat Moor or Junee Cave, allowing a better representation of the population. Identification of the species (including potentially new species) is based on the diagnoses in Ahyong (2016). Herein, we will focus only on three species (lineages) – *A. richardsoni* (Mt Field), *A. eberhardi* and *Anaspides* sp. nov. 2 – occurring in proximity in the Mt Field National Park and the adjacent Junee–Florentine karst.

The DNA extraction was performed using the DNeasy Blood and Tissue Kit (Qiagen, Hilden, Germany), following the manufacturer´s instructions. The mitochondrial marker COI was partially sequenced. The polymerase chain reaction (PCR) had a total volume of 30 mL containing 3 mL of each primer (each 10 mM), 3 mL 10× buffer (Sigma Aldrich), 3 mL dNTP mix (2 mM, Biozym), 2.58 mL $MgCl_2$ (25 mM, Sigma Aldrich), 0.12 mL Taq-polymerase (Sigma Aldrich), 10.71 mL ultrapure water and 4.5 mL of the DNA extract. Primers were LCO2 (50-TCN ACH AAY CAT AAA GAY ATT GGA AC-30) (Richter et al., 2018) and HCO2198 (50-TAA ACT TCA GGG TGA CCA AAA AAT CA-30) (Folmer et al., 1994). PCR amplification programs comprised an initial denaturation step at 94°C for 1 min, followed by 38 amplification cycles (94°C for 30 s, 50°C for 30 s, 72°C for 60 s) and a final elongation step at 72°C for 5 min. All PCR reactions were performed with a Mastercycler gradient (Eppendorf). PCR products were visualised by gel electrophoresis, using 5 mL of the PCR product with 1.5 mL loading buffer DNA b II (AppliChem) on a 1.2% agarose/TAE gel stained with 5 mL Rotisafe (Carl Roth). PCR products were purified using paramagnetic beads (High Prep PCR, Magbio) following the manufacturer's instruction with a final volume of 25 mL. Sequencing of PCR products was performed in Lightrun96 well plates by the company Eurofins Genomics. The resulting chromatograms were manually checked and adjusted with

Geneious 2019.1.3 (Biomatters Limited). All sequences were deposited in GenBank (Benson et al., 2003) (COI: PV937831–PV938053; ddRAD: BioProject ID: PRJNA1291715). The sequences were aligned using GeneiousAlign implemented in Geneious Prime 2019.1.3 (Biomatters Limited). Phylogenetic networks were calculated with Network 5.0.1.1 (Fluxus Technologies) by using the median–joining method with the parameter epsilon set to 10.

Molecular clock analyses were performed in BEAST 2.4.6 (Bouckaert et al., 2014). The input files for BEAST were created with Beauti as part of the BEAST package, with each haplotype included only once. Mutation rates for each gene were based on averages of reported divergence rates for Crustacea: 1.4 % per million years (Knowlton & Weigt, 1998), 1.66 % per million years (Schubart et al., 1998) and 2.33 % per million years (Schubart et al., 1998) for COI (substitution rate 0.9 % per million years). In addition to setting the mean rates, the original rates were set as maximum or minimum rate constraints, respectively. A strict clock with a Yule tree prior and default parameters was employed with the GTR + I + G nucleotide substitution model. The first 20 % of trees were discarded as burn-in and the posterior probability limit was set to 0.5 in TreeAnnotator 2.4.6 (Bouckaert et al., 2014).

ddRAD

For ddRAD analyses we largely followed Schwentner & Lörz (2021). We added four random nucleotides in one adapter to allow the downstream detection and removal of PCR duplicates (similar to Franchini et al., 2017). The DNA concentration of each DNA extract was quantified on a Qubit 3.0 (Invitrogen). From each DNA extract, 150–250 ng DNA was brought to 24 µl with H_2O. Samples were always processed in batches of eight, which were pooled prior to PCR amplification (each of these eight share the index added by PCR, but received individual barcodes during adapter ligation) and which always had the same DNA concentration. 1.5 µl fastdigest MspI, 1.5 µl fastdigest EcoRI (20000U/ml) and 3 µl 10× buffer (all Thermo Fisher) were added to each DNA sample and incubated for at least 4 hr at 37°C. Digested DNA was cleaned with 45 µl magnetic beads (AmpliClean Cleanup Kit, Nimagen) following the manufacturer's recommendations and eluted with 21 µl H_2O, of which 19 µl were transferred for adapter ligation. All adapters were diluted in annealing buffer (10× annealing buffer comprises 500 mM NaCl, 100 mM Tris-Cl, 10 mM EDTA) to 2 µM (EcoRI adapters) or 31.6 µl (MspI adapters), respectively (following Peterson et al., 2012). 16 EcoRI and 8 MspI adapter variations with unique barcodes (MspI adapters with additionally four random nucleotides following the barcode; Franchini et al., 2017) were used to tag each library with a unique adapter combination within each batch of eight samples. Barcode sequences were derived from Peterson et al. (2012). Ligation reactions comprised 19 µl digested DNA, 3 µl EcoRI adapter, 3 µl MspI adapter, 2 µl T4 Ligase (2 Weiss units; Thermo Fisher Scientific, Germany), and 3 µl 10× T4 ligase buffer and was incubated at 22°C for 1 hr and then heat killed at 65°C for 10 min. Subsequently, the eight samples of each batch were pooled and each pool cleaned with 360 µl magnetic beads, eluting in 32 µl TE buffer. Size selection was carried out on a BluePippin (1.5% dye free cassettes with marker L; Biozym) for each pool independently, selecting the 'tight' option with a mean size of 300 bp (range 261–339 bp). To reduce amplification biases during PCR, four PCR replicates were run for each pool. Each PCR comprised 0.3 µl (10 nM) of each primer, 5 µl 2× Kappa HIFI HotStart ReadyMix (Roche) and 4.4 µl of a pool after size selection. A 2-step PCR program of 95°C initial denaturation and 12–15 cycles of 98°C for 20 s and 72°C for 25 s plus a final elongation step of 1 min at 72°C was run. Forward and reverse primers were available with eight different 8 bp indices each and combined to add a unique index combination for each pool. After PCR, the four PCR replicates

of each pool were mixed and cleaned with 40 µl magnetic beads (eluting in 20 µl H_2O). Concentrations of all cleaned pools were measured with Qubit 3.0, and correct fragment size length (~350 bp) was assessed on a Tapestation (D1000 ScreenTape; Agilent). All libraries were mixed at equal molarity into a final pool of 20 nM in 60 µl. Paired-end sequencing with 100 bp each was carried out on one Illumina HiSeq4000 lane by Macrogen. Upon sequencing, Macrogen pre-demultiplexed the data into the respective pools (based on provided index combinations).

We did not include ddRAD data from *A. swaini* and *A. tasmaniae* because they are only distantly related to the "central clade" (Richter et al., 2018; Höpel et al., 2023b, Höpel et al., 2025). As our focus is on the species from Mt Field and the Junee–Florentine Karst area, which are the most basal branching lineages according to Höpel et. al. (2025), we used only *A. richardsoni* from Lightning Plains (population B in Höpel et al. 2025) as a representative for the remaining derived lineages. Höpel et al. (2025) showed that there is no evidence of introgression or gene flow into the herein studied species from the remaining lineages, respectively, species of the *A. richardsoni* species clade.

Using STACKS v2.59 (Rochette et al., 2019) and the clone_filter program we removed PCR duplicates. Subsequently the process_radtages program was used to demultiplex these pools into the individuals by their unique barcodes. The program denovo_map.pl was then used to create a catalog of loci (parameters: -m 3, -M 7, -n 7).

We created four different datasets to analyse the ddRAD data on different levels (table 1). The first three datasets comprise the three species of the Mt Field National Park and Junee–Florentine karst: *A. richardsoni* (Mt Field metapopulation), *A. eberhardi* and *Anaspides* sp. nov. 2; and are used to test for monophyly and the relationships between these three species, as well as to search for coancestry or interbreeding between them. Dataset (4) was used for a detailed population genetic analysis of *A. eberhardi*. Dataset 1 and 2 also include *Anaspides* sp. nov. 1, which was used as outgroup and is also found in the Mt Field National Park. Additionally, we included in dataset 1 *A. richardsoni,* specimens from Lightning Plains as a representative of the various derived lineages that were studied by Höpel et. al. (2025). We have greatly increased the number of specimens and sampling sites for *A. richardsoni* (Mt Field), *A. eberhardi* and *Anaspides* sp. nov. 2 compared to Höpel et al. (2025).

Table 1: ddRAD Datasets used in this study with number of specimens, loci, polymorphic loci, SNPs and included species.

dataset	specimens	loci	polymorphic loci	variable sites (SNPs)	species included
1	261	1815	1776	18163	*Anaspides* sp. nov. 1, *Anaspides* sp. nov. 2, *A. richardsoni* (Mt Field), *A. richardsoni* (Lightning Plains), *A. eberhardi*

2	254	1866	1823	17627	*Anaspides* sp. nov. 1, *Anaspides* sp. nov. 2, *A. richardsoni* (Mt Field), *A. eberhardi*
3	202	2165	2047	14850	*Anaspides* sp. nov. 2, *A. richardsoni* (Mt Field), *A. eberhardi*
4	118	2443	1773	5202	*A. eberhardi*

Maximum-Likelihood (ML) and Maximum-Parsimony (MP) analyses were used to infer phylogenetic relationships between the species using dataset 1. We are using the .var.phy file generated by the populations program in STACKS. The maximum-likelihood tree was inferred with IQ–TREE 2 (Minh et al., 2020) with the GTR+G+I model and 1,000 bootstrap pseudoreplicates applied. The best fit model of evolution was determined by the implemented model test in RaxML GUI 2.0.8 (Darriba et al., 2020). The console version of TNT v1.6, June 2021 (Goloboff & Catalano, 2016) was used to conduct the Maximum-Parsimony analysis with New Technology Search (Torres et al., 2021). The script PhylogenomicSearch.run (Torres et al., 2021) was applied with the following arguments specified: search, nt; level, 10; hits, 5; output, newick. Resulting trees were visualized with Fig.Tree v.1.4.2 (Rambaut, 2014) and Corel Draw 2020. The script PhylogenomicSupport.run was run to obtain the support values using the following arguments: reftree, StrictConsensus_tnt.tre; format, tnt; sites, boot; replic, 1000; search, nt; level, 5; output, newick.

We used dataset 3 and 4 for population structure inference, proportion of admixture and coancestry, applying a principal component (PCA), fineRADstructure (Malinsky et al., 2018) and STRUCTURE analyses. For PCA and STRUCTURE analyses we were following the ipyrad workflow using STRUCTURE 2.3.4 (Pritchard et al., 2000). These STRUCTURE and PCA analyses are using multilocus genotype data to determine population structure and to identify hybrid zones, migrants and levels of admixture (Pritchard et al., 2000). Both analyses are only using one randomly chosen SNP per locus to minimize the effect of linkage between neighboring SNPs, which may bias the analyses. For the STRUCTURE analyses, we tested k-values, i.e., the putative number of ancestral groups, from 1–20 and conducted 20 replicate runs for each k-value. Based on these calculations, we used the StructureSelector website to select the optimal number of clusters (Li & Liu, 2018). The high resolution fineRADstructure, which uses haplotype linkage information and constructs coancestry matrices was run with default parameters (Malinsky et al., 2018). Subsequent results were plotted with the fineRADstructure GUI. To further quantify genetic differentiation among the sampling sites we calculated the F_{ST} and d_{xy} values using the program populations in STACKS v2.59. To further analyse potential introgression events and their direction as well as gene flow within species, we used the programs DSuite (Malinsky, 2021) as well as TreeMix (Pickrell, 2012) to analyse dataset 2. To calculate the D-statistics/ABBA-BABA tests with DSuite we used the Dtrios method for all possible population trios with *Anaspides* sp. nov. 1 (dataset 2) set as outgroups.

The TreeMix analysis was run for m-values, i.e., the number of independent migration events, ranging from 1–10 with 10 replicate runs per m-value. To calculate the optimal number of migration events we used the OptM package (Fitak, 2021) in R.
All resulting trees, plots, statistics and Figures were post–processed with Corel Draw 2020. The complete and well-documented bioinformatic analysis pipeline including custom scripts and the commands for third-party programs can be found at Github (https://github.com/ch515/Mt_field_Comparative_phylogeography_and_speciation_Anaspides).

Results

Distribution of *Anaspides* in the Mt Field National Park & the Junee–Florentine area

We *a priori* distinguish six species, using the diagnostic morphological characters described by Ahyong (2016) and Höpel et al. (2023a, 2025), of which four are known to science and two potentially new species. The latter are herein referred to as *Anaspides* sp. nov. 1 and *Anaspides* sp. nov. 2 (following Höpel et al., 2025). The four described species are *A. eberhardi*, *A. richardsoni*, *A. swaini* and *A. tasmaniae* (Fig. 1).

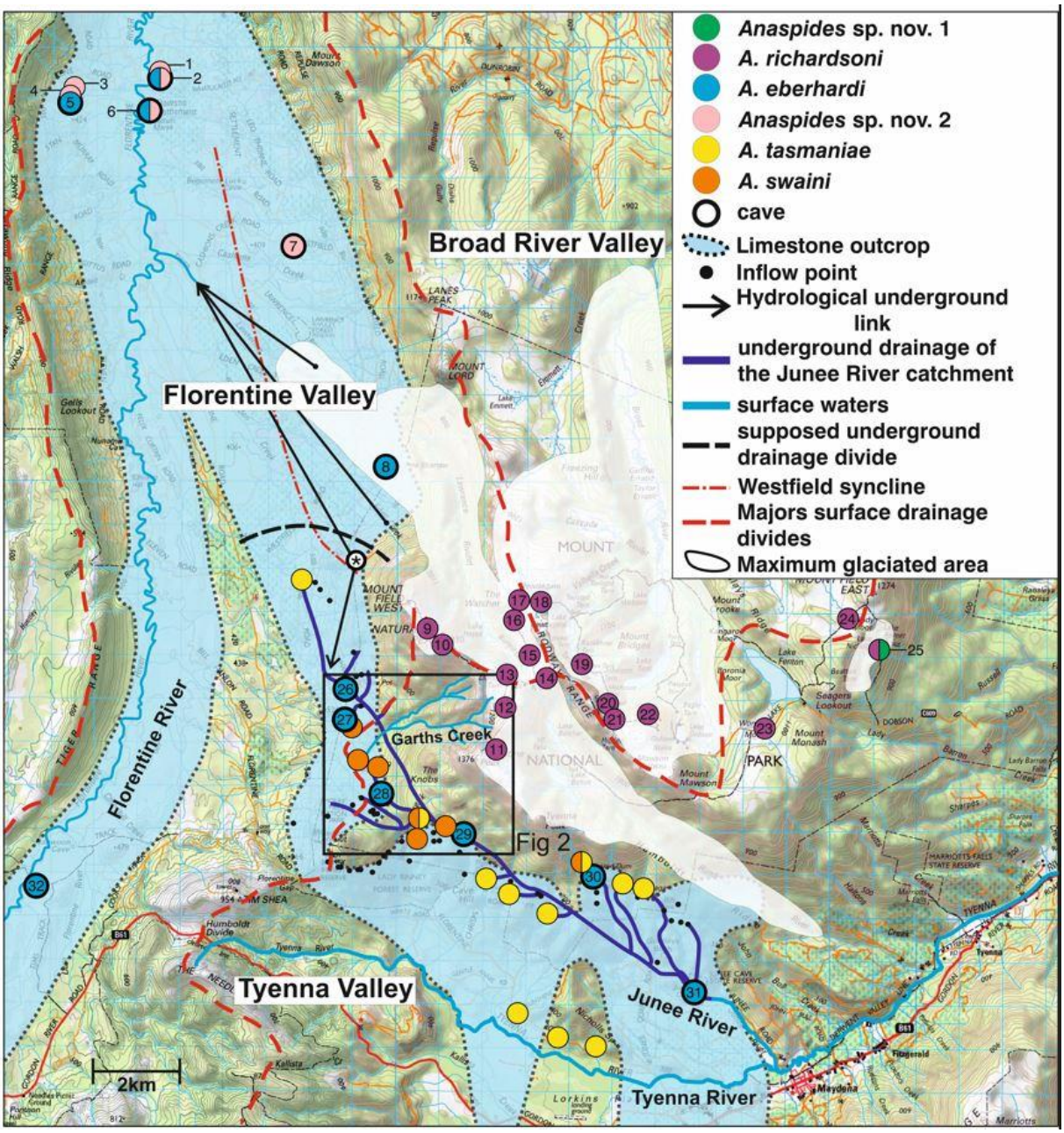


Fig. 1: Topographical map of the Mt Field National Park, and the adjacent Junee–Florentine karst and Florentine Valley with collection sites of *Anaspides*. Numbers correspond to the sampling sites of *A. richardsoni* (purple), *A. eberhardi* (blue), *Anaspides* sp. nov. 1 (green) and 2 (light pink). 1. Nameless Spring, outflow 2. Nameless Spring, 3. cave JF-576, 4. outflow cave JF-104, 5. cave JF-104, 6. Settlement Cave, 7. Cashions Creek Cave, 8. Welcome Stranger Cave, 9. pool on plateau Mt. Field West, 10. creek near Naturalist Peak, 11. Florentine Peak, 12. tarn on the west side of the ridge between Clemes Tarn and Florentine Peak, 13. small tarn near Clemes Tarn, 14. K-Col, 15. pool between K-Col and Newdegate Pass, 16. creek near Newdegate Pass, 17. Newdegate Pass II, east 18. Newdegate Pass I, west 19. James Tarn, 20. Robert Tarn, 21. small pool near Robert Tarn, 22. small tarn near ski huts, 23. Wombat Moor, 24. Windy Moor 25. Lake Nicholls 26. Porcupine Pot, 27. Gormenghast Cave, 28. Growling Swallet, 29. Niggly Cave, 30. Khazad Dum, 31. Junee Cave, 32. Toolshed cave. Orange circles indicate cave inflows which are inhabited by *A. swaini*, while yellow circles indicate cave inflows which are inhabited by *A. tasmaniae* except for three creeks which are creeks below the limestone outcrop. Shared circles indicate syntopy. Black box indicates zoomed in area of Fig. 2. Cryptic Cowry cave (JF-655) is indicated with an asterisk. The limestone outcrop was marked after Kiernan 1992, Eberhard 1998. The maximum glaciated area was marked after Kiernan et al. 2001.

The stygomorphic *Anaspides eberhardi* inhabits the caves of the Junee-Florentine karst and was collected in two different water catchments, the Florentine River catchment and the Junee River catchment (Fig. 1). In the Florentine River catchment *A. eberhardi* was collected from JF-104, Nameless Spring, Settlement Cave and Welcome Stranger Cave in the lower (northern) part of the river catchment, and Toolshed Cave in the upper (southern) part of the catchment. In the Junee River catchment this species was collected at multiple sites in Porcupine Cave, Gormenghast Cave, Growling Swallet, Niggly Cave, Khazad Dum and Junee Cave (Fig. 2). Within these cave systems, *Anaspides eberhardi* appears to be restricted to the deeper base level conduits and tributaries and has so far not been detected in the higher-level cave passages close to the surface inflow points. In Settlement Cave and Nameless Spring, *A. eberhardi* is syntopic with *Anaspides* sp. nov. 2 the latter was also collected in Cashions Creek Cave and one surface locality, the outflow creek of cave JF-104. However, *Anaspides* sp. nov. 2 was only found near the outflow (up to 50 m) and not further downstream in the same creek. The cave-dwelling specimens of *Anaspides* sp. nov. 2 showed slight stygomorphic features, mainly the loss of body pigmentation, whereas the specimens collected in the surface outflow creek of cave JF-104 were normally pigmented. *Anaspides richardsoni* is found in alpine tarns, pools and runnels on the mountain ranges of Mt Field National Park including Lake Nicholls, Windy Moor, Wombat Moor, Robert Tarn, Tarn Shelf, K-Col, Newdegate Pass to Mt Field West and Florentine Peak (Fig. 1). *Anaspides* sp. nov. 1 is currently known only from Lake Nicholls, where it is syntopic with *A. richardsoni*. The distantly related *Anaspides swaini* and *Anaspides tasmaniae* were collected mainly in the inflows of the Junee-Florentine caves (Fig. 1). In contrast, *A. richardsoni* and *A. eberhardi* were not detected near the inflow point or surface outflow of any caves. We define inflows here as the point at which surface water sinks into a cave, and including then stream reach extending for a distance of ~100 m upstream (surface stream reach) and ~100 m downstream (cave stream reach) of the inflow point. *Anaspides tasmaniae* was found in the inflow reach of Rainbow Cave, Trapdoor Swallet, Bunyips Lair, Rescue Pot, Ring Hole, Satans Lair, Niggly Cave and Khazad Dum, where in the latter, it is sympatric with *A. swaini*. Additionally, *A. tasmaniae* was found at three lowland sites in creeks crossing the Florentine Road (Höpel et al., 2021), which do not represent cave inflows. *Anaspides swaini* is found in the inflow of Gormenghast Cave, Growling Swallet (i.e. Garths Creek), Boulder Jenga, Niggly Cave/Delta Variant (same inflow waters), North Crisps Swallet, Cauldron Pot and Niagara Pot (Supplement table 1). In Gormenghast cave, *A. swaini* was collected close to base level at 112 m depth below the surface inflow point, where it was collected with *A. eberhardi*. *Anaspides swaini* was not detected further downstream in Gormenghast, albeit, the cave specimens exhibited body depigmentation, as did *A. tasmaniae* sampled in Niggly Cave.

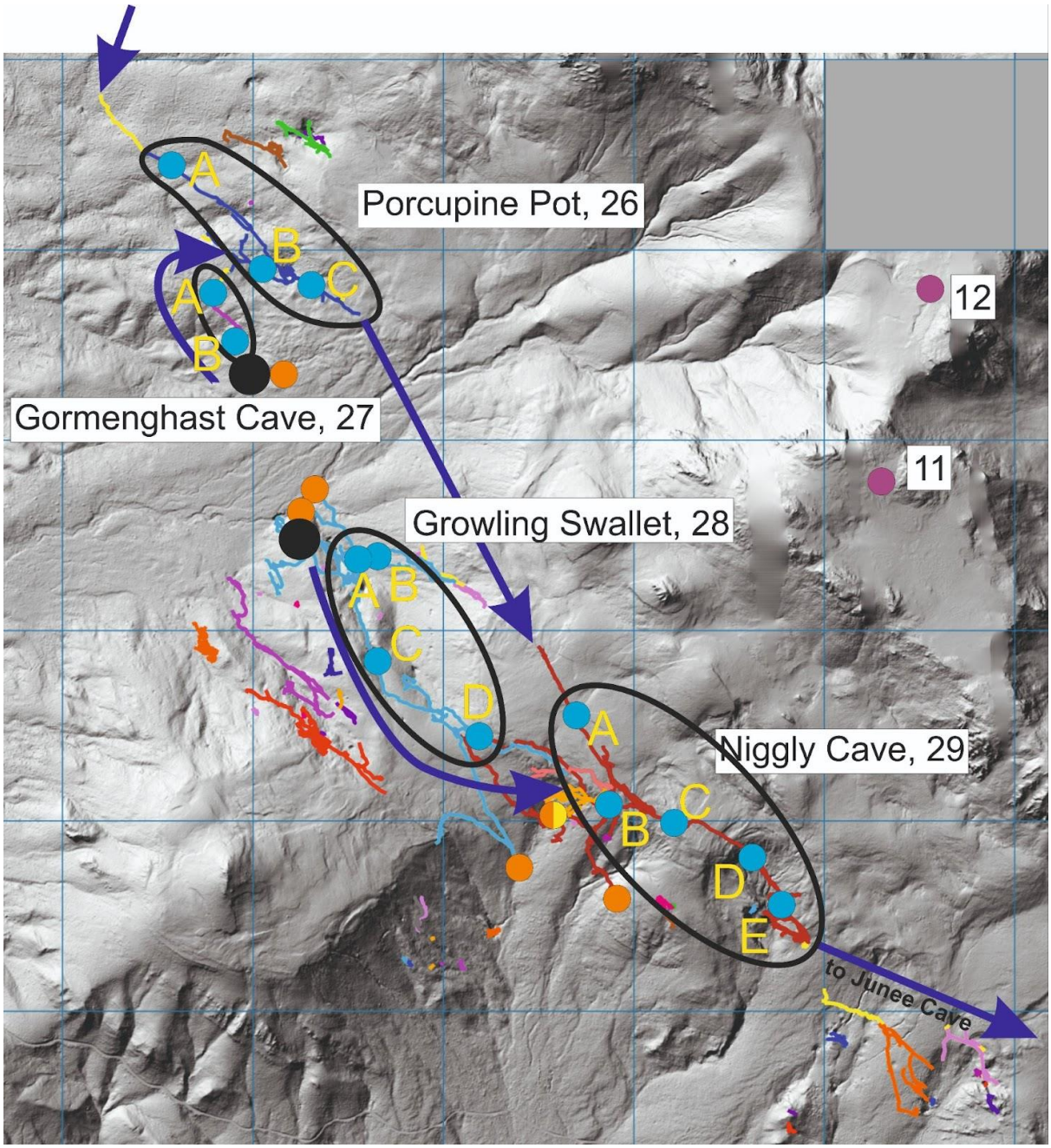


Fig. 2: Mapped cave passages (underground) of the upper Junee-River catchment, with the four major caves Porcupine Pot (26) in dark blue, Gormenghast Cave (27) in purple, Growling Swallet (28) in light blue and Niggly Cave (29) in dark red. Colours correspond to different caves. Light blue dots with yellow letters correspond to the specific sampling site within each of these four caves. Big blue arrows indicate the direction of water flow. Black dots correspond to the major inflows into Gormenghast Cave and Growling Swallet (different surface waters entering these two caves). Purple dots mark surface sampling sites of *A. richardsoni* and numbers correspond to the numbers in Fig. 1. Orange dots mark surface sampling sites of *A. swaini* and yellow dots of *A. tasmaniae.* Shared circles indicate syntopy.

ddRAD data

Both phylogenetic analysis approaches (MP and ML) recovered *Anaspides* sp. nov. 1, *Anaspides* sp. nov. 2, *A. eberhardi*, *A. richardsoni* from the Mt Field plateau area (Fig. 1, location 25 – 9) and *A. richardsoni* from Lightning Plains as monophyletic groups (dataset 1)

with high support values (all 100) (Fig. 3A, B), which is also supported by the principal component analysis (PCA) (Supplement Fig. 1). In these analyses (and some of the following population genetic analyses) we used *Anaspides* sp. nov. 1 as outgroup. Höpel et al. (2025) recovered it as the sister group of the *A. richardsoni* species complex within the "central clade". *Anaspides richardsoni* from Lightning Plains was used as a representative of the various *A. richardsoni* lineages uncovered in Höpel et al. (2025), which will not be discussed in detail here. *Anaspides richardsoni* from Mt Field and *A. eberhardi* are sister lineages. Both phylogenetic analyses reveal a strong correlation between locality and lineages, with some exceptions in *A. eberhardi* and to a minor degree in *Anaspides* sp. nov. *2*.

Within *A. eberhardi* both analyses uncovered mostly the same relationships. The lineage comprising the specimens from Toolshed Cave (the most geographically separated popuation located in the upper Florentine River, 32) is always sister group to the remaining lineages. One of these lineages comprises specimens collected in the lower Florentine Valley from four different caves, namely Welcome Stranger Cave (8), Settlement Cave (6), Nameless Spring (2) and cave JF-104 (5). The other lineage, which is sister group to the lower Florentine lineage comprises the specimens from the Junee River catchment, including the caves Porcupine Pot (26), Gormenghast Cave (27), Growling Swallet (28), Niggly Cave (29), Khazad Dum (30) and Junee Cave (31). Within the lower Florentine Valley lineage, the specimens from Welcome Stranger Cave are the sister group to the remaining specimens. Furthermore, specimens from JF-104 form a discrete lineage that is nested within a paraphyletic grouping of specimens from Settlement (6) and Nameless Spring (2), but specimens from the latter two caves do not clusters according to locality. From the Junee River catchment, only specimens from Khazad Dum were recovered as a distinct clade, whereas we could not detect any discrete grouping regarding the sampling locality for the other five caves.

In the fineRADstructure analysis (dataset 3), the three species show higher coancestry between specimens of each species than between species (Fig. 4A). Each sampling site formed its own distinct cluster with higher coancestry between specimens of the same sampling site than between specimens of different localities (Fig. 4A, black boxes). However, there were a few exceptions, mostly in *A. eberhardi*, where specimens from Settlement Cave (6) and Nameless Spring (2) formed one cluster, as did specimens from Porcupine Pot, Gormenghast Cave, Growling Swallet and Niggly Cave. The latter cluster also shows a high degree of coancestry with Junee Cave. As in the fineRADstructure analyses, the STRUCTURE analyses uncovered three distinct clusters that correspond to the three species when using k=3. The best detected k value, however, was k=5, where *A. richardsoni* (Mt Field) and *A. eberhardi* were further subdivided into two clusters each. In *A. richardsoni* (Mt Field) one cluster comprises the specimens from the eastern part of Mt Field (23–25) and one comprising the specimens from the middle to western part of the Mt Field plateau (9–22). In *A. eberhardi* one cluster comprises the specimens from the Florentine River catchment (2, 5, 6, 8, 32) and the other, the specimens from the Junee River catchment (26–31). One interesting finding was some shared genetic signal between *A. richardsoni* (Mt Field) and *A. eberhardi*. In the fineRADstructure analyses 11 specimens from Porcupine Pot (Fig. 2, A), Growling Swallet (Fig.

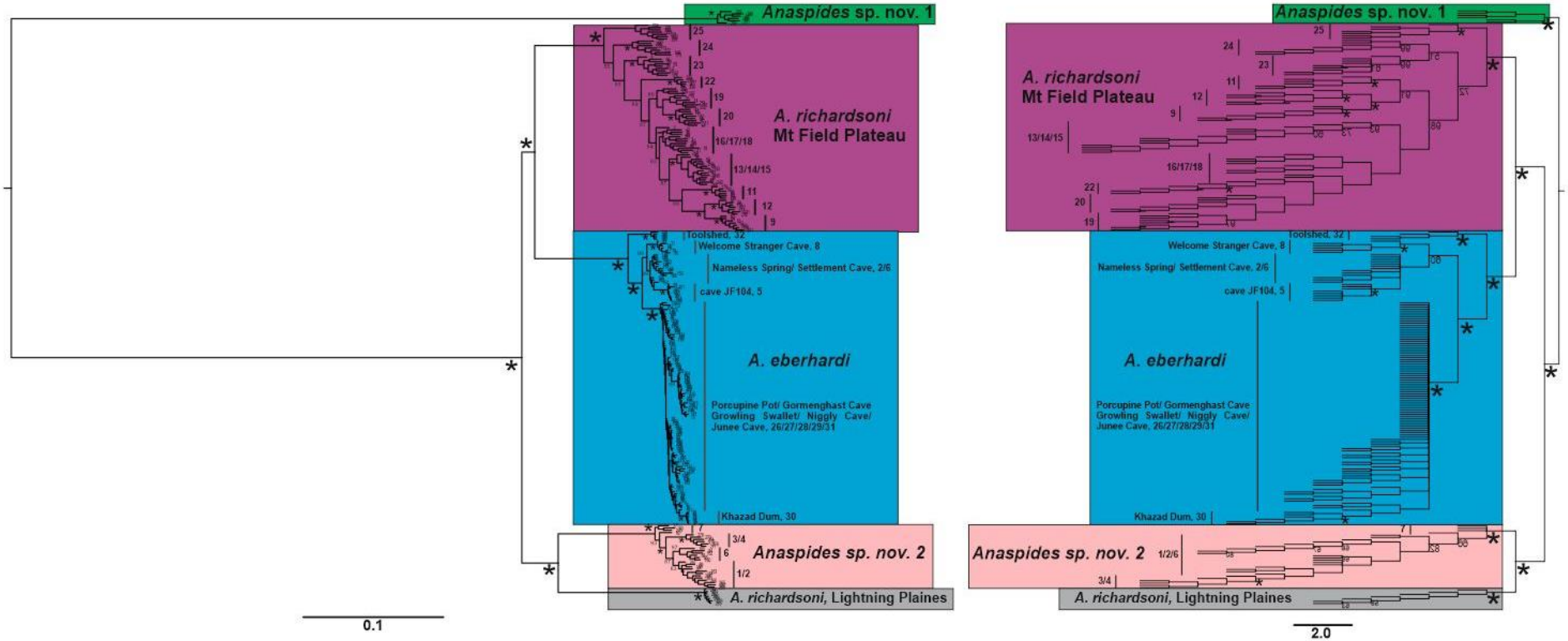


Fig. 3: (A) Maximum Likelihood phylogram (left) calculated with IQ–TREE 2.3.6 (GTR+G+I Model, 1000 Iterations) and (B) Maximum Parsimony phylogram (right) calculated with TNT v1.6. using the script PhylogenomicSupport.run (Torres et al. 2021) of ddRAD dataset 1 (261 specimens, 1815 loci, 1776 polymorphic Loci, 18163 SNPs). *Anaspides* sp. nov. 1 was set as outgroup following Höpel et al. (2025). *Anaspides richardsoni* from Lightning Plains was used as the representative for the more derived lineages of *A. richardsoni*. Bootstrap values >50 are shown for the respective major branches and clades. Asterisks indicate bootstrap value 100. Numbers after vertical bars correspond to the sampling locality in Fig. 1. Best score for MP analyses was 25517.

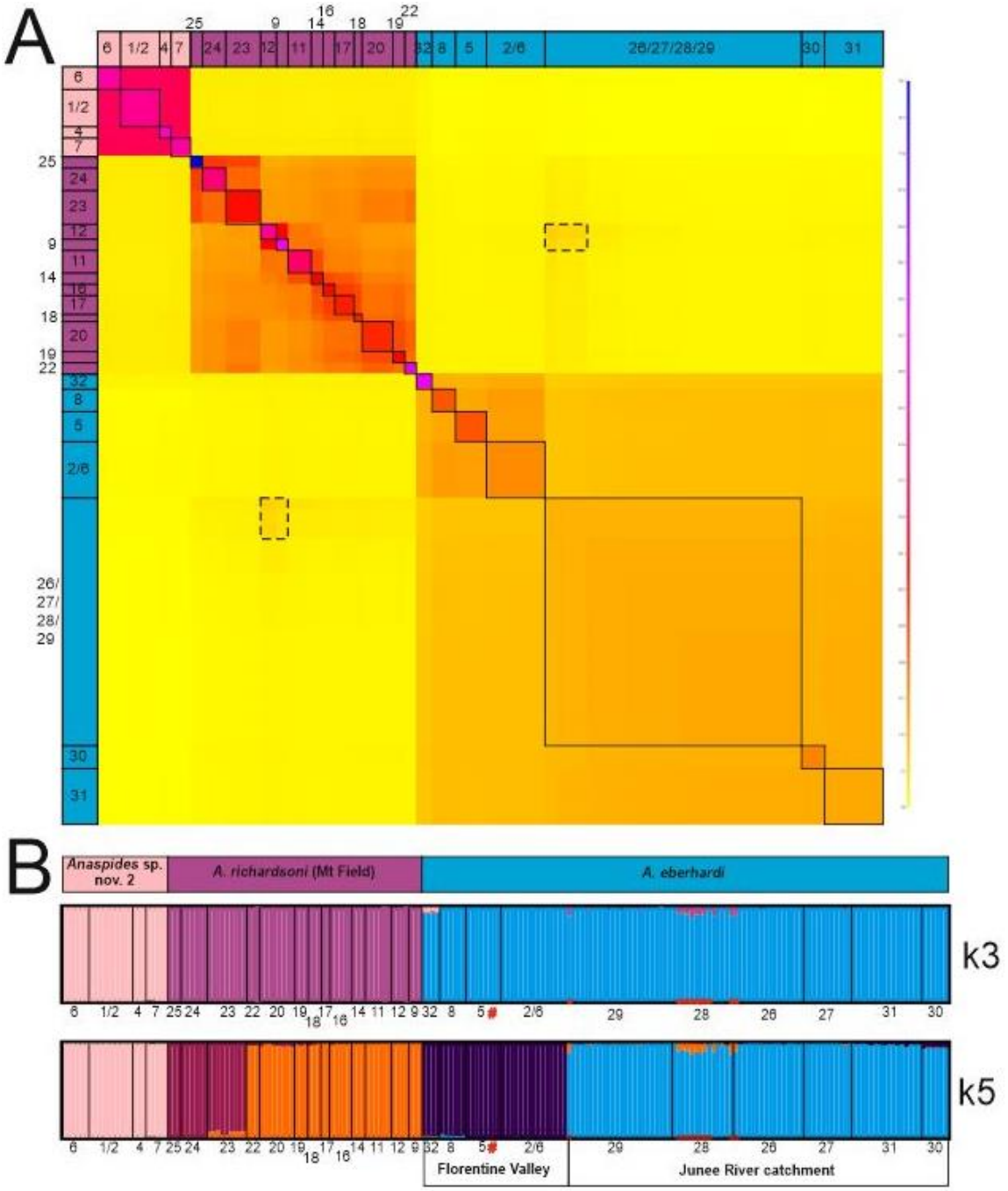


Fig. 4: Clustered fineRADstructure co–ancestry matrices (A) and Structure analyses (showing k=3 and5) based on nuclear ddRAD dataset 3 (202 specimens, 2165 Loci, 2047 polymorphic, 14850 SNPs) of *A. eberhardi* (blue), *A. richardsoni* from Mt Field (purple) and *Anaspides* sp. nov. 2 (light pink). Numbers correspond to the sampling locality in Figure 1. (A) Darker blue and purple colors in the matrix indicate higher proportion of loci with shared coancestry. Black lined boxes were manually added to highlight the clusters with higher coancestry, representing the potential populations. Black broken lined boxes were

2, A–C) and Niggly Cave (Fig. 2, B), show slightly higher coancestry with specimens of *A. richardsoni* from locations 12 and 9 (Fig. 4A, broken lined box). These same specimens of *A. eberhardi* share genetic signal with the mid–western cluster of *A. richardsoni* (sampling sites 9–22) in the STRUCTURE analyses (Fig. 4B, both k values, dataset 3). To test for potential

introgression and its direction, we treated these eleven specimens in the following DSuite and TreeMix analyses as a separate cluster. Although most of the signals of gene flow shown in DSuite (dataset 2) were between clusters of the same species, we also detected a slight signal of gene flow between *A. richardsoni* (Mt Field) and *A. eberhardi*. Here, the strongest signal suggests gene flow from *A. richardsoni* sampling site 12 into the *A. eberhardi* cluster comprising the above mentioned eleven specimens. We further used TreeMix (dataset 2) to estimate the direction and migration weight of gene flow, respectively introgression events. The best supported number of migration events by the OptM package was three. Two of these events were again between specimens of the same species, namely between *A. richardsoni* specimens. The third migration event was found again between *A. richardsoni* (Mt Field) and *A. eberhardi* suggesting introgression. We detected gene flow from *A. richardsoni* sampling site 12 into the cluster comprising the eleven specimens with higher coancestry in the fineRADstructure analyses.

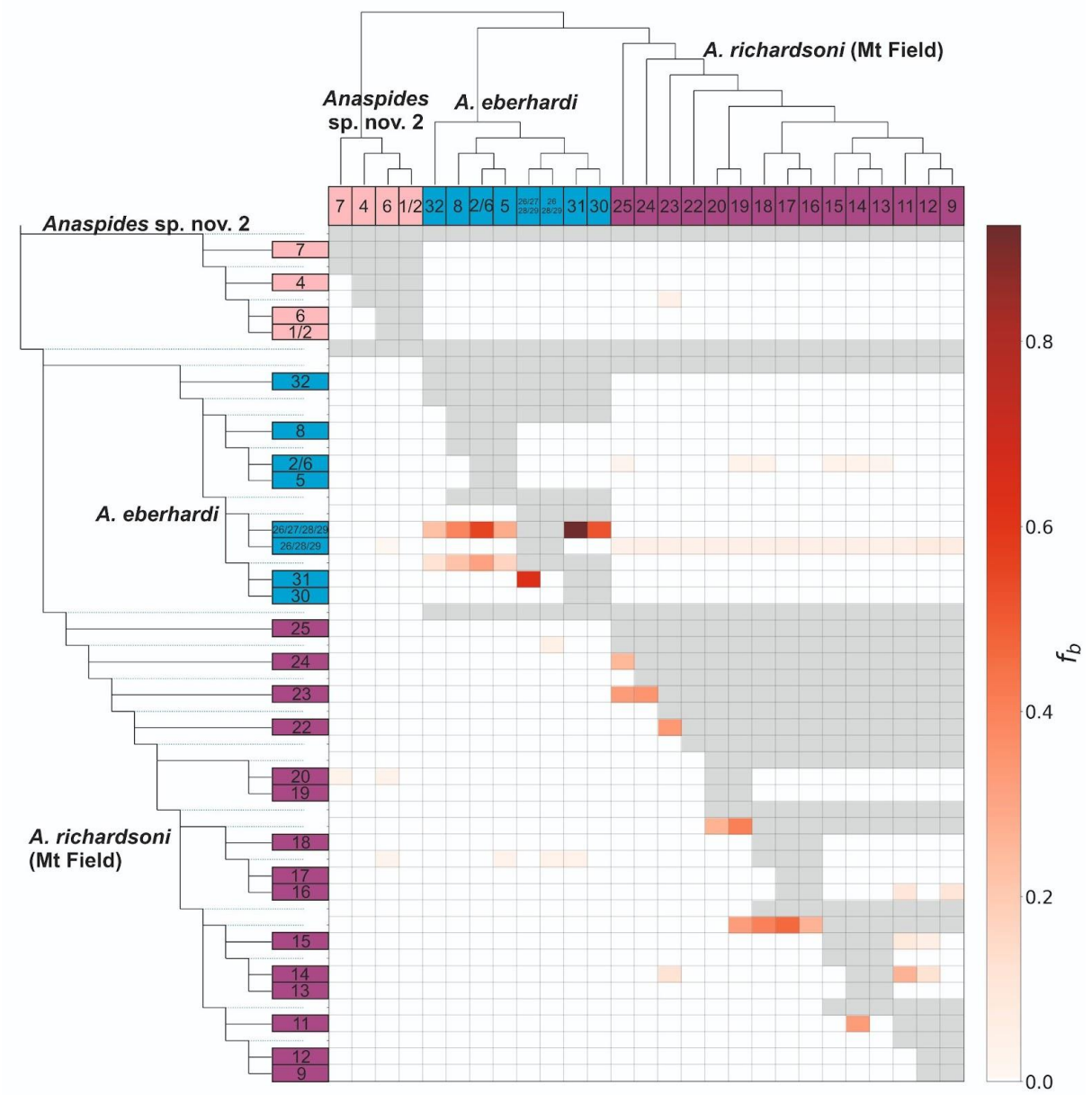


Fig. 5: DSuite analysis of dataset 2 (254 specimens, 1866 Loci, 1823 polymorphic, 17627 SNPs). *Anaspides* sp. nov. 1 was used as outgroup. The genetic groups were chosen after the clusters delineated in Figure 4A (black boxes) with the exception of the 11 specimens of *A. eberhardi* showing higher coancestry which were treated as a separate genetic group. The letters correspond to the locations in Figure 1. Topology is based on the phylogeny in Figure 3A. Coloured boxes correspond to the morphological delineated species: Purple: *A. richardsoni* (Mt Field), Blue: *A. eberhardi*, Light Pink: *Anaspides* sp. nov. 2.

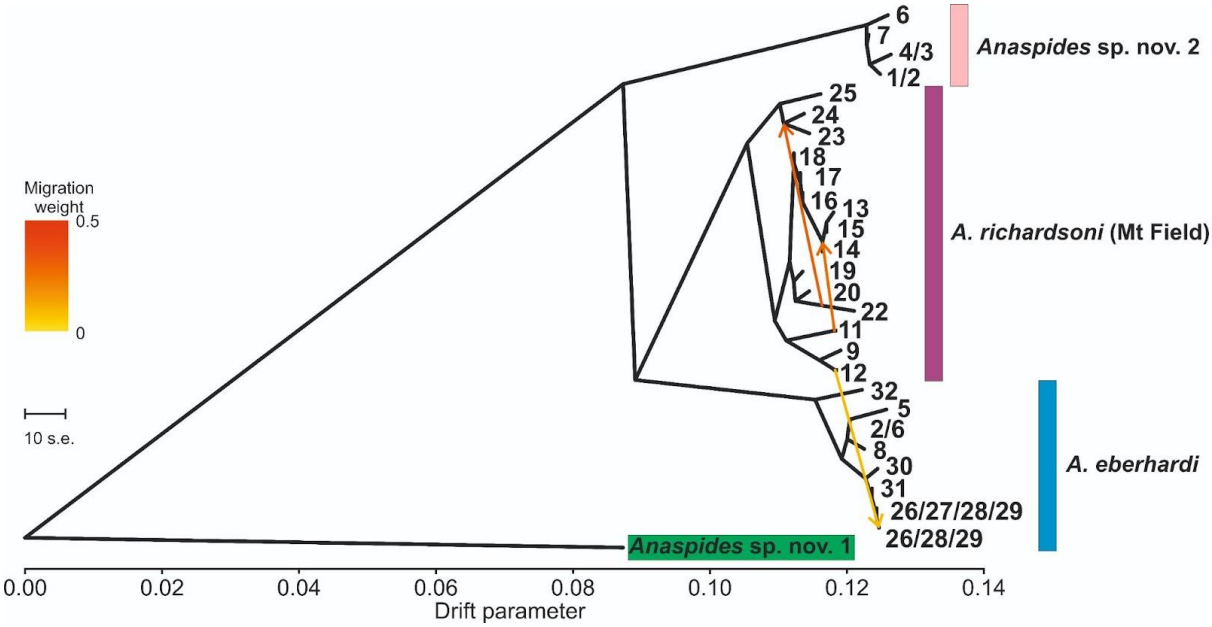


Fig. 6: Treemix analyses of dataset 2 (254 specimens, 1866 Loci, 1823 polymorphic, 17627 SNPs) with the best value for m being 3. The genetic groups were chosen after the clusters delineated in Figure 4A (black boxes) with the exception of the 11 specimens of *A. eberhardi* showing higher coancestry which were treated as a separate genetic group. The letters correspond to the locations in Figure 1. Arrows indicate putative gene flow, respectively introgression events.

COI

In contrast to the ddRAD data, the COI sequences show major differences. In both analyses (haplotype network and molecular clock analyses) none of the three species is recovered as monophyletic (Fig. 7, Supplement Fig. 2). In the phylogram all species even appear as polyphyletic, although no shared haplotypes were recovered. In the haplotype network and molecular clock we have three major clusters respectively lineages (>2.5% difference). The first major cluster (cluster 1) comprises specimens solely of *A. eberhardi*. Within this cluster there are two subgroups (>1% difference), one with a single haplotype comprising the specimens from Toolshed (32), and the other with four haplotypes comprising mainly specimens from Junee Cave (31) and to a lesser extend specimens from Niggly Cave (29) and Growling Swallet (28). Major cluster 2 is composed of specimens from *A. richardsoni* (Mt Field) and *A. eberhardi.* It is also subdivided into two smaller clusters (>1% difference), one with two haplotypes comprising two specimens from Wombat Moor (23, *A. richardsoni*), and the other with four haplotypes with two comprising specimens from the tarn on the west side of the ridge between Clemes Tarn and Florentine Peak (12, *A. richardsoni*), one comprising the specimens from Khazad Dum (30, *A. eberhardi*) and the last one being a single specimen from Porcupine Pot (26, *A. eberhardi*) having also the unusual number of telson spines. One of the

haplotypes comprising *A. richardsoni* is the central haplotype with the other three grouped around it with one, and two mutations difference, respectively. The last major cluster (cluster 3A, B) comprises 45 haplotypes from *A. richardsoni* (Mt Field), *A. eberhardi* and *Anaspides* sp. nov. 2. This cluster shows a complex structure, but no shared haplotypes between species were found. The three cluster were also detected in the Molecular Clock, with clusters 1 and 3 being sister lineages and cluster 2 being sister lineage to them. The separation between clusters 2 and 1/3 is dated to ~2.8 mya, while the split between cluster 1 and 3 to ~2.19 mya. The earliest split in cluster 1 is datetd to ~0.93 mya, in cluster 2 to ~1.06 mya and in cluster 3 to ~1.22mya (Supplement Fig. 2).

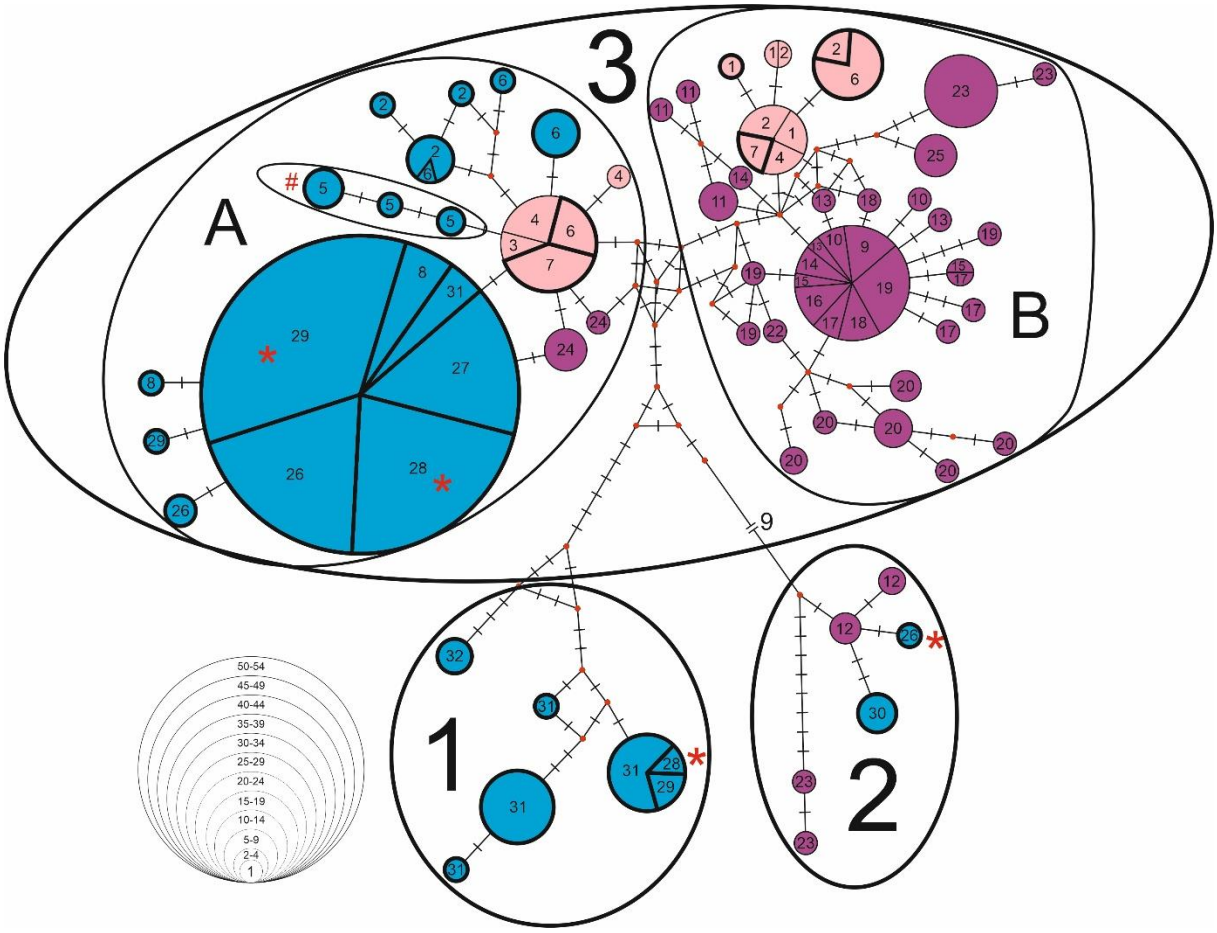


Fig. 7: Median joining haplotype network of *A. eberhardi* (blue), *A. richardsoni* from Mt Field (purple) and *Anaspides* sp. nov. 2 (light pink) calculated for the COI dataset. The dataset comprises 295 specimens and 607 bp. Numbers correspond to the sampling locality in Fig. 1. The size of each haplotype corresponds to the number of individuals sharing that specific haplotype (see scale). Each dash corresponds to one mutation. Circles in bold indicate cave inhabiting specimens. Red asterisks indicate specimens with the unusual number of telson spines (15–23 spines) and red hashtag indicates the *A. eberhardi* population from cave JF–104 with the unusual number of clasping spines (2 clasping spines).

Anaspides eberhardi

Our data (dataset 4) reveal a strong correlation of population structure and geographic distribution. In PC0/1 we can distinguish four clusters within *A. eberhardi* corresponding to major cave and drainage systems (Fig. 8A, B). The first cluster comprises all specimens from

the Junee River catchment (locations 26–31). The second cluster comprises the specimens from Toolshed (32, upper Florentine catchment). The third and fourth cluster comprise specimens from the lower Florentine catchment, with one cluster comprising the specimens from cave JF-104 (5) and the other comprising the specimens from Nameless Spring (2), Settlement Cave (6) and Welcome Stranger Cave (8). The greatest separation is seen in PC0 (explaining 28.7%), dividing the three clusters of the Florentine Catchment from the cluster comprising the specimens from the Junee River catchment (locations 26–31). In PC1 we further have a separation of the upper and lower Florentine catchment clusters. In PC2/3 we can further subdivide specimens from the Junee River catchment into two clusters: one comprising the specimens from Khazad Dum, another comprising the specimens from Porcupine Pot (26), Gormenghast Cave (27), Growling Swallet (28) and Niggly Cave (29) and Junee Cave with the Junee Cave specimens showing a tendency for separation from the above mentioned caves, also visible in the STRUCTURE analyses. The Junee Cave specimens show a mixture of first (26–29) and the second cluster (30) in the ratio ⅔ to ⅓. The remaining clusters were also found in the STRUCTURE analyses (k=5) with the exception of the lower Florentine specimens grouping as a single cluster. In PC2/3 we can also further subdivide the cluster comprising Nameless Spring (2), Settlement Cave (6) and Welcome Stranger Cave (8) into two distinct clusters: one comprising the specimens from Welcome Stranger Cave (8) and the other the specimens from Nameless Spring (2) and Settlement Cave (6). All the above-mentioned clusters and groupings were also found as distinct clusters in the fineRADstructure analyses (Fig. 8C). It was even possible in this analysis to further separate Nameless Spring (2) and Settlement Cave (6) into two distinct groupings with higher coancestry, albeit with very low F_{ST} (0.013) and d_{xy} (0.0028) values (Supplement table 2). The unusual pattern of many small "clusters" (mostly one specimen) in the lower right corner, shows the specimens from Porcupine Pot (26), Growling Swallet (28) and Niggly Cave (29) that have a small proportion of shared genetic information with *A. richardsoni* (Mt Field). These specimens were also found in the STRUCTURE analyses with some genetic signal (green in Fig. 8D) from the *A. richardsoni* specimens from locality 12 from the plateau (see Fig. 4–6). A majority of these specimens also have an unusual number of telson spines (15–23). Nevertheless, these small clusters have extremely high coancestry with the remaining specimens of Porcupine Pot (26), Gormenghast Cave (27), Growling Swallet (28) and Niggly Cave (29), again with extremely low F_{ST} (0.001–0.037) and d_{xy} (0.0024–0.0025) values (Supplement table 2).

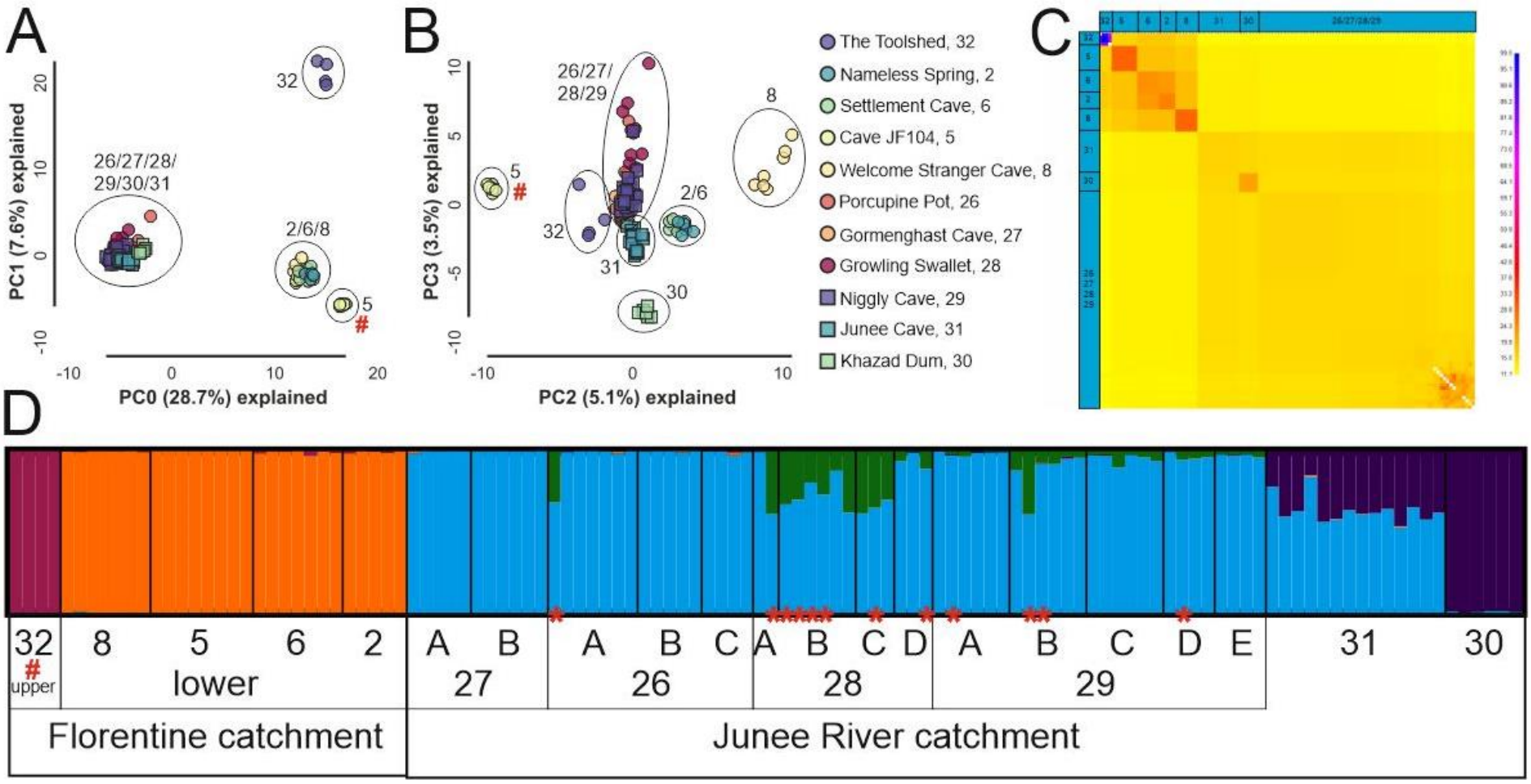


Fig. 8. PCA (A, B), FineRADstructure (C) and STRUCTURE (D) analyses of *Anaspides eberhardi* from Mt Field National Park using dataset 4, (118 specimens, 2443 loci, 1773 polymorphic, 5202 snps). Numbers correspond to the sampling localities in Figure 1. (A) PC0/1; (B) PC2/3; (D) best k–value was k5. Red asterisks indicate specimens with the unusual number of telson spines (15–23 spines) and red hashtag indicates the *A. eberhardi* population from cave JF–104 with the unusual number of clasping spines (2 clasping spines). Black circles in (A) and (B) were drawn by hand to highlight certain genetic groupings.

Discussion

Species, speciation and introgression

Herein, we focus mainly on the stygomorphic species, *A. eberhardi*. The species is clearly monophyletic. The indicated long separation of *A. richardsoni* and *A. eberhardi* (long branches in the ML analyses, low coancestry, and higher FST values ranging from 0.31 to 0.71) also corroborates *A. eberhardi* being a separate species. Accepting *A. richardsoni* as a paraphyletic species, with the Mt Field population as a monophyletic sub-group (Höpel et al. 2025), implies that the common ancestor of *A. eberhardi* and *A. richardsoni* (Mt. Field) needs to be considered as *A. richardsoni* as well, implying that the stem species survived the speciation event. Our analysis also recovers *Anaspides* sp. nov. 2 as a monophyletic lineage, supporting its species status.

We did not detect any signs of interbreeding (based on ddRAD) between the syntopic *A. eberhardi* and *Anaspides* sp. nov. 2 populations in Nameless Spring (2) and Settlement Cave (6). Cave JF-104 population of *A. eberhardi* is a special case, because the three adult males collected here possess two clasping spines. This population from JF-104 might be in an early stage of speciation, given its nested position within *A. eberhardi* and low F_{ST} values (0.13 to Settlement Cave). However, the low number of males studied make it difficult to currently determine if they represent a separate species. The two clasping spines might result from ancient hybridization between the two species, as seen in the COI haplotype network (Fig. 7, cluster 3), but there is no indication of such hybridization in the genomic data.

In contrast to the previous species pair, we detected slight signals of introgression between *A. eberhardi* and *A. richardsoni* (Mt Field), which is nevertheless very localized. Especially evident in the TreeMix analyses, the introgression appears to have come from the *A. richardsoni* population from the tarn on the west side of the ridge between Clemes Tarn and Florentine Peak (12) into the *A. eberhardi* population comprising specimens from Porcupine Pot – Niggly Cave (26–29). More precisely, this signal of introgression is strongest in eleven specimens from this population, of which nine are from Growling Swallet (29). This introgression is also evident in the COI data in haplotype cluster 2 (Fig. 7). As seen in Fig. 2, this surface tarn on the west side of the ridge between Clemes Tarn and Florentine Peak (12) and the Growling Swallet cave (29) are hydrologically connected via Garths Creek, which originates on the Mt Field plateau and sinks into Growling Swallet Cave. During glacial times, this *A. richardsoni* population (12) was probably forced downslope and would have inhabited lower areas of Garths Creek, facilitating this introgression. However, Garths Creek itself and the inflow waters to the cave are currently inhabited by the distantly related species *A. swaini* (Fig. 1, 2). At the four collection sites within Growling Swallet (Fig. 2, 29 A–D), we also found the highest abundance of *A. eberhardi* specimens showing the unusual number of telson spines (15–23), many of which belong to the eleven specimens with signs of introgression. We hypothesise that the introgression from *A. richardsoni* (Mt Field) is responsible for the abnormal number of telson spines.

The mito-nuclear discordance is particularly evident at the level of species delimitation. The COI data fails to detect the three well-separated lineages (*A. eberhardi*, *A. richardsoni* (Mt

Field), and *Anaspides* sp. nov. 2). In fact, in COI, the intraspecific distances (>3% in some cases) are higher than the interspecific distances (0.16% or one mutation difference regardless of the species). This would likely lead to grouping all lineages into a single species, despite distinct morphological differences and clear monophyly in the ddRAD data.

We suggest that the three COI haplotype clusters represent the "original" haplotype groups of *A. eberhardi* (cluster 1), *A. richardsoni* (Mt Field) (cluster 2), and *Anaspides* sp. nov. 2 (cluster 3), which implies that that the mito-nuclar discordance as well as the mismatch between COI and the morphological species identification is the result of several introgression events rather than incomplete lineage sorting in COI. In our view, COI cluster 1 includes the original haplotypes for *A. eberhardi* (or at least are close to the original haplotypes), because it includes the one of the most basal lineages (Toolshed, 32; based on ddRAD) and comprises exclusively specimens of *A. eberhardi*. The *A. eberhardi* haplotypes in cluster 3A are suggsted to be the result of introgressions from *Anaspides* sp. nov. 2. This is especially evident in JF-104 (location 5, Fig 7, red hash), which includes *A. eberhardi* specimens with two clasping spines (similar to *Anaspides* sp. nov. 2) and also plausible giving the overall close geographical proximity of the two species in the lower Florentine Valley (locations 1-7). These introgressed haplotypes then apparently became the dominant haplotypes for *A. eberhardi* (the apparent dominance may also be biased by regional sampling), replacing the original haplotypes. This probably happened before *A. eberhardi* crossed the border between the lower Florentine valley and the Junee River catchment, which is supported by the presence of the same haplotype in Welcome Stranger Cave (8). The original haplotype, however, is still present in low numbers (seen in cluster 1, with 4 specimens form Niggly Cave, respectively Growling Swallet, locations 28, 29). The potential causes underlying the successful spread of their mitogenomes remains elusive. We hypothesize that the introgressed mitogenome featured one or several selectively advantageous mutations (not necessarily in the COI locus studied herein). Furthermore, the *A. richardsoni* haplotypes in cluster 3A and 3B are also the result from introgression from *Anaspides* sp. nov. 2. As this left no signal in the nuclear genome of *A. richardsoni*, introgression probably occurred via very few females. This introgression must have happened before the recolonisation of the plateau. In cluster 2 the *A. eberhardi* haplotyes are apparently the result from introgression from *A. richardsoni* plateau population 12 (which is also seen in the ddRAD data).

Population structure and phylogeography

Herein, we mainly discuss the ddRAD results, as these extensive datasets clearly give a more detailed picture than the single mitochondrial locus (COI) dataset. The almost identical stygomorphic morphology of all *A. eberhardi* populations, coupled with its clear monophyly in the phylogenomic analyses, suggests a single colonization event of the ancestor of *Anaspides eberhardi* into the subterranean environment, followed by underground diversification and dispersal.

Following the topology (both ML and MP), with the upper Florentine River catchment lineage (Toolshed, 32) being the first branching lineage, followed by the lower Florentine River catchment lineage (2, 5, 6, 8) and the Junee River catchment lineage (26–31), we can infer

that *A. eberhardi* originated in the Florentine River catchment. Our molecular clock approach suggests that the ancestor of *A. eberhardi* colonized the Junee-Florentine caves during the Pleistocene. If assuming that cluster 1 represents the original *A. eberhardi* haplotype (only *A. eberhardi* specimens in this cluster) then the colonization is at least 0.93 mya old (with a 95% confidence interval of 0.6–1.3 mya) and possibly up to 2.19 mya (split of cluster 1 and 3) (Supplement Fig. 2).

The Pleistocene saw multiple glaciation events across Tasmanian mountain ranges, including Mt Field National Park and surrounding landscapes. Like other regions of Tasmania, glaciation and ice advances were most extensive during the early Pleistocene, becoming less pronounced in subsequent glacial events. However, the Florentine Valley, the centre of origin of *A. eberhardi*, was not overridden by glacial ice (Fig. 1). During glacial maxima, when most water was bound in glaciers, conditions became drier, leaving mostly cave waters as refugia. For example, Bradbury (1986) found that the latest Pleistocene climate of Mt Field was drier than in the Holocene. Additionally, speleothem dating suggests several drier phases within the Pleistocene, with little to no stalagmite growth (e.g., 70–30 ka in Xia et al., 2001 or around 117–100 ka in Zhao et al., 2001). If the molecular clock dating is partially accurate, *Anaspides eberhardi* must have survived several glacial and periglacial cycles within the cave systems, spreading and diversifying. In contrast, any remaining surface population of *A. richardsoni* in the Florentine Valley became locally extinct.

Within the Florentine Valley we can find a series of smaller, hydrologically discrete, cave drainage systems that ultimately drain into the Florentine River (Eberhard, 1996). All of the upper and most of the lower Florentine Valley karst can be characterized as low relief valley-floor karst. The most significant caves, such as Welcome Stranger Cave (Fig. 1, location 8) or Cashions Creek Cave (Fig. 1, location 7), are horizontal stream passages with only a few hundred metres of passages. Each cave has its own genetically well-separated population of *A. eberhardi*. Moreover, we observe a distinct separation between the upper (Toolshed, 32) and lower (Welcome Stranger Cave 8, Nameless Spring 2, Settlement Cave 6, Cashions Creek 7) valley clusters (13–18 km beeline apart). Probably no recent permanent passable underground connections exist between these caves in this low-relief karst (Kiernan 2018). Dispersal via surface waters seems unlikely for this strictly stygomorphic species owing to unsuitable habitat conditions (e.g., elevated water temperature) and epigean predators, but there can be water flow under peat, on forest floors, and through the interstices of slope deposits. Alternatively, *A. eberhardi* might have used ancient subterranean connections during glacial or interglacial periods.

An underground connection might still exist in the Nameless–Settlement system. We detected only very shallow population-level differentiation between *A. eberhardi* from these two caves (F_{ST} values 0.013, only separate clusters in the fineRADstructure analyses of dataset 4, still with high coancestry), which suggests that *A. eberhardi* might be able to more easily move between these two caves. In contrast, in the same two caves, we observe a clearer distinction between specimens belonging to *Anaspides* sp. nov. 2 (forming distinct populations), suggesting that this slightly stygomorphic and less cave-adapted species does not use these underground connections as often. Furthermore, the data imply that *Anaspides* sp. nov. 2 is

also not using the possible surface connections, possibly because of the higher temperature of the streams further away from the caves.

The next step in the (hypothesized) dispersal route that needs to be explained is the expansion of *A. eberhardi* from the Florentine River catchment into the Junee River system. It has been suggested that these systems are separated by a well-demarcated hydrogeological boundary formed by non-karstic rock units (Fig. 1) within the Westfield syncline (Eberhard, 1998). However, this boundary is not as impermeable as previously suggested. Recent water tracing tests with fluorescent dyes at Cryptic Cowry Cave (JF-655), located at the supposed hydrogeological boundary of both systems (and cutting across the Westfield Syncline), detected a hydrological connection between both drainage systems. After sinking into Cryptic Cowry, the water course appears to split, with a portion draining to Lawrence Rivulet Rising and another portion unexpectedly draining to Junee Cave (Fordyce, 2021). Our findings support that limestone is indeed continuous beneath the siltstone core of the Westfield syncline. Conceivably, an underground stream flows (which might have been more substantial in the past) beneath it at depth (Eberhard, 2020), representing most likely the historic pathway for *A. eberhardi* into the Junee River system. Specimens from Welcome Stranger Cave (8, lower Florentine catchment, closest cave to the Westfield syncline) and the Junee River System (26–29, 31) share the same haplotype in COI, corroborating this hypothesis.

Today, most of the water entering the karst in the south-east of the area resurges at Junee Cave near Maydena, the underground drainage breaching the surface divide between the Florentine and Tyenna valleys (Kiernan, 1992). Flow-through time is rapid, confirming that a well-developed and integrated cave drainage system connects the stream–sinks and this resurgence.

Another element for the current distribution of *A. eberhardi* throughout the whole underground Junee River system (26–31), must have been past drainage modification in the karst. Parts of the underground drainage that belonged to the Florentine catchment were captured by the Tyenna River catchment via its tributary, the Junee underground river, which included among others, Porcupine Pot (26), Gormenghast Cave (27), and Growling Swallet (28) (Kiernan, 2018). Our results do not allow for a precise dating of this capture event; however, it might also be correlated with glacial events. Kiernan et al. (2001) state that during times when glaciers were most extensive, the catchment of the underground Junee River was greatly increased because ice overran present-day fluvial divides, and meltwater under pressure in englacial and subglacial tunnels could flow uphill over bedrock ridges (Ford et al., 1983; Kiernan, 1984).

In contrast to the Florentine Valley caves, the caves of the Junee River catchment are all hydrologically connected via underground streams and can be divided into three subsystems based on hydro-geographic context (Eberhard, 1997), from north to south: (1) Rainbow–Porcupine subsystem (>5 km of mapped passages draining into the Growling–Niggly subsystem); (2) Growling–Niggly subsystem (>23 km of mapped passages, draining to the 10 km distant Junee Cave); (3) Khazad Dum area subsystem (closest to Junee Cave). Each subsystem comprises a cluster of several caves within geographic proximity of each other, and all three subsystems are ultimately connected by hydrology and discharge at Junee Cave. Our

data clearly show that the third subsystem (Khazad Dum, 30) has a separate population forming a discrete cluster in all analyses and showing elevated F_{ST} values (0.064–0.174). In contrast, populations in subsystems one (Porcupine Pot, 26; Gormenghast Cave, 27) and two (Growling Swallet, 28; Niggly Cave 29) are more similar to each other with low F_{ST} values (0.007–0.031), with "higher" values being skewed by the observed introgression of *A. richardsoni* (Mt Field). Another interesting finding is that the specimens from Junee Cave are differentiated from those of the Porcupine Pot – Niggly Cave population and from the nearby Khazad Dum population. Junee Cave specimens form a separate cluster in the PCA and fineRADstructure analyses (Fig. 8) and have slightly elevated F_{ST} values (up to 0.075). As expected, they share genetic signals with both populations mentioned above; however, the proportion of shared genetic signals (⅓ from Khazad Dum, ⅔ from Porcupine–Niggly) is stable in this cave.

Moreover, we did not find a single specimen in Junee Cave with the full genetic signal of either of the other populations, and no specimens in the other populations with a shared signal. This suggests that Junee Cave might be considered a distinct eco-hydrological subsystem (at least in terms of *Anaspides eberhardi* population structure), and also interestingly, that migration between cave subsystems may be more constrained than the rapid dye trace through-flow indicates, not only upstream but also downstream.

CRH or ASH?

Although the indicated long separation of *A. richardsoni* and *A. eberhardi* (long branches in the ML analyses, low coancestry, and higher FST values ranging from 0.31 to 0.71) makes it more difficult to determine the exact mode of speciation, our data support the Climate Relict Hypothesis (CRH). Paleoclimatic reconstructions suggest that caves were used as refuges, followed by the extinction of the surface population. Today, *A. eberhardi* is only found in the deep zone of caves in the Junee–Florentine karst, and never in the inflows or twilight zones. The absence of *A. richardsoni* is evident in the Florentine Valley and on the slopes of Mt. Field. Although many plateau creeks now drain into the caves of the Junee–Florentine karst, the two species do not appear parapatrically, as the inflows and upper cave passages are inhabited by two other species of *Anaspides*, namely *A. tasmaniae* and *A. swaini*, and surprisingly never by their most closely related surface-living species, *A. richardsoni*. These two species might have displaced *A. richardsoni*, as this species inhabits inflows, outflows, and lowland caves in other areas of Tasmania (e.g., Mole Creek caves or Lightning Plains). Furthermore, the evidence of very localized recent hybridization between *A. eberhardi* and *A. richardsoni* (Mt Field), only from one specific *A. richardsoni* population (12) into only a few specimens of one *A. eberhardi* population (26–29), is also consistent with the CRH. This introgression happened after the divergence, and we have no evidence for gene flow during divergence. That the latter cannot be fully excluded is a general problem related to the CRH.

Conservation

The Mt Field National Park and adjacent Junee–Florentine karst can be considered as one of the major hotspots of *Anaspides* diversity in Tasmania in terms of species (see also Höpel et

al., 2021). With the discovery of two potentially new species, one in the Florentine Valley and one in Lake Nicholls, we can now observe six *Anaspides* species species in this mountain massif and its drainage catchments. It is also one of the few places in Tasmania where species of *Anaspides* can be found in syntopy (*A. eberhardi* + *Anaspides* sp. nov. 2 in Settlement Cave and Nameless Spring, *A. tasmaniae* + *A. swaini* in the inflow of Khazad Dum and Niggly Cave/Delta Variant, *A. richardsoni* + *Anaspides* sp. nov. 1 in Lake Nicholls as well as historically also *A. richardsoni + Anaspides* sp. nov. 1 in Robert Tarn and on the Mawson Plateau, see Ahyong (2016).

Mt Field and the Junee–Florentine karst are not only a hotspot in terms of species number, but also genetic diversity, population structure and morphological variation as outlined above. This is an aspect that needs to be the focus of future conservation efforts (Balint et al., 2011). Our findings clearly show an allopatric separation of most populations. Most caves have genetically unique populations, especially seen in A*. eberhardi* in the Florentine Valley and *Anaspides* sp. nov. 2, sometimes corresponding with different morphology as in *A. eberhardi* from JF-104 having two instead of the usual one clasping spine. Moreover, even in the hydrologically connected Junee River system, we detected three different populations of *A. eberhardi* (1: Porcupine Pot – Gormenghast Cave – Growling Swallet – Niggly Cave, 2: Junee Cave, 3: Khazad Dum)*,* showing the great significance of protecting whole eco- and cave systems and not only parts of them (Kiernan, 2018).

Acknowledgements

We want to thank David Butler, Michael Driessen, Rolan Eberhard, Janine McKinnon, John Oxley, Andrew Palfreyman, Cathy Plowman, Alastair Richardson, Chris Sharples and Richard Tunney for collecting various specimens in Tasmania as well as for their advice and guidance. Further specimens were collected by Karina Anders, Alan Jackson, Ciara Smart and Peter Smejkal. We thank Kevin Kiernan for his comments concerning Tasmanian geomorphology. We further thank the University of Tasmania, Institute for Zoology, especially David Green, for providing us with scientific equipment for our field trips. We are thankful to the Department of Natural Resources and Environment Tasmania (NRE) and the Parks and Wildlife Service Tasmania for supporting and facilitating our research. Specimens were collected in 2017, 2019, 2022, 2023 and 2024 (Permits of the Tasmanian Government, Department of Primary Industries, Parks, Water & Environment, nos. FA16347, FA18250, FA21214, FA22411 and FA 23244 respectively). We further thank the Tasmanian Museum and Art Gallery (TMAG) for the loan of specimens from Lightning Plains, the SFM Lenah Estate and John Webb for granting us access to certain areas in the Florentine Valley that include Nameless Spring and Settlement Cave. We are grateful to Markus Grams, Fabio Oliveira, Marian Reinhardt, Birk Rillich, Alexander Rixen, Malte Weiler, Christian Wirkner, (all Universität Rostock), Lena Götz and Louisa Höpel for assistance in the field. Collecting was funded by the German Science Foundation (DFG RI 837/22–1,2). Advanced education and collecting in 2019 was partly funded by the DAAD (Nr. 57438025, Kurzstipendien für Doktoranden, 2019/2020) and the University of Rostock (Promotionsstipendienprogramm, ‘Unsere Besten promovieren in Rostock’). Ralf Bastrop (University of Rostock) provided the infrastructure for sequencing

some of the data. The ddRAD library preparations were conducted in cooperation with the National History Museum Vienna. The present project is funded by the Deutsche Forschungsgemeinschaft (DFG RI 837/22–1, 2, 3).

Data Availability statement

All sequences were deposited in GenBank (Benson et al., 2003) (COI: PV937831–PV938053; ddRAD: BioProject ID: PRJNA1291715). The complete and well–documented bioinformatic analysis pipeline including custom scripts and the commands for third–party programs can be found at Github (https://github.com/ch515/Mt_field_Comparative_phylogeography_and_speciation_Anaspides).

References

Ahyong ST. The Tasmanian mountain shrimps, *Anaspides* Thomson, 1894 (Crustacea, Syncarida, Anaspididae). *Records of the Australian Museum* 2016; 68(7): 313–364.

Ahyong ST., Alonso-Zarazaga MA. Anaspidesidae, a new family for syncarid crustaceans formerly placed in Anaspididae Thomson, 1893. *Records of the Australian Museum* 2017; 69(4): 257–258.

Baker JM. Adaptive speciation: the role of natural selection in mechanisms of geographic and non–geographic speciation. *Studies in History and Philosophy of Science Part C: Studies in History and Philosophy of Biological and Biomedical Sciences* 2005; 36(2): 303–326.

Bálint M, Domisch S, Engelhardt CHM, Haase P, Lehrian S, Sauer J, Nowak C. Cryptic biodiversity loss linked to global climate change. *Nature climate change* 2011; 1(6): 313–318.
Benson DA, Karsch–Mizrachi I, Lipman DJ, Ostell J, Wheeler DL. Genbank. *Nucleic Acids Research* 2003; 31(1): 23–27.

Borowsky R. The evolutionary genetics of Cave fishes: convergence, adaptation and pleiotropy. *Biology of Subterranean Fishes. Enfield: Science Publishers* 2010; 141–168.

Bouckaert R, Heled J, Kühnert D, Vaughan T, Wu CH, Xie D, Drummond AJ. BEAST 2: a software platform for Bayesian evolutionary analysis. *PLoS computational biology* 2014; 10(4): e1003537.

Bowden AR. Coastal sands of Northeastern Tasmania: geomorphology and groundwater hydrology 1981; Doctoral dissertation, University of Tasmania.

Bradbury JP. Late Pleistocene and Holocene paleolimnology of two mountain lakes in western Tasmania. *Palaios* 1986; 381–388.

Colhoun EA, Kiernan K, Barrows TT, Goede A. Advances in Quaternary studies in Tasmania. *Geological Society, London, Special Publications* 2010; 346(1): 165–183.

Darriba D, Posada D, Kozlov AM, Stamatakis A, Morel B, Flouri T. ModelTest–NG: a new and scalable tool for the selection of DNA and protein evolutionary models. *Molecular biology and evolution* 2020; 37(1): 291–294.

Desutter–Grandcolas L, Grandcolas P. The evolution toward troglobitic life: a phylogenetic reappraisal of climatic relict and local habitat shift hypotheses. *Mém Biospéol* 1996; *23*: 57–63.

Eberhard R. Inventory and Management of the Junee River Karst System, Tasmania. *Report to Forestry Management* 1996.

Eberhard R. Age constraints for clastic sediments from two caves in the Junee–Florentine karst. In *Papers and Proceedings of the Royal Society of Tasmania* 1997; 131: 67–72.

Eberhard R. Planning for karst management in multiple–use forest: The Junee–Florentine karst study. *Tasforest–Hobart* 1998; 10: 33–48.

Eberhard R. 2020. JF–665 Cryptic Cowrie Cave. *Speleo Spiel* 2020; 439: 5.

Fitak RR. OptM: estimating the optimal number of migration edges on population trees using Treemix. *Biology Methods and Protocols* 2021; 6(1): bpab017.

Ford DC. Effects of glaciations upon karst aquifers in Canada. *Journal of Hydrology* 1983; 61: 149–158.

Franchini P, Monné Parera D, Kautt AF, Meyer A. quaddRAD: A new high-multiplexing and PCR duplicate removal ddRAD protocol produces novel evolutionary insights in a nonradiating cichlid lineage. *Molecular Ecology* 2017; *26*(10): 2783–2795.

Goede A. Hydrological observations at the Junee Resurgence and a brief regional description of the Junee area, Tasmania. *Helictite* 1973; *11*(1): 3–22.

Goede A, Harmon, RS. Radiometric dating of Tasmanian speleothems—evidence of cave evolution and climatic change. *journal of the Geological Society of Australia* 1983; 30: 89–100.

Goloboff PA, Morales ME. TNT version 1.6, with a graphical interface for MacOS and Linux, including new routines in parallel. *Cladistics* 2023; 39(2): 144–153.

Holsinger JR. Ecological derivation, colonization, and speciation. *Ecosystems of the World* 2000; 399–416.

Höpel CG, Ahyong ST, Kapun M, Schwentner M, Richter S. Phylogeography of the *Anaspides richardsoni* species clade (Anaspidacea, Anaspidesidae): glaciation and recolonization of the Tasmananian Central Plateau and the question of paraphyletic species. Cladistics 2025.

Höpel CG, Ahyong ST, Richter S. Genetic structure and new occurrence records of the iconic Tasmanian mountain shrimp *Anaspides tasmaniae* (Thomson, 1893) (Anaspidesidae: Anaspidacea) reveal relictual distribution in southern Tasmania. *Australian Journal of Zoology* 2021; 68(1): 45–53.

Höpel CG, Richter S, Ahyong ST. A new species of Tasmanian mountain shrimp, *Anaspides driesseni* sp. nov. (Malacostraca, Anaspidacea, Anaspidesidae). *Records of the Australian Museum* 2023a; 75(1): 25–43.

Höpel CG, Yeo D, Ahyong ST, Meier R, Richter S. First mitochondrial genomes of Anaspidacea (Malacostraca, Crustacea) and the phylogenetic relationships of mountain shrimps (*Anaspides* Thomson, 1894) and their relatives within Anaspidesidae. *Journal of Crustacean Biology* 2023b; 43(2): ruad028.

Houshold I., Jackson A. Tasmania. In: Webb J, White S, Smith GK, (ed). Australian Caves and Karst Systems. Heidelberg: Springer International Publishing, 2023; 43–73.

Juan C, Guzik MT, Jaume D, Cooper SJ. Evolution in caves: Darwin's 'wrecks of ancient life in the molecular era. *Molecular Ecology* 2010; 19(18): 3865–3880.

Howarth FG. The zoogeography of specialized cave animals: a bioclimatic model. *Evolution* 1980, 394-406.

Kiernan K. Morphological karst on some New Zealand glaciers. *Journal of the Sydney Speleological Society* 1984; 24: 257–273.

Kiernan K. The management of soluble rock landscapes 1988. University of Tasmania.

Kiernan K. Karst Hydrogeology in Tasmania. In: Back W, Herman J, Paloc H. (ed). Hydrogeology of Selected Karst Region. *International Contributions to Hydrogeology* 1992; 13: 377–392.

Kiernan K. An Atlas of Tasmanian Karst: Tasmanian Forest Research Council 1996; Hobart.

Kiernan K. Eroding the Edges of Nature. Hobart: Fullers Publishing Pty Ltd, 2018.

Kiernan K, Lauritzen SE, Duhig N. Glaciation and cave sediment aggradation around the margins of the Mt Field Plateau, Tasmania. *Australian Journal of Earth Sciences* 2001; 48(2): 251–263.

Klaus S, Mendoza JC, Liew JH, Plath M, Meier R, Yeo DC. Rapid evolution of troglomorphic characters suggests selection rather than neutral mutation as a driver of eye reduction in cave crabs. *Biology letters* 2013; 9(2): 20121098.

Knowlton N, Weigt LA. New dates and new rates for divergence across the Isthmus of Panama. *Proceedings of the Royal Society of London B: Biological Sciences* 1998; 265(1412): 2257–2263.

Li YL, Liu JX. StructureSelector: A web-based software to select and visualize the optimal number of clusters using multiple methods. *Molecular ecology resources* 2018; 18(1): 176–177.

Mackintosh AN, Barrows TT, Colhoun EA, Fifield LK. Exposure dating and glacial reconstruction at Mt. Field, Tasmania, Australia, identifies MIS 3 and MIS 2 glacial advances and climatic variability. *Journal of Quaternary Science: Published for the Quaternary Research Association* 2006; 21(4): 363–376.

Malinsky M, Matschiner M, Svardal H. Dsuite-Fast D-statistics and related admixture evidence from VCF files. *Molecular ecology resources* 2021; 21(2): 584–595.

Malinsky M, Trucchi E, Lawson DJ, Falush D. RADpainter and fineRADstructure: population inference from RADseq data. *Molecular Biology and Evolution* 2018; 35(5): 1284–1290.

Medina MJ, Antić D, Borges PA, Borko Š, Fišer C, Lauritzen SE, Reboleira ASP. Temperature variation in caves and its significance for subterranean ecosystems. *Scientific reports* 2023; 13(1): 20735.

Minh BQ, Schmidt HA, Chernomor O, Schrempf D, Woodhams MD, Von Haeseler A, Lanfear R. IQ–TREE 2: new models and efficient methods for phylogenetic inference in the genomic era. *Molecular Biology and Evolution* 2020; 37(5): 1530–1534.

Niemiller ML, Fitzpatrick BM, Miller BT. Recent divergence with gene flow in Tennessee cave salamanders (Plethodontidae: *Gyrinophilus*) inferred from gene genealogies. *Molecular ecology* 2008; 17(9): 2258–2275.

O'Brien DP. The conservation status of the mountain shrimp (*Anaspides tasmaniae* and *Anaspides spinulae*): a report on its distribution, ecology and taxonomy, including recommendations for management. Department of Parks, Wildlife and Heritage 1990.

Peck SB, Finston TL. Galapagos islands troglobites: the questions of tropical troglobites, parapatric distributions with eyed–sister–species, and their origin by parapatric speciation. Mémoires de Biospéologie 1993; 20: 19–37.

Peterson BK, Weber JN, Kay EH, Fisher HS, Hoekstra HE. Double digest RADseq: an inexpensive method for de novo SNP discovery and genotyping in model and non–model species. *PloS one* 2012; 7(5): e37135.

Pickrell J, Pritchard J. Inference of population splits and mixtures from genome–wide allele frequency data. *Nature Precedings* 2012; 1–1.

Pritchard JK, Stephens M, Donnelly P. Inference of population structure using multilocus genotype data. *Genetics* 2000; 155(2): 945–959.

Rambaut A. *Tree Figure Drawing Tool Version 1.4.* Institute of Evolutionary Biology, University of Edinburgh 2014.

Richter S, Schwentner M, Wirkner CS, Ahyong ST. Phylogeny and species diversity of Tasmanian mountain shrimps and their relatives (Crustacea, Anaspidesidae). *Zoologica Scripta* 2018; 47(1): 84–105.

Rivera MAJ, Howarth FG, Taiti S, Roderick GK. Evolution in Hawaiian cave-adapted isopods (Oniscidea: Philosciidae): vicariant speciation or adaptive shifts? *Molecular Phylogenetics and Evolution* 2002; 25(1): 1–9.

Rochette NC, Rivera-Colón AG, Catchen JM. Stacks 2: Analytical methods for paired-end sequencing improve RADseq-based population genomics. *Molecular ecology* 2019; 28(21): 4737–4754.

Schubart CD, Diesel R, Hedges SB. Rapid evolution to terrestrial life in Jamaican crabs. *Nature* 1998; 393(6683): 363.

Schwentner M, Lörz AN. Population genetics of cold-water coral associated Pleustidae (Crustacea, Amphipoda) reveals cryptic diversity and recent expansion off Iceland. *Marine Ecology* 2021; 42(1): e12625.

Stamatakis A. RAxML version 8: a tool for phylogenetic analysis and post–analysis of large phylogenies. *Bioinformatics* 2014; 30(9): 1312–1313.

Swain R, Reid CI. Observations on the life history and ecology of *Anaspides tasmaniae* (Thomson) (Syncarida: Anaspididae). *Journal of Crustacean Biology* 1983; 3(2): 163–172.

Thomson GM. Notes on Tasmanian Crustacea, with descriptions of new species. *Papers & Proceedings of the Royal Society of Tasmania* 1893; 45–76.

Torres A, Goloboff PA, Catalano SA. Parsimony analysis of phylogenomic datasets (I): scripts and guidelines for using TNT (Tree Analysis using New Technology). *Cladistics* 2022; 38(1): 103–125.

Vaccarelli I, Colado R, Pallares S, Galassi DM., Sanchez–Fernandez D, Di Cicco M, Mammola S. A global meta–analysis reveals multilevel and context–dependent effects of climate change on subterranean ecosystems. *One Earth* 2023; 6(11): 1510–1522.

Vrijenhoek R. DNA primers for amplification of mitochondrial cytochrome c oxidase subunit I from diverse metazoan invertebrates. *Molecular Marine Biology and Biotechnology* 1994; 3(5): 294–299.

Williams WD. Ecological notes on Tasmanian Syncarida (Crustacea: Malacostraca). with a description of a new species of Anaspides. *Internationale Revue der Gesamten Hydrobiologie und Hydrographie* 1965; 50(1): 95–126.

Wolf JB, Lindell J, Backström N. Speciation genetics: current status and evolving approaches. *Philosophical Transactions of the Royal Society B: Biological Sciences* 2010; 365(1547): 1717–1733.

Xia Q, Zhao JX, Collerson KD. Early–Mid Holocene climatic variations in Tasmania, Australia: multi–proxy records in a stalagmite from Lynds Cave. *Earth and Planetary Science Letters* 2001; 194(1–2): 177–187.

Zhao JX, Xia Q, Collerson KD. Timing and duration of the Last Interglacial inferred from high resolution U–series chronology of stalagmite growth in the Southern Hemisphere. *Earth and Planetary Science Letters* 2001; 184(3–4): 635–644.

Eigenständigkeitserklärung der Kapitel 2-6

Die für die zugrundeliegenden Publikationen (Kapitel 2-6) essentiellen Individuen wurden während diverser Forschungs- und Sammlereisen nach Tasmanien gesammelt in den Jahren 2006, 2013, 2017, 2019, 2022, 2023, 2024, 2025. Den Hauptteil der für die hier dargelegten Untersuchungen wichtigen Tiere wurde dabei in den Jahren 2017-2024 gesammelt. Der Großteil der Tiere wurde von Stefan Richter, Shane Ahyong und mir selbst gesammelt. Darüber hinaus hatten wir Hilfe im Feld während der Forschungsreisen von Christian Wirkner (2006), Marian Reinhard (2017), Markus Grams (2019, 2022), Fabio Oliveira (2022), Malte Weiler (2022), Alexander Rixen (2023) Birk Rillich (2023), Christopher Schreier (2025) und George Wilson (2025). Des Weiteren sammelten und halfen uns beim Sammeln sowie beim Finden diverser Orte (insbesondere von Höhlen) Cathie Plowman, David Butler, Alastair Richardson, Stefan Eberhard, Rolan Eberhard, Chris Sharples, John Oxley, Stephen Jacobs, John Webb, Janine McKinnon, Richard Tunney, Arthur Clarke, Henry Shannon, Stephen Fordyce, Peter Smejkal, Alan Jackson, Karin Anders, Ciara Smart, Clair Capper, Michael Driessen und Andrew Palfreyman.

Kapitel 2

Die Idee und das Konzept zu der Untersuchung wurden gemeinsam mit Stefan Richter und Shane Ahyong entwickelt und ausbearbeitet. Die genetischen Untersuchungen, einschließlich DNA Isolation, PCR, Magnetischer Beads Aufreinigung, Sequenz Kontrolle, Alignment und anschließender phylogenetischer Analysen wurden durch mich durchgeführt. Die Sequenzierung übernahm die Firma Eurofins Genomics, sowie Ralf Bastrop von der Universität Rostock. Das Erstellen der Abbildungen und die Ausarbeitung des Manuskriptentwurfs erfolgten durch mich. Manuskript und Abbildung wurden anschließend gemeinsam mit Stefan Richter und Shane Ahyong diskutiert und überarbeitet. Eine sprachliche Korrektur fand durch den Muttersprachler Shane Ahyong statt.

Kapitel 3

Die Idee und das Konzept zu der Untersuchung entstand in Abstimmung mit Stefan Richter und Shane Ahyong. Neben den selbst gesammelten Tieren wurde weiteres Museumsmaterial des Australian Museum in Sydney unter Leitung von Shane Ahyong bearbeitet. Zu diesem Zweck hospitierte ich einen Monat in Sydney am Museum um Techniken der taxonomischen

Arbeit zu lernen. Hierbei wurden die artspezifischen Merkmale durch mich erarbeitet und von Shane Ahyong überprüft. Die genetischen Untersuchungen, einschließlich DNA Isolation, PCR, Magnetischer Beads Aufreinigung, Sequenz Kontrolle, Alignment und anschließender phylogenetischer Analysen wurden durch mich durchgeführt. Die Sequenzierung übernahm die Firma Eurofins Genomics sowie Ralf Bastrop von der Universität Rostock. Die Zeichnungen stammen von Shane Ahyong und mir, wobei der überwiegende Teil von Shane Ahyong gezeichnet wurde. Das Erstellen der Abbildungen und die Ausarbeitung des Manuskriptentwurfs erfolgten durch mich und Shane Ahyong. Manuskript und Abbildungen wurden anschließend von Stefan Richter, Shane Ahyong und mir diskutiert und überarbeitet. Eine sprachliche Korrektur fand durch den Muttersprachler Shane Ahyong statt.

Kapitel 4

Die Idee und das Konzept zu der Untersuchung wurden gemeinsam mit Stefan Richter und Rudolf Meier entwickelt und ausbearbeitet. Die DNA Isolation wurde von mir durchgeführt. Die weitere Library Präparation, das Genome Skimming und das Assembly der Mitogenome wurde in Singapur im Labor von Rudolf Meier durch Darren Yeo durchgeführt. Die für das Baiting notwendigen COI und 16S Sequenzen wurden von mir generiert. Dabei wurden von mir PCRs und magnetische Beads Aufreinigungen durchgeführt und die Sequenzierung fand mittels der Firma Eurofins Genomics statt. Die Annotation der Mitogenome wurde von mir durchgeführt. Die weitere Datenaufbereitung, das Erstellen der Abbildungen und die Ausarbeitung des Manuskriptentwurfs erfolgte durch mich. Teile des Abschnitts Material und Methoden stammen von Darren Yeo. Manuskript und Abbildungen wurden anschließend von Stefan Richter, Rudolf Meier, Shane Ahyong und mir diskutiert und überarbeitet. Eine sprachliche Korrektur fand durch den Muttersprachler Shane Ahyong statt.

Kapitel 5

Die Idee und das Konzept zu der Untersuchung wurde gemeinsam mit Stefan Richter und Martin Schwentner entwickelt und ausbearbeitet. Die notwendigen Schritte für die Sanger Sequenzierung, einschließlich DNA Isolation, PCR, Magnetischer Beads Aufreinigung, Sequenz Kontrolle, Alignment und anschließender phylogenetischer Analysen wurden durch mich durchgeführt. Die Sequenzierung übernahm die Firma Eurofins Genomics. Die für die Untersuchung essentiellen ddRAD Analysen wurden in Kooperation und unter Leitung von Martin Schwentner teilweise am Naturhistorischen Museum in Wien in den Zentralen

Forschungslaboratorien und teilweise an der Uni Rostock durchgeführt. Dabei hospitierte ich für die ersten zwei Durchläufe (je 240 Individuen) an der Uni Wien zum Erlernen dieser genetischen Methode und führte die folgenden drei Durchläufe selbständig an der Universität Rostock in den Laboratorien der Allgemeinen und Speziellen Zoologie durch. Die für die ddRAD notwendigen Laborarbeiten wie die die DNA Analyse, das Messen der DNA Gehalte, sowie die vollständige Library Preparation wurden durch mich durchgeführt. Die Sequenzierung der ddRAD Libraries übernahm die Firma Macrogen. Die bioinformatische Aufarbeitung fand in Kooperation mit Martin Schwenter und Martin Kapun (beide Naturhistorisches Museum Wien) statt. Hierfür hospitierte ich wieder in Wien zum erlernen bioinformatischer Methoden unter Anleitung von Martin Schwenter und Martin Kapun, wobei ich alle bioinformatischen und phylogenetischen Analysen selbst durchgeführt habe. Das Erstellen der Abbildungen und die Ausarbeitung des Manuskriptentwurfs erfolgten durch mich. Manuskript und Abbildungen wurden anschließend von Stefan Richter, Shane Ahyong, Martin Schwentner, Martin Kapun und mir diskutiert und überarbeitet. Eine sprachliche Korrektur fand durch den Muttersprachler Shane Ahyong statt.

Kapitel 6

Die Idee und das Konzept zu der Untersuchung wurde gemeinsam mit Stefan Richter entwickelt und ausbearbeitet. Die notwendigen Schritte für die Sanger Sequenzierung, einschließlich DNA Isolation, PCR, Magnetischer Beads Aufreinigung, Sequenz Kontrolle, Alignment und anschließender phylogenetischer Analysen wurden durch mich durchgeführt. Die Sequenzierung übernahm die Firma Eurofins Genomics. Die für die Untersuchung essentiellen ddRAD Analysen wurden in Kooperation und unter Leitung von Martin Schwentner teilweise am Naturhistorischen Museum in Wien in den Zentralen Forschungslaboratorien und teilweise an der Uni Rostock durchgeführt. Dabei hospitierte ich für die ersten zwei Durchläufe (je 240 Individuen) an der Uni Wien zum Erlernen dieser genetischen Methode und führte die folgenden drei Durchläufe selbständig an der Universität Rostock in den Laboratorien der Allgemeinen und Speziellen Zoologie durch. Hierbei wurden die DNA Analyse, das Messen der DNA Gehalte, sowie die vollständige Library Preparation durch mich durchgeführt. Die Sequenzierung der ddRAD Libraries übernahm die Firma Macrogen. Die bioinformatische Aufarbeitung fand in Kooperation mit Martin Schwenter und Martin Kapun (beide Naturhistorisches Museum Wien) statt. Hierfür hospitierte ich wieder in

Wien zum erlernen bioinformatischer Methoden unter Anleitung von Martin Schwenter und Martin Kapun, wobei ich alle bioinformatischen und phylogenetischen Analysen selbst durchgeführt habe. Das Erstellen der meisten Abbildungen und die Ausarbeitung des Manuskriptentwurfs erfolgten durch mich. Das Basisgrafik für Abbildung 2 dieses Kapitels wurde von Stephen Fordyce erstellt. Manuskript und Abbildung wurden anschließend von Stefan Richter, Shane Ahyong, Stefan Eberhard, Stephen Fordyce, Martin Schwentner, Martin Kapun und mir diskutiert und überarbeitet. Eine sprachliche Korrektur fand durch die Muttersprachler Shane Ahyong und Stefan Eberhard statt.

Selbstständigkeitserklärung

Ich versichere hiermit an Eides statt, dass ich die vorliegende Arbeit selbstständig angefertigt und ohne fremde Hilfe verfasst habe. Dazu habe ich keine außer den von mir angegebenen Hilfsmitteln und Quellen verwendet und die den benutzten Werken inhaltlich und wörtlich entnommenen Stellen entsprechend als solche kenntlich gemacht.

Rostock, 14.08.2025

Christoph Gert Höpel

Lebenslauf

Persönliche Daten

Name:	Christoph Gert Höpel
Geburtsdatum, -ort:	25.12.1993 in Grevesmühlen
Email	christoph.hoepel@uni-rostock.de
	c.hoepel@melica-mv.de

Schulbildung

08/2000 - 07/2004	Grundschule Dassow
08/2004 - 09/2012	Ernst-Barlach-Gymnasium Schönberg, Abschluss: Abitur, Note: 1.9

Studium und Ausbildung

10/2012 - 09/2016	Bachelor of Science in Biowissenschaften an der Universität Rostock, Bachelorarbeit: Nahrungsanalysen an Kormoranen (*Phalacrocorax carbo sinensis*) der Insel Heuwiese Abschluss: Bachelor of Science, Note: 2.6
2016	Ausbildung zum wissenschaftlichen Taucher an der Universität Rostock
10/2016 – 09/2018	Master of Science in Integrative Zoologie an der Universität Rostock, Masterarbeit: Tasmanian mountain shrimps (*Anaspides*, Anaspidacea, Malacostraca) - Phylogeography, endemism and multiple immigrations into caves Abschluss: Master of Science, Note: 1.1
Seit 01.10.2018	Anfertigung einer Dissertation an der Universität Rostock (Mitglied der Graduiertenakademie) mit dem Thema: Systematik, Taxonomie und Phylogeographie der Tasmanischen Berggarnelen der Gattung Anaspides (Anaspidesidae, Anaspidacea, Malacostraca).

Berufliche Tätigkeit

01/2021 – 12/2023	Wissenschaftlicher Mitarbeiter in der Allgemeinen und Speziellen Zoologie an der Universität Rostock (DFG Projekt DFG RI 837/22-2, “The Tasmanian Mountain Shrimps (Anaspidacea, Malacostraca) – from the surface to the underground: independent colonization and adaptations”)
02/2024 – 07/2025	Wissenschaftlicher Mitarbeiter in der Allgemeinen und Speziellen Zoologie an der Universität Rostock (DFG Projekt DFG RI 837/22-3, “The Tasmanian Mountain Shrimps (Anaspidacea, Malacostraca) – from the surface to underground: independent colonization and adaptations”)

Nebentätigkeit

2014	Studentische Hilfskraft in der Allgemeinen und Speziellen Botanik an der Universität Rostock
2016	Studentische Hilfskraft in der Allgemeinen und Speziellen Zoologie an der Universität Rostock, Magenanalysen bei Kormoranen der Insel Heuwiese
2016 -2018	Mithilfe als wissenschaftlicher Taucher im Rahmen des Projektes TRANSCOAST
2016 – 2017	Wissenschaftliche Hilfskraft in der Allgemeinen und Speziellen an der Universität Rostock, Betreuung des Masterkurses: Biologie der Fische
2017	Wissenschaftliche Hilfskraft am Meeresmuseum Stralsund, Magenanalysen an Kegelrobben, Seehunden und Schweinswalen
2017 – 2018	Wissenschaftliche Hilfskraft in der Allgemeinen und Speziellen an der Universität Rostock, Betreuung des Masterkurses: Grundlagen Evolutionärer Morphologie
2018 – 2025	Leitung von Zoologischen Feldexkursionen im Rahmen des Moduls Einheimische Flora und Fauna an der Universität Rostock
2018	Wissenschaftliche Hilfskraft in der Allgemeinen und Speziellen an der Universität Rostock, Leiter des Tutoriums für Allgemeine und Spezielle Zoologie
2018	Wissenschaftliche Hilfskraft in der Allgemeinen und Speziellen an der Universität Rostock, Molekulare Untersuchungen von Polychaeten atlantischer Seeberge
2022	Arbeit als wissenschaftlicher Taucher am Institut für Angewandte Ökosystemforschung (IfAÖ)

Publikationen

2021	Höpel, C.G., Ahyong, S.T., & Richter, S. (2021). Genetic structure and new occurrence records of the iconic Tasmanian mountain shrimp *Anaspides tasmaniae* (Thomson, 1893) (Anaspidesidae: Anaspidacea) reveal relictual distribution in southern Tasmania. Australian Journal of Zoology, 68(1), 45–53. (https://doi.org/10.1071/ZO20100).
2022	Höpel, C.G., Yeo, D., Grams, M., Meier, R., & Richter, S. (2022). Mitogenomics supports the monophyly of Mysidacea and Peracarida (Malacostraca). Zoologica Scripta, 51, 603–613. (https://doi.org/10.1111/zsc.12554).
2022	Hazerli, D., Höpel, C.G., & Richter, S. (2022). New insights into the evolution of portunoid swimming crabs (Portunoidea, Heterotremata, Brachyura) and the brachyuran axial skeleton. Frontiers in Zoology 19(1), 24. (https://doi.org/10.1186/s12983-022-00467-8).

2023 Höpel, C.G., Richter, S. & Ahyong, S.T. (2023). A New Species of Tasmanian Mountain Shrimp, *Anaspides driesseni* sp. nov. (Malacostraca, Anaspidacea, Anaspidesidae). Records of the Australian Museum, 75(1), 25–43. (https://doi.org/10.3853/j.2201-4349.75.2023.1829).

2023 Höpel, C.G., Yeo, D., Ahyong, S.T., Meier, R. & Richter, S. (2023). First mitochondrial genomes of Anaspidacea (Malacostraca, Crustacea) and the phylogenetic relationships of mountain shrimps (*Anaspides* Thomson, 1894) and their relatives within Anaspidesidae. Journal of Crustacean Biology, 43(2), ruad28. (https://doi.org/10.1093/jcbiol/ruad028).

2023 Schmidt, J., Kleeberg, A., Kornmilch, J., Bachmann, O., Albe, F., Dörnbrack, F., Ehlermann, J., Erber, T.M., Guschker, L.V., Höpel, C.G., Lappe, V., Lembach, L., Morana, M., Riegert, J.W., Ruf, J., Schmitt, F., Schneider, J., Taege, T.J., Thiesen, P., & Naumann, B. (2023). Erfassung von Arthropoden an der Lübecker Bucht im Rahmen einer Studienexkursion der Universität Rostock – Ergebnisbericht 2023. Archiv Natur- und Landeskunde Mecklenburg-Vorpommern, 59, 65–96. (https://doi.org/10.30819/anlk.59.05)

2024 Schmidt, J., Bachmann, O., Ewald, J., Frase, T., Höpel, C.G., Hoffmann, H., Kornmilch, J.-C., Lehmann, J.F., Martin, D., Wilde, M., Winter, J. & Naumann, B. (2024). Erfassung von Arthropoden in Nordwestmecklenburg im Rahmen einer Studienexkursion der Universität Rostock – Ergebnisbericht 2024. Archiv Natur- und Landeskunde Mecklenburg-Vorpommern 60: 3–11. (https://doi.org/10.30819/anlk.60.04)

2025 Schmidt, J., Höpel, C.G., & Russow, B. (2025). Erstnachweis von *Bembidion normannum* (Coleoptera: Carabidae) an der Küste Mecklenburg-Vorpommerns: Bislang übersehen oder ein Profiteur von Klimaerwärmung und Meeresspiegelanstieg? Angewandte Carabidologie 15: 28–42. (https://doi.org/10.54336/AC1504)

2025 Höpel, C.G., Ahyong, S.T., Kapun, M., Schwentner, M., & Richter. S. (2025). Phylogeography of the *Anaspides richardsoni* species clade (Anaspidacea, Anaspidesidae) - glaciation and recolonisation of the Tasmanian Central Plateau and the question of paraphyletic species. Cladistics. (https://doi.org/10.1111/cla.70005)

Tagungsbeiträge und eingeladene Vorträge

2018 Poster: Höpel, C., Bastrop, R., Ahyong, S., Richter, S. (2018): Phylogeography of the Tasmanian mountain shrimps (*Anaspides*; Malacostraca) - Multiple immigrations into subterranean habitats and biodiversity. 111. Annual Meeting of the German Zoological Society (DZG), Greifswald, 10. – 15. September 2018.

2019 Vortrag: Höpel, C.G., Bastrop, R., Ahyong, S., Richter, S. (2019): Glacial influence on the phylogeographic pattern in Tasmanian mountain shrimps

(*Anaspides*, Anaspidacea, Malacostraca). 112. Annual Meeting of the German Zoological Society (DZG), Jena, 09. – 13. September 2019.

2022 Vortrag: Höpel, C.G., Richter, S. (2022): Die Tasmanischen Berggarnelen (*Anaspides*, Anaspidacea) – von der Oberfläche in den Untergrund. 20. Treffen der Deutschen Crustaceologen, Kiel, 07. – 10. April 2022.

2022 Vortrag: Höpel, C.G., Yeo, D., Meier, R., Richter, S. (2022): Phylogeny of Malacostraca with special focus on the Anaspidesidae (Anaspidacea) based on full mitochondrial genomes. 39th Annual Meeting of the Willi Hennig Society, Helsinki, 24. – 28. Juli 2022.

2022 Vortrag: Höpel C.G., Schwentner, M., Richter, S. (2022): Speciation in correlation with cave immigration in Tasmanian mountain shrimps (*Anaspides*, Anaspidacea, Malacostraca). 114. Annual Meeting of the German Zoological Society (DZG), Bonn, 12. – 16. September 2022.

2023 Vortrag: Höpel, C.G., Schwentner, M., Richter, S. (2023): Speciation in correlation with cave immigration in Tasmanian mountain shrimps (*Anaspides*, Anaspidacea, Malacostraca). 40th Annual Meeting of the Willi Hennig Society, Ithaca, 09. – 13. Juli 2023.

2023 Poster: Höpel, C.G., Eberhard, S., Kapun, M., Ahyong S.T., Schwentner, M., Richter, S. (2023): Speciation in correlation with cave immigration in Tasmanian mountain shrimps (*Anaspides*, Anaspidacea, Malacostraca). 63th Phylogenetic Symposium, Greifswald, 24. – 26. November 2023.

2024 Vortrag: Höpel, C.G., Richter, S. (2024): Systematics and Phylogeography of Tasmanian Mountain Shrimps (*Anaspides*, Malacostraca, Crustacea). Mexico City (Mexico), 28. Juli – 01. August 2024.

2024 Vortrag: Höpel, C.G., Schwentner, M., Richter, S. (2024): Die Tasmanischen Berggarnelen (Anaspidacea, Malacostraca) im Mole Creek Karst – unabhängige Höhleneinwanderung und Anpassung. 21. Treffen der Deutschen Crustaceologen, Rostock, 25. – 27. April 2024.

2024 Vortrag: Höpel, C.G., Richter, S. (2024): Systematics and Phylogeography of Tasmanian Mountain shrimps (*Anaspides*, Malacostraca, Crustacea). 41th Annual Meeting of the Willi Hennig Society, Mexico-Stadt (Mexiko), 28. Juli - 01. August 2024.

2025 Vortrag: Höpel, C.G., Richter, S. (2025): Comparative phylogeography and speciation in correlation with glaciation and cave colonization in Tasmanian mountain shrimps (*Anaspides*, Anaspidacea, Crustacea). Gastvortrag an der Fakultät für Lebenswissenschaften der Universität Wien. 29.04.2025.

2025 Vortrag: Höpel, C.G., Richter, S. (2025): Comparative phylogeography and speciation in correlation with glaciation and cave colonization in Tasmanian mountain shrimps (*Anaspides*, Anaspidacea, Crustacea). Gastvortrag im Seminar „Frontiers in Molecular Systematics“ des Naturhistorischen Museum Wien. 28.04.2025.

2025	Vortrag: Höpel, C.G., Ahyong S.T., Kapun, M., Schwentner, M., Richter, S. (2025): Comparative phylogeography and speciation in correlation with glaciation and cave colonization in Tasmanian mountain shrimps (*Anaspides*, Anaspidacea, Crustacea). The Crustacean Society (TCS) Summer Meeting (Paris). 07. – 10. Juli 2025.

Auszeichnungen

10/2018	Auszeichnung der Mathematisch Naturwissenschaftlichen Fakultät für die beste Masterarbeit in einem Biologischen Masterstudium 2018.
01/2019 – 12/2020	Stipendium "Unsere Besten promovieren in Rostock" der Universität Rostock
2021	Best Student Paper Award Australian Journal of Zoology: Höpel, C. G., Ahyong, S. T. & Richter, S. (2021). Genetic structure and new occurrence records of the iconic Tasmanian mountain shrimp *Anaspides tasmaniae* (Thomson, 1893) (Anaspidesidae: Anaspidacea) reveal relictual distribution in southern Tasmania. Australian Journal of Zoology, 68(1), 45–53. (https://doi.org/10.1071/ZO20100).
04/2022	Auszeichnung für den drittbesten Studierendenvortrag. 20. Treffen der Deutschen Crustaceologen, Kiel, 07. – 10. April 2022
07/2022	Willi Hennig Award für den besten Studierendenvortrag. 39th Annual Meeting of the Willi Hennig Society, Helsinki, 24. – 28. Juli 2022
08/2024	Kurt Milton Pickett Intercontinental Award. 41th Annual Meeting of the Willi Hennig Society, Mexiko City, 28. Juli - 01. August 2024.
08/2024	Lars Brundin Award für den zweitbesten Studierendenvortrag. 41th Annual Meeting of the Willi Hennig Society, Mexiko City, 28. Juli - 01. August 2024.
07/2025	Award für den zweitbesten Studierendenvortrag eines TCS Mitglieds. The Crustacean Society (TCS) Summer Meeting (Paris). 07. – 10. Juli 2025.

Gutachten für wissenschaftliche Zeitschriften

Marine Biology Research

Organisms Diversity & Evolution

Forschungsreisen

2013	Forschungsreise nach Burkina Faso im Rahmen des Projektes WASCAL
2014	Forschungsreise nach Burkina Faso im Rahmen des Projektes WASCAL
2017	Forschungs- und Sammelreise nach Tasmanien mit Fokus auf die Anaspidesidae

2019	Forschungs- und Sammelreise nach Tasmanien mit Fokus auf die Anaspidesidae und Koonungidae
2022	Forschungs- und Sammelreise nach Tasmanien mit Fokus auf die Anaspidesidae
2023	Forschungs- und Sammelreise nach Tasmanien und New South Wales mit Fokus auf die Anaspidesidae und Psammaspididae
2024	Forschungs- und Sammelreise nach Tasmanien mit Fokus auf die Anaspidesidae
2024	Forschungsreise nach Peru in den Tieflandregenwald, Biodiversitätsmonitoring und Katierung mit Fokus auf Pfeilgiftfrösche und Vögel
2025	Forschungs- und Sammelreise nach Tasmanien mit Fokus auf Anaspidesidae und Phreatoicidae
2025	Forschungsreise nach Nepal in den Himalaya, Biodiversitätsmonitoring und Geländekartierung mit Fokus auf die Carabidae

Mitgliedschaften

Deutsche Zoologische Gesellschaft (DZG), Willi Hennig Society (WHS), The Crustacean Society, Northern Caverneers of Tasmania (NC), Arbeitsgemeinschaft für Karstkunde Harz e.V., Verein der Freunde und Förderer der Zoologischen Sammlung der Universität Rostock e.V., Vogelschutzverein Langenwerder e.V., Plant for Future e.V.

Danksagung

Als Erstes und in ganz besonderem Maße gilt mein Dank meinem Betreuer, Prof. Dr. Stefan Richter, für die Möglichkeit, dieses faszinierende Promotionsprojekt zu bearbeiten und diese einzigartigen Tiere kennen und lieben zu lernen. Ohne dich wäre dieses gesamte Projekt nicht möglich gewesen. Vielen Dank für deine kontinuierliche fachliche und freundschaftliche Betreuung und Unterstützung, für die vielen wundervollen Forschungsreisen und gemeinsamen Momente sowie für die Gelegenheit, an zahlreichen spannenden Tagungen weltweit teilzunehmen. Einen besseren Betreuer hätte ich mir nicht wünschen können!

I would like to express my special thanks to Shane Ahyong for his continuous support throughout the project—be it assistance in the field, many scientific discussions, content and language revisions of the manuscripts, or the opportunity to spend a month in Sydney under his guidance, gaining valuable insights into good taxonomic practices.

Für die wunderbare Arbeitsatmosphäre und die vielen schönen gemeinsamen Erlebnisse möchte mich besonders bei allen derzeitigen und ehemaligen Mitarbeitenden, Kolleginnen und Kollegen sowie Doktorandinnen und Doktoranden der Allgemeinen und Speziellen Zoologie bedanken: Markus, Alice, Sören, Christian, Benni, Yannic, Achim, Kerstin, Antje, Scholle, Alex, Max, Basti, Jens, Torben, Thomas, Andreas, Helmut, Marion, Helga, Olaf, Kati, Birk, Dennis, Fabio und Christopher. Es war eine Freude, jeden Tag zur Arbeit zu kommen und euch von den neusten *Anaspides*-News zu berichten. Besondere möchte ich hierbei nochmal Markus Mendes-Grams danken, mit dem mich viele schöne Erlebnisse auf diversen Forschungsreisen und Tagung verbinden, ebenso wie zahlreiche fachliche Diskussionen weit über *Anaspides* hinausgehend.

Mein Dank gilt auch Martin Schwentner für die Einführung in genetische Analysemethoden, die Möglichkeit, mehrfach in Wien zu hospitieren und die Methoden der ddRAD-Sequenzierung und -Auswertung zu erlernen, sowie für viele fachliche Gespräche über *Anaspides* und Artbildung. Ebenso danke ich Martin Kapun für seine Unterstützung bei den bioinformatischen Analysen. Mein Dank geht auch an alle Mitarbeitenden des Naturhistorischen Museums Wien, die mir während meines Aufenthalts dort geholfen und die Zeit sehr angenehm und kurzweilig gestaltet haben.

A special thanks goes to all people in Tasmania, many of whom have become good friends over the years, who helped us during and between our field trips, collecting various specimens and helping us to collect, guiding and advising us, organizing permits, providing us with the all materials and scientific gear we needed as well as discussing our results and showing us the beautiful nature of Tasmania. These people are: Cathie Plowman, David Butler, Alastair Richardson, Stefan Eberhard, Rolan Eberhard, David Green, Chris Sharples, John Oxley, Steve Jacobs, Stephen Fordyce, John Webb, Kevin Kiernan, Janine McKinnon, Richard Tunney, Arthur Clarke, Henry Shannon, Peter Smejkal, Alan Jackson, Karin Anders, Ciara Smart, Serena Benjamin, Janice March, Claire Capper, Jenny Sprent, Jia Huan Liew, Henry Garrat, Harry Driessen, Ben Masterman, Michael Driessen und Andrew Palfreyman. Without your efforts, this study in its extend and detail would not have been possible. I further want to thank to the Department of Natural Resources and Environment Tasmania (NRE), the Parks and Wildlife Service Tasmania and the University of Tasmania for supporting and facilitating our research.

Ich möchte mich auch bei Ralf Bastrop für seine fachliche Hilfe und den Sequenzierservice, insbesondere während meiner Masterarbeit und zu Beginn meiner Promotion bedanken. Rudolf Meier und Darren Yeo danke ich für die Möglichkeit, die Analyse der mitochondrialen Genom

durchzuführen. Darüber hinaus möchte ich George ‚Buz' Wilson, Malte Weiler, Marian Reinhard, Alexander Rixen, Birk Rillich, Fabio Oliveira, Christopher Schreier und Markus Grams für ihre Hilfe im Feld während unserer Forschungsreisen nach Tasmanien danken.

Für die finanzielle Förderung meiner Doktorarbeit danke ich der Deutschen Forschungsgemeinschaft (DFG), der Universität Rostock sowie dem DAAD.

Ich möchte allen Freuden danken für ihre moralische Unterstützung, die vielen schönen und lustigen Momente, die tollen Gespräche und langen Abende während meiner Zeit in Rostock.

Ich möchte von ganzem Herzen meiner ganzen Familie – meiner Mutter Gudrun, Volker, meiner Schwester Louisa, meinem Vater Ralf, meinen Großeltern und meiner Freundin Anna - bedanken. Ohne eure Hilfe, Unterstützung, euer Verständnis und Rückhalt wäre mein Studium und diese Arbeit nicht möglich gewesen. Besonders danke ich meiner Freundin Anna für ihr Verständnis, wenn ich wieder einmal länger gearbeitet habe oder wochenlang auf Forschungsreise war, sowie für die vielen schönen Momente und Ablenkungen in stressigen Phasen. Im besonderen Maße möchte ich nochmals meiner Mutter Gudrun danken – ohne ihre konstante Unterstützung, Förderung, ihren Rückhalt und ihren Glauben an mich, wäre ich heute nicht da, wo ich bin.